โครงสร้างและการเปลี่ยนแปลงระบบประสาทสร้างโกนาโดโทรปินรีลิสซิงฮอร์โมน–1 ในช่วงฤดูสืบพันธุ์ของปลาทู *Rastrelliger brachysoma* (Bleeker, 1851) จากจังหวัดสมุทรสงคราม

นายศิลปชัย เสนารัตน์

วิทยานิพนธ์นี้เป็นส่วนหนึ่งของการศึกษาตามหลักสูตรปริญญาวิทยาศาสตรดุษฎีบัณฑิต
สาขาวิชาวิทยาศาสตร์ทางทะเล ภาควิชาวิทยาศาสตร์ทางทะเล
คณะวิทยาศาสตร์ จุฬาลงกรณ์มหาวิทยาลัย
ปีการศึกษา 2558

STRUCTURE AND ALTERATION OF GONADOTROPIN RELEASING HORMONE–1 PEPTIDERGIC NEURONAL SYSTEM DURING BREEDING SEASON OF SHORT MACKEREL *Rastrelliger brachysoma* (Bleeker, 1851) FROM SAMUT SONGKHRAM PROVINCE

Mr. Sinlapachai Senarat

A Dissertation Submitted in Partial Fulfillment of the Requirements
for the Degree of Doctor of Philosophy Program in Marine Science
Department of Marine Science
Faculty of Science
Chulalongkorn University
Academic Year 2015

Thesis Title	STRUCTURE AND ALTERATION OF GONADOTROPIN RELEASING HORMONE–1 PEPTIDERGIC NEURONAL SYSTEM DURING BREEDING SEASON OF SHORT MACKEREL *Rastrelliger brachysoma* (Bleeker, 1851) FROM SAMUT SONGKHRAM PROVINCE
By	Mr. Sinlapachai Senarat
Field of Study	Marine Science
Thesis Advisor	Jes Kettratad, Ph.D.
Thesis Co-Advisor	Assistant Professor Wannee Jiraungkoorskul, Ph.D.

Accepted by the Faculty of Science, Chulalongkorn University in Partial Fulfillment of the Requirements for the Doctoral Degree

.....Dean of the Faculty of Science
(Associate Professor Polkit Sangvanich, Ph.D.)

THESIS COMMITTEE

.....Chairman
(Associate Professor Voranop Viyakarn, Ph.D.)
.....Thesis Advisor
(Jes Kettratad, Ph.D.)
.....Thesis Co-Advisor
(Assistant Professor Wannee Jiraungkoorskul, Ph.D.)
.....Examiner
(Associate Professor Charoen Nitithamyong, Ph.D.)
.....Examiner
(Assistant Professor Sukanya Jaroenporn, Ph.D.)
.....External Examiner
(Apichart Termvidchakorn, D.Agri.)

ศิลปชัย เสนารัตน์ : โครงสร้างและการเปลี่ยนแปลงระบบประสาทสร้างโกนาโดโทรปินรีลิสซิงฮอร์โมน–1 ในช่วงฤดูสืบพันธุ์ของปลาทู *Rastrelliger brachysoma* (Bleeker, 1851) จากจังหวัดสมุทรสงคราม (STRUCTURE AND ALTERATION OF GONADOTROPIN RELEASING HORMONE–1 PEPTIDERGIC NEURONAL SYSTEM DURING BREEDING SEASON OF SHORT MACKEREL *Rastrelliger brachysoma* (Bleeker, 1851) FROM SAMUT SONGKHRAM PROVINCE) อ.ที่ปรึกษาวิทยานิพนธ์หลัก: อ. เจษฎ์ เกษตระทัต, อ.ที่ปรึกษาวิทยานิพนธ์ร่วม: วรรณีย์ จิรอังกูรสกุล, 200 หน้า.

ปลาทู (*Rastrelligerbrachysoma* (Bleeker, 1851)) จัดเป็นปลาเศรษฐกิจที่สำคัญและถูกพัฒนาเป็นปลาสำหรับเพาะเลี้ยงแต่อย่างไรก็ตามการเพาะเลี้ยงปลาชนิดนี้ยังมีปัญหาทางด้านการสืบพันธุ์และการผลิตเซลล์สืบพันธุ์ในสภาพกักขังการเข้าใจเรื่องโครงสร้างด้านระบบนิวโรเอนโดไครน์ที่เกี่ยวข้องกับการสืบพันธุ์ทั้งปลาทูในธรรมชาติและภายใต้โรงเพาะฟักจึงมีความสำคัญและจำเป็นต้องศึกษา รังไข่ของปลาทูเป็นชนิดasynchronous developmental type ซึ่งภายในรังไข่ประกอบด้วยระยะเซลล์ไข่ 7 ระยะ เมื่อพิจารณาจากโครงสร้างทางด้านมิญชวิทยาได้แก่ oogonium, chromatin nucleolar, perinucleolarnucleolar, lipid droplet and cortical alveolar, early vitellogenic, late vitellogenic และ post vitellogenic stages อัณฑะของปลาทูเป็นชนิด unrestricted spermatogonial type ซึ่งสามารถแบ่งตามขดตัวของเส้นใยโครมาตินและลักษณะอื่นๆได้เป็น5 ระยะการได้แก่spermatogonium, secondary spermatogonia, primary spermatocytes, secondary spermatocyte, spermatids และ spermatozoa โครงสร้างทางด้านกายวิภาคและมิญชวิทยาของสมองปลาทูจากส่วนหน้า (anterior region) ถึงส่วนหลัง (posterior region) ประกอบด้วย 5 ส่วน ได้แก่ telencephalon, mesencephalon, diencephalon, metencephalon และ myelencephalon กลุ่มเซลล์ประสาทที่สร้าง sbGnRHภายใน nucleus preopticus-periventricularis ของสมองปลาทูเพศเมีย สามารถพบได้ 3 บริเวณได้แก่ nucleus periventricularis, nucleus preopticus และ nucleus lateralistuberis นอกจากนี้เส้นใยประสาทสร้าง sbGnRH ยังยื่นเข้าไปยังบริเวณ proximal par distalis โดยแสดงปฏิกิริยากับ GtH จากการศึกษาปลาทูเพศเมียในฤดูสืบพันธุ์การเปลี่ยนแปลงของจำนวนเซลล์ประสาทสร้าง sbGnRH และเซลล์สร้าง GtH ในสมองมีระดับสูงกว่าในปลาทูเพศเมียนอกฤดูการสืบพันธ์อย่างมีนัยสำคัญทางสถิติในขณะที่มีเพียงปริมาณ LH เท่านั้นที่สูงสุดในช่วงสืบพันธุ์และต่ำสุดในช่วงนอกฤดูสืบพันธุ์ จำนวนและปริมาณของเซลล์ประสาทสร้าง sbGnRH และเซลล์สร้าง GtH ในสมองของปลาทูในธรรมชาติสูงกว่าปลาทูภายใต้โรงเพาะฟัก โดยในปลาทูเพศผู้การกระจายของเซลล์ประสาทสร้าง sbGnRH และเซลล์สร้าง GtH ในสมองจะคล้ายคลึงกับปลาทูเพศเมีย จากผลการศึกษาทั้งหมดแสดงให้เห็นว่าการปรากฏของเซลล์ประสาทสร้าง sbGnRH และเซลล์สร้าง GtH เกี่ยวข้องกับการสืบพันธุ์ในปลาทูภายในความสัมพันธ์ของระบบsbGnRH-GtH นอกจากนี้ยังพบว่าปลาทูในธรรมชาติมีกระบวนการสืบพันธุ์ดีกว่าปลาทูที่เลี้ยงภายใต้โรงเพาะฟักซึ่งอาจเกิดจากความเสียหายของระบบต่อมไร้ท่อและความเสียหายของระบบสืบพันธุ์ของปลาทูที่เลี้ยงในระบบโรงเพาะฟัก

ภาควิชา	วิทยาศาสตร์ทางทะเล	ลายมือชื่อนิสิต	.....
สาขาวิชา	วิทยาศาสตร์ทางทะเล	ลายมือชื่อ อ.ที่ปรึกษาหลัก	.....
ปีการศึกษา	2558	ลายมือชื่อ อ.ที่ปรึกษาร่วม	.....

5672846423 : MAJOR MARINE SCIENCE
KEYWORDS: GNRH / RASTRELLIGER BRACHYSOMA / REPRODUCTVE SYSTEM

SINLAPACHAI SENARAT: STRUCTURE AND ALTERATION OF GONADOTROPIN RELEASING HORMONE–1 PEPTIDERGIC NEURONAL SYSTEM DURING BREEDING SEASON OF SHORT MACKEREL *Rastrelliger brachysoma* (Bleeker, 1851) FROM SAMUT SONGKHRAM PROVINCE. ADVISOR: JES KETTRATAD, Ph.D., CO-ADVISOR: ASST. PROF. WANNEE JIRAUNGKOORSKUL, Ph.D., 200 pp.

The Short mackerel (*Rastrelligerbrachysoma*) is one of the most economically important and a mariculture candidate fish in Thailand. Nevertheless, it is plagued by reproductive problems that cause low production of gamete in the captivity. An understanding about the neuroendocrine system which involves with the reproductive activity of the wild and captive *R. brachysoma* is needed in order to clarify the situation. Based on their histological characteristics, the ovary of *R. brachysoma* is considered as an asynchronous developmental type. Oogenic cells was found in this type. These cells could be classified into six stages i.e. oogonium, chromatin nucleolar, perinucleolarnucleolar, lipid droplet and cortical alveolar, early vitellogenic, late vitellogenic and post vitellogenic stages. The testicular parenchyma of this fish species was a lobular organ, which is considered as an unrestricted spermatogonial type. Based on the pattern of chromatin condensation and other characterizations, the spermatogenetic stage could also be divided into six stages including primary spermatogonium, secondary spermatogonia, primary spermatocytes, secondary spermatocyte, spermatids and spermatozoa stages. The results revealed that a detailed anatomy and histological structure of the brain consisted of telencephalon, mesencephalon, diencephalon, metencephalon and myelencephalon. In female *R. brachysoma* brain, the distribution pattern of sbGnRH-immunoreactive neurons was structurally present in the nucleus preopticus-periventricularis in three areas including: nucleus periventricularis, nucleus preopticus and nucleus lateralistuberis. Additionally, the sbGnRH neuronal immunoreactive fibers protruded into the proximal par distalis where these cells positively reacted with GtHsimmunoreactivty (ir) (FSHβ – ir and LHβ – ir). The number of sbGnRH and GtHs in both number and mRNA level from the breeding season was significantly higher ($P<0.05$) than the fish from the non-breeding season. Only the mRNA level of the sbGnRH from the non-breeding season fish was significantly higher ($P<0.05$) than the fish from the breeding season. Moreover, the number and mRNA levels in all hormones (sbGnRH, FSHβ and LHβ) from the wild fish were significantly higher ($P<0.05$) than the cultured broodstock. In *R. brachysoma* male, the distribution of the sbGnRH-immunoreactive neurons and GtHs immnoreactivity in brain were similar to that of female fish. This study also suggested that the wild fish tended to have better reproductive system than hatchery fishes. This could be related to the endocrinological dysfunction and the reproductive failure in the hatchery condition.

Department:	Marine Science	Student's Signature	.....
Field of Study:	Marine Science	Advisor's Signature	.....
Academic Year:	2015	Co-Advisor's Signature	.....

ACKNOWLEDGEMENTS

I would like to express my sincere gratitude and deepest appreciation to my supervisor, Lect. Dr. Jes Kettratad, and my co-advisor, Assist. Prof. Dr. Wannee Jiraungkoorskul, for their guidance, encouragements, kindness and constructive comments. Both of them played an influential role in encouraging and stimulating activities at every phase in my laboratory work.

I am deeply indebted to my thesis committee members, Assoc. Prof. Dr. Voranop Viyakarn, Assoc. Prof. Dr. Charoen Nitithamyong, Assist. Prof. Dr. Sukanya Jaroenporn and Dr. Apichart Termvidchakorn, for their valuable suggestions and comments.

I would like to thanks Assist. Prof. Dr. Pisit Poolprasert, Ms. Ezra Mongkolchaichana, Assoc. Prof. Nittharatana Paphavasit, Dr. Watiporn Yenchum, Lect. Dr. Niwat Kangwanrangsan, Lect. Dr. Waristha Angsirijinda, Lect. Dr. Sansareeya Wangkulangkul, Assist. Prof. Dr. Sirichai Dharmvanij, Assoc. Prof. Dr. Sehanat Prasongsuk, Lect. Dr. Koraon Wongkamhaeng, Lect. Dr. Jirawat Saeton, Assoc. Prof. Dr. Chanpen ChanChao, and Lect. Dr. Natapot Warrit, for their helpful advice and valuable suggestions.

I would like to specially thanks Prof. Dr. Akio Shimizu and Prof. Dr. Masafumi Amano, for the donation of anti-sebremGnRH (sbGnRH), FSHβ and LHβ, Prof. Dr. Makito Kobayashi and Ms. Yuyu Kunimura, for their help on the antibody preparation and Dr. Thitiya Poonpet, for her advice on the investigation of the gene expression, Ms. Piyakorn Boonyong, Miss Jirapa Kumrak and Ms. Kanda Tongmitr, for their assistance to suggest in the immunohistochemical techniques.

I would also like to acknowledge Mr. Wicha Luengthong and his family, local fishermen at Samut Songkhram Province, Mr. Sasipong Tipdomrongpong and my colleage for specimen collecting.I would also like to thank Mr. Watcharapong Hongjamrassilp and Mr. Teeratas Kijpornyongpan, for accessing to several publications.

This research work was financially supported from The 100th Anniversary Chulalongkorn University Fund for Doctoral Scholarship.

Last but definitely not least, I am grateful to my parents and my sister for their support, understanding and patience.

CONTENTS

Page

Page

Page

Page

LIST OF TABLES

LIST OF FIGURES

Chapter I
INTRODUCTION

The short mackerel, *Rastrelliger brachysoma* (Bleeker, 1851) is one of the most important fishery resources of the Gulf of Thailand. Interestingly, the *R. brachysoma* culture project is set up in the Samut Sakhon Fisheries, Sumut Sakhon Province, Thailand. The goals of this project were to increase the number of fish population and to manage the fish in natural resources. This project was quite successful in terms of survival rate of the larvae. However, sexually matured fishes used in this project were obtained from the natural population. In captive breeding condition, broodstock caught from the wild population and maintained in the captive condition usually showed the endocrinological dysfunction preventing completion of the reproductive system such as reduction of gonadosomatic index (GSI) and decrease of germ cells in both quality and quantity. These changes may be influenced by the lacking of gonadotrophin releasing hormone (GnRH) that is synthesized and the released from the brain into the pituitary gland for the stimulation and releasing of Luteinizing hormone (LH) (Shiraishi et al., 2005). The lacking of this hormone was caused by the differences between the culturing condition and their natural environment. These differences lead to acute and chronic stresses on reproductive physiology of the fishes (Selvaraj et al., 2009, Zohar & Mylonas, 2001). To overcome this problem, various aquaculture techniques to increase the reproductive performance have been introduced, for examples, endocrine manipulative strategies, hormone priming, artificial fertilization, and production of recombinant fish gonadotropins. However, in order to optimize these manipulative procedures, a well understanding of basic knowledge of structure and regulation system

of the reproductive neuroendocrine mechanisms of the fish is needed. Unfortunately, such information is still unknown for *R. brachysoma*.

In this research, juvenile and sexually matured, *R. brachysoma* were caught from natural habitats in the Upper Gulf of Thailand. These fishes were mainly studied for the role of their neuroendocrine system during non-breeding and breeding seasons which is vital for understanding reproductive physiology in multiple spawned fishes. The study focused on the changes of the level, distribution and localization of the gonadotropin-releasing hormone–gonadotropin system (GnRH-GtH system) in the brain because GnRH-1 has been clearly demonstrated to play the master signaling neuroendocrine decapeptide and central regulator for controlling growth and reproductive hormones in scombrids (Selvaraj et al., 2012a, Selvaraj et al., 2012b, Selvaraj et al., 2009). Structure, chemical details and gametogenesis of gonadal tissue were also investigated by histology and histochemistry. Ultrastructure of gametogenesis was observed. Additionally, differences of mRNA GnRH and GtH levels between wild caught fish and hatchery fish was also investigated. This study provided the basic knowledge of the reproductive neuroendocrine mechanisms underlying juvenile and sexual maturity of the species. The knowledge gained by this study could potentially be applied to the maturation regulation and the spawning induction, which will improve the breeding aquaculture system. Moreover, an understanding of reproductive biology of *R. brachysoma* will serve as the scaffold for equipping scientific advice to fisheries management in the future.

Objectives

The objectives of this study are as follows:

1. To investigate structure, immunoreactivities and mRNA levels of the gonadotrophin releasing hormone–1–gonadotropin (luteinizing hormone, LH and follicle stimulating hormone, FSH) system (GnRH–1–GtH system) in the brain of juvenile and sexually matured, *Rastrelliger brachysoma* in the Upper Gulf of Thailand during breeding and non-breeding seasons

2. To study structural classification, chemical details and ultrastructure of germ cells of the juvenile and the sexually matured, *Rastrelliger brachysoma* in the Upper Gulf of Thailand

3. To compare the mRNA levels of GnRH–1–GtH system between wild caught *Rastrelliger brachysoma* and sexual matured *R. brachysoma* raised from hatchery

Chapter II
LITERATURE REVIEW

Biology of *Rastrelliger brachysoma* and study area

Taxonomy and morphology of the *R. brachysoma*

The short body mackerel belongs to Phylum Chordata, Class Actinopterygii, Order Perciformes, Family Scombridae, Subfamily Scombridae, Genus *Rastrelliger* and Species *Rastrelliger brachysoma* (Bleeker, 1851). The morphological features of this fish are as followed: body laterally compressed, dorsal fins spinous and the yellowish with a black edge. Pectoral and pelvic fins are dusky (Figure 2.1). Head depth is 3.7–5.2 times in fork length. Intestine is 1.4–3.6 times in fork length (FAO, 1999). The maximum fork length of this species is approximately 34.5 cm, but they are commonly found between 15 to 20 cm. The size at first maturity is about 13.4 cm total length and about 17.5 cm for the fully sexual matured fish (Department of Fisheries, 1965, Menasveta, 1980).

Distribution and habitat of the *R. brachysoma*

Rastrelliger brachysoma is an epipelagic fish commonly found in tropical and subtropical ocean along the coastal areas of the Central Indo-West Pacific Ocean from the Eastern Andaman Sea to Thailand, Indonesia, Papua New Guinea, Philippines, Solomon Islands, and Fiji (FAO, 1999, FAO, 2010).

Reproductive biology of the *R. brachysoma*

Current investigations on the spawning season and migration of *R. brachysoma* in the Gulf of Thailand are hypothesized as follows. The peak of reproductive season extended from September to November. During this time, the spawning ground is located near Samut Sakhon and Samut Songkhram Provinces (Figure 2.2*)*. I selected this area as our study area (Figure 2.3). After that, this fish migrates to two main spawning grounds located at Prachuap Khiri Khan, Chumporn and Surat Thani Provinces during January and March (Department of Fisheries, 1965, Menasveta, 1980) (Figure 2.2). The predicted spawning season of this species was determined mainly on GSI and external characterization of gonads (Sritakon, 2006, Sutthakorn, 1998). However, some histological studies reported that the increased GSI was due to testicular atrophy caused by fat accumulation in testicular tissue rather than normal testicular maturation. Moreover, histological evaluation on the fine scale structures of gametogenesis could be used as an accurate indicator of spawning based on the process of gametogenesis and gonadal development. It has a greater reliability in separating mature from immature individuals than the traditional macroscopic evaluations such as GSI (Tomkiewicz et al., 2003). In Thailand, *R. brachysoma* is considered as one of the most economically important fishery resource in the Gulf of Thailand. In 2009, 115,400 tons of *R. brachysoma* were caught. The catch from year 2009 was significantly less from those of approximately 143,500 tons from year 2005 to 2008. The depletion of *R. brachysoma* wild population may due to overfishing and deterioration of their natural habitat (Department of Fisheries, 2009). If the decrease still continues at this rate, *R. brachysoma* will be extinct from the Gulf of Thailand and food security will become

a major issue in the near future. *R. brachysoma* has therefore been considered as one of the potential marine fish species for aquaculture.

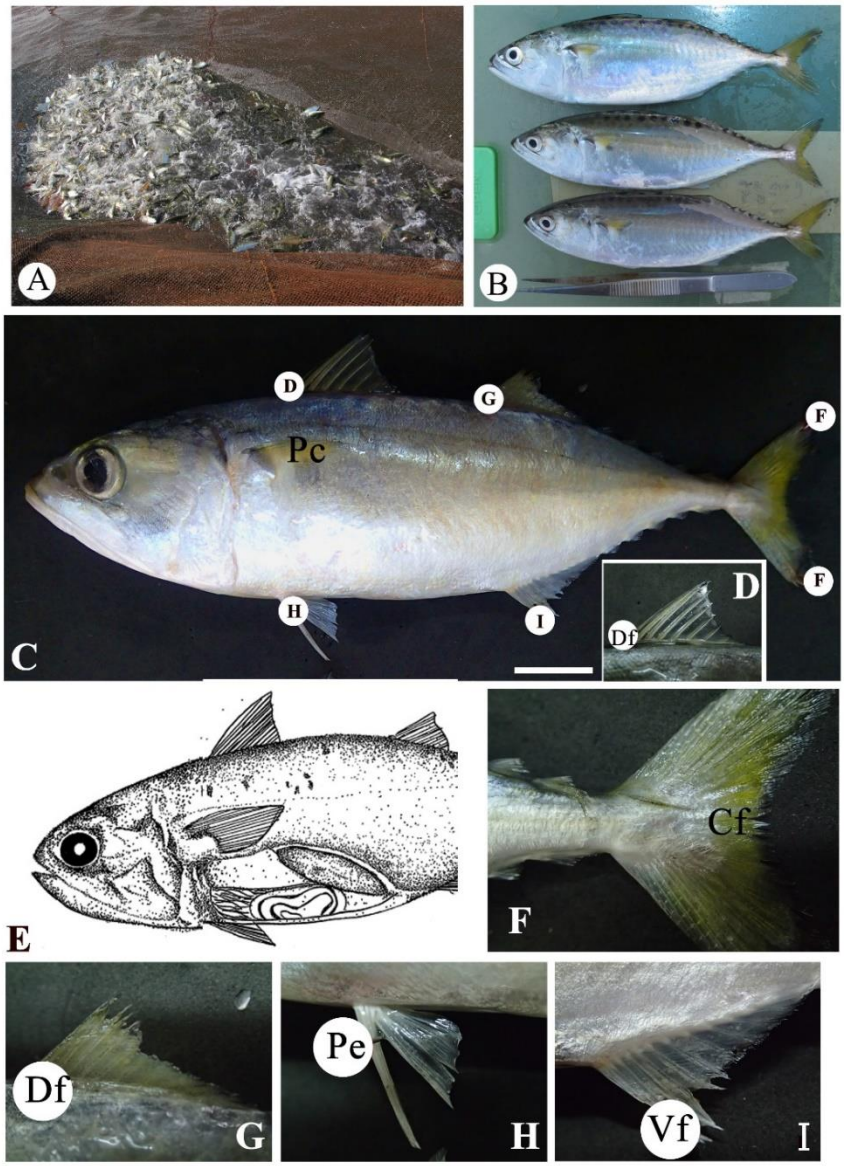

Figure 2.1 Wild *Rastrelliger brachysoma* captured from bamboo strake trap (A-C, F-I) and Drawing shows internal organ body plan of *R.brachysoma*, lateral view (E); Scale bar = 1 cm. *Cf = caudal fin, Df = dorsal fin, Pc = pectoral fin, Pe = pelvic fin, Vf = ventral fin.*

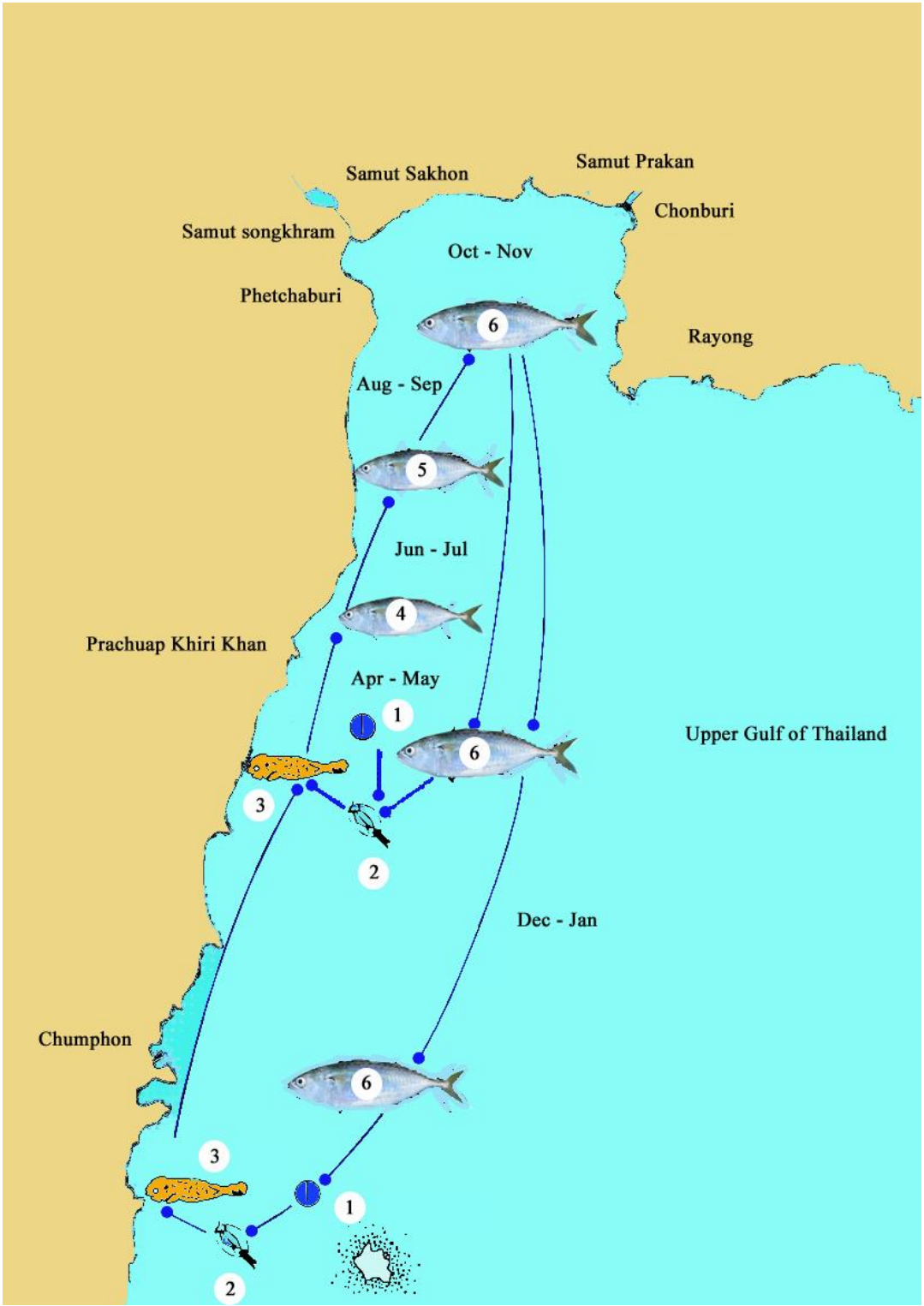

Figure 2.2 Life cycle of short mackerel, *Rastrelliger brachysoma* (1 = egg, 2 - 3= larval stage, 4 = juvenile, 5 = adult and 6 = sexual maturation) adapted from *(Department of Fisheries, 1965, Menasveta, 1980)*.

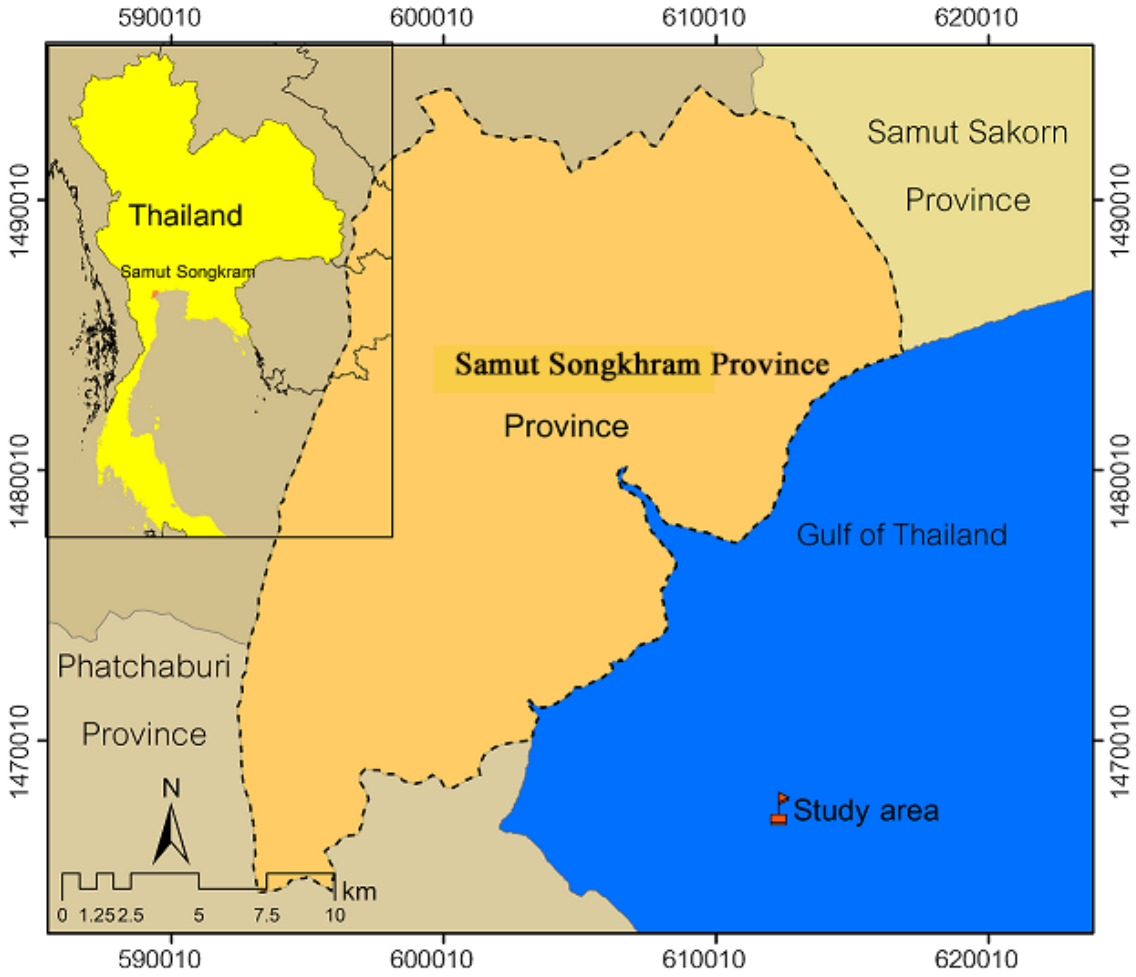

Figure 2.3 Map of the Samut Songkhram Province in the Upper Gulf of Thailand and the sampling locality (13°16'18.4" N, 100°02'13.4" E)

Aguacultural development of *Rastrelliger brachysoma*

The Samut Songkhram fishery research stations was set up for the breeding project of this fish (Figure 2.4). The goals of this project were to increase the number of fish in the wild and to optimize the fisheries management on the natural habitat for this species. Up until the late 2011, the first culture technique was quite successful, and could be considered as the first report for this species. However, success rate were slightly low and the brood stocks were collected from the wild (Personal communication). In captive breeding condition, brood stock that were caught from the

wild population usually showed the endocrinological dysfunction preventing the completion of the reproductive system, such as reduction of GSI, decrease of germ cells in both quality and quantity. These changes was responsible by the lacking of GnRH that is synthesized and released from the brain into pituitary gland because of the inappropriate environmental change could lead to acute and chronic stress in fishes (Selvaraj et al., 2009, Zohar & Mylonas, 2001). To overcome this problem, various aquaculture techniques to increase the reproductive performance have been introduced, for examples, endocrine manipulative strategies, hormone priming, artificial fertilization, and production of recombinant fish gonadotropins (Zohar & Mylonas, 2001). However, to optimize these manipulative procedures, well understanding of basic knowledge of structure and regulation system of the reproductive neuroendocrine mechanism of the fish is needed. Unfortunately, such information is still unknown in the *R. brachysoma*.

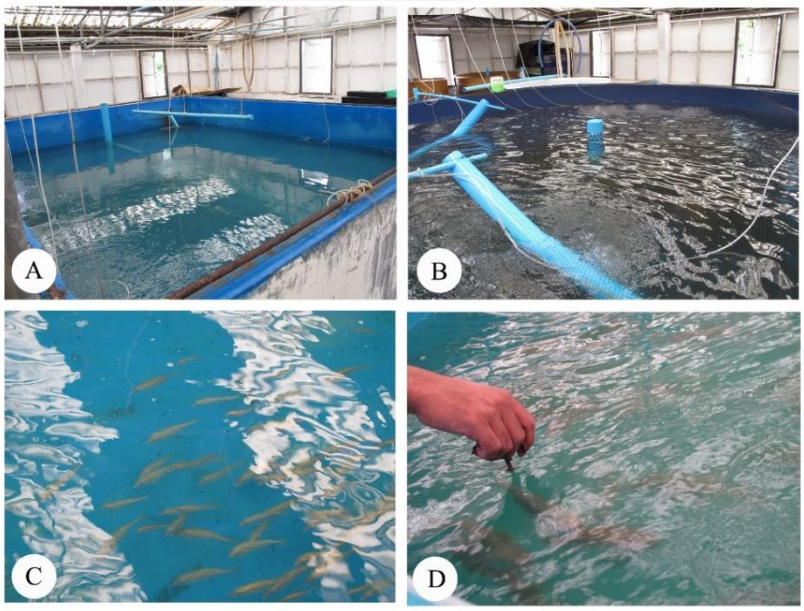

Figure 2.4 *Rastrelliger brachysoma* hatchery at the Samut Songkhram Fishery Research Stations, Samut Songkhram Province

Reproductive physiology of teleost fishes

The central nervous system neuroendocrine is a special mechanism responding to the environmental stimuli by perceiving and controlling the signaling pathway which results in the changes of endocrine system in teleost fish (Zohar et al., 2010). The environmental stimuli can be perceived by many specialized sense cells in the olfactory organ and eye that directly associated with GnRH neuronal system within the brain. These neuron fibers perceive and act in the signaling pathway to mediate and produce GnRH. The GnRH, a conserved amino-acid neuropeptide (pGlu-His-Trp-Ser-Tyr-Gly-Leu-Arg-Pro-Gly-NH2), acts as the master hormone that plays an important role as a neurotransmitter and a neuromodulator in the stimulation of the growth controlling and the reproduction of the fish (Zohar et al., 2010). Three GnRH isoform (GnRH-1, 2 and 3) in teleost fish species were classified based on primary structure or complementary DNAs (cDNAs), neuroanatomical distributions based on immunocytochemistry and *in situ* hybridization (Fernald & White, 1999). GnRH-2 and GnRH-3 expressed mainly in olfactory bulbs, midbrain tegmentum, ventral telencephalon, and preoptic area. They play an important role in reproductive behavior (Kauffman & Rissman, 2004, Volkoff & Peter, 1999). GnRH–1 is a hydrophysiotropic form and mainly expressed of neuronal population in the ventral surface of the forebrain, associated with the ventral telencephalon, preoptic area and hypothalamus. Therefore, only GnRH–1 fibers plays an important role in the reproduction of fish, especially in Scombridae i.e., *Scomber japonicas* (Selvaraj et al., 2009) (Figure 2.5). These neurons innervated into the pituitary gland and play a pivotal role in reproduction in all vertebrates by stimulating GtH secretion (González‐Martínez et al., 2001, Gothilf et al., 1997, Guilgur et al., 2006, Kah et al., 2007, Okubo & Nagahama, 2008, Palevitch et al., 2009).

Gonadotropins, (GtHs: GtH I (FSH-like) and GtH II (LH-like)) were produced by gonadotrops of the pituitary gland (Sherwood & Adams, 2005). Previous investigations have shown that GtH I gonadotrophs increased significantly in immature fish, whereas GtH II gonadotrophs later dominated in mature fish (Naito et al., 1991). Therefore, it has been suggested that GtH I and GtH II possessed different functions in fishes. GtH I contributed to early spermatogenesis and follicular growth, while GtH II encouraged the maturation of gametes and was induced in spermiation and ovulation (Planas et al., 1993, Tyler et al., 1991).

Due to the pathaway of sbGnRH and GtHs, it is possible that the changes of the cell size/cell numbers of the GnRH–gonadotropin–immunoreactivity (GnRH–GtH–ir) system in the brain may correlate with gonadal development and gonadal maturation. Report concerning about GnRH-GtH-ir is scanty; however, extensive investigation on the changes of GnRH–immunoreactivity (GnRH–ir) have shown the significant correlation between cell size/cell numbers in the brain and gonadal development in many fishes (Dellovade et al., 1995a, Dellovade et al., 1995b, Halpern‐Sebold et al., 1986). For examples, the change of GnRH cell number in preoptic area of the brain related to gonadogenesis in *Amphiprion melanopus* (Elofsson et al., 1997). Halpern‐Sebold et al. (1986) have also reported that a gradual change of preoptic area GnRH neuronal cells which positively correlated to cell number during the beginning of sexual maturation in *Xiphophorus maculatus*. Similarly, the preoptic GnRH cell number has been reported to correlation with the onset of gonadal maturation in *Porichthys notatus* (Grober et al., 1994).

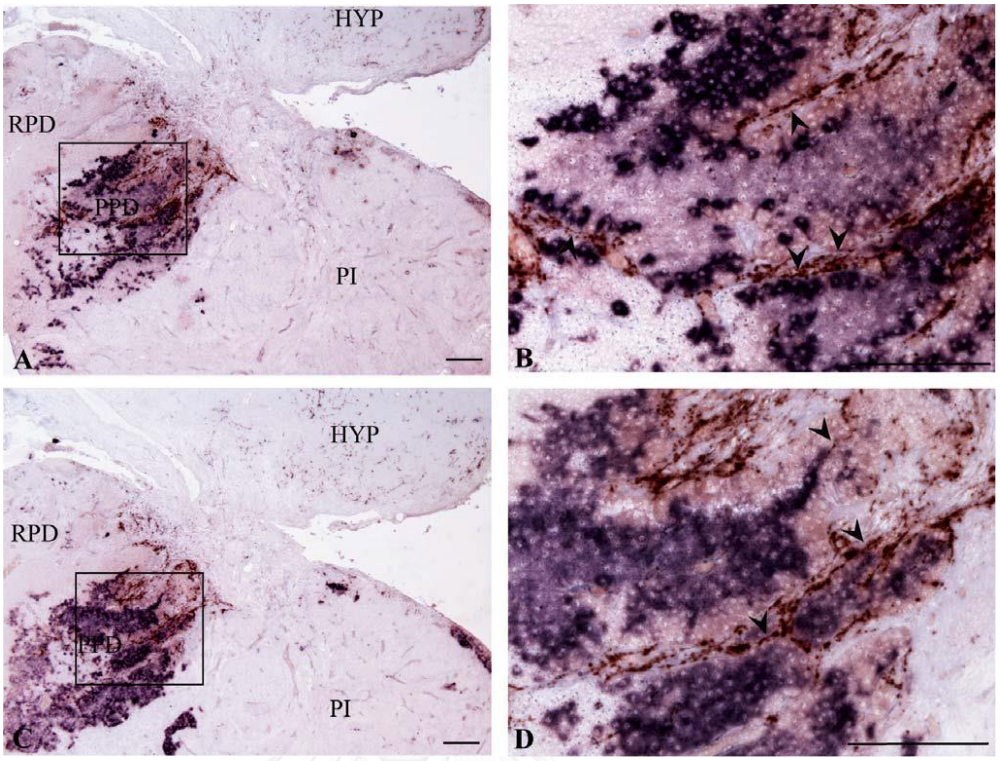

Figure 2.5 Colocalization of sbGnRH-ir fibers (brown) and gonadotrophs (blue) in sagittal sections of the pituitary. Low (A) and higher (B) magnifications of the localization of sbGnRH-ir fibers with adjacent the follicle stimulating hormone (FSH) cells. Low (C) and (D) high magnification of the localization of sbGnRH-ir fibers near luteinizing hormone (LH) cells. Scale bar: 100 µm. *HYP = hypothalamus, RPD = rostral pars distalis, PPD = proximal pars distalis, PI = pars intermedia (Selvaraj et al., 2009).*

Previous studies also found that the increasing of the activity of GnRH neuronal cells depends on the environmental factors such as photoperiod and water temperature (Andersson et al., 2001, Okuzawa et al., 2003). In the same way, the GnRH mRNA levels in brain of *Sparus auratus* was showed to significantly increased when the day length increased (Okuzawa et al., 2003).To detail, the initial of large mRNA product is originated from transcription inside the nucleus and then transferred into a precursor peptide called prepro-GnRH. It consists of prohormone and a signal peptide that allows the protein to be transferred to the endoplasmic reticulum and then to the Golgi apparatus. The final product is GnRH peptidegenic hormone (Zohar et al., 2010). The

GnRH mRNA levels were measured by radioimmunoassay (RIA), enzyme immunoassay (EIA) and high performance liquid chromatography (HPLC) but these technique are a summation of the synthesis, release and degradation of GnRH at a given point in development (Amano et al., 2004, Andersson et al., 2001). Therefore, it is necessary to confirm by real-time quantitative PCR to measure GnRH gene expression in the brain for each type of GnRH to clarify the function of GnRH in reproduction (Amano et al., 2004). Thus, it could be hypothesized that the parallel changes occur of GnRH neuronal system and GnRH mRNA levels using real-time quantitative PCR characterized the increasing of the expression during breeding season and gonadal maturation.

There has not been a study on the GnRH-Gonadal development system that links to the GtH-gonadal development system in Scombrid fishes. However, these two systems are highly linked in other fishes. Therefore, it is also possible that its development is related the expression of the GnRH-GtH system of the brain; however, it is not well understood. Previous investigations have reported that the possibilities of the gonadal development associated with the cluster of GtH (FSH and LH) expressing neurons in *Scomber japonicas* (Scombridae) (Nyuji et al., 2012b, Nyuji et al., 2011). Nyuji et al. (2011) showed that a cluster of FSH-ir increased rapidly from immature to the completion of vitellogenesis, whereas LH-ir was increasingly observed from the early vitellogenesis to the post-spawning. Similarly, testicular development in male *S. japonicas* was also correlated by the level of GtH-ir (Nyuji et al., 2012a). Therefore, an understanding of detailed histology and development of gonadal tissue is required before examining the correlation with GnRH-GtH activities. Recent results revealed that histological and ultrastructural techniques have been primarily used for the

investigation of scombrid reproductive systems such as *Thunnus japonicus* (Hara & Okiyama, 1998), *Istiophorus albican* (Mattei, 1991), *S. australasicus* (Hara & Okiyama, 1998) and *S. japonicas* (Hara & Okiyama, 1998). It is important to apply both techniques because the gonadal tissue at the cellular and organism levels provide not only detailing of its structure, but also the understanding of gonadal processes under neuroendocrine control. Therefore, histological and ultrastructural techniques will be used for the investigation of the gonadal structure and ultrastructural details in this fish.

Chapter III

OVARAIN HISTOLOGY AND ULTRASTRUCTURE IN SHORT MACKERAL *Rastrelliger brachysoma* (Bleeker, 1851) FROM SAMUT SONGKHRAM PROVINCE

Introduction

The short mackerel, *Rastrelliger brachysoma* (Bleeker, 1851) is the principal resource supporting a large industrial fishery and has considerable commercial value in Thailand. Current hypothesize reproductive scheme of the *R. brachysoma* in the Gulf of Thailand can be classified into three periods. The first period extends from January to March and the second period is from June to August. Both periods are in the vicinity of spawning groud of the Prachuap Khiri Khan and Surat Thani Provinces. The third reproductive season extends from October to November. The third reproductive season extends from October to November. The spawning ground in this period is in the vicinity of Samut Sakhon and Samut Songkram Provinces (Menasveta, 1980). This hypothesized reproductive scheme was based on the gonadosomatic index (GSI), the gross morphology and coloration of the ovarian tissue (Saidapur, 1978, Sritakon, 2006) . Nonetheless, the ovarian tissues in *R. brachysoma* have not yet been identified by their histological aspects. Using such techniques will give more accurate results and would increase the baseline knowledge of their reproductive development and reproductive cycle. However, note that only in ultrastructural study in teleost fish is possible to investigate the details of gametogenic processing at cellular and organelles levels (Grier, 2000). There have been many investigations of the oogenic ultrastructure in different aspects including concerning the development of oogenic stage (Abascal &

Medina, 2005), development of cytoplasmic organelles and follicular cells (Cruz-Landim & Cruz-Hofling, 2001).

Although, the scombroid species is composed of several high commercial values species for fisheries, it has rarely been selected for examination. Only one Scombroid (*T. thymus*) has been described in oogenesis (Abascal & Medina, 2005). It is necessary not only to provide understanding of the basic ultrastructural pattern and developmental processing including oogenesis, steroidogenesis and vitellogenesis in this family but also to apply for possible applications in aquaculture. In this article was primarily attempted to identify the ovarian structure, ultrasture and reproductive mode of *R. brachysoma* during its annual reproductive season using histological and histochemical analyses. Surely, our information novel provided and could be also vital for the provision of scientific advice to aquaculture development, which can help to increase the natural population of this species.

Materials and methods

Fish collection

Adult short mackerel, *Rastrelliger brachysoma* with a standard body length about 15-19 cm (average 16.5±0.49 cm) and total weight about (68.68±0.67 g) were were considered as late – development stage of the ovarian histology. They were obtained by bamboo strake trap during non-breeding (October to November 2013, n = 30) and breeding seasons (January to February 2014, n = 30) from the area of Samut Songkhram Province in the Upper Gulf of Thailand (13°16’18.4” N, 100°02’13.4” E). The identification of all fish was according to the taxonomic key of FAO (FAO, 2010). Fish were euthanized by rapidly cooling shock (Wilson et al., 2009).

Light microscopic observation

The ovarian tissue was fixed in Davidson's fixative and then they were processed using standard histological techniques. The gonadal paraffin block was cut at 5 µm thickness and stained with Harris's hematoxylin and eosin (H&E) and Masson's trichrome (MT), periodic acid-schiff (PAS), germ positive (GMS), alcian blue pH 2.5 (AB) and reticulin (Rt) methods, as followed from Bancroft & Gamble (2008), Puchtler & Waldrop (1978), Vidal (1988). Additionally, frozen tissues were cut at 10 µm thicknesses and stained with oil red O (ORO) (modified from Culling (2013)). The ovarian structure, ultrastructure and oogenesis with size measurement was assessed as to detail according to the guidelines of Dietrich & Krieger (2009) and Brown-Peterson et al. (2011) under light microscope. Additionally, it was microscopically examined to assess the histological stage of the atretic follicles according to the guidelines of Ganias et al. (2003).

Ultrastructural observation

Small pieces of ovarian tissue were cut and rapidly pre-fixed in 2.5% glutaraldehyde in 0.1 M phosphate buffer, pH 7.4 at 4 °C and washed in the buffer fixative solution. Thereafter, they were post-fixed with 1% osmium tetraoxide (OsO_4) and then they were processed using standard ultrastructural techniques. The thin sections were cut by ultramicrotome about 90 nm thicknesses, stained with uranyl acetate and lead citrate. Lastly, the ultrathin sections were observed and photographed using a JEM-2100 at 200kV.

Results

Anatomy, histology and histochemistry of *R. brachysoma*

Based on anatomical analysis, the asymmetrical elongation of *R. brachysoma* ovaries were paired organs located in the abdominal cavity (Figures 3.1A-3.2C). Cross sections of the immature ovary in non-breeding season were histologically surrounded by tunica albuginea including a thick layer of connective tissue and numerous blood vessels (Figures 3.2a-3.2c). They were suspended by mesovarium from the peritoneal dorsal wall. Overall histological sections in both immature and mature ovaries revealed that the ovigerous fold protruded into a central lumen where it could be distinguished into two compartments: (i) a germinal compartment which was covered with the ovigerous fold. The ovigerous fold was composed of epithelial cells and oogonia. (ii) A stromal compartment which contained the different of oogenic stages. The ovary in this species was described to be an asynchronous developmental type, which was distinctly classified into seven stages based on the cell size, histological features of each developing oocyte and staining properties are given as follows (Figures 3.2 and 3.3).

Oogonium, the smallest among oogenic cells, were located and scattered within the somatic epithelial cells in the germinal epithelium. It was oval-rounded cell about 25-30 μm in diameter. This cell contained a spherical nucleus (18-20 μm in diameter) with a prominent nucleolus about 3-4 μm in diameter. Its cytoplasm was stained, slight blue by H&E. It was noted that the oogonium was attached within clusters or oogonial cysts inside the ovigerous fold. Each oogonium was surrounded by a few squamous-shaped prefollicular cells (Figures 6.3a, 6.3h).

Chromatin nucleolar stage oocyte significantly increased in size (30-40 μm). The nucleus of oocytes (15-20 μm) was a weakly basophilic nucleoplasm showing a

spherical form and enlarged in size. Single and large spherical nucleoli were present. The ooplasm had a thin layer of progressively basophilic cytoplasm. Their follicle cells form squamous cells layer which completely surrounded the oocyte (Figures 3.3b, 3.3h).

Perinucleolar stage oocyte was 80-100 µm in diameter. The nucleus, about 50 µm in diameter was in the central area. Multiple nucleoli at 5-8 µm in diameter were spherical shape and arranged around the nuclear membrane. Balbiani's bodies were first present around the periphery. There was a slight decrease basophilic property of the ooplasm. Then, the circumnuclear ring was seen during the oocyte under light microscope. The follicle cells were elongated and flat around the oocyte (Figures 3.3c, 3.3i).

Oil droplets and cortical alveolar stage oocyte were large. They attained the size of 150-180 µm in diameter. Multiple nucleoli at the periphery of nuclear membrane progressively decreased in size (about 3-4 µm). At first appearance, spherical oil droplets were seen primarily encircling the nucleus. Their sizes were 10 µm in diameter. Later, oval cortical alveoli appeared with clear content as the vesicle. At the end, oil droplets and cortical alveoli increased in both numbers and size throughout the ooplasm as basophilic area. During the stage, the zona pellucida as an acidophilic acellular layer was first detected. The layer of simple granulose cells and theca cells were similar to what was seen in the previous stage (Figures 3.3d, 3.3j).

Early vitellogenesis stage oocyte was characterized by an increase in cell size to about 250-320 µm in diameter and decrease of basophilia cell. The beginning of ooplasm of the oocyte filled the numerous small yolk granules. The oil droplets increased in size and began to migrate throughout of the ooplasm. Numerous cortical

alveoli were still detected in increasing amounts. The follicular complex of this oocyte consisted of three well-developed layers: zona pellucida, granulosa cell and theca cell. The zona pellucida was 20 µm thick. It was thicker tha tthe previous stage. It was distinctly striated and strongly positive with eosin. In this stage, the layer of granulosa cell underwent morphological change in shape from squamous into low columnar epithelium. Basement membrane and theca cells were seen (Figures 3.3e, 3.3k, 3.3o).

Late vitellogenesis stage oocyte was 280-350 µm in diameter. It displayed reddish-stain with acidophilic according to the most accumulation of yolk deposition (10-15 µm). In the periphery of the ooplasm was filled by lipid globules and a few cortical alveoli (around 15-18 µm in diameter). Irregular and eccentric nucleus appeared to move near the animal pole. Later, the micropyle in an oocyte was well-developed and occurred in the zona pellucida. The zona pellucida was also presented as thick and striated. In addition, its zona pellucida can be separated into two layers; a thick internal layer and a thin external layer. The layers of granulosa and theca cells were similar to those described in the previous stage (Figures 3.3f, 3.3l, 3.3p).

Post vitellogenesis stage oocyte or maturating oocyte was the largest in size (320-370 µm diameters) among oogenic stage because the yolk granules of oocyte were not completely fused as homogenous material. An enlarged yolk granules were were also present at this stage. The nucleus was not visible at this stage. A few lipid droplets and cortical alveoli were rarely observed at the periphery of the ooplasm. Follicular complex was slightly flattened under histological changes, but zona pellicida can be distinctly classified into two layers: the outer layer was located near granulosa cells, whereas the inner layer was exhibited near the oocyte surface (Figures 3.3g, 3.3m, 3.3q).

Protein

Histochemistry of the ovarian tissue revealed that numerous cortical alveolar were positively stained to MT as bluish and PAS as pinkish. This indicated that the presence of a glycoprotein. Also, it slightly stained with AB as bluish, indicating the presence of carbohydrate or acid mucopolysaccharide (Figures 3.3-3.4). Another inclusion, yolk granules in the vitellogeneic stage also strongly stained to MT as reddish and slightly stained with PAS reactions (Figures 3.3n, 3.3b, 3.3e). The zona pellucida also strongly showed PAS-slight reaction during lipid droplet and cortical alveolar stage throughout the post vitellogenic stage, indicating the presence of the protein (Figures 3.3a-3.3c). Surprisingly, in the post vitellogenic stage showed that the inner zona pellucida was exclusively seen than the outer zona pellucida (Figure 3.3d).

Lipids

Lipid droplet and cortical alveolar stage, the most intense ORO reaction positively appeared in the lipid droplets. It first appeared near nuclear membrane and then, it distributed along the mid and peripheral regions. This distribution can be found throughout the post vitellogenic stage (Figures 3.3e-3.4h). Furthermore, MT, PAS and AB negatively stained as empty vesicles (Figures 3.3 and 3.4).

Fiber composition

MT staining was positive at the connective tissue with covering epithelial cells that separated the two compartments of the ovary. Additionally, the positively reticulin stained cell located at the basement membrane of the active germinal epithelium. This germinal epithelium included the separation between the germinal epithelium and the

ovigerous fold from the stromal compartment (Figure 3.5a) and the separation between the granulosa cells and the thecal cell layers (Figures 3.5e-3.5f). Moreover, oogonia within the cell nest were also separated from the ovigerous fold by the same basement membrane (Figures 3.5b-3.5c). Based on the Masson's trichrome (MT) and reticulin (Rt) stain, the reticulated fiber was found in the connective tissue that formed compartmentalization.

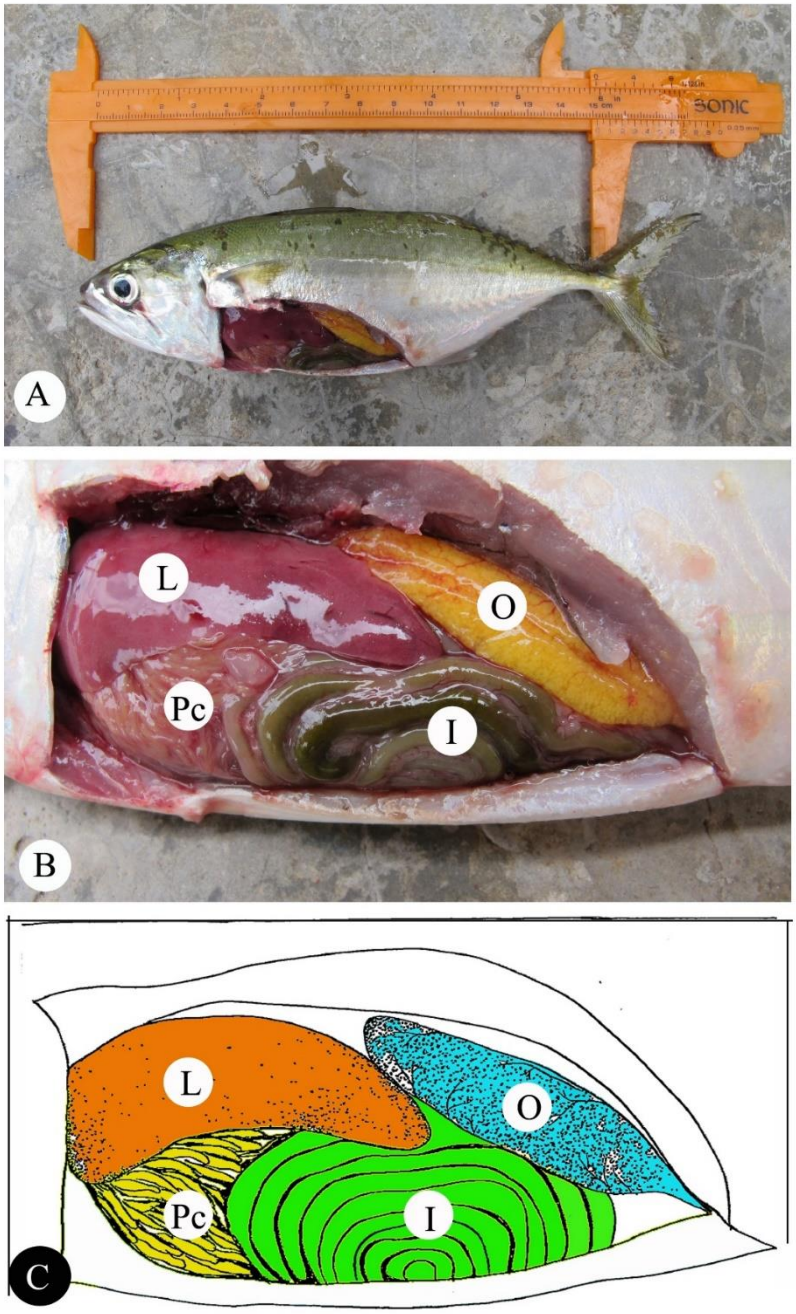

Figure 3.1 Gross antomy of ovarian tissue (O) of *Rastrelliger brachysoma*. Scale bar: 1 cm. *I = intestine, L = liver, Pc = pyloric cacae.*

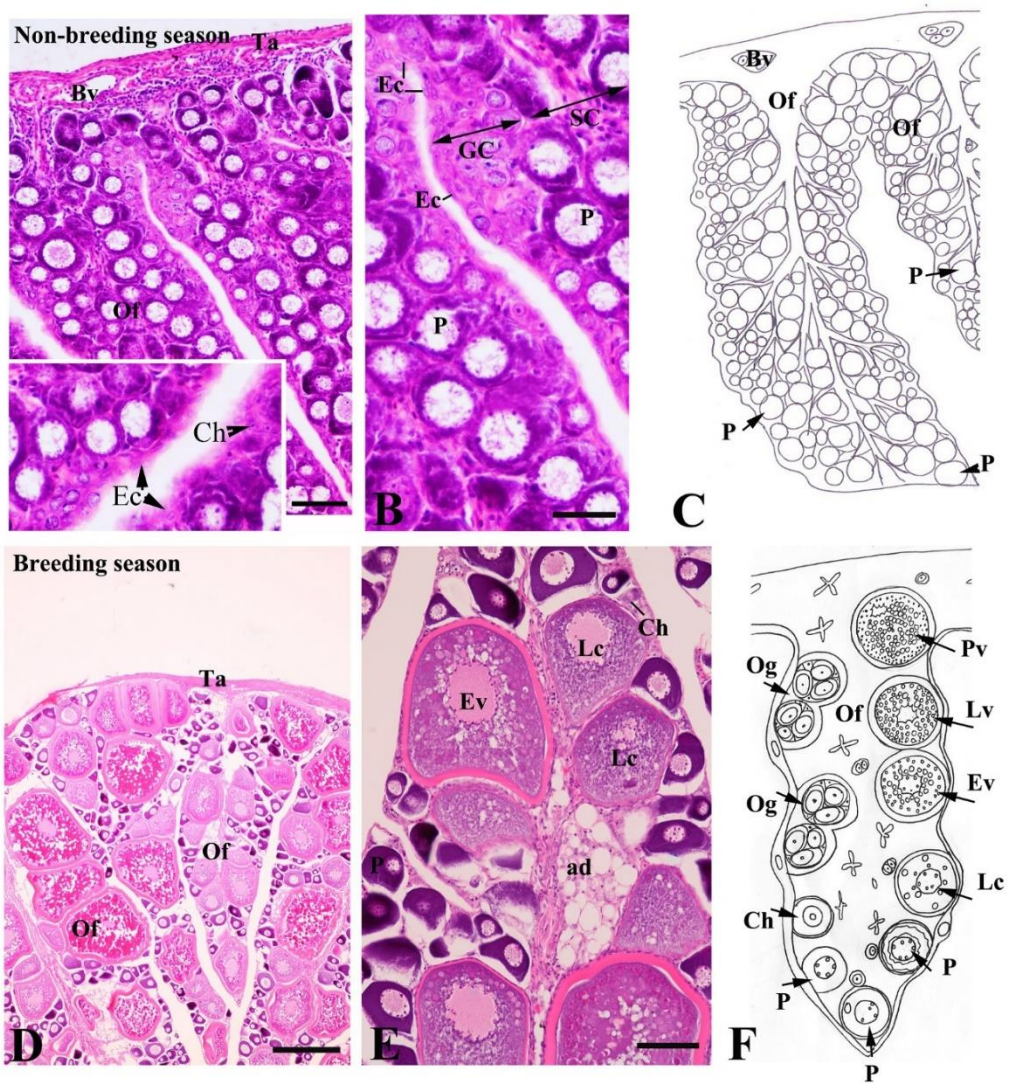

Figure 3.2 Light photomicrograph (a, b, c, e, f) and schematic summary of ovarian structure (d, g) of *Rastrelliger brachysoma*. Scale bar: 100 µm (a, c, f), 200 µm (e). *ad = adipose tissue, Bv = blood vessel, Ch = chromatin nucleolar stage, Ec = epithelium cells, Ev = early vitellogenic stage, GC = germinal compartment, Lc = lipid and cortical alveoli stage, Lv = late vitellogenic stage, Of = ovigerous fold, Og = oognia, P = perinucleolar stage, Pv = post vitellogenic stage, SC = stromal compartment, Ta = tunica albuginea.*

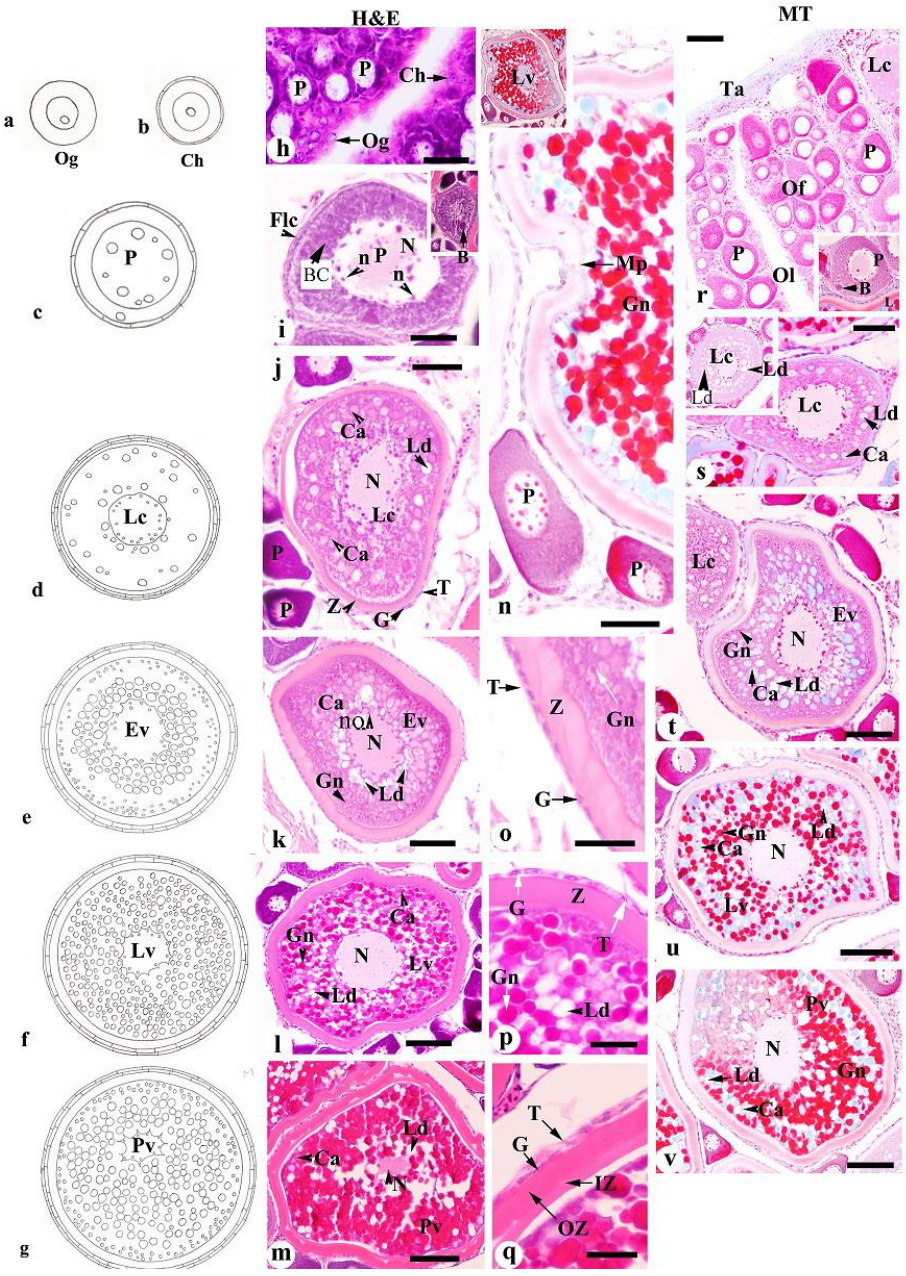

Figure 3.3 Schematic summary (a-g) and light photomicrograph (h-v) of oogenesis of *Rastelliger brachysoma*. h-m, o-q based on H&E and n, r-v based on MT. Scale bar 100 µm (i-v), 20 µm (h)**.** *B = Balbiani's bodies, Bc = circumnuclear ring, Ca = cortical alveoli, Ch = chromatin nucleolar stage, Ev = early vitellogenic stage, Flc = follicular complex, G = granulosa cells, Gn = yolk granules, IZ = inner zona pellucida, Lc = lipid and cortical alveoli stage, Ld = lipid droplets, Lv = late vitellogenic stage, Mp = micropyle, N = nucleus, no = nucleolus, Of = ovigerous fold, Og = oognia, OI = ovigerous lamellae, OZ = outer zona pellucida, P = perinucleolar stage, Pv = post vitellogenic stage, T = theca cell, Ta = tunica albuginea, Z = zona pellucida.*

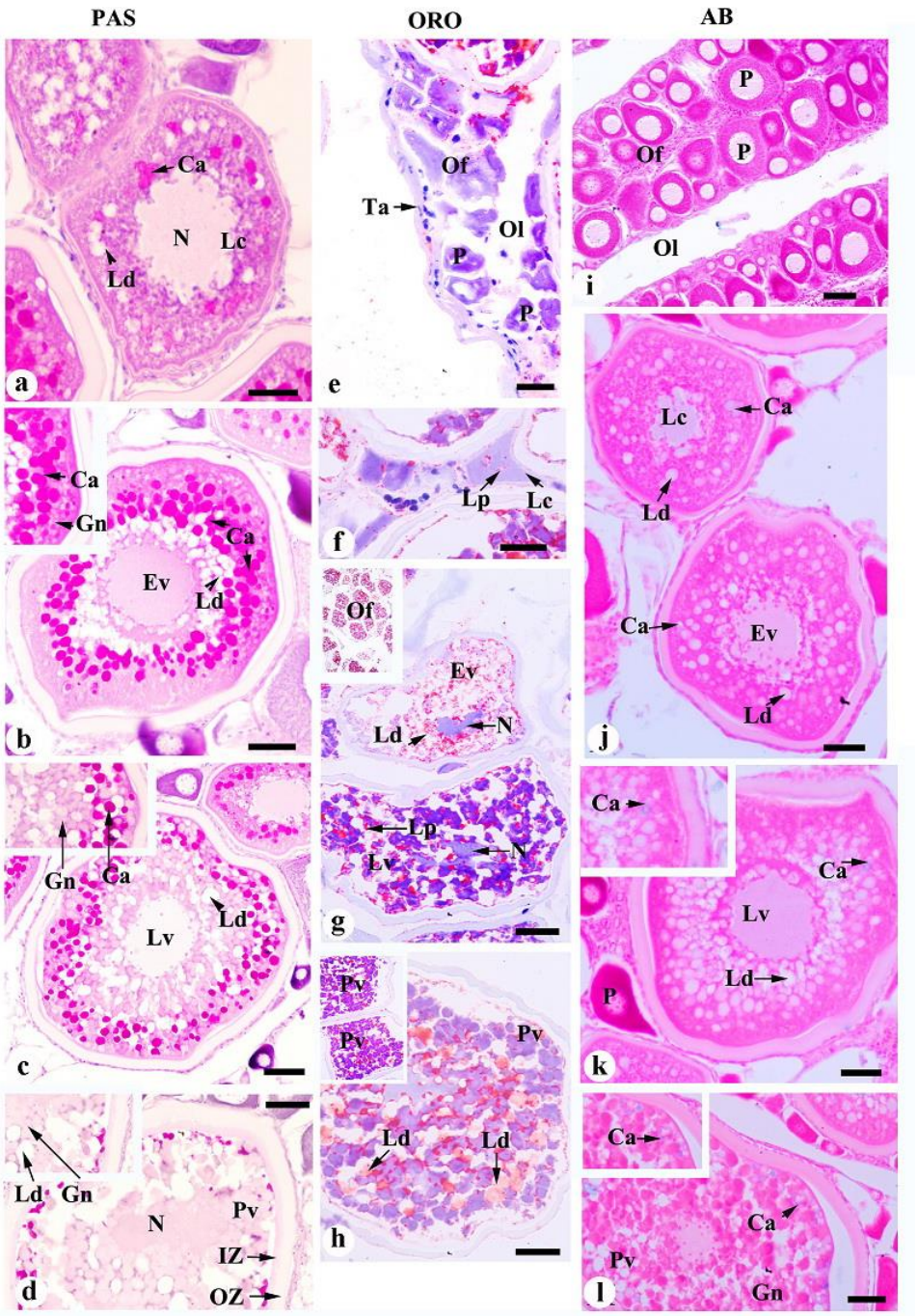

Figure 3.4 Light photomicrograph of oogenesis of *Rastrelliger brachysoma*. a-d based on PAS, e-h based on ORO and i-l based on AB. Scale bar: 40 µm (a-d, f-h, j-l), 100 µm (e, i). *Ca = cortical alveoli, Ev = early vitellogenic stage, Gn = yolk granules, IZ = inner zona pellucida, Lc = lipid and cortical alveoli stage, Ld = lipid droplets, Lv = late vitellogenic stage, N = nucleus, O = ovary, Of = ovigerous fold, Ol = oviferous lamellae, OZ = outer zona pellucida, P = perinucleolar stage, Pv = post vitellogenic stage, Ta = tunica albuginea.*

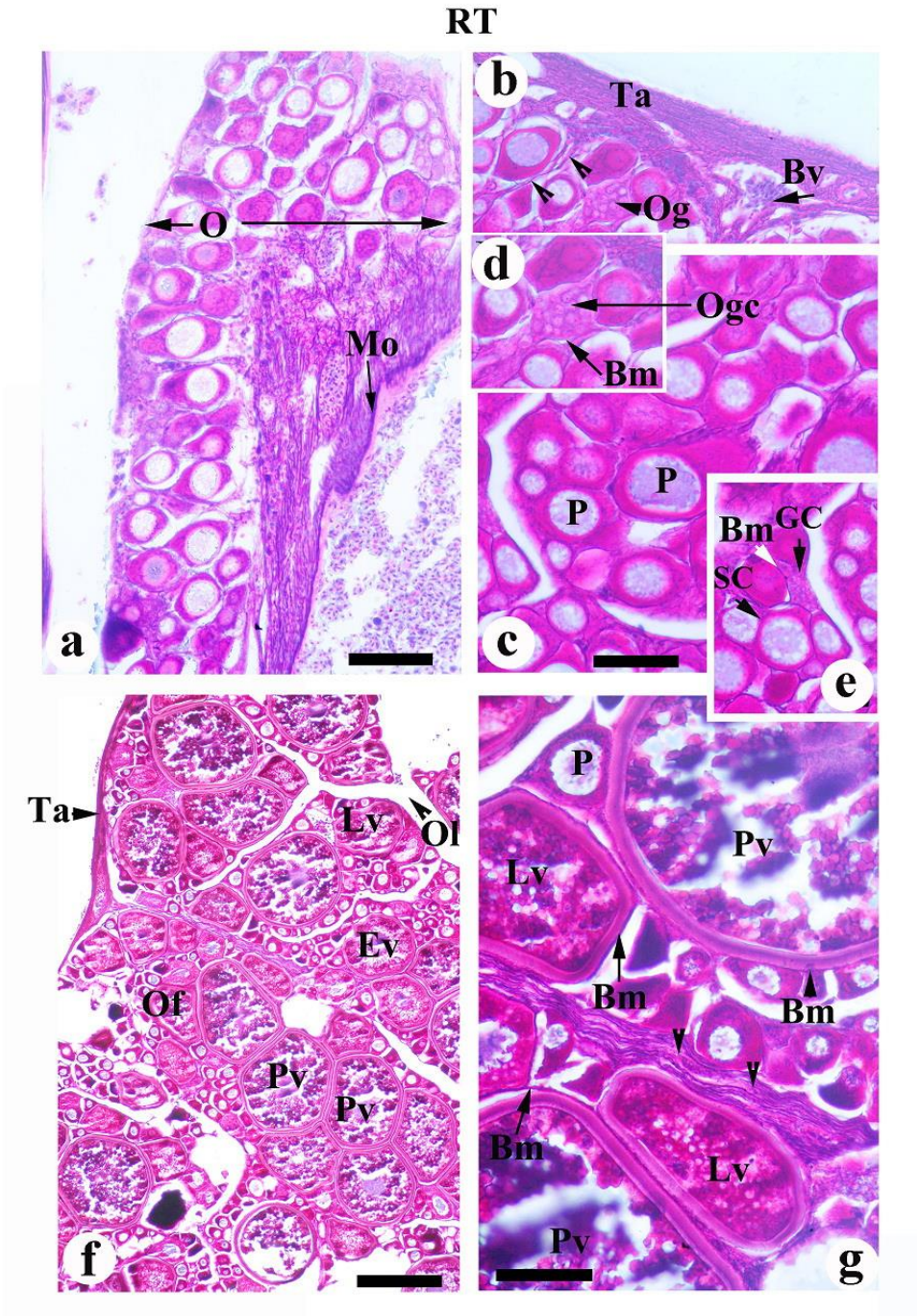

Figure 3.5 Light photomicrograph of ovarian structure (O) and oogenesis of *Rastrelliger brachysoma*. a-g based on RT. Scale bar: 100 µm (a, c, g), 200 µm (f). *Bm = basement membrane, head arrow = Elastic fiber, Bv = blood vessel, Ev = early vitellogenic stage, GC = germinal compartment, Lv = late vitellogenic stage, Mo = mesovarium, Of = ovigerous fold, Og = oognia, Ogc = oogonia cyste, Ol = oviferous lamellae, P = perinucleolar stage, Pv = post vitellogenic stage, SC = stromal compartment, Ta = tunica albuginea.*

Histology and histochemistry of atretic follicle in *R. brachysoma*

The gross anatomy of ovaries in the *R. brachysoma* during the breeding season had paired and elongated structures showing yellow color (before fixation) and white color (after fixation) within the peritoneal cavity (Figures 3.6A and 3.6B). At the light microscopic level, the analysis of ovaries of *R. brachysoma* obviously exhibited during breeding season as containing the differential stages of oocyte because it was considered as asynchronous developmental oocytes according to MT staining (Figures 3.6C to 3.6D). In this study, it could be classified into two phases based on size, histological structure and staining properties as follows:

Phase I the classification of the atretic follicle during previtellogenic stage

The characterization of atretic follicle in the previtellogenic stage was similarly seen with normal stage, but the ooplasm shown as basophilic cytoplasm with a surrounding thin follicular layer (PAS staining) (Figures 3.7Aand 3.7B).

Phase II the classification stage of the atretic follicles during vitellogenic stage

In general, the characterization of normal vitellogenic stage based on histology and histochemistry was 250-300 μm in diameter with numerous small yolk granules. Among its yolk granules, the oil droplets and cortical alveoli were distinctly detected. Also, this stage was surrounded by follicular complex which was clearly divided into three well-developed layers: (i) zona pellucida composing of two layers; inner and outer zona pellucida, (ii) granulosa and (iii) theca cells, respectively. Among normal vitellogenic stage, histological details of several atretic follicles during vitellogenic stage in this species were detected. It could be completely divided into four steps

according to shape, characterizations of nucleus and follicle complex (Figures 3.7D to 3.7I).

Stage I, the histological appearance in this stage was quite similar to that of normal vitellogenic stage, but some microstructures were initially seen including nucleic disintegration with irregular shapes. Some areas of yolk granules were digested, especially in the periphery of the ooplasm. Irregularity in shape and degeneration with separation between inner and outer layers of the zona pellucida were initially and continuously detected. Additionally, hypertrophies together with pyknosis of some granulosa and theca cells were detected (Figures 3.7C and 3.7K). Based on histochemistry, the cortical alveoli were still positive with MT as reddish and AB as bluish. Other characterizations, yolk granules with slight positively stain with PAS reaction, were specially surrounded by basement membrane (black line with RT) (Figures 3.7L to 3.7O).

Stage II, the early stage of stage II was irregular in shape. A sequence of event characterization as follows: the degradation and regression of yolk granules in some area located in the peripheral ooplasm were detected more than in the previous stage, as indicated by the fusing granules. According to H&E, the inner zona pellucida became broken down and fragmented from the degenerating of oocyte, whereas the outer zonapellucida increased highly, containing several fragments as well as islets greater than the inner zonapellucida. The hypertrophy of granulosa cells were also continuously proliferated, which each cell had a spherical nucleus with surrounding the eosinophilic cytoplasm. Externally, the thecal cell layer was located around few blood vessels (Figures 3.7J and 3.7P). AB, MT and PAS reactions conformed to previous stage but

RT reaction distinctly showed the degeneration due to the fragment of basement membrane (Figures 3.7Q to 3.7T).

Stage III, the disorganizations both irregular in shape and shrinkage were obviously seen when compared with the prior stage. The nucleus in this stage was seen and slightly observed in some oocytes among the degeneration and digestion of yolk granules. The highly increasing fragmentations of zona pellucida gradually continued more than in the previous stage. Exclusively, it was also confirmed that inner layers of zonapellucida were first degenerated and continuously observed in its outer layer. The granulosa and theca were not separated and rarely seen. Surprisingly, in this stage, the leucocytes were mostly found and continued to be found near oocyte (Figures 3.7U and 3.7V). Histochemically, the cortical alveoli were slightly seen and began to degenerate (AB and MT stains) whereas RT reaction confirmed that no basement membrane was seen during this stage (Figures 3.7W to 3.7Z).

Stage IV, the cell size was intermediately decreased when compared to former stage. Unlike the previous stage, the zona pellucida was greatly degenerated among liquefaction of yolk granules. During reabsorption, some area in the ooplasm was shown to contain the vacuoles, referred as empty space. Then, the follicular cells became phagocytize degenerating materials because several leucocytes were presented among a few blood vessels (Figures 3.7Z1 and 3.7a). No mucopolysaccharide was observed according to AB and MT, indicating the complete degeneration of cortical alveoli (Figures 3.7b and 3.7e).

Stage V follicle was an amoeboid-shape and decreased in size. The follicle (both yolk granules and zona pellucida) itself was completely digested. The large vacuole associated with yellow-brownish pigments within the ooplasm was accumulated

(Figures 3.7Z2 and 3.7f). Some follicular cells were also presented. Moreover, this stage was surrounded by fibroblast-like cells, as strongly positive with MT and PAS stained (Figures 3.7g and 3.7h). It should be noted that this stage could potentially cause by the apoptosis under RT reaction (Figure 3.7j). The leucocytes were found around the apoptotic follicles (based on RT stained).

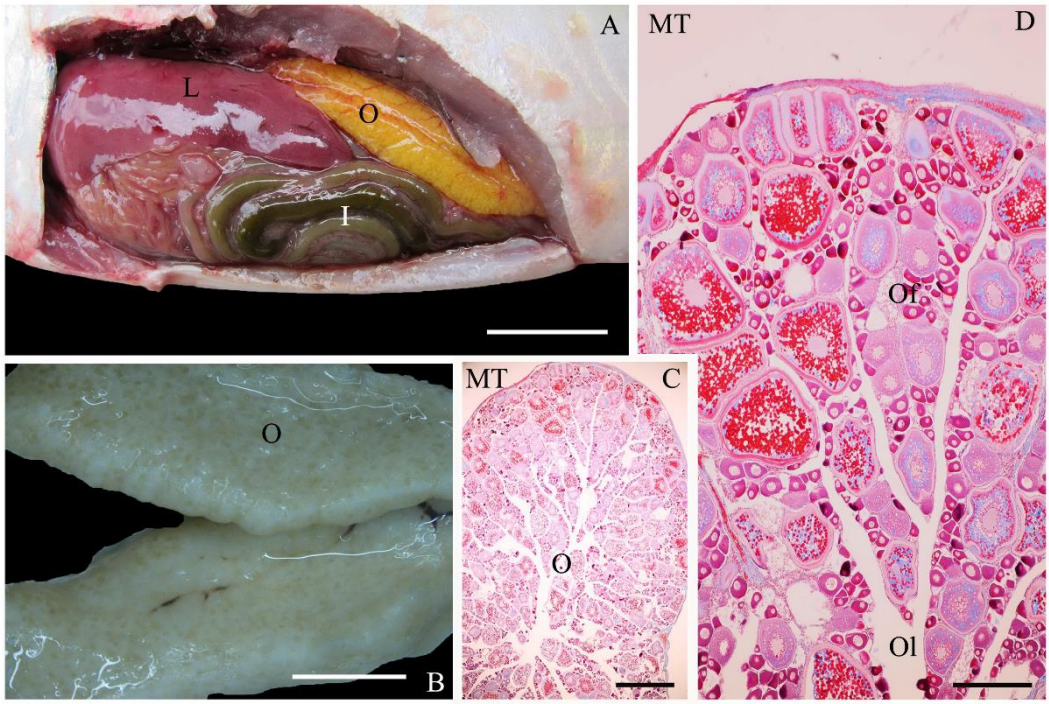

Figure 3.6 Micrograph of gross anatomy and histology of ovaries in *Rastrelliger brachysoma* during breeding season; (A) ovarian morphology (pre-fixation) = 1 cm; (B) ovarian morphology (post-fixation) = 1 cm; (C-D) ovarian histology = 200 µm. *I = intestine, L = liver, O = ovarain tissue, Of = ovigerous fold; Ol = ovarian lumen. (MT = Masson's trichrome stain)*

.

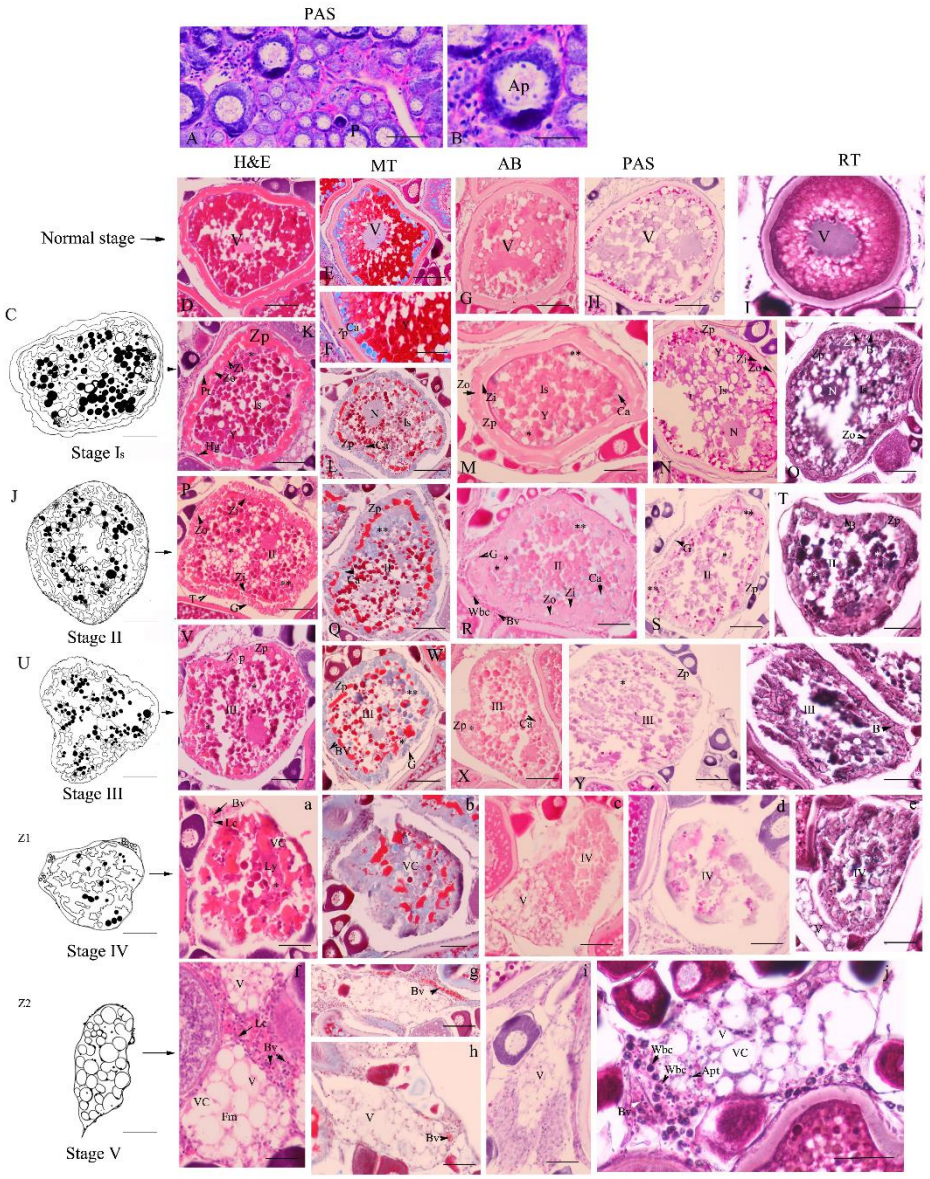

Figure 3.7 Schematic diagram, micrograph of histology and histochemistry of atretic follicles in *Rastrelliger brachysoma*; (A-B) atretic follicle of previtellogenic stage (Ap), A = 100 µm, B = 50 µm; (D-I) Normal vitellogenic stage (V) = 70 µm; (C, K-O) Stage Is = 50 µm; (J, P-T) Stage II = 50 µm; (U-Z) Stage III = 50 µm; (Z1, a-e) Stage IV = 50 µm; (Z2, f-j) Stage V = 50 µm; *Apt = apoptosis, B = basement membrane, Bv = blood vessel, Ca = Cortical alveoli, G = granulosa cell, Hg = hypertrophy of granulosa cell, Lc = lymphocytes, Ly = liquefaction of yolk granules, N = nucleus, P = previtellogenic stage, Pt = pynotic nuclei, T = theca cell, VC = vacuole, Wbc = white blood cells, Y = yolk granules, Zi = inner layer of zonapellucida, Zo = outer layer of zonapellucida, Zp = zonapellucida, * = degeneration of yolk granule, ** = degeneration of cortical alveoli.(MT = Masson's trichrome, PAS = periodic acid-schiff, AB = aniline blue, Rt = reticulin method).*

Morphology and histology of reproductive oviduct

The gross anatomy of the oviduct of *R. brachysoma* had two lateral parts: left and right oviducts. Each oviduct, a thin and tubular organ was connected with the ovary in the dorsal part before joined into the genital duct and cloaca in the ventral part (Figure 3.8). This anatomical structure agreed with previous reports of Dietrich & Krieger (2009) and Selman & Wallace (1989), who discussed the oviduct in some teleost fish. However, it could be not classified into four major regions: oviduct, nidamentary gland, uterus and vagina, which are principally found in *Dasyatis bleekeri* (Chatchavalvanich & Visattipat, 1997). The significance of the uterus and vagina in the oviduct has not only been shown in chondrichthyes (Dodd, 1983), but also in lizards, including *Crotaphytus collaris* and *Eumeces obsoletus* (Guillette et al., 1989). At light microscopic level in both section and semithin section, the basic histological organization was similarly shown along the oviduct. There were four layers, including tunica mucosa, tunica submucosa, tunica muscularis and tunica serosa layers that were shown in the oviductal wall (Figure 3.9A-3.9B, 3.9G-3.9H). These results were similar to those described in several fish including *A. alburnus* (Lahnsteiner et al., 1997), *R. lentiginosus* (Hamlett et al., 1998) and *X. maculatus* (Potter & Kramer, 2000).

The mucosal layer as well as the innermost layer was composed of a few longitudinal folds, referred to as fimbriae. Folds were branched to different degrees, becoming primary and secondary folds. Also, this mucosal layer was composed of two sub-layers: epithelial layer and lamina propria. High magnification of a section of the epithelial layer showed it was covered by low simple columnar epithelium. This presence of oviduct structure was similarly reported in another fish, *A. alburnus* (Lahnsteiner et al., 1997). Moreover, three different cell types with different heights

were identified, including ciliated epithelial, mucous secretory and basal cells (Figures 3.9C-3.9D). The first cell type, the most abundant of the ciliated epithelial cells, was the elongated cell containing cilia. A prominent nucleus was basophilic stain and surrounded by eosinophilic cytoplasm. However, its function and mechanism is unknown. The second cell type, the mucous secretory cell, was located among the epithelial cell, but unlike epithelial cell because it was positively detected in the AB and PAS reactions. It was indicated that the secretory cell produced mucopolysacchraide and glycoprotein. As reported in a previous study, the role of these substrates may be to produce and secrete during gamete transport (McMillan, 2007). Additionally, the appearance and the secretion of the glycoprotein profile are also suggested to be related to physiological function and ovarian hormones (Buhi, 2002). The mucous secreting cell in *R. brachysoma* may have a close relation to the non-ciliated cells of the oviduct, which are found in other vertebrates including Chinese Meishan pig (Abe, 1994) and some other mammals (Abe & Oikawa, 1992) because this cell synthesizes and releases the glycoprotein. Therefore, this might be an evolutionary trend that conserves the structural function of this cell in the oviductal epithelium.

The final cell type, the basal cell, was mostly located between the epithelial layer and the basement membrane. It was less frequent and relatively smaller in size. Under the epithelial layer in the present study was the thin layer of lamina propria, which contained various compositions, particularly fibroblasts and loose fibrous connective tissue. This connective tissue was positively stained, as shown by MT technique. Underneath the mucosal layer, the thin layer of submucosa contained the loose connective tissue and several blood vessels. Our findings showed the tunica muscularis layer in this species was composed of two smooth muscle layers: inner

circular muscle and outer few longitudinal muscles. It had clearly defined the smooth muscle fibers. It is possible that tunica muscularis was associated with movement of the oviduct structure. Another important finding was that the thin layer of serosa finally surrounded the tunica muscle, forming simple squamous epithelium, a small amount of loose connective tissue and nerves to gather with many blood vessels (Figure 3.9).

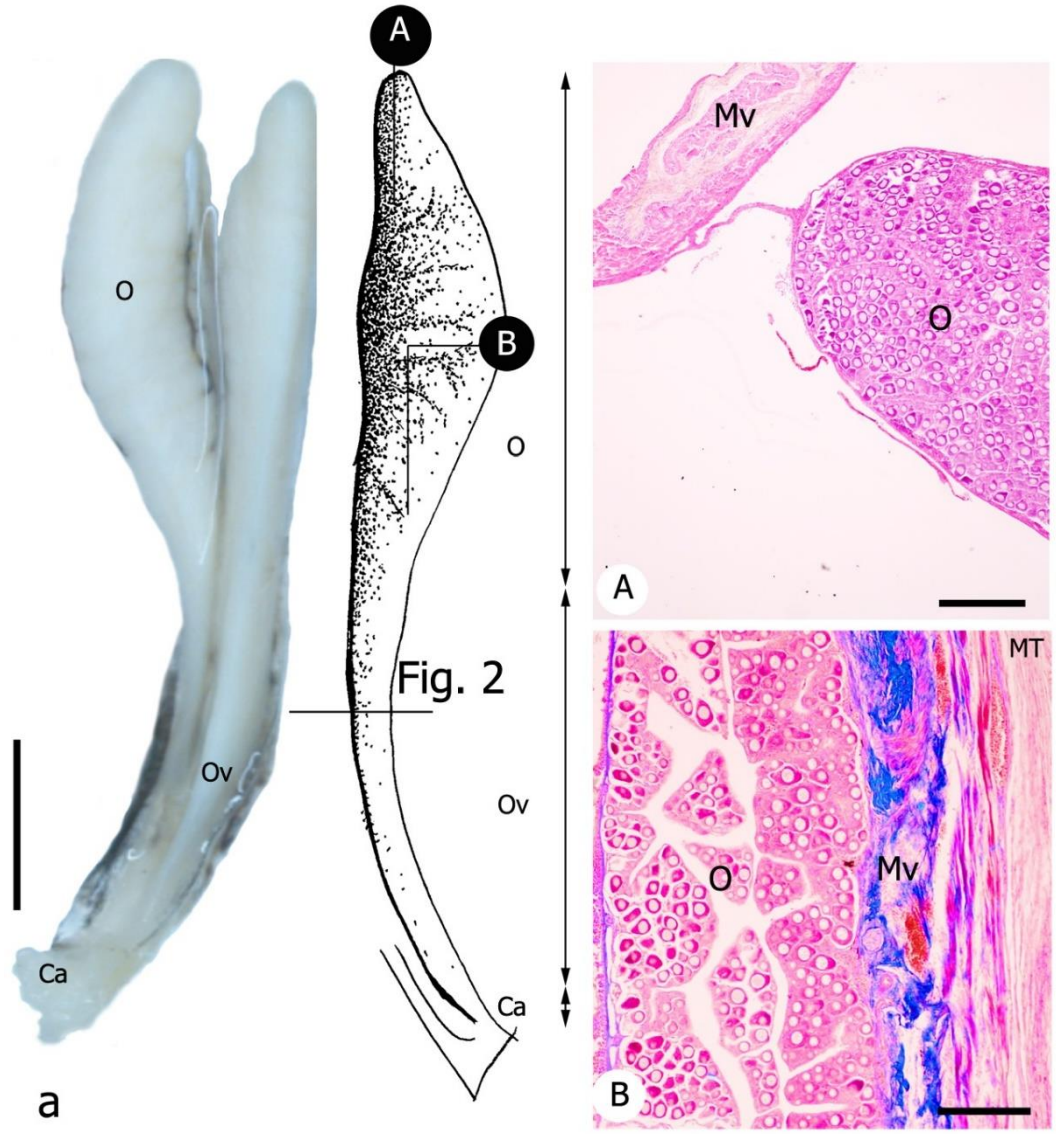

Figure 3.8 (a) Morphology (A-B) and light micrograph of the oviduct (Ov) of *Rastrelliger brachysoma* during non-breeding season. Scale bar: a, 1 cm, A-B, 350 µm. *Ca = cloaca, O = ovary, Mv = mesovarium. (Hematoxylin and eosin (H&E) and Masson's trichrome (MT))*

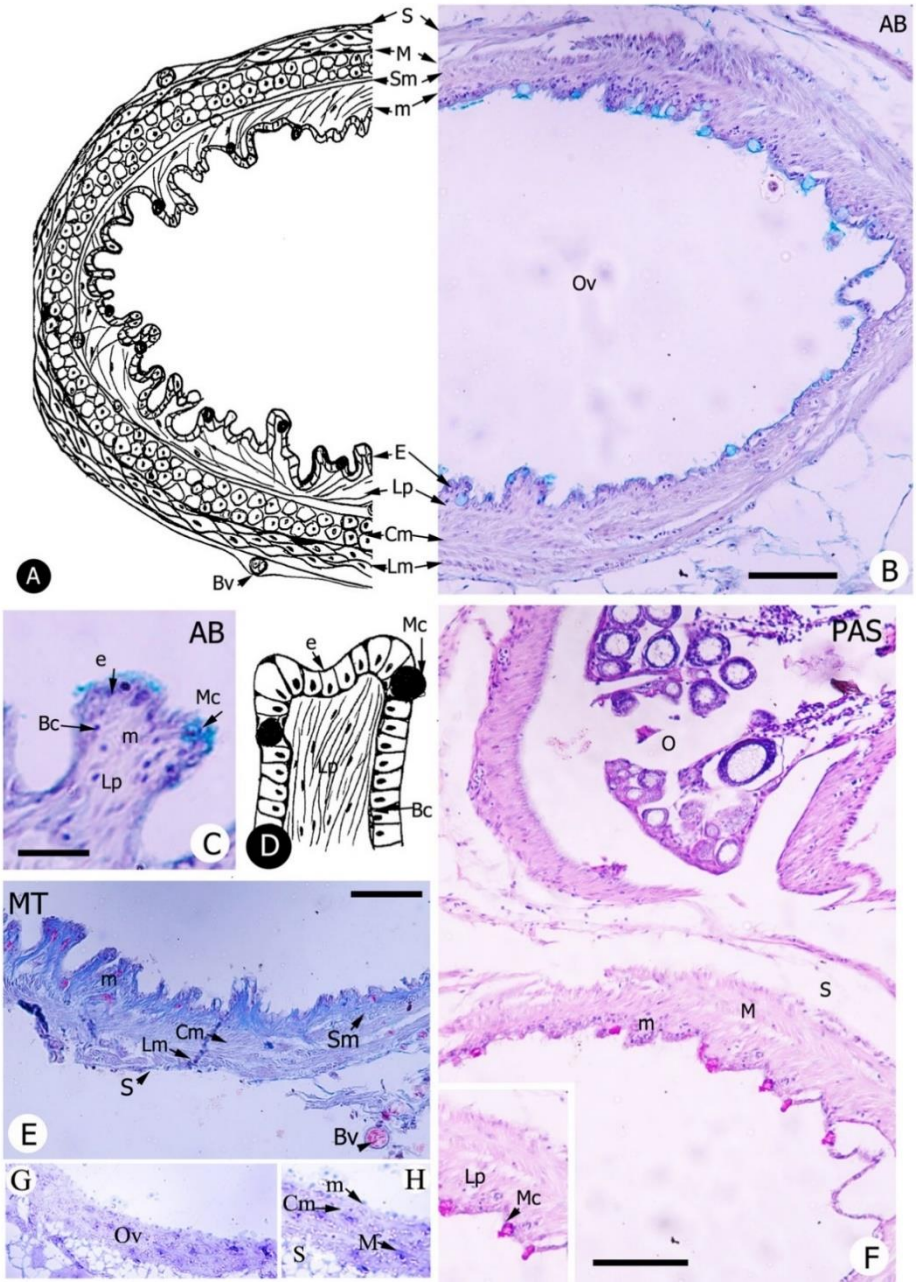

Figure 3.9 Light micrograph of the oviduct (Ov) of *Rastrelliger brachysoma.* Scale bar B, E and F, 100 µm, C, 20 µm. *Bc = basal cell, Bv = blood vessel, Cm = circular muscle, e = epithelial cell, Lm = longitudinal muscle, Lp = lamina propria, m = tunica mucosa, M = tunica muscularis, Mc = mucous secreting cells, O = ovary, S = tunica serosa, Sm = tunica submucosa. (Masson's trichrome (MT), Periodic Acid-Schiff (PAS) and aniline blue (AB)*

Histology of the blood vessel in the ovarian tissue

In this study, the arteriole, the capillaries and the small veins were commonly-seen in the ovarian vessel (Figure 3.10). These blood vessels were linked and separated from dorsal aorta before branching into ovarian artery from the dorsal aorta. The arteriole or small artery was not easily distinguished staining with H&E and negative stained with ORO. However, based on histochemical techniques including MT and RT stains, it was covered by a thin squamous epithelium in the tunica intima. This was similar reported in previous studies (Grizzle & Rogers, 1976). However, it was different from *Parika scaber* because it was covered by arteriolar cuboidal epithelium (Davison et al., 1997). The subendothelial sub-layer was indistinct here under light microscope. Tunica media was more prominent than other layers. This layer distinctly composed of smooth muscular tissue about two or three layers with MT stain and elastic fiber with RT stain. Tunica media characterization has been known to play important roles in many physiological responses to neurocrine, endocrine and paracrine stimuli (Satchell, 1991). The tunica adventitia, forming in the outermost wall contained a thin connective layer. The capillary was the smallest vessel and tube-shaped, when compared to other vessels. The wall was composed of only a single layer of endothelial cell. Additionally, it was surrounded by basement membrane. This observation was similarly reported in *Cyprinus carpio* (Genten et al., 2008) and mammals (Genten et al., 2008, Satchell, 1991). The small vein revealed that it rarely observed with irregular or oval in shapes under longitudinal sections. The tunica intima and the tunica media were proportionally decreased and not distinct. This was similarly observed in *Ictalurus punctatus* (Grizzle & Rogers, 1976). Additionally, lymphatic vessel was also found in the ovarian tissue. Its wall was a single epithelial layer and enclosed by connective tissue. The roles of this

vessel might be involved in transportation of lymphatic fluid and leucocytes (Harder, 1975).

Ultrastructure of the blood cells in the ovarian capillaries

Based on ultrastructual levels, follicular complex was found near small capillaries in previtellogenic stage. The most abundant types in this vessel contained a variety of blood cells including erythrocytes and leucocytes (eosiophils and lymphocytes) (Figure 3.11). As to detail, the diameters of erythrocytes were 7.3 μm in length and about 2.3 μm in width. This was similarly reported in *Dicentrarchus labrax* L. (Esteban et al., 2000), *Oreochromis niloticus* (Ueda et al., 2001) and *Cichlasoma dimerus* (Vázquez & Guerrero, 2007). It had biconvex and elongated in shape. Its average oval nucleus diameter was about 1.78 μm. It contained the condense heterochromatin which surrounded by electron-dense. The function of this cell concerns with carrying oxygen and carbon dioxide in teleost fish Genten et al. (2008). Only the round vesicles were occasionally found in the neutrophils. The range of cell sizes was 4.0 μm to 4.2 μm. By TEM, they were both round to oval shape cells and contained the bilobed nucleus shaped (1.8 μm mean in diameter). Cytoplasm of this cell contained globular mitochondria, ER, round vesicle and especially numerous granules as well as cytoplasmic rod-shaped granules. The range of the lymphocytes was 3.4 μm to 3.6 μm in diameter. They were small round cell with a large and spherical or centrally located nucleus. A thin rim cytoplasm contained mitochondria and several granules. Previous studies suggested that it is conceded as the most important to the immune response in fish (Jalali et al., 2009). The presence the lymphocytes in the ovarian tissue

of *R. brachysoma* may suggested that the individual may be infected. Hence, they could be unhealthy fish, which needs to be further investigated.

Systematic blood vessel in the ovarian tissue

Most investigations about the systematic blood vessels have been especially shown in some fish (Roberts, 2012), however; the vessel in ovarian teleosts has not yet been reported. In the present study, we provide a novel description about systematic ovarian tissue in the *R. brachysoma* (Figures 3.12-3.13). The systematic blood vessel of the ovarian tissue was easily seen in ovarian arteries. It was more prominent during the breeding season than non-breeding season. Histologically, the systematic ovarian artery was separated from the dorsal aorta along the body and branched into the arterioles at the mesovarium. Then, it reached into tunica albuginea with decreasing in size. The systematic ovarian arteries could be classified into two patterns according to different seasons. The ovarian tissue during non-breeding season was the ovarian arteriole branches, which were found along the mesovarium both cross and longitudinal sections (H&E and MT stains). After then, the branching of ovarian arteriole became many small arterioles along the tunica albuginea and penetrated directly to the ovigerous fold. It decreased in size and became capillaries. Hence, it is concluded that the major blood vessel in the ovary was the capillary vessel. Additionally, the termination or blind tube of the capillaries was distributed and nearly seen at the previtelligenic stage. When considering the role of capillaries, it is believed to be most involved in supplying both oxygen and nutrient and in particular, sex hormones (Olson KR, 2000, Ostrander, 2000). During breeding season, all blood vessels were increased in size, especially capillaries vessel. It was possible that this characterization may be

related with the ovarian development, which might supply the endocrine activities including vitellogenin uptake and estrogenic control. Additionally, the environmental problems in natural habitat of this fish may be the cause in the characterization of blood vessel, which needs to be clarified. Another observation, the systematic venous vessels were hard to notice in ovarian tissue under the light microscopic analysis.

Under histological images, this study also concluded that the ovarian vessels including arterioles, capillary, small vein and lymphatic vessel were present in the *R. brachysoma*. The systematic ovarian vessels particular arterial system could be identified into two patterns according to different seasons. Note that the increasing in the ovarian arterial vessels both amount and size from non-breeding to breeding seasons were observed in this article. However, the systematic venous vessels were not easily seen in ovarian tissues.

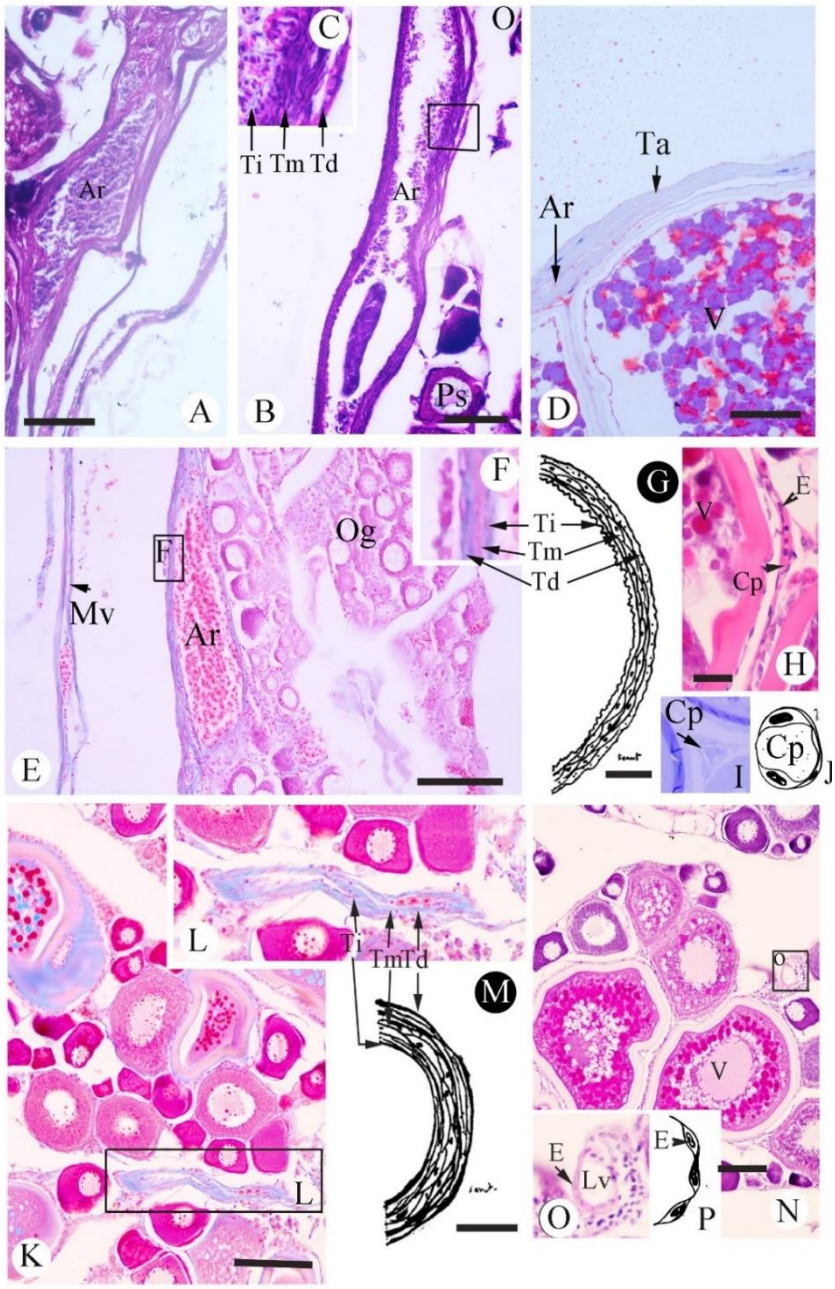

Figure 3.10 Light micrograph and schematic diagram of ovarian vessels in *Rastrelliger brachysoma*. Sclae bar: 50 µm (A, B, E, K, N), 20 µm (D), 10 µm (G, H, M). *Ar = Arterioles, Cp = capillaries, E = endothelium, Ef = elastic fiber, Lv = lymphatic vessel, O = ovary, Mv = mesovarium, Og = ovigerous fold, Ps = previtellogenic stage, Ta = tunica albuginea, Td = tunica adventitia, Ti = tunica intima, Tm = tunica media, V = vitellogenic stage.*

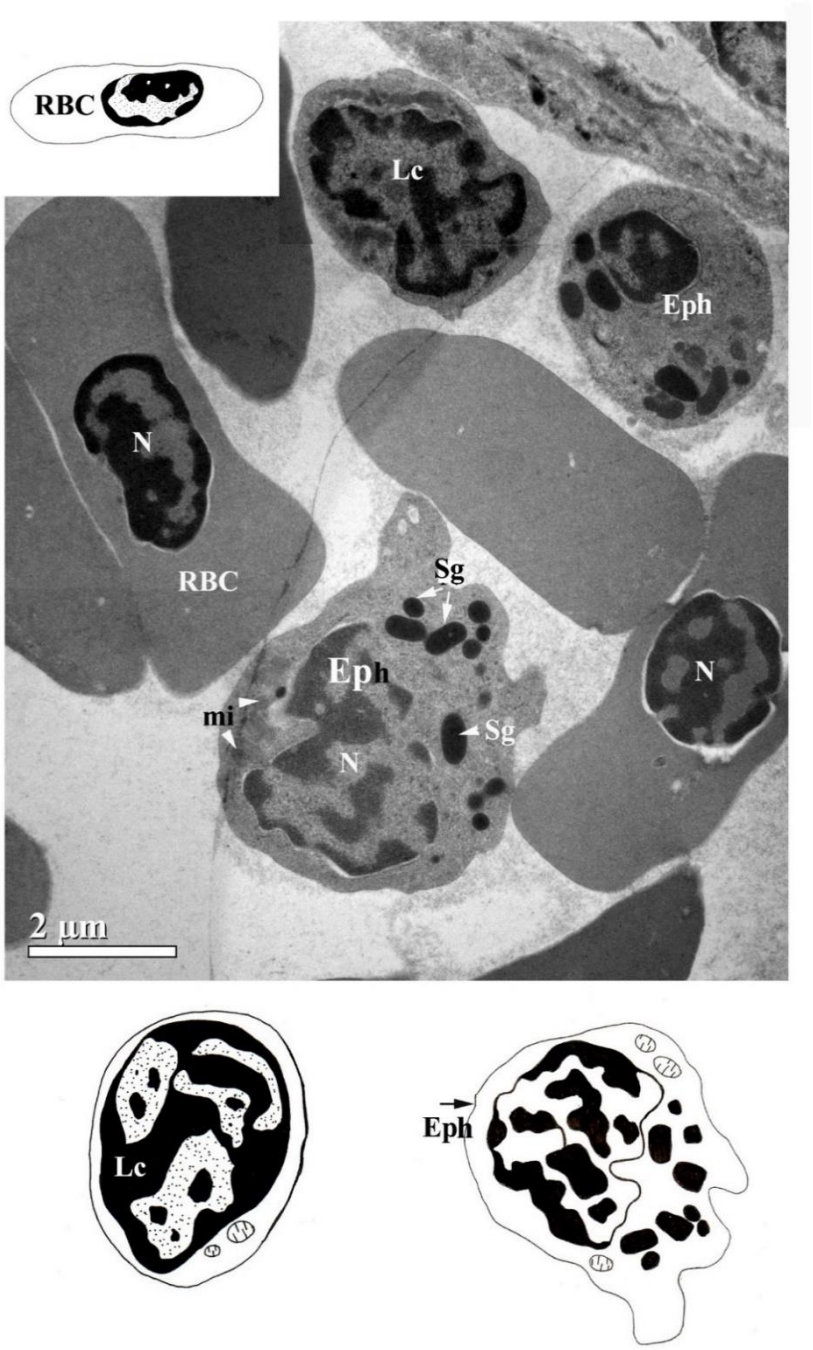

Figure 3.11 Electron micrograph and schematic diagram of blood cells in *Rastrelliger brachysoma* capillaries. *Eph = eosinophils; Lc = lymphocytes; mi = mitochondria, N = nucleus; RBC = red blood cells; Sg = specific granules*.

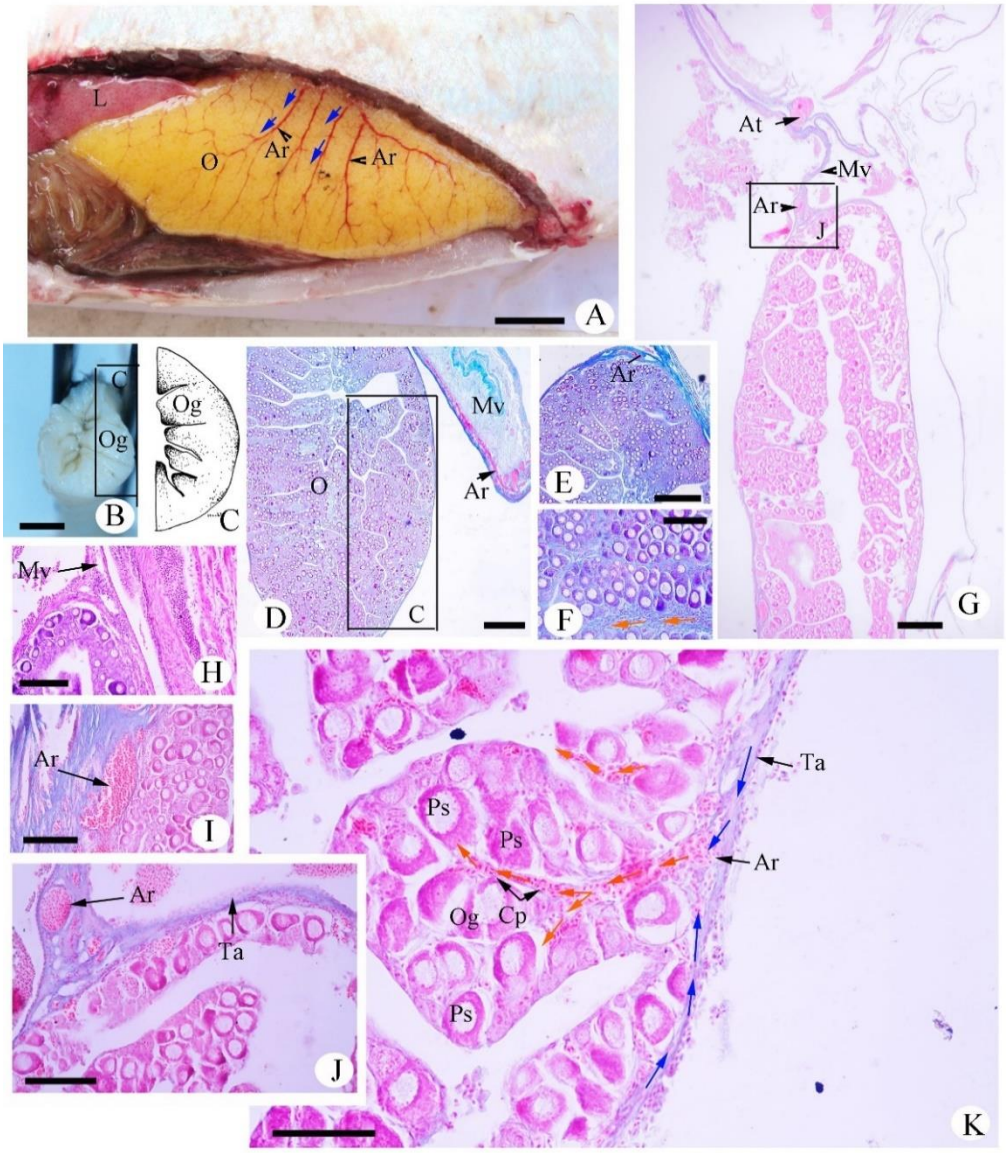

Figure 3.12 Gross anatomy and schematic diagram of ovarian tissue with showing of the systematic ovarian vessel in *Rastrelliger brachysoma*. The systematic ovarian tissue showed that arterioles flowed throughout tunica albuginea (blue arrow) and then it breached and penetrated to ovigerous fold, as called capillary (orange arrow). Sclae bar: 1 cm (A), 1 mm (B), 200 μm (D, G), 100 μm (E, H, I, J, K). Ar = arteriole, *At = artery, Cp = capillaries, L = liver, Mv = mesovarium, O = ovary, Og = ovigerous folds, Ps = previtellogenic stages, Ta = tunica albuginea.*

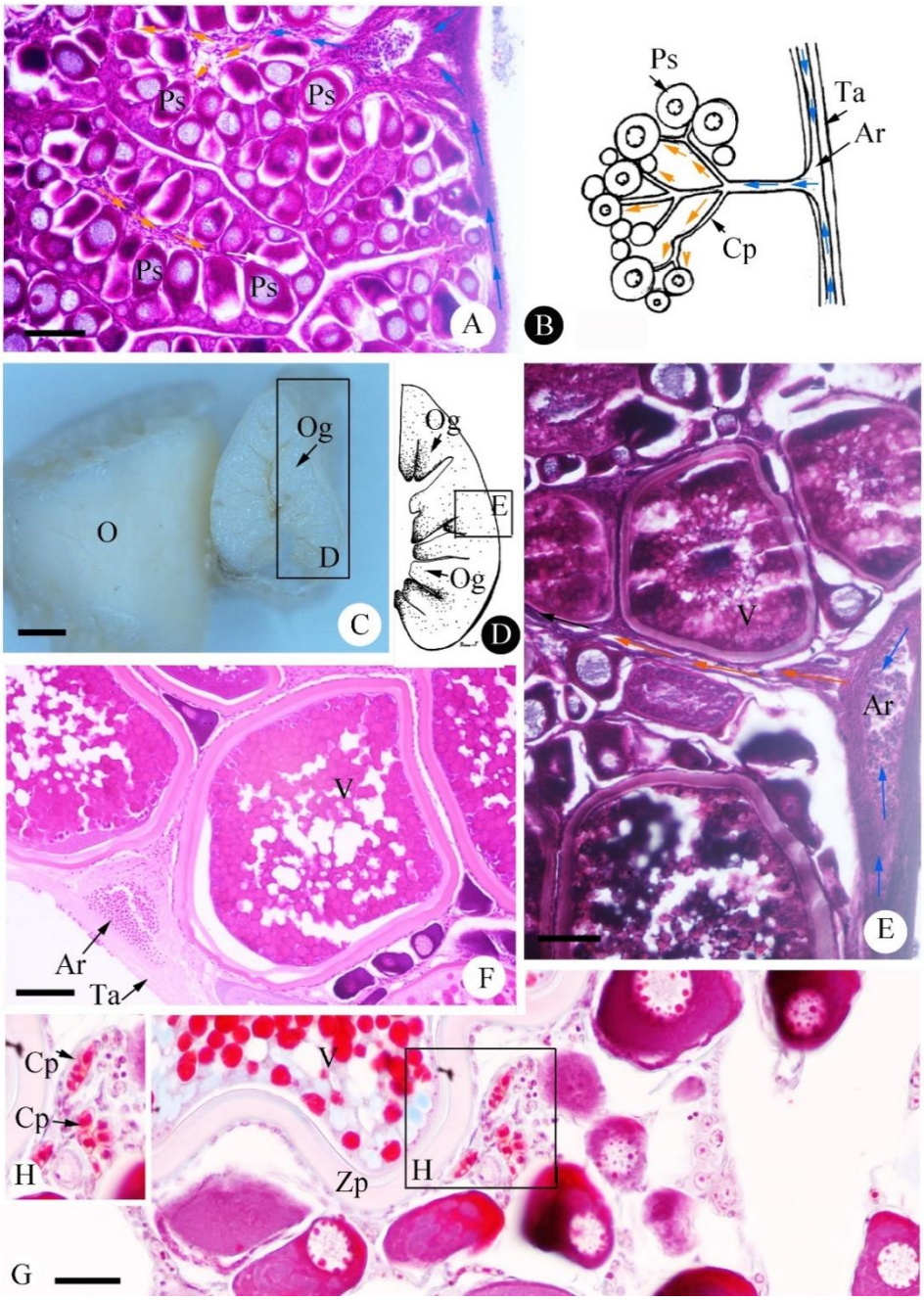

Figure 3.13 Comparison of the systematic ovarian tissue between non-breeding (A-B) and breeding seasons (C-G) in *Rastrelliger brachysoma*. (Arterioles flowed throughout tunica albuginea (blue arrow) with penetrating into ovigerous fold (orange arrow). Scale bar: 0.5 cm (C), 100 µm (A), 50 µm (E, F, G). *Ar = arteriole, Cp = capillaries, Mv = mesovarium, O = ovary, Og = ovigerous fold, Ps = previtellogenic stage, Ta = tunica albuginea, V = vitellogenic stage, Zp = zona pellucida.*

Oogenic structure and ultrastucture of *R. brachysoma*

Based on histological and semithin sections, the ovarian tissue of *R. brachysoma* was asynchronously developed. Consequently, all stages of their oocyte development could be divided into 5 stages based on size, nuclear characterization and cytoplasmic organizations and schematic diagram: oogonium, previtellogenic, lipid and cortical alveolar, early and late vitellogenic stages (Figures 3.14-3.16).

According to structure and ultrastructural studies, the epithelial and stromal compartments were observed in the ovarian tissue. In the epithelial compartment was contained both germinal epithelium and somatic prefollicular cells, which were associated with oogonial cyst. Especially in the first sub-compartment, their germinal epithelium with forming into squamous epithelial cell covered the ovigerous fold (Figures 3.14C-3.14E). The characterization of its elongated cell was an irregular and flattened nucleus with a prominent a single nucleolus. Within the nucleoplasm, the condensed chromatin was also first present near nuclear membrane, whereas the information constitutions including globular mitochondria, endoplasmic reticular (ER) and electron-dense particles were poor in the cytoplasm. Sometimes, the extravascular space had relatively lucent electron-density and was also located above the basement membrane of epithelial cells (Figure 3.14B). The last sub-compartment, the cytoplasm processes of the somatic prefollicular cells were observed and extended around the cell nest. The presence in each cell had a triangular shape with an irregular nucleus.

The outline in a cell nest, oogonium was observed in germinal compartment and rarely appeared. Note that it was the smallest cell within the oogenic stage with a diameter at 7-8 μm in size under divided mitotically. The characterization of oogonium was unique and mainly exhibited by round nucleus (5-6 μm in diameter). Also, it

contained the syntonemal complex with a majority of finely granular chromatin. Together with nuclear components, the small single nucleolus (about 1 μm in diameter) also slightly seen. Its nucleopores were numerous as electron-dense and granular material along the nuclear membrane. As following, nuages as polymorphic organelle frequently first appeared in ultrathin section and were usually associated with mitochondria (Figures 3.14F-3.14H). Moderate amount of cytoplasm in this stage had few organelles and were poorly-developed including ribosome and ER. Mitochondria were shown a round appearance with few cristae. During this stage, the cell was surrounded by pre-follicular cells, which were joined by desmosome.

In this study, the oogonium then continues growing into the primary oocyte stage, as called the early meiotic oocyte, was look like oogonium (Figure 3.15A). However, the characterization of this stage rarely displayed the nucleolus. Small patches of heterochromatin increased and were scatted within nucleoplasm. Golgi complex and well-development of ER in this stage were visible in ooplasm (Figures 3.15B-3.15E).

The term "the stromal compartment" seems to observe in several oocytes that the complete oogenic process could be classified into four successive stages according to the characterizations of nuclear and cytoplasmic organelles; previtellogenic, lipid and cortical alveoli, early and late vitellogenic stages. Initially, the previtellogenic stage with referring to pre-vitellogenic stage of *R. brachysoma* was more spherical than oogonium with about 20–60 μm in diameter (Figures 3.15F-3.15J). Under nuclear events progress, as so-called a new feature, the nuclear membrane had numerous pores, whereas multiple micronucleoli first appeared and were scattered around the periphery of the nuclear membrane. Occasionally in electron micrographs, some nucleolus clearly showed two parts at this stage was only detectable using eletron microscropy; inner

fibrillar core and outer granular periphery (Figure 3.15H). The lucent electron-density of cytoplasmic organelles occasionally increased the number of abundant ribosomes, irregular shape (globular and tubular), whereas a few lamellar cristae of mitochondria well developed. Electron-dense and nuage bodies were also seen. At the same time in surrounding events, the layers of the follicular complex began to change (Figure 3.15I). The small layer of the vitelline envelope began to appear the homogeneous and moderately electron-dense material, while the granulosa cell layer exclusively started to form as elongated-flatten cells. Some microvilli of granulosa cell became longer and extended toward the oocyte surface. A distinct thin basement membrane separated the granulosa and theca layers. A continuous follicular complex, theca cell were seen. Not that, a thin squamous layer contained the small block heterochromatin and a single nucleolus.

The lipid and cortical alveolar stage commenced during the beginning of secondary oocyte growth (Figures 3.15K-3.15N). Ultrastructural study revealed the initiation of the accumulation in two inclusions (lipid droplets and cortical alveoli) during this stage. At the beginning, the lipid (120–250 μm in diameter) synthesis was first observed as homogeneous and moderate electron-dense. During our observations, its synthesis and accumulation increased in size and number, continuing throughout the vitellogenic stage, whereas cortical alveoli with fine granular materials were obviously present in the periphery of the ooplasm. Numerous organelles of weakly basophilic cytoplasm (compared to previous stage) were also exhibited such as nuage bodies, mitochondria and ER cisterna. During this stage, the vitelline envelope was clearly deposited, lightly thickened (compared to previous stage) and had longer microvilli because this characterization gradually extended from granulosa cells. Specifically, the layer of

theca cell was distinctly classified into two layers; outer and inner theca cells (Figures 3.15M-3.15N).

The vitellogenic stage could be classified into two stages; early and late vitellogenic stages. In early vitellogenic stage (Figures 3.16A-3.16G), the ooplasm contained the organelles-rich cytoplasm. Surprisingly, the initial stage was characterized by increasingly larger sized oocyte because it began to uptake and accumulates the yolk granules with moderate electron-density in the peripheral ooplasm. Therefore, it reflected the fact that the early vitellogenic stage had well-developed microvilli as abundant finger-like projections. It was exclusively embedded in the vitelline envelope while reaching maximum thickness. Moreover, according to our understanding, the events of the vitelline envelope could be classified into three layers according to localization and electron-densities. The low electron-density of outer layer (Z1) was located near the granulosa cell. The intermediated layer (Z2) was thickest layer of electron-density and strongly seen, while the electron-density of the inner layer (Z3) was exhibited near oocyte surface, respectively. The granulosa cells were distinctly seen, whereas the outer thecal layer was observed as fibroblast shape. From the ultrastructure, the exogenous uptake mechanism showed that the electron-lucent materials or transport vesicles appeared in the cytoplasm of granulosa cell. At high magnification, the materials entering to pits and endocytotic vesicles (or pinocytotic vesicles) were seen to be clathrin-coated. This indicates that it is a vselective transport. After that, single or multiples of coated vesicles were found in membrane of vitelline envelope. Finally, these coated vesicles coalesced to be larger vesicles (endosome) and large yolk granules at the peripheral ooplasm. Each yolk granule was composed of two parts; dense central core and the peripheral granular

matrix. The dense central core as electron dense was surrounded by the peripheral granular matrix as lucent electron dense. The cortical alveoli and the lipid droplet also increased in number and size. Moreover, they continued to accumulate their vesicles and were present in the periphery of oocyte. Cytoplasmic organelles appeared as well-developed of mitochondria, free ribosome and ER.

At the beginning of the late vitellogenic stage, no nucleus was observed in the ooplasm. Throughout this stage, yolk granules coalesced into large electron-dense yolk granules, measuring about 3-5 µm in diameter, whereas cortical alveoli also began to fuse into larger inclusions. Surrounding events, the layered vitelline envelops were still thick and followed the disorganization, respectively. Within ooplasm, the groups of mitochondria and lipid droplets were intermingled among yolk granules (Figures 3.16H-3.16M). Moreover, regression and degeneration of oocytes were normally observed during reproductive cycle in the species (Figures 3.17A-3.17D).

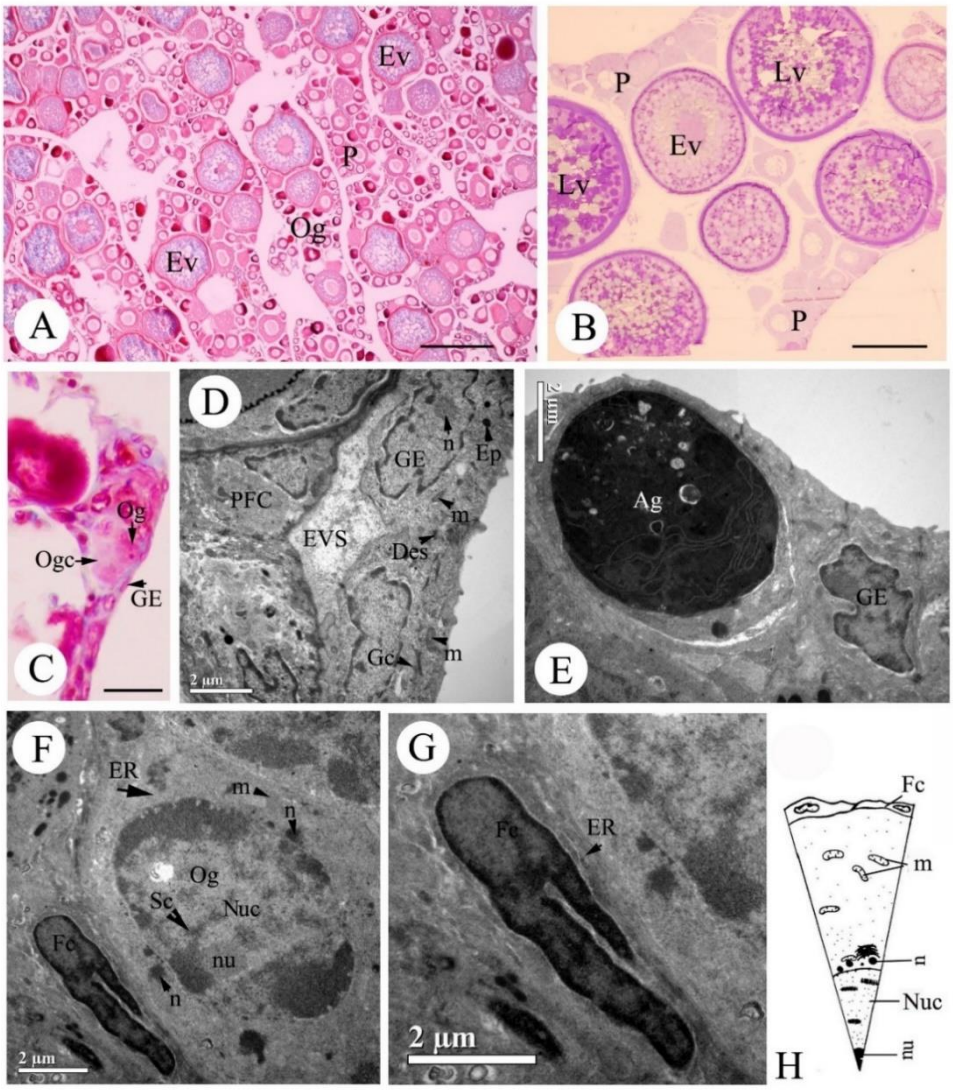

Figure 3.14 Light microscopic (A), transmission electron micrographs and schematic diagram of oogenesis in *Rastrelliger brachysoma* (A-H) including oogonia (Og), previtellogenic (P), lipid and cortical alveoli (Ld), early (Ev) and late (Lv) vitellogenic stages (A-B). Histological and thin sections showing the germinal epithelium (GE) and extracellular space (EVS) (C-E). Oogonia (Og) with surrounding the pre-follicular cell (PFC) (F-H). Scale bar: 200 µm (A), 50 µm (B), 20 µm (C). *Ag = atretic follicle of oogonia, Des = desmosome, ER = endoplasmic reticulum, Goc = Golgi complex, m = mitochondria, n = nuage, Nuc = nucleus, nu = nucleolus, Sc = syneptonemal complex.*

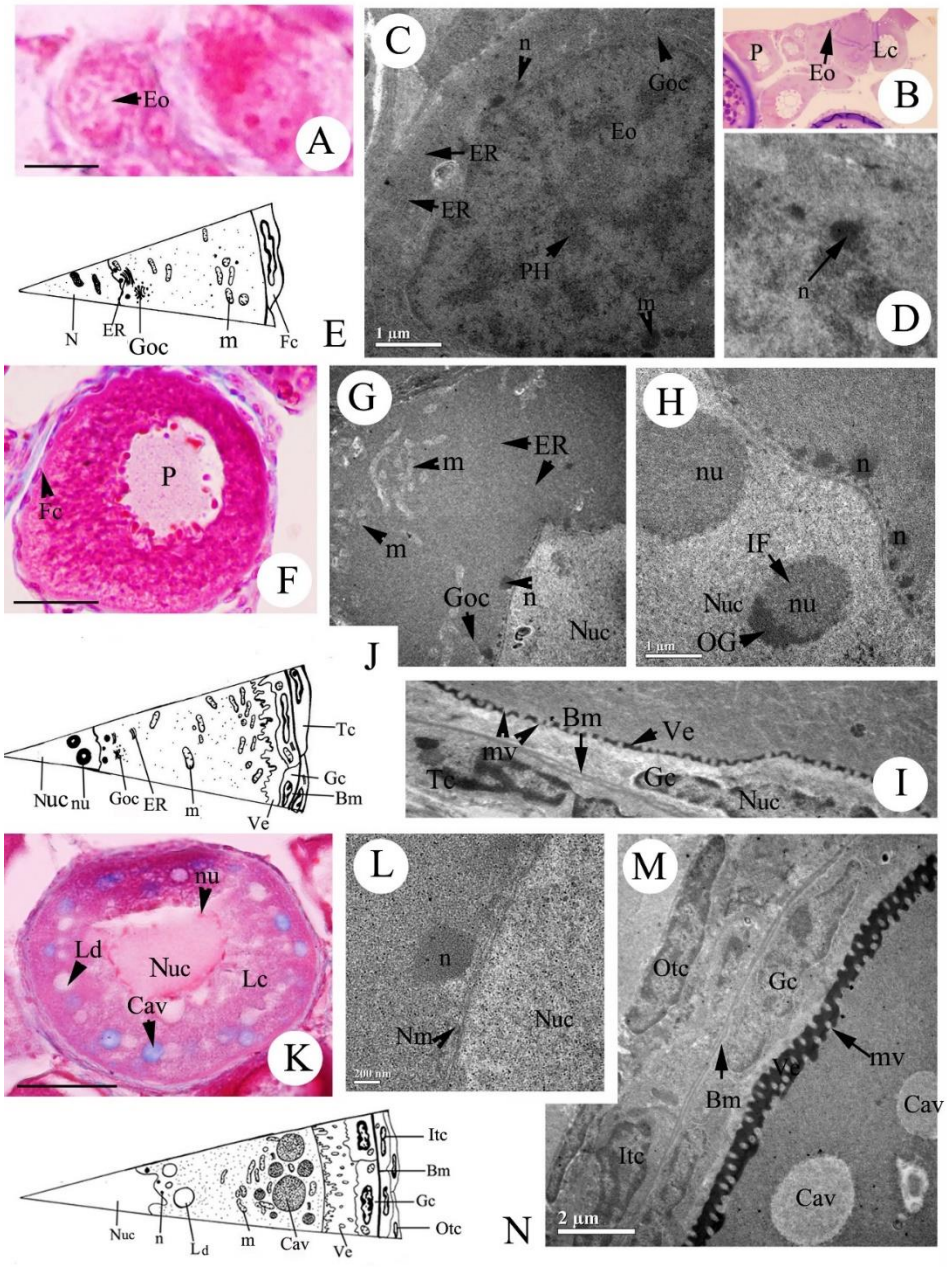

Figure 3.15 Light microscopic, transmission electron micrographs and schematic diagram of early meiotic oocyte (Eo), previtellogenic (P) and lipid and cortical alveoli (Lc) stages in *Rastrelliger brachysoma* (A-M). Scale bar: 20 µm (A,F,K*). bm = basement membrane, Cav = cortical alveoli, ER = endoplasmic reticulums, Fc = follicular cell, Gc = granulosa cell, Goc = Golgi complex, IF = inner fibrillar core, Itc = inner theca cell, Ld = lipid droplet, m = mitochondria, mv = microvilli, n = nuage, Nuc = nucleus, Nm = nuclear membrane, nu = nucleolus, Otc = outer theca cell, Tc = theca cell, Ve = vitelline envelope.*

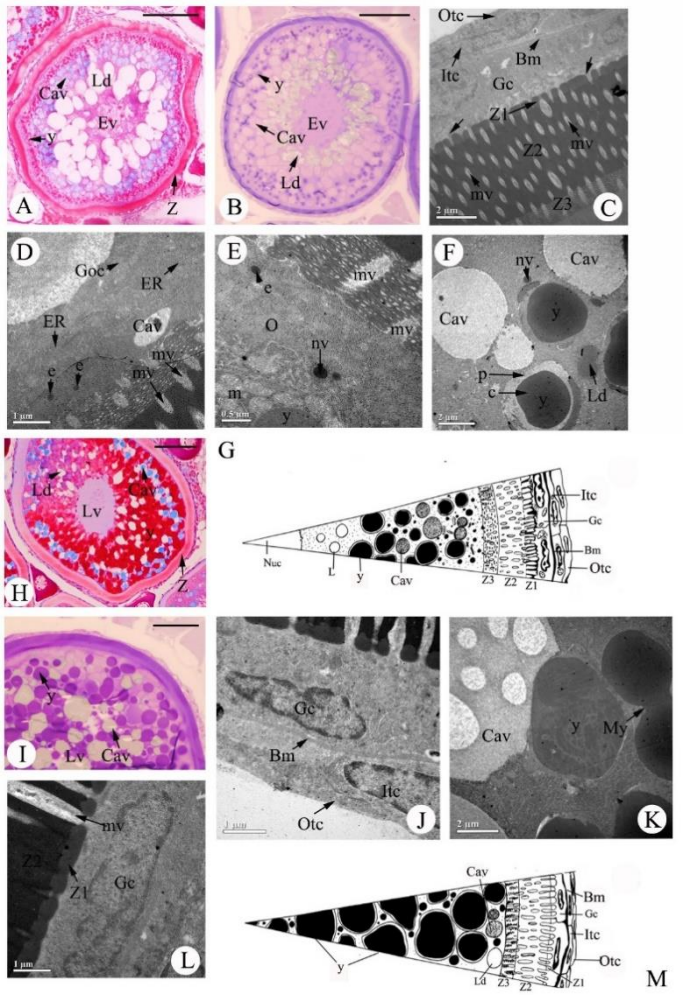

Figure 3.16 Light microscopic, transmission electron micrographs and schematic diagram of early and late vitellogenic stages in *Rastrelliger brachysoma* (A-M). Histological and semithin sections of early vitellogenic stage (Ev) (A-B).Ultrathin sections showing the detail of the increasing of vitelline envelope with consisting of 3 layers: outer (Z1), intermediate (Z2) and inner layers (Z3) with several organelles in ooplasm (C-G). Scale bar: 50 µm (A,B,H,I). *bl = basement membrane, c = dense central core, Cav = cortical alveoli, e = uncoated endocytotic vesicles (endosome), Gc = granulosa cell, Goc = Golgi complex, Itc = inner theca cell, Ld = lipid droplet, m = mitochondria, mv = microvilli, N = nucleus, ny = nascent yolk platelets, O = ooplasm, Otc = outer theca cell, p = peripheral granular matrix, RER = rough endoplasmic reticulum, SER = smooth endoplasmic reticulum, y = yolk granules, arrow = material from granulosa cell with sending to pass microvilli, arrowheads = gathering of oocyte microvilli into bundles.*

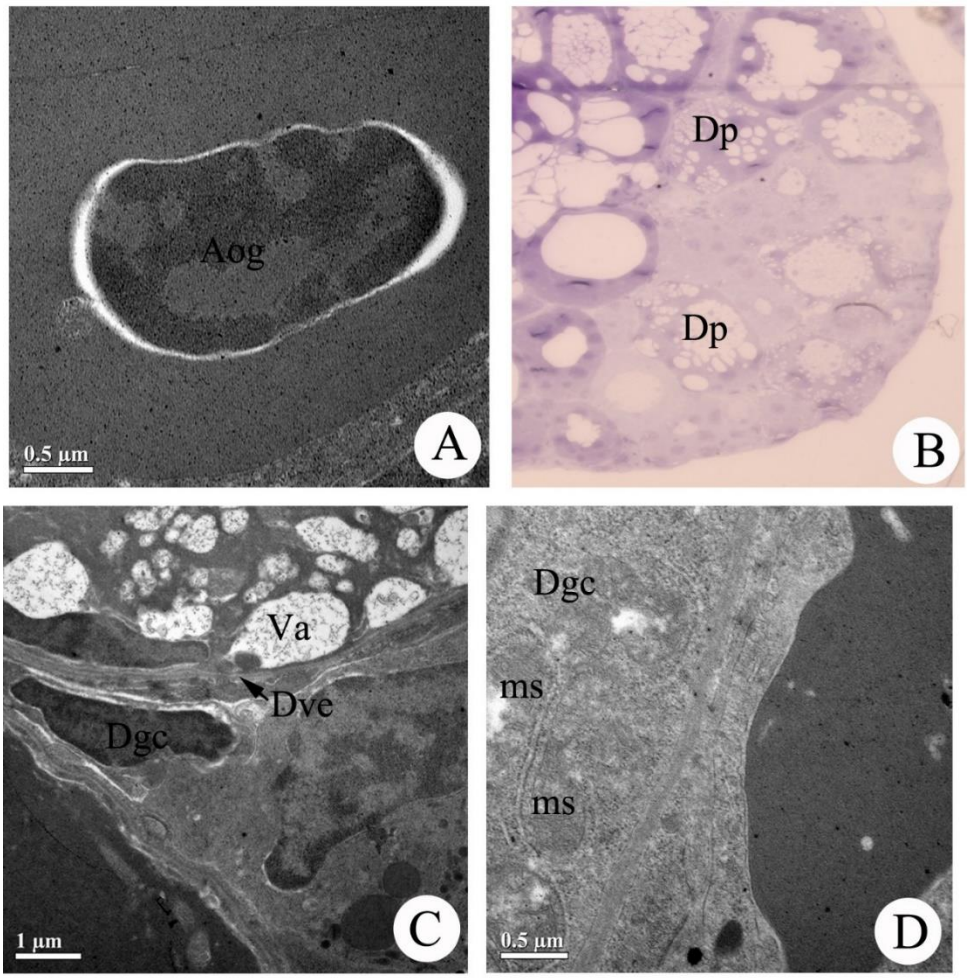

Figure 3.17 Transmission electron and light microscopic micrographs of atretic follicle of oogoonia (Aog) and degeneration of previtellogenic stage (Dp) in *Rastrelliger brachysoma*. *Dgc = degernartion of granulosa cell, Dve = degeneration of vitelline envelope, ms = mitochondrial swelling, Va = vacuolar*.

Discussion

Based on the histological structure, the ovarian tissue of *R. brasochyma* was the asynchronous oocyte development type which is similar all other scombrids (Chellappa et al., 2010). This indicated a protracted spawning period with multiple spawning. At the initiation phase of oogenic stage, the oogonium was observed and they were the smallest among female germ cells. It was proliferate within cell nest. They were characterized as being enclosed by prefollicular cells in the germinal compartment. This feature was commonly found in most teleost (Grier, 2000, Selman et al., 1993). Then, it progressed to the primary growth stage. In this fish, the primary growth stage is characterized by basophilic cell due to a period of intense RNA synthesis together with ribosome production to support the oocyte development (Wallace & Selman, 1990). Generally, this stage can be also divided into two phases based on nuclear morphological characteristics: (i) the chromatin nucleolus and (ii) the perinucleolar stages, as in this species. The characterization of the chromatin nucleolus stages of this fish were seen but are rarely observed, as shown by *Thunnus orientalis* (Okochi et al., 2016) and other teleost oocytes (Sarasquete et al., 2002). This probably was caused by the transformation of oogonia tured into chromatin nucleolus stage and then it tured into the perinucleolar stage, as suggested by Mandich et al. (2002) and Sarasquete et al. (2002). The perinucleolar stage was the firstly observed in the Balbiani's body as non-homogeneous structure. Its oval shape with containing the basophilic staining located near the nucleus membrane. A similar characteristic was also found in *Oryzias latipes* (Wallace & Selman, 1981). The functional structure of Balbiani's body was uncertain, but it was believed to be a center for the formation of various organelles. It was regions rich in nucleic acid (Hamaguchi, 1993), RNA and proteins (Selman & Wallace, 1989).

Afterwards, two types of inclusion occured, lipid droplet and cortical alveoli. Lipid droplet inclusion occurred prior to the cortical alveoli inclusion in the cortical alveolar stages. Sequential of these inclusion were used in the egg type postulation in most teleost fishes (Brown-Peterson et al., 1988, Selman & Wallace, 1989). These ovary patterns of *R. brachysoma* agreed with the some marine fishes including *Dicentrachus labrax* (Mayer et al., 1988) and *C. undecimalis* (Neidig et al., 2000). Our inclusion sequential confirmed that the egg of *R. brachyoma* is a pelagic type. Although, the structural role of lipids is still unclear, it concerned with energy sources for embryo development (Wiegand, 1996) whereas, cortical alveoli were negatively stained with H&E and ORO, but they were strongly positive to MT as greenish color, indicating the presence of the polysaccharide. The staining pattern in *R. brachysoma* similar to other fish species (Selman et al., 1988, Wallace & Selman, 1990). The role and function of this inclusion concerned with physiological roles, especially the prevention of polyspermy after ovulation (Nagahama, 1983).

The early vitellogenic oocyte started to either synthesis or accumulation of yolk granules. Hence, it increased in size. Wallace & Selman (1990) reported that these yolk granules where the material stored during the secondary growth stage. Their structural roles were usually related to to the nutrition and metabolic activities in the embryonic development as described in most fish species (Selman & Wallace, 1989). Then, entering into late vitellogenic stage it showed several processes in both cytoplasm and nucleus. In the cytoplasm, the characterization of yolk granule in this species is similar to *Serra spanish* (Chellappa et al., 2010). It was not fused until it entered into mature stage. This feature was suggested to be typical of pelagic egg (Wallace & Selman, 1981), which was different from demersal eggs, in which the beginning of yolk fusion

was observed during the early vitellogenesis stage. This was also found in *Gasterosteus aculeatus* and *Apeltes quadracus* (Selman & Wallace, 1989). Then, the nucleus of the late vitellogenesis stage first migrates to the animal pole and the micropyle was observed. This pattern also observed in *R. brachysoma* oocyte (present study), *Fundulus heteroclitus* (Kuchnow & Scott, 1977) and *T. orientalis* (Okochi et al., 2016). The micropyle function concerned with the entering location of the spermatozoa to the oocyte surface without acrosomal reaction (Bartsch & Britz, 1997). The final stage of oocyte in this species is the post ovulatory stage or mature oocytes with processes involving the nucleus region. No nucleus with germinal vesicle breakdown was observed under the first meiotic cell division. This breakdown is widely used as an indicator of the final maturation in the teleost fish (West, 1990).

Oogenic ultrastructure in teleost fish is considered a complex process, which provides understanding of differential fine structure relating to hormonal control (Selman et al., 1986). In this study we reveal the first reported ultrastructural analysis mainly as used to assess the oogenic step in *R. brachysoma* and classified the differentiating oocytes into five stages including oogonium, early meiotic stage, primary (referring to previtellogenic stage) and secondary (referring to lipid-cortical alveolar and vitellogenic stages) growth stages throughout the degeneration of oocytes. Although to study the oogenic ultrastructure of *R. brachysoma* has been similarly described in some fishes (Abdalla & Cruz-Landim, 2003, Abdel-Aziz et al., 2012), the use of TEM provided us to better the understanding the components in both cellular and organelles during oogenic process of this species. The prominent characterization of oogonium as well as earliest stage had nucleolar materials with several nuages, in which the common feature did not differ from previously described in several authors

(Abdalla & Cruz-Landim, 2004). The appearance of the nuages in this stage, *R. brachysoma* referring to the electron-dense masses, from the fact that were scatted and observed in association with mitochondria near nuclear membrane throughout the lipid and cortical stage, as similar to that of *Piaractus mesopotamicus* (Abdalla & Cruz-Landim, 2004). Previous suggestion is supported that nuage may involve the oogenic development for fishes because the synthetic activity of the ribonucleoprotein with ribosomic content is found in this structure (Alberts et al., 2000). As in different teleosts, the unique complexity of the primary growth stage was pronounced initially by increasing basophilia with reflecting to the active synthesis of RNAs and the accumulation of ribosome with mitochondria, while the nucleus contained the multiple nucleoli in a perinuclear position of the nuclear membrane (Selman & Wallace, 1986, Selman et al., 1986). Prominent characterization of this stage in agreement with previous findings in *Dicentrachus labrax* (Mayer *et al*., 1988) and *R. brachysoma* (present study).

Other important findings during the following secondary growth stage, the small lipid droplets first appeared, gradually became more abundant and increased in size at the vitellogenic stage, which is dominantly characterized as commonly observed in some marine fishes (de Vlaming, 1983). Under light microscopy, the accumulation of lipid droplet showed the empty apace or vacuolar because of the extraction of its content during the histological method, however, Oil red O staining was positively reacted (Senarat et al., unpublished data). Recent data with the multifunction of this structure is well-known and associated with the nutrients for the development of the future embryo (Abascal & Medina, 2005). As following to the cortical alveoli were continuously developed and gradually increased in the ooplasm, suggesting that this

was highly active in glycoprotein synthesis activity (based on MT stating (Unpublished data). This feature is similarly reported in many other fish species (de Vlaming, 1983, Selman et al., 1986, Selman et al., 1988). The development of the cortical alveoli may be involved in processing the cortical reaction at fertilization and polyspermy (de Vlaming, 1983, Selman et al., 1986, Selman et al., 1988).

When oocytes turn into vitellogenesis, the formation of the small yolk granules in ooplasm of the early vitellogenic stage and their large granules in later stage (late vitellogenic stage) were seen. A parallel fluctuation to morphological events during oogenic process, the vitelline envelope was also interestingly formed. Particularly clear evidence at the previtellogenic stage, the vitelline envelope was first seen and distinctly embedded by several microvilli that extended from granulosa cells. Then, the vitelline envelop became the thickest layer together with several microvilli during vitelligenic stages. Hence, it is apparent that these changes are closely associated to be highly specific with an increasing level of vitellogenin as well as yolk granules, which is highly observed in vitellogenic stage. This feature is similarly reported in several marine fish, as for instance, in *Pagrus major* (Matsuyama et al., 1991) and *Chionodraco hamatus* (Baldacci et al., 2001). It is well known that this process is normally regulated by hypophyseal hormones as well as hypothalamo-pituiatry gonadal axis, like other fishes (Selman and Wallace, 1986b; Selman *et al*., 1988). The pathway of yolk uptake into the ooplasm, this is well known with reporting in several species for example *Cyprinodon variegatus* (Selman & Wallace, 1982) and *Fundulus heteroclitus* (Selman & Wallace, 1983). All cases and our observation showed that circulating macromolecules are passed to endothelial cells of the thecal capillaries and then transported to granulosa cell (referred as follicle cells) and through the pore channels

of vitelline envelope. When the uptake of yolk granules from the granulosa cell to ooplasm, it was also selective by endocytosis, then translocate to the nascent yolk platelets and yolk granules, as confirmed by Yön & Akbulut (2012) too. In further work, the direct experimental evidence supporting the purification and level of vitellogenin from ovarian tissue using SDS-PAGE and western blot analyses remains unknown, which are still to be explored.

Interestingly, we also showed the organization of vitelline envelope in the vitellogenic stage, three layers; the outer, intermediate and inner layers were found, as like to *Serrasalmus spilopleura* (Quagio-Grassiotto & Guimarães, 2003). However, in some species, it differed from other fish species such as two layers in *P. major* (Matsuyama et al., 1991). Considering this characterization would suggest the layer of vitelline envelope; it may be associated with types of reproductive strategies. Quagio-Grassiotto & Guimarães (2003) provided evidence that the vitelline envelope of oviparous species was thicker than viviparous. This result had led to the suggestion that *R. brachysoma* was considered as oviparous.

Conclusion

An important conclusion from in this study was that, the histological and histochemical characteristics of the ovarian tissue in *R. brachysoma*, a highly attractive marine fish of commercial importance in Thailand is received and considered the first report from Thailand. Additionally, we found that the oogenic ultrastructure of *R. brachysoma* female was classified into five stages including oogonium, previtellogenic, lipid and cortical alveolar and vitellogenic stages, is novel with particular arrangement of nucleus, cytoplasmic organelles and follicular complex.

Therefore, our findings accurately provided a better understanding during oogenic processing, will improve and increase the *R. brachysoma* productivity during aquacultural development as well as Scombridae group.

Chapter IV

TESTICULAR STRUCTURE AND ULTRASTRUCTURE OF THE SHORTMACKERAL*Rastrelliger brachysoma* (Bleeker, 1851) FROM SAMUT SONGKHRAM PROVINCE

Introduction

Investigations on the testicular structure and spermatogenesis under light microscopic level have been observed in several orders of teleost i.e., perciform, cypriniform, atheriniform and beloniform (Dietrich & Krieger, 2009, Parenti & Grier, 2004). Similarly, ultrastructural studies of the spermatogenic stages have also been investigated in teleost fish in Families: Anguillidae (Todd, 1976), Mugilidae (Bruslé, 1981), Poeciliidae (Billard, 1984), Sparidae (Gwo et al., 1993), Characidae (Romagosa et al., 1999), Scombridae (Abascal et al., 2002) and Gobiidae (Chung, 2008). The sperm morphology was particularly investigated because it varied in its shape when compared to other vertebrate groups (Jamieson & Leung, 1991, Mattei, 1991). Also, the interest in sperm morphology involved many aspects in fish biology such as reproductive biology, physiology, phylogenetic analysis and breeding (Jamieson & Leung, 1991, Mattei, 1991). Similalry in previous observation, the spermatozoa morphology in teleost fish have been used as a powerful tool in taxonomic and phylogenetic classification (Jamieson & Leung, 1991, Mattei, 1991). Not only a useful tool for the systematical analysis, but also for the diversity of habitats and reproductive modes of the fishes. Surprisingly, spermatozoa morphology can be mainly classified into two types. A simple first type is the aquasperm spermatozoon which characterized by a round head with a short neck region (mid-piece), few

mitochondria, whereas in the second type, the introsperm spermatozoon has the elongated head and other derived features including absence of the mid-piece and nuclear rotation (Jamieson & Grier, 1993, Mattei, 1991). Differences between these two types reflect to the mode of fertilization in fishes (Jamieson & Grier, 1993). Among fishes, several scombrids such as *Scomberomorus tritor* (Mattei, 1991), *Thunnus thynnus* and *Euthynnus alletteratus* (Abascal et al., 2002), *Scomber australasicus* (Hara & Okiyama, 1998), *S. japonicas* (Hara & Okiyama, 1998, Mattei, 1991) and *Cybium tritor* (Mattei, 1991) have especially observed due to their economical important value and investigated in male germ cells based on fine structure. Unfortunately, no information has been done on the structure using light and electron microscopes of the spermatogenesis in the short mackerel *Rastrelliger brachysoma.* It is considered as the only marine species that is successfully managed in Thailand. However, due to recent reducing in sign of age of maturity, The Thai government is operaly aquaculture program for it. Therefore, it is the best candidate for further research as it is the up promising prospect for aquaculture in Thailand.

Hence, in this study, the testicular structure and spermatogenic stages of the *R. brachysoma* living in the Upper Gulf of Thailand were clarified using light and transmission electron microscopes.

Materials and methods

Fish collection and sampling

Adult *R. brachysoma* (15 to 18 cm standard length) were used in this study. Fish were collected by bamboo strake trap from Samut Songkhram Province on the Upper Gulf of Thailand (13°16’18.4”N, 100°02’13.4”E), during non-breeding season

(October to December 2013, n = 20) and breeding season (January to February 2014, n = 20). All fish were euthanized by rapidly cooling shock (Wilson et al., 2009). The experimental protocol was approved by the Animal Care and Use Committee of Faculty of Science in accordance with the guide for the care and use of laboratory animal prepared by Chulalongkorn University (Protocol Review No. 1423003).

Light microscopic observation

The testis tissues were immediately fixed in Davidson's fixative for 48 h at room temperature and processed using standard histological techniques. The testicular paraffin blocks were cut at 5 µm thickness and stained with Harris's hematoxylin and eosin (H&E) (Bancroft & Gamble, 2008). For histochemical technique, the basement membrane, reticular fiber, protein, carbohydrate and lipid contents of testis tissue were specific stained with Masson's trichrome (MT), periodic acid-schiff (PAS), alcian blue pH 2.5 (AB) and reticulin (RT) staining methods (modified from Bancroft & Gamble (2008), Puchtler & Waldrop (1978), Vidal (1988). Additionally, frozen tissues were cut at 10 µm thickness by freezing microtome, and stained with oil red O (ORO) (modified from Culling (2013)). Overall, the testicular structures and spermatogenesis were measured according to the guidelines of Dietrich & Krieger (2009).

Ultrastructural observation

Small pieces of testicular tissue (approx. 1 mm^3 in size) were cut and rapidly prefixed in 2.5% glutaraldehyde (phosphate buffer pH 7.3) for 24 h at 4°C and postfixed in 1% osmium tetroxide. Testicular tissues were dehydrated in serial graded ethanol and embedded in epoxy resin (Epon 812). The semithin tissues were cut at 500 nm

thicknesses and stained with toluidine blue. Ultrathin sections were cut at 90 nm thickness and then stained with uranyl acetate and lead citrate. The sections were observed with a JEM-2100 (200kV) transmission electron microscope (TEM, JEOL, Japan).

Results

Histology of testicular tissue

Asymmetrical anatomy of *R. brachysoma* testes had paired organs and heart shape in cross section (Figures 4.1A – 4.1C). They situated in the dorsal part of the abdominal cavity, under the kidney. The cross sections revealed that the parenchyma of the testicular tissue was the anastomosing lobular type, which was surrounded by tunica albuginea. Its tunica albuginea was covered by mesothelium (Figure 4.2A). The projection of tunica albuginea extended into the testicular parenchyma, forming lobules in the dorsal region, which was divided into two compartments (Figures 4.1A, 4.1D): (i) the interstitial compartment which contained the blood/lymphatic vessels, perilobular myoid cells and steroidogenic Leydig cells (Figures 4.2R, 4.2S). Perilobular myoid cells were elongated in shape. The weakly acidophilic cells with surrounding the lobular. Steroidogenic Leydig cells had a large polygonal shape and were usually represented as small groups near blood capillaries in the interstitial compartment. Their nuclei were basophilic containing one nucleolus. (ii) The germinal compartment contained the numerous seminiferous lobules. The testis of *R. brachysoma* was classified as unrestricted spermatogonial type because the spermatogonia occurred and were distributed along the entire length of the germinal compartment of the lobules (Figure 4.1E). Each seminiferous lobule composed of spermatogenic and somatic

sertoli cells. The somatic sertoli cells had triangular nuclei with large, prominent nucleoli and slightly acidophilic cytoplasm. They were usually presented in low numbers and located adjacent to lobular septa. Each stage of spermatogenesis was synchronously developed, called spermatocyst. Based on the structural features, such as cell size, shape, nuclear characteristics, chromatin condensation, amount of cytoplasm and staining properties, the spermatogenic process of *R. brachysoma* can be classified as follows:

Primary spermatogonium was the largest among the spermatogenic cells with diameter about 10-12 µm. It was generally found as single cell, near the seminiferous epithelial compartment. The center of the oval nucleus contained a very prominent single nucleolus with weakly basophilic neucleoplasm. The granular cytoplasm contained moderate amounts (pale vesicle) (Figure 4.2F).

Secondary spermatogonium derived from the primary spermatogonium by mitosis division. This stage was similar in character to the previous stage, but the nucleus had stronger basophilia than the primary spermatogonium, due to the increase of heterochromatin condensation along the nuclear membrane. Each group (generally more than 4 cells) with 12-15 µm in diameter was the commonly found in cysts formation, called spermatocysts (Figures 4.2C, 4.2G).

Primary spermatocyte was formed when the secondary spermatogonia enter in meiosis. Its size (7-8 µm) was smaller than secondary spermatogonia and still occurred inside spermatocyst. The spherical or oval nucleus of secondary spermatocyte had a granule and stained as a basophilic cell with no prominent nucleolus. It exhibited a moderate amount of distinct acidophilic cytoplasm (Figure 4.2H).

Secondary spermatocyte developed from primary spermatocyte under the first meiotic division. It was relatively smaller in size about 6-7 µm than primary spermatocytes. It was contributed to the largest spermatocyst (35-40 µm). The distinguishing feature of this stage was a change in shape and color of the nucleus; round nucleus increasingly condensed near the nuclear membrane without nucleolus (5 µm) as basophilic chromatin, which did not contain. The basophilic staining of the 2nd spermatocyte decreased as it depended (Figure 4.2I). However, it was rarely observed throughout the testis.

Spermatid derived from secondary spermatocyte after the second meiotic division. It was still inside spermatocyst. The oval nucleus was small with intensive basophilic. Rims of eosinophilic cytoplasm were shown, due to the losing of its cytoplasm during spermiogenesis (Figures 4.2C, 4.2J).

Spermatozoon was the smallest spermatogenic cell. It was found in the lumen because of the spermatocyst capsule breaking out and then being released into vasa defferentia. It can be morphologically distinguished into 2 regions: head and tail. The ovoid shape head of the spermatozoon was responsible from its' chromatins became completely condensed and was represented as strongly basophilic. The tail was a strongly acidophilic with rarely apparent uniflagella in histological sections (Figures 4.2C, 4.2K).

The spermatozoa within lumen were released during spermiation into the ventral region were called as the anastomosing zone before opening, continued with the vasa efferent and testicular duct, respectively. In a study involving the morphological localization of the testicular duct of *R. brachysoma*, it descended along the lateral side of testis and then it connected with cloaca (Figure 4.3A). Histologically, section of this

structure was found similar to oviductal female, which was composed of tunica mucosa, tunica submucosa, tunica muscularis and tunica serosa. No longitudinal fold in the mucosal surface was observed in all specimens. Their mucosa surface was lined with low simple columnar epithelium. This layer was surrounded by tunica submucosa, which was rarely identified in testicular duct. The layer of the tunica muscularis showed within duct with consisting of a few muscular tissue, whereas the serosa was slightly seen in this duct. Through this duct, the mature sperm as well as final sperm maturation were also found (Figures 4.2B-4.2D).

Histochemistry of testicular tissue

Protein and carbohydrate

Histochemistry of the testicular tissue was detected by AB (Figures 4.4A, 4.4B) as slightly positive as well as MT (Figures 4.4E, 4.4F, 4.4G). PAS (Figures 4.4H, 4.4I, 4.4J) had strong positives for tunica albuginea and interstitial connective tissue, while spermatogonia and primary spermatocytes were slightly positive with PAS reaction. Both Leydig cells and somatic Sertoli cells were moderately stained with the same reaction.

Lipid

Overall testicular tissues were unstained with ORO, indicating the absence of lipids (Figures 4.4C, 4.4D).

Fiber composition

Reticulin reaction from the longitudinal section revealed that the several blind ends of the lobule testis were established and protruded by tunica albuginea. Moreover, cross sections from the testis parenchyma were also revealed similar pattern. Basement membrane was obviously observed between germinal and interstitial compartments, respectively (Figures 4.5A, 4.5B)

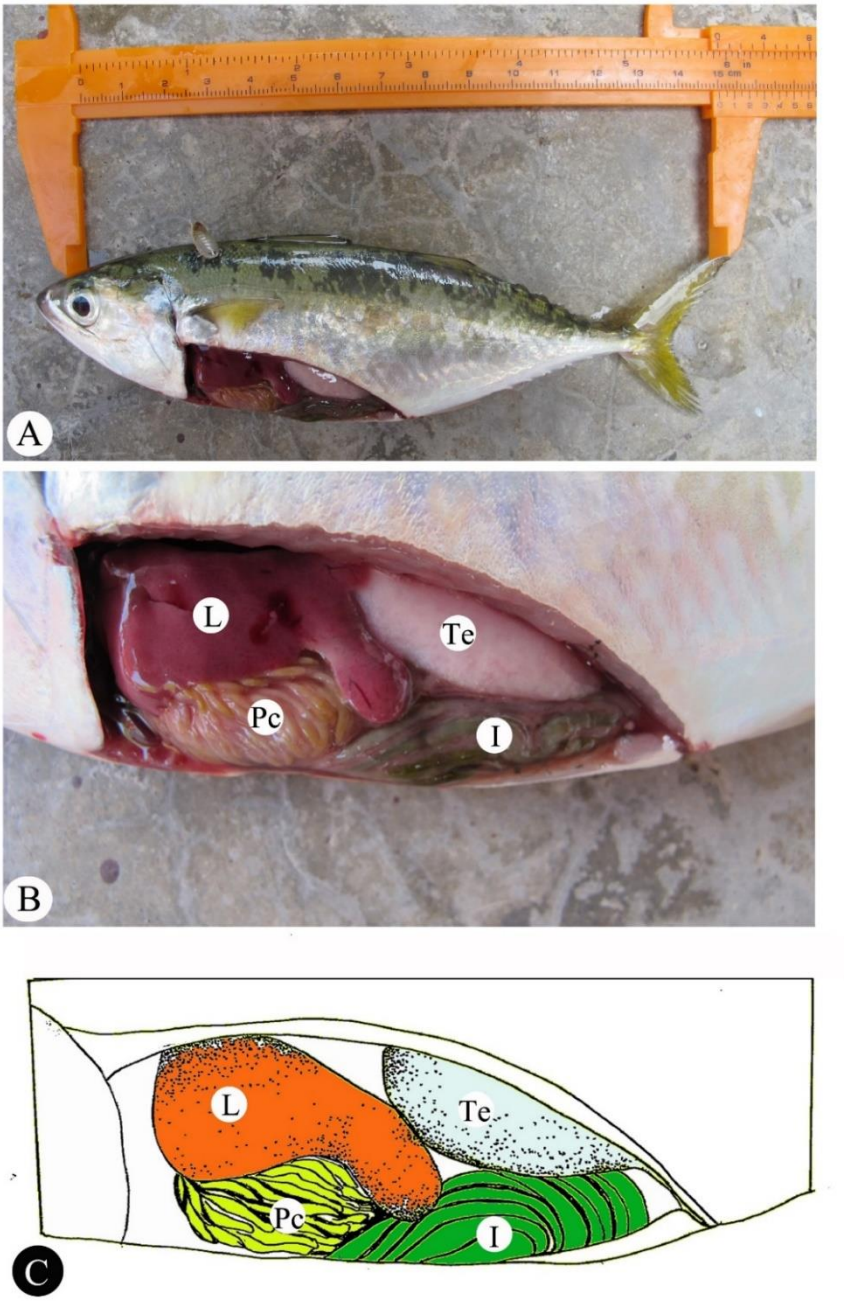

Figure 4.1 Gross anatomy and schematic diagerm of the testicular structure in *Rastrelliger brachysoma* (A-C). *I = intestine, L = liver Pc = pyloric caeca, Te = testicular tissue.*

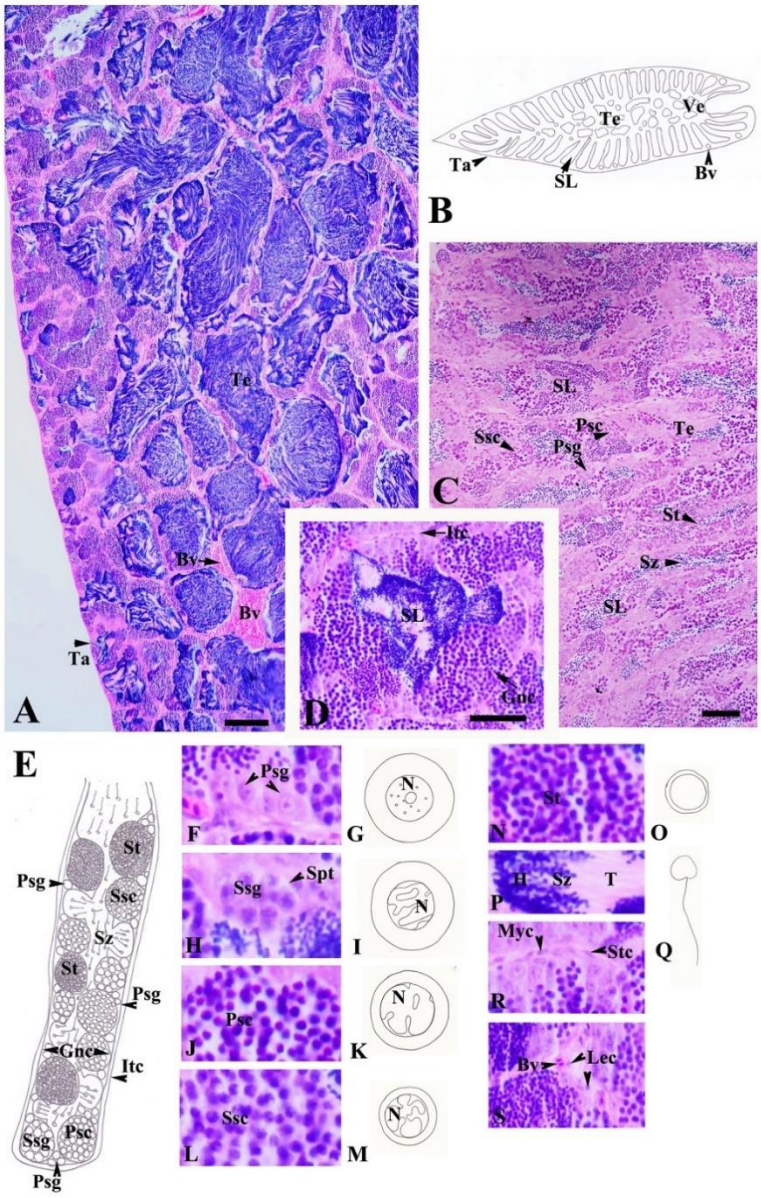

Figure 4.2 Light photomicrograph and schematic summary of testicular structure (A-E) and spermatogenesis (F-S) in *Rastrelliger brachysoma.* Scale bar; 100 µm (A, C, D).*Bv = blood vessel, Gnc = germinal compartment, H = head of spermatozoa, Itc = interstitial compartment, Lec = Leydig cells, Myc = myeoid cell, N = nucleus, Psc = primary spermatocyte, Psg = primary spermatogonia, SL = seminiferous lobule, Spt = spermatocyst, Ssc = secondary spermatocyte, Ssg = secondary spermatogonia, St = spermatids, Stc = sertoli cell, Sz = spermatozoa, T = tail of spermatozoa, Ta = tunica albuginea, Te = testis, Ve = vasa efferentia.*

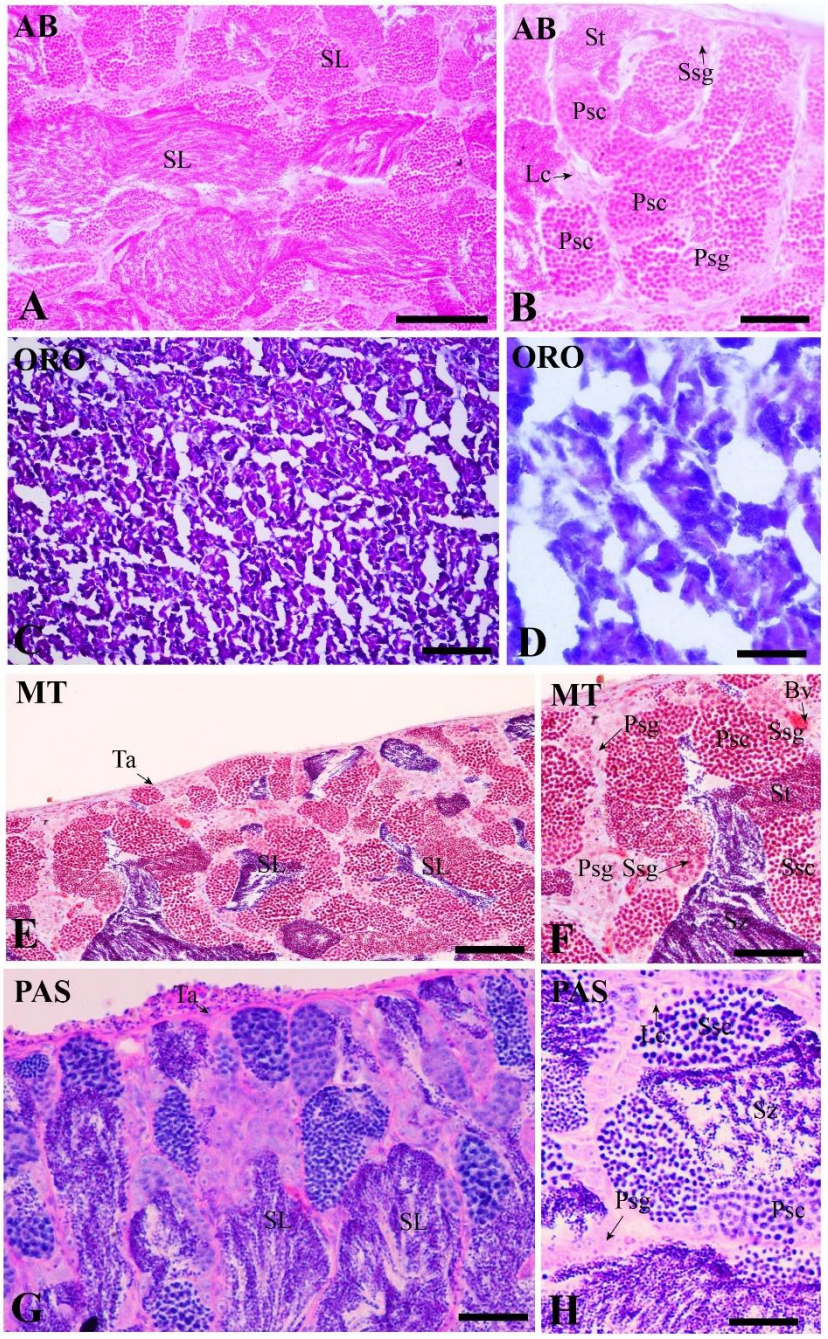

Figure 4.3 Light photomicrograph of testicular structure and spermatogenesis in *Rastrelliger brachysoma.* A-B based on alcian blue pH 2.5 (AB), C-D based on oil red O (ORO), E-I based on Masson's trichrome (MT) and H-J based on periodic acid-schiff (PAS). Scale bar: 100 µm (A, D, E, F, G, H), 50 µm (B, C, I, J). *Bv = blood vessel, Lc = Leydig cell, Psc = primary spermatocyte, Psg = primary spermatogonia, SL = seminiferous lobule, Ssc = secondary spermatocyte, Ssg = secondary spermatogonia, St = spermatids, Sz = spermatozoa, Ta = tunica albuginea.*

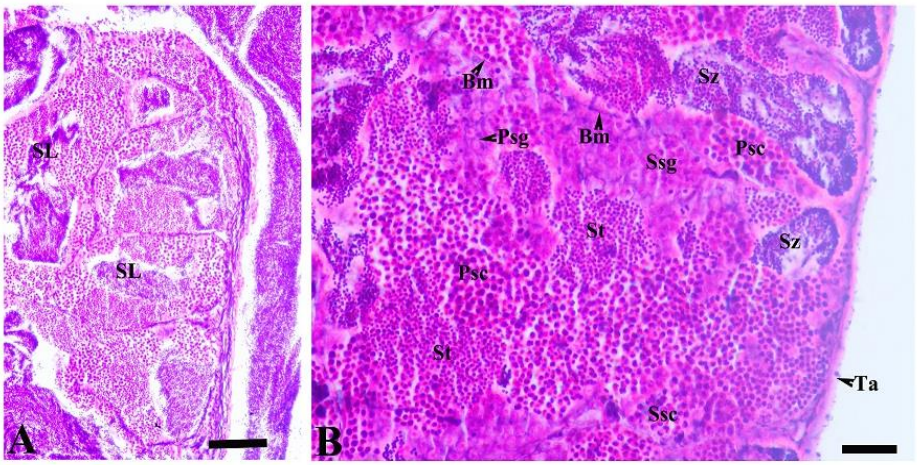

Figure 4.4 Light photomicrograph of testicular structure and spermatogenesis (A-B) in *Rastrelliger brachysoma*. Scale bar: 50 µm (A, B). *Bm = basement membrane, Psc = primary spermatocyte, Psg = primary spermatogonia, SL = seminiferous lobule, Ssc = secondary spermatocytes, Ssg = secondary spermatogonia, St = spermatids, Sz = spermatozoa, Ta = tunica albuginea.*

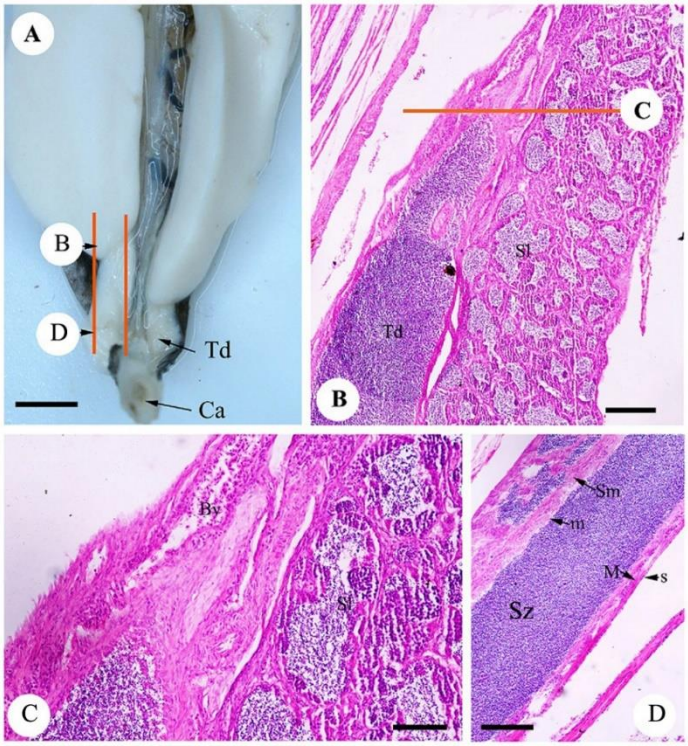

Figure 4.5 Morphology (A) and light micrograph of the testicular duct (Td) in *Rastrelliger brachysoma* (B-D). Scale bar: 0.3 cm (A), 200 µm (B), 50 µm (C-D). *Bv = blood vessel, Ca = cloaca, m = tunica mucosa, M = tunica muscularis, s = tunica serosa, Sm = tunica submucosa, Sl = seminiferous lobule, Sz = spermatozoa.*

Ultrastructure of spermatogenesis

Based on semithin section, normal testis of the adult *R. brachysoma* revealed that the lobular lumen in germinal compartment contained various stages of spermatogenic cells during the reproductive season. Ultrastructure evidences e.g., cytoplasmic morphology and chromatin condensation of the nucleus were observed with TEM. Spermatogenesis in this species could be classified into 4 successive stages as the following.

Spermatogonium (approx. 10-12 µm) was the largest male germ cells and occurred in small groups at the periphery of the seminiferous lobule (Figure 4.6A). TEM revealed that the spermatogonium was either slightly spherical or oval in shape. Its nucleus was large and prominent oval in shape, which occupied by the presence of the fine granular chromatin throughout the nucleoplasm. At this stage, a few cytoplasmic organelles such as several globular mitochondria were present (Figure 4.6B).

Primary spermatocyte originated mitotically from the spermatogonium. During the beginning of meiotic prophase, it was smaller than spermatogonia with approx. size of 8-9 µm (Figure 4.6C). Under TEM, the nucleus of primary spermatocyte was the central oval - shape and the nucleolus was not visible. At this stage, the nucleus was also contained densely packed chromatin as a heterochromatic nucleus (compared to spermatogonia). During pychytene stage under the meiotic division I, this was an increasing of the condensation of the heterochromatin among several synaptonemal complexes within the nucleus. The cytoplasm contained the endoplasmic reticulum, the electron dense particles, nuage and several mitochondria that became irregular in shape

and electron dense matrix (Figures 4.6D, 4.6E). Intercellular bridge was observed at this stage.

Secondary spermatocyte was produced from the first mitotic division of primary spermatocytes. They could be identified at the structure level by having larger cysts when compared the previous stages, but they were rarely seen with seminiferous lobules. A characterization of the cell and nucleus were reduced in sizes (6-7 µm), when it compared with the primary spermatocyte (Figure 4.6F). Ultrastructurally, the identifying characteristic of spherical nucleus was the appearance of the heterochromatin pattern around the nuclear membrane. The cytoplasm was reduced and still contained a few organelles. Intercellular bridge also frequently connected adjacent secondary spermatocytes (Figure 4.6G). This stage gave rise to spermatids under meiotic division II.

Spermatid was seen under chromatin condensation and cytoplasmic organelles changes during spermatid differentiation that called spermiogenesis (Gwo et al., 1993, Lahnsteiner & Patzner, 1990). It could be classified into three morphological stages based on the modified criterion used in other families (Gwo et al., 1993, Manni & Rasotto, 1997, Quagio-Grassiotto & Oliveira, 2008). The early spermatid of spermiogenesis (approx. 4.0-4.5 µm) had a large and round nucleus shape (Figure 4.7A). Under TEM, remodeling of the chromatin condensation appeared, resulting in a granular-chromatin mass (Figure 4.7B). At this time, cytoplasmic organelles, such as spherical-mitochondria and centriole initially, accumulated at the posterior regions (data not shown). The intermediate spermatid showed that the chromatin condensation of nucleus transformed into a more compact form, when compared with the previous stage. Also at this stage, the sphere-shaped mitochondria were located near the posterior

region of the nucleus (Figures 4.7C, 4.7D). The late spermatid, the proximal centriole was located within the nuclear fossa. Their flagellum axoneme which was arranged by mitochondria and was located the midpiece. They were also separated from the flagellum by the cytoplasmic canal (Figures 4.7A, 4.7E, 4.7F). The chromatin completely condensed throughout the nucleus due to the increasing of dense and thick chromatin granules. The cytoplasm started to degenerate. The residual bodies in a various sizes and shapes were also found in the cytoplasm (Figure 4.7G).

Spermatozoon, the mature spermatozoon had three distinct regions: a head, mid-piece and tail region (flagellum). Based on our observation, the spermatozoon of *R. brachysoma* had characteristic of those belonging to the primitive type, named aquasperm primitive type. If it is considered based on sperm characterization as follows to van der Straten et al. (2006), it will be classified as Type II. The asymmetrical head region appeared as ovoid nucleus, about 2-3 µm in length and 3-4 µm in width, due to the extreme granular chromatin condensation with an acrosome-less head in the anterior region. The short mid-piece was cylindrical with approximately 0.5 µm. Inserted in the mid-piece, the centriolar complex was present outside the shallow nuclear fossa in bell-shape of ultrathin sections which was composed of the (i) proximal centriole was near the nucleus envelope and (ii) distal centriole giving rise to the sperm flagellum. This region completely composed of several spherical mitochondria (approx. 0.5-0.7 µm) which were irregular cristae and moderately electron-dense. The sperm tail (flagellum), without lateral fins of this species, was estimated about 15-18 µm. It was mainly consisted of nine triplet's doubles of peripheral microtubules and two central singlet microtubules. Thus, each axonemal pattern of the flagella has a typical 9+2 arrangement of microtubules as typically presented in primitive species. In a cross section of mid-

piece was interconnected by Y-shaped bridge with enclosing by a flagellum plasma membrane and the flagella had no lateral fins were exhibited (Figures 4.7B, 4.7G, 4.8A, 4.8G, 4.9).

During the reproductive season, somatic sertoli cell and perilobular myoid cell were also observed. The localization of somatic sertoli cell was exclusively found in the periphery of the lobule and around the spermatogonia, sertoli cell occurred within the germinal compartment of the spermatogonia. Under light microscope, they were difficult to identify (Figure 4.10A) but they had a triangular or oval shape which nucleus was regular oval with scatting dense heterochromatin under TEM (Figure 4.10B). Also, the cytoplasm specially contained a few glycogen and several residual bodies which could be classified into two types: laminar bodies and lipofuscin pigments (Figure 4.10C). Therefore, this characterization underwent active phagocytosis. Several mitochondria and rough endoplasmic reticulum were observed. Each cell was joined by desmosome and tight junctions. Perilobular myoid cells were present near somatic sertoli cell (Figure 4.10A). Ultrastructurally, they had irregular shape with containing oval or irregular nucleus. The cytoplasm of this cell was mainly filled the high concentration of contractile filaments. Mitochondria and caveolae-like vesicles were commonly found in this cell (Figure 4.10D). Each cell was joined by hemidesmosome junctions.

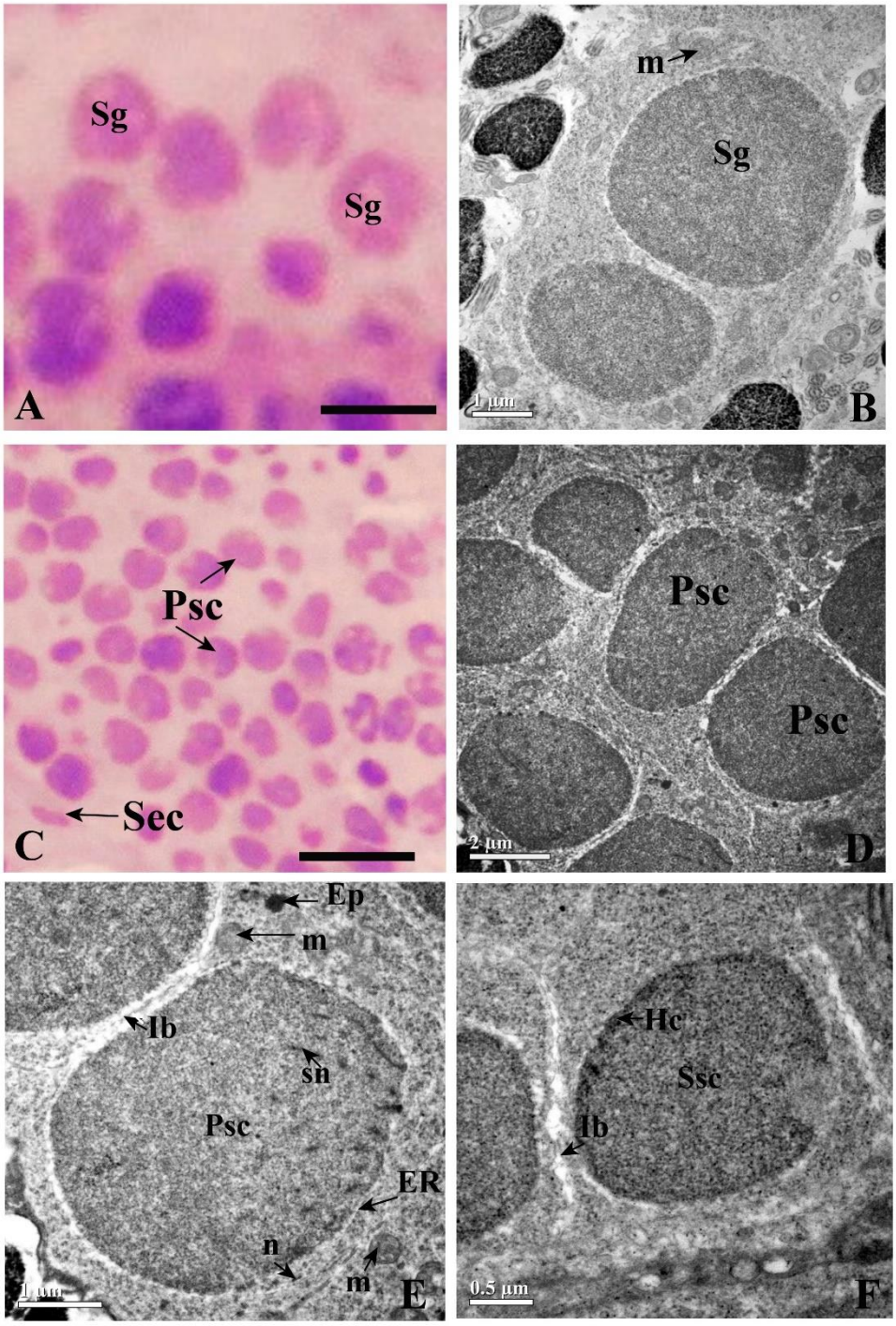

Figure 4.6 Photomicrographs and transmission electron micrographs of spermatogenesis showing different types of male germ cells. A and B spermatogonia (Sg), C-E primary spermatocyte (Psc), F and G secondary spermatocyte (Ssc). Scale bar A = 25µm; C and F = 20µm. *Ep = electron dense particle, ER = endoplasmic reticulum, H = heterochromatin, Hc = patch of herterochromatin, Ib = intercellular bridge, m = mitochondria, n = nuage, Sec = somatic sertoli cell, Sn = syntoplasmic complex.*

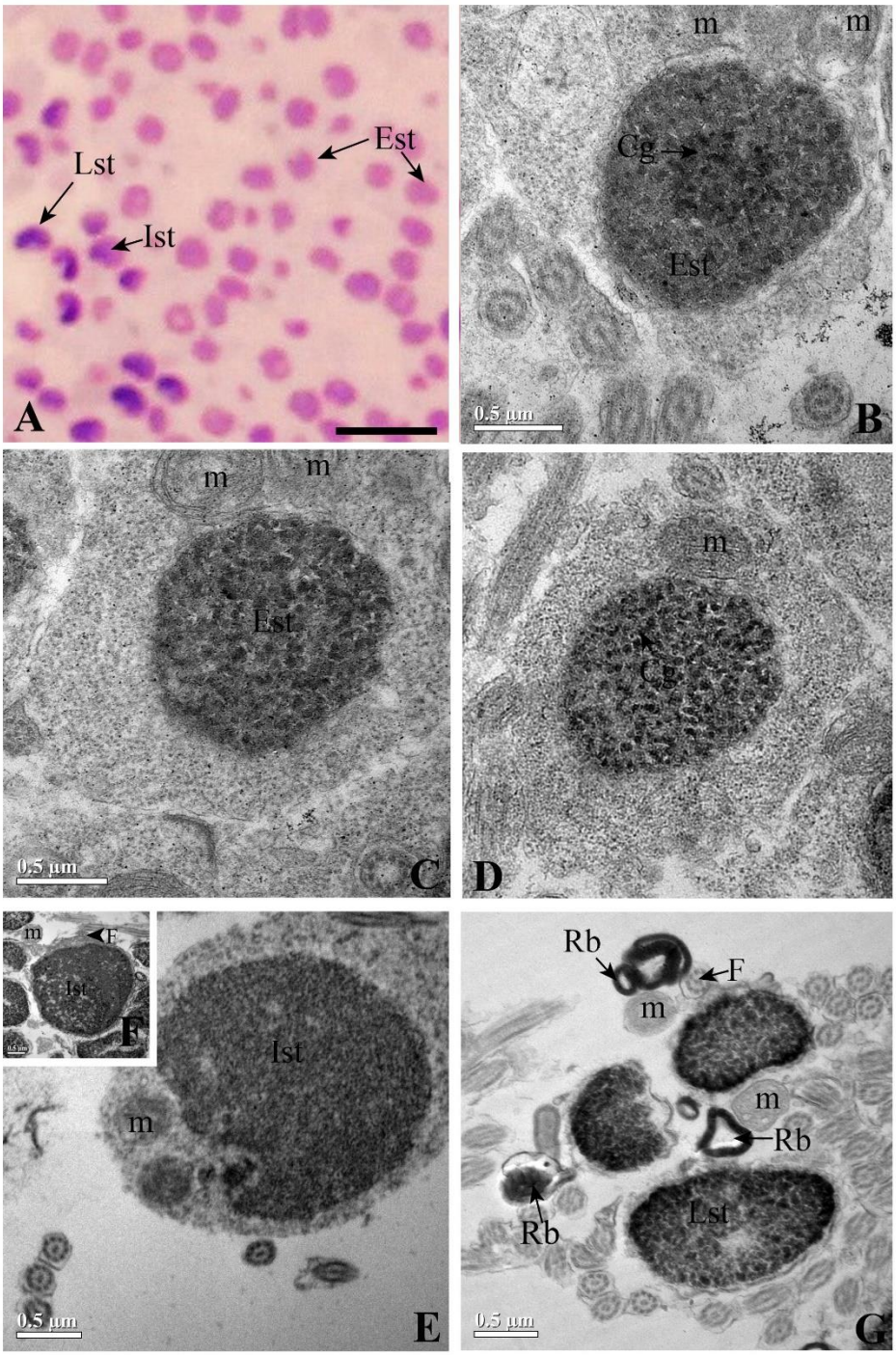

Figure 4.7 Photomicrograph and transmission electron micrographs showing different stage of spermatids. A semithin section of various spermatids, B and C early spermatids (Est), D-F intermediate spermatids (Ist); G late spermatids (Lst). Scale bar A = 25 µm. *Cg = chromatin granule, F = flagella, m = mitochondria, N = nucleus, Nf = nuclear fossa, Rb = residual bodies.*

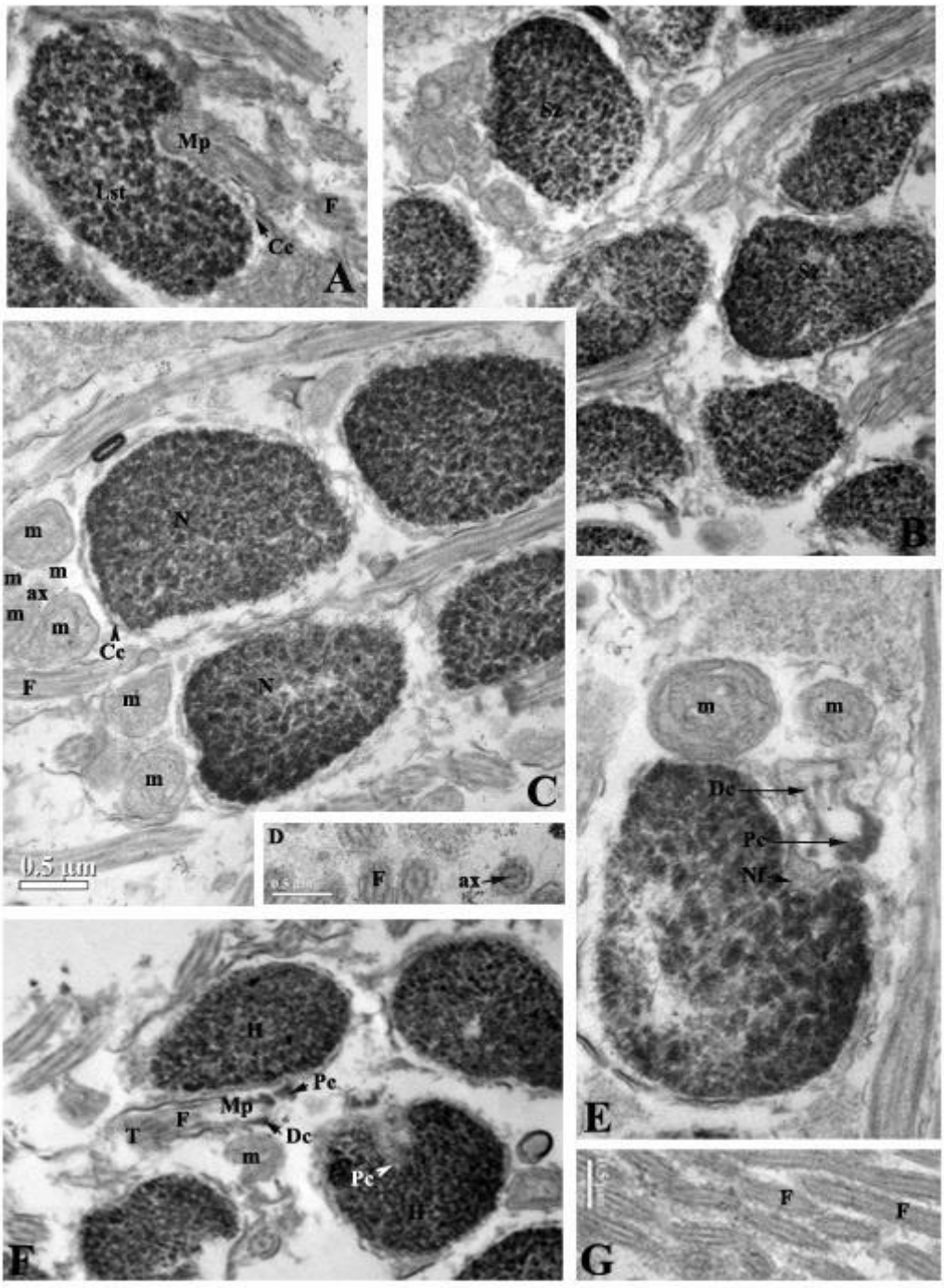

Figure 4.8 Transmission electron micrographs showing spermatozoa (Sz). A late spermatids, B-G the characterization of spermatozoa. *ax = axoneme, Cc = cytoplasmic canal, Dc = distal centriole, F = flagella, H = head, m = mitochondria, Mp = mid-piece, N = nucleus, Nf = nuclear fossa, Pc = proximal centriole, T = tail.*

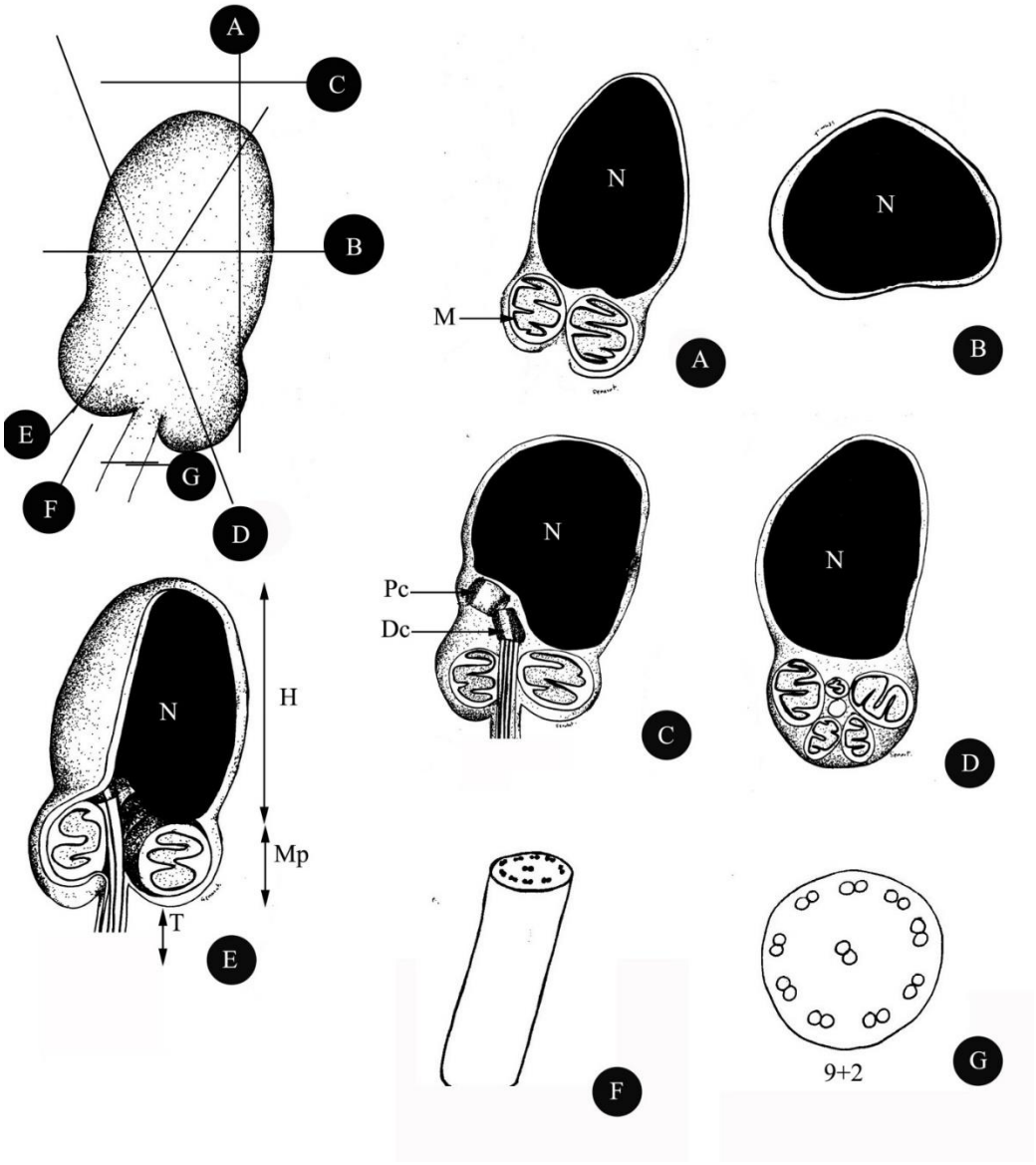

Figure 4.9 Schematic several sections showing the characterization of spermatozoa. *Dc = distal centriole, H = head, M = mitochondria, Mp = mid-piece, N = nucleus, Pc = proximal centriole, T = tail.*

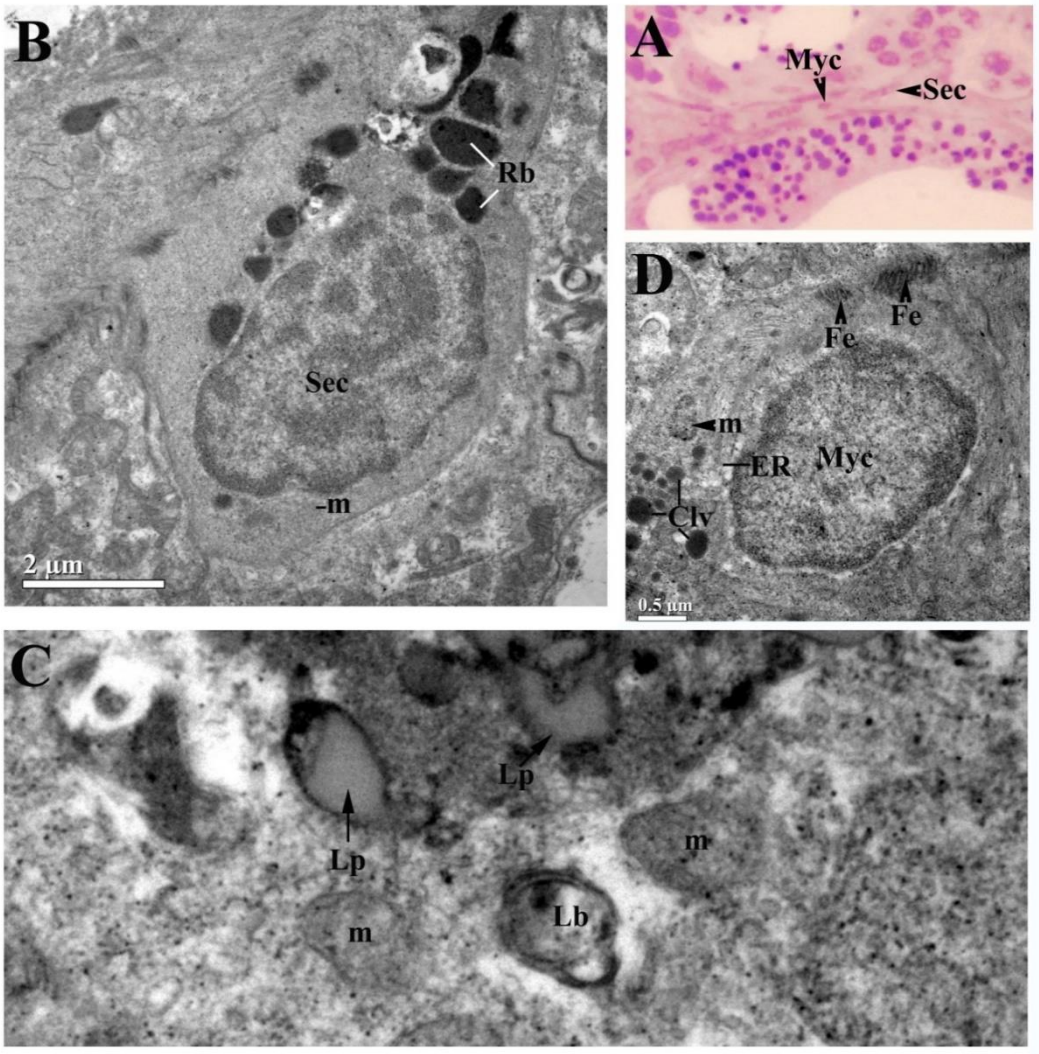

Figure 4.10 Photomicrograph and transmission electron micrographs showing somatic sertoli cell (Sec) and perilobular myoid cell (Myc). A semithin section of somatic sertoli cell and perilobular myoid cell. B-C the characterization of somatic sertoli cell containing various types of residual bodies (Rb), laminar bodies (Lb), lipofuscin pigments (Lp). D the characterization of perilobular myoid cell containing caveolae-like vesicles (Clv), endoplastic reticulum (ER), filaments (Fe), mitochondria (m).

Discussion

Structure of testicular tissue and spermatogenic stages

The testicular parenchyma consists of two parts, the germinal and interstitial compartments. The lobular testis in germinal compartment was the first reported in *R. brachysoma* in this study, quite similar to those of scombridae group such as *Thynnus thynnus* (Abascal et al., 2004), *Scomber japonicas* (Nyuji et al., 2012b) and *Rachycentron canadum* (Brown-Peterson et al., 2002). The testicular structure of this fish was also classified as an unrestricted spermatogonial type due to the presence of spermatogonia along the germinal compartment. It has been commonly observed in most teleost fish, except the atherinomorphs (Dietrich & Krieger, 2009, Grier, 1993, Parenti & Grier, 2004). The detection of polysaccharides and proteins of PAS reaction in the interstitial compartment was presented in the *R. brachysoma*. They were suggested that they concerned the synthesis and secretion of sugars and proteins. Moreover, two mainly cell types were seen within the interstitial compartment, both perilobular myoid cell and steroidogenic Leydig cells. The perilobular myoid cells were also found, which similar to those of teleost fish (Billard, 1970, Grier et al., 1989). Its functions concerned the contractile of the sperm in environment during spawning within seminiferous lobules (Billard, 1970, Grier et al., 1989). The steroidogenic Leydig cells were also mainly presented as cluster cells (about 4-5 cells) near blood vessels, as like other teleost fishes (Billard, 1983, Dietrich & Krieger, 2009, Nagahama, 1983). Its function has been reported in teleost fishes, including *Synbranchus senegalensis*, *Padogobius martensi* (Cinquetti & Dramis, 2003) and *S. marmotatus* (Nostro et al., 2004), which were investigated by histochemical analysis. All these

studies were strongly positive to 3β-hydroxysteroid dehydrogenase and were confirmed to produce the androgens inside the testis.

In the germinal compartments, this part was composed of various seminiferous lobules including somatic Sertoli cells and spermatogenesis agreed with the previous reports (Billard, 1992, Dietrich & Krieger, 2009, Nagahama, 1983). Additionally, seminiferous lobules of *R. brachysoma* also showed PAS positive, indicating the secreting fluid that may be composed of neutral glycoproteins, acid glycoconjugates, acid carboxylate and sialomucins (Santos et al., 2010). The cytoplasmic processes of the somatic sertoli cells surrounded each spermatocyste as a cyst-liked structure where were contained many different stages of spermatogenesis (Billard, 1992, Dietrich & Krieger, 2009, Nagahama, 1983) as those of *R, brachysoma*. As to the functions of somatic sertoli cells, they were concerned with metabolites transport (Billard et al., 1982, Grier, 1975) and phagocytosis of residual bodies and degenerating germ cells, including residual sperms (Grier, 1993, Grier & Taylor, 1998) Though, the characterizations of spermatogenesis like the spermatogenic stages (except primary spermatogonium and spermatozoa) were presented within spermatocysts. The present result differed from that of García-López et al. (2005), who reported that only primary and secondary spermatogonia were presented in the spermatocysts. At the final stage, spermatozoa were centrally located in the seminiferous lobules before they released into environment, similar to that described in *Thunnus obesus* (Hashimoto et al., 2003). This stage started the beginning of the fertilization.

Ultrastructure of spermatogenic stages

Ultrastructural features of spermatogenic stages are interestingly seen in teleost fish (Fishelson et al., 1990, Quagio-Grassiotto & Oliveira, 2008). Initially, the spermatogonium of *R. brachysoma* was a large cell. Dense osmiophilic material or nuage was also normally occurred at this stage and scatted throughout the cytoplasm, as reported in different species of fishes such as *Poecilia reticulata* (Billard, 1984), *Oryzias latipe* (Hamaguchi, 1993) and *T. thynnus* (Abascal et al., 2004). However, nuage structure in this species was the smallest structure and it could be the first found in primary spermatocyte which was unclear throughout this research. It was possible that ultrasection (approx. 90 nm) in this study was still too thick resulting in losing the detail of spermatogonia stage. This particular feature involving origin and function associated with the synthetic activity of spermatogenic step due to composing the ribonucleoproteins and mRNA (Hamaguchi, 1993, Nostro et al., 2003). After mitosis, the spermatogonia successively became primary spermatocytes. The characterization of the *R. brachysoma* primary spermatocytes was similar to other teleost fishes (Bhatti & Al-Daham, 1978, Bruslé, 1981). The nucleus of primary spermatocyte contained high dense chromatin (compared to spermatogonia) and the synaptomemal complexes, particularly pachytene phase. This structure was basically presented in *Piaractus mesopotamicus* (Romagosa, 1991) and *T. thynnus* (Abascal et al., 2004). On the other hand, secondary spermatocytes in *R. brachysoma* were rarely observed. This was similar to those found in several teleost fishes, probably due to their short-term appearance under rapidly dividing (Bhatti & Al-Daham, 1978, Bruslé, 1981, Burke & Leatherland, 1984, Grier, 1976). Another intercellular bridge, referred the cytoplasmic bridge was normally observed connecting during spermatogenic stage (Billard, 1984,

Selman & Wallace, 1986). Their bridges were found through spermatocytes to spermatids in this fish.

During spermiogenesis, spermatids were differently found under chromatin condensation and cytoplasmic organelles changes (Gwo et al., 1993, Lahnsteiner & Patzner, 1990). The developmental pattern of spermatid in this fish could be prominently classified into three morphological stages; early, intermediate (referred to middle) and late spermatids, following the modified criterion from other family fish (Lahnsteiner & Patzner, 1990, Manni & Rasotto, 1997, Quagio-Grassiotto & Oliveira, 2008). At the beginning of spermiogenesis, the early spermatid of this fish was characterized to condense as granular-chromatin mass and the nucleus was completely condensed in the late spermatid. These features have been documented in teleost fish (Bruslé, 1981, Gwo et al., 1993, Sprando & Russell, 1988, Todd, 1976).

Finally, the pattern of spermatozoa morphology could be distinctly classified into two types based on the external and internal mode of the fertilization of the fishes (Jamieson & Leung, 1991, Jamieson & Grier, 1993). The spermatozoa ultrastructure of *R. brachysoma* had characteristic of that belonging to the primitive type, named aquasperm primitive type, which preferred to an external fertilization, according to descriptions by Jamieson & Leung (1991), similar to *Makaira indica* (van der Straten et al., 2006) and *T. thynnus* (Abascal et al., 2002). The introsperm type differed from internal fertilization type which had elongated head and complicated mid-piece structure (Lahnsteiner & Patzner, 1990). So, the type of spermiogenesis was established to type I and II in this present study with similar with the report by van der Straten et al. (2006). In *R. brachysoma*, the spermatozoon is considered to the type II because of the shallowness of the nuclear fossa and nucleus outsides the fossa. This type was

evolutionarily more advanced than the type I sperm (Jamieson & Leung, 1991). A similar appearance had been described in scombrid group; Trichiuridae-*Trichiurus japonicus* (Hara & Okiyama, 1998), Scombridae-*S. australasicus* and *S. japonicus* (Hara & Okiyama, 1998), *S. japonicas* and *S. tritor* (Mattei, 1991) and *E. alletteratus* and *T. thynnus* (Abascal et al., 2002). Other sperm characterizations of *R. brachysoma* included the asymmetrical morphology of the head appeared as an ovoid nucleus with an acrosome-less in the anterior region, very similar to several scombrid species (Mattei, 1991) such as *T. thynnus* (Abascal et al., 2002). It was well understood that its acrosome-less head was correlated with an egg micropyle (Chung, 2008, Romagosa et al., 1999). Short mid-pieces were presented with several spherical mitochondria. This result agreed with the study in spermatozoon of *S. australasicus* (Hara & Okiyama, 1998), *Spiraea japonica* (Hara & Okiyama, 1998) and *T. thynnus* (Abascal et al., 2002).

An asymmetric uniflagella was described here similar to those described in most of the teleost species, *S. tritor* (Mattei, 1991), *E. alletteratus* (Abascal et al., 2002), *S. australasicus* (Hara & Okiyama, 1998) and *S. japonicas* (Hara & Okiyama, 1998, Mattei, 1991). On the other hand, biflagella was only found in few teleost, such as *Ictalurus punctatus* (Poirier & Nicholson, 1982), *Malapterurus* sp. (Mattei, 1988) and *Pimelodidae rhamdiasapo* (Jamieson & Leung, 1991). The flagellum of this species consisted of nine triplet's doubles of peripheral microtubules and the two central singlet microtubules. Thus, each axonemal pattern of the flagella in this fish was a typical 9+2 arrangement of microtubules as typically presented in primitive species(Romagosa, 1991).

Generally, the function of somatic sertoli cell concerned the nutrition, phagocytosis and steroidgenesis (Gresik et al., 1973). The ultrastructure of sertoli cell

was changed during the reproductive season, possible that the materials within cytoplasm were correlated with reproductive function. A few glycogen particles were found, as like in *Boleophthalmus pectinirostris,* which these particles were concerned with spermatid nutrition during spermiogenesis (Chung, 2008). However, the study about nutrient during spermatids is unclear. Moreover, somatic sertoli cells in some fish displayed ultrastructural feature which the change related to gametogenic cycle (Cinquetti & Dramis, 2003). Testicular tissue was distinctly observed during regression as well as spermiation. Therefore, residual bodies normally observed, indicated the phagocytic function. This was also reported in several teleost (Grier et al., 1980) as well as in mammals (Fawcett, 1975). Perilobular myoid cells, which its function concerned the synthesis of the basement membrane (Skinner, 1991), did not degenerate during season. This is also found in many studies (Cinquetti, 1994, Cinquetti & Dramis, 2003). Moreover, contractile network could facilitate the ejection of sperm from the lobules during spawning (Grier et al., 1980) because it exclusively contained the filamentous microfilament. This information was similar to our observations. Therefore, on the basis of fine structure of perilobular myoid cell in this fish directly correlated with its spermiation.

Conclusion

This study analyzed the histological and histochemical characteristics of the testicular tissue in *R. brachysoma*, a commercial importance marine fish in Thailand. The present result is considered the first report about the spermatogenic stage under light and electron microscopic level. It is also the important information for the

phylogeny and systematics, which will be applied or used for the development of aquaculture technology.

Chapter V
ANATO-HISTOLOGY OF THE BRAIN IN THE SHORT MACKERAL, *Rastrelliger brachysoma* (Bleeker, 1851)

Introduction

Recent publications showed that the nervous system in fish is the important orans with multiple functional machnism to response in both internal and external envionments (Genten et al., 2008). In many fishes for example *Scyliorhinus canicula* (Turkmen et al., 2007) and *Epinephelus coioides* (Savari et al., 2013), two majors division including the central nervous system (CNS) and the peripheral nervous system (PNS) were observed in the nervous system. The CNS is also consists of the brain and spinal cord with containing the spinal nerve and ganglia. Defining the precise of the characterization and anatomy of the fish brain is well-estrablised due to its reflecting to lifestyle and specific function such as motor coordination, behavior and metabolic regulation (Butler, 2011). Many studies have also been made that the relationships between size and development of brain structure is particularly recommended in some fishes (Bauchot et al., 1977, Kotrschal & Junger, 1987), that is, large brains is demonstrated that this feature has been serves with multiple factors in habitat complexity or locomotor performance (Bauchot et al., 1977, Bauchot et al., 1988, Northcutt, 1981). As noted by Kotrschal & Junger (1987) reported that the relative development of the telencephalon and the cerebellum is particularly related to differences in microhabitat. Similar study in term of the large telencephalon in fishes, although the function of this area is little known, it has been recently related and lived in spatially structured environments (Huber et al., 1997).The enlarge telecephalon in

both *Carcharhinus falciformis* and *C. hippurus* may be correlated to behaviors for example pair formation and communication (Bshary et al., 2002, Kotrschal & Junger, 1987), whereas the relative size of the cerebellum may be also related to locomotion and posture (Bauchot et al., 1977, New, 2001). Based on the histological observation of the brain, there were several studies examining telesost fish and it is consists of five regions including telencephalon, diencephalon, mesencephalon, metencephalon and myelencephalon, respectively. Intestingly, an important site of the dencephalon is correctly described and contained in both the hypothalamus and pituitary gland (Nagahama, 2000) where various hormones under the hypothalomo–pituitary–gonadal axis (HPG) are to stimulate gonad development and maturation in teleost fish (King & Millar, 1992, Sherwood, 1997), such as *Scomber japonicas* (Selvaraj et al., 2009), *Trachurus japonicas* (Imanaga et al., 2014, Nyuji et al., 2012a) and *Takifugu obscurus* (Yang & Chen, 2004).

The short mackerel, *Rastrelliger brachysoma* is one of the most important fishery resources in Thailand. Up to date, the increased over-exploitation and deterioration of their habitat is gradually caused a serious decline in the number of *R. brachysoma*. This fish has been, therefore, considered to be a marine fish species with the potential for aquaculture. During this time, the Samut Sakhon Fishery Research Station, Samut Sakhon Province has set up for a breeding project for this fish. The goals were to increase the number of fish in the wild and to optimize the fisheries management of the natural habitat. Early culture techniques used with *R. brachysoma* in the late 2011indicated that it was quite successful. In contrast, several problems have been gradually increasing particularly the low success rates of larval stages and gonadal

disorganization. Another finding was that the major source of sexually mature fishes was located in the Upper Gulf of Thailand.

A review investigation of the hatchery condition for broodstocks generally caught from wild population showed endocrinological dysfunction preventing completion of the reproductive system, such as reduction of gonadosomatic index (GSI) and decrease in the quality and quantity of the germ cells. These changes may be influenced by the lack of gonadotrophin releasing hormone (GnRH) that is synthesized and released from the brain into the pituitary gland for the stimulation and release of luteinizing hormone (LH) (Shiraishi et al., 2005, Zohar & Mylonas, 2001). A need to report the basic knowledge of anatomical and structural details of the central nervous system is important, and primarily required before investigating the regulation of neuroendocrine mechanism, especially the GnRH as the master signaling neuroendocrine decapeptide and the central regulator for controlling reproductive growth of the fishes (Zohar et al., 2010).

The intent of this study was to describe the basic anatomy and histological structure of the central nervous system (CNS) and special sensory organ in the sexually matured, *R. brachysoma* living in Upper Gulf of Thailand. This article provides information about the basic knowledge of the structural and cell components in the *R. brachysoma* CNS, as well as the special sensory orhans. Additionally, this information can be presented as reference material breeding aquaculture system, neurophysiology and neuropathology.

Materials and methods

Fish sampling

Sexually matured *Rastrelliger brachysoma* (approx. >16.5 cm in total length, n = 20) were used in our research and caught by bamboo strake traps in Samut Songkhram Province (Figure 5.1), the Upper Gulf of Thailand (13°16’18.4” N, 100°02’13.4” E) during breeding period (December 2013 to February 2014). The specimens were identified with the key (FAO, 2010). The experimental protocol was approved by the Animal Care and Use Committee of Faculty of Science in accordance with the guide for the care and the use of laboratory animals prepared by Chulalongkorn University (Protocol Review No. 1423003).

Gross anatomy and histological analysis

All samples were euthanized by rapid cooling method (Wilson et al., 2009). Then, their whole brains were anatomically observed to detail under stereo microscope. The brain and eye were carefully removed and fixed overnight in a solution containing Davidson's fixative at room temperature (Dietrich & Krieger, 2009) and dehydrated through a graded series of ethyl alcohol concentrations. They were then infiltrated and embedded in paraffin. A serial of 5-6 µm sections of the tissue blocks were cut by rotary microtome. The sagittal and cross sections were then histologically stained with Harris’s hematoxylin and eosin (H&E) (Bancroft & Gamble, 2008, Humason, 1979). Consecutive sections were histochemically stained with Masson's Trichrome (MT), Periodic Acid-Schiff (PAS) and Reticulin (RT) (Bancroft & Gamble, 2008, Humason, 1979). The general structure, together with the cell components of the brain and eye of

all slides, were identified under a light microscope and photographed with a Canon EOS 1100D digital camera.

Results and discussion

Neuroanatomic localization of the *R. brachysoma* brain

The central nervous system (CNS) of *R. brachysoma* is composed of a brain, continuing to form the spinal cord (Figure 5.1), in agreement with the prior reports (Butler, 2011, Genten et al., 2008). Anatomy nomenclature of the *R. brachysoma* brain is basically embedded in the skull, and covered by meninx primita (meninges), seen under a stereo microscope (Figures 5.1a-5.1c). Five regional anatomies, including telencephalon, mesencephalon, diencephalon, metencephalon and myelencephalon, were also clearly described in the brain. Our observations were basically divided into 2 views; dorsal and ventral views. Our observations were divided into two views; dorsal and ventral views (Figures 5.1b-5.1c). In the dorsal view, similar to *Amia calva* (Northcutt, 1981), the largest part of the brain, optic tectum, was well-developed under the mesencephalon. It possible that this fish may be involves the important of vision in pelagic enviroment, as similar to other fishes including *Thunnus audax* and *Katsuwonus pelamis* (Brill et al., 1993, Cayré, 1991). The cerebellum of the metencephalon was moderately sized, located between the optic tectum and medulla oblongata. The feature may be related to important in motor coordination during swimming, which it is also always swimming clockwise in pelagic environment, as similar investigations such as *Rhyacichthys aspro* (Bauchot et al., 1989) and *Pseudopimelodus bufonius* (Abrahão & Shibatta, 2015). The telencephalic region of the cerebral hemispheres was situated anteriorly in the nostrils, followed by olfactory lobes. In the ventral view, the optic tract

and optic chiasma, connecting to the eye, were anteriorly located to the pituitary gland. The largest part of the hypothalamus, the inferior lobes, was situated in the center of the diencephalon. The large inferior lobes of the hypothalamus were seen in the middle of the diencephalon. Lastly, the myelencephalon contents, particularly the narrow medulla oblongata and vagal lobes, are the most posterior parts of the brain.

Figure 5.1 Sampling locality and bamboo strake trap from Samut Songkhram Province.

Histologic organization of *R. brachysoma* brain

Figures 5.2-5.7, showed the 5 main regions and histologically and histochemically identified in the brain, based on sections staining procedures. The telencephalon was first located anterior to the brain, and was less developed than that of other higher vertebrate (Harder, 1975). In the anterior part of the brain, *R. brachysoma* is composed of a pair of olfactory lobes, followed by a pair of cerebral hemisphere (cerebrum). Furthermore, the cerebral hemisphere structure of this fish was without a neocortex, and principally contained various interconnected neurons because it was supported by neurogila and neuronal fibers. Several studies have reported that the roles of this region were important in reproductive behavior, color vision and learning (Roberts, 2012). The diencephalon distinctly composed of 3 zones, including the dorsal epithalamus, the middle thalamus, and the ventral hypothalamus, was highly in accordance with other fishes (Genten et al., 2008, Sattari, 2002). The main role of this region involves maintenance of muscle, eye stimulation, and reproductive physiology (Genten et al., 2008). Note that the dorsal epithalamus was situated beneath the optic tectum, and comprised of the pineal complex and the habenular ganglion (data not shown), which are involved in coordinating outputs between the telencephalon and thalamus. A neuronal fiber of this region was also connected to the optic chiasma and retina, respectively (Roberts, 2012). Moreover, saccus dorsalis or tela choroidia, was seen in the dorsal-rostal evagination of the diencephalon roof. Its histological structure contained several fibers lining by the epithelial layer, covered by the meninx primitive. The basement membrane of this organ was also seen using RT staining method. In the thalamus, it was in the middle, located between tegmentum and the hypothalamus under the third ventricle. The hypothalamus is the most posterior region of the diencephalon,

being the major structural complex due to its function related to olfactory, gustatory and other sensory impulses seen in some other teleost (Genten et al., 2008, Groman, 1982). This region is ventrally located and consists of the infundibular region and the inferior lobes, as well as specialized appendages, including saccus vasculosus and pituitary gland, which are innervated in the hypothalamus. Form the results of histological studies, the saccus vasculosus was seen more obviously, and lined between the caudal parts of the inferior lobes of the hypothalamus, beneath the glomerular nucleus, referred to as nucleus glomerulosus. It contained several neurons, as similarly reported in *Scyliorhinus canicula* (Turkmen et al., 2007) and *Epinephelus coioides* (Savari et al., 2013). The succus vasculosus was histologically surrounded by a thin tunica albuginea, as well as a prominent connective tissue. Within its structure were several folded walls, consisting of blood sinuses as well as red blood vessels, were covered by pseudostratified cuboidal epithelium on the basement membrane. In this context, these epitheliums could also be classified into 2 epithelial cell types. The large of Coronet (crown) cells with basal nucleus were generally extended into the lumen. Globular expansions of the ciliary processes extended from the apical portion. The supporting cells, located with oval or triangular in shapes of the nucleus were principally located at the apical portion of the epithelial layer. Additionally, melanomacrophage centers (MMC) can be mostly observed in some areas of the succus vasculosus. The function of this organ is uncertain. However, Khanna & Singh (1967) stated that it was involved with the secretion of the acid mucopolysaccharides. In another hypothesis, Butler (2011) noted that it can also detect the water pressure. In regard to the hypothalamus-hypophyseal system, the pituitary gland in this fish species was attached to the infundibular stalk. This organ could be distinctly divided into 2

areas according to histological localization and cell types: neurohypophysis and adenohypophysis. The neurohypophysis could be easily distinguished due to the composition of hypothalamic neurosecretory neuronal fibers without cell bodies, blood sinuses and pituicytes. The adenohypophysis, consisting of several different cell types. However, the histological techniques used in this species were not able to investigate or classify the pituitary details. Another immunohistochemistry technique, using specific classification of cell types, is further required for pituitary analysis.

Under sagittal sections, the mesencephalon was the largest component in *R. brachysoma* brain. The wall of its structure was surrounded by a thin meninx primtiva containing several blood vessels. The optic tectumwas complex area was consisted of six histologically distinct layers including stratum marginale, stratum oa complex area, which consisted of 6 histologically distinct layers; stratum fibroetgricialem stratum album central, stratum griseum central and stratum periventriculae. Beneath the optic tectum was the third ventricle, surrounded by ependymal lining. In the metencephalon, the major component of this region was the cerebellum, which could also be prominently divided into 2 sub-regions; corpus and vulvula cerebelli. Note that in term of localization, corpus cerebelli was laid on the rostal zone of the optic tectum, whereas vulvula cerebelli projected forward under the optic tectum. However, the histological structure was similarly seen into 3 different layers based on histological organization including outer molecular, Purkinje cell and inner granular layers. An outer molecular layer contained parallel fibers, Purkinje cells dendrite (rounded or pear-shaped), and satellite cells. The inner granular layer contained small multipolar neurons as granule cells. In the rostral region the myelencephalon principally composed of medulla oblongata, as the stem of the brain

and the paired vagal lobes. In terms of function, this region is responsible to integrating the reticulomotor system, taste and auditory senses (Lagler et al., 1977). Another characterization of this region is that it was connected with the cerebellum to the diencephalon. The central canal, as well as the fourth ventricle (fossa rhomboidea), was found in the middle of the caudal medulla oblongata. This region was also covered by ependymal cells. The histological details of the medulla oblongata consist of neurons and different cell types. The neurogails were small cells with a few nucleuses, whereas Nissl bodies were basophilic cells, as well as big circular cells. Another pair of lobes, the vegal lobes, was evident in the dorsal medulla oblongata. Lastly, the spinal cord of this species was jointed and extended from medulla oblongata along the length of the body. The prominent feature of this region contained neurons, neuroglia, and the neuronal fibers. The nucleus in each neuron was oval shape, deeply surrounded by an eosinophilic cytoplasm.

Conclusion

This study revealed that the histological characterization of brain was basically similar to other fishes. It showed 5 regions, including telencephalon, mesencephalon, diencephalon, metencephalon and myelencephalon of the brain. Among its region, the two optic lobes of the mesencephalon were the largest part with six histologically distinct layers; stratum marginale, stratum opticum, stratum fibroetgricialem stratum album central, stratum griseum central and stratum periventriculae. Further, our investigation on the identification of neurotransmitters and neuropeptides as well as biomolecules in this species will be further observed.

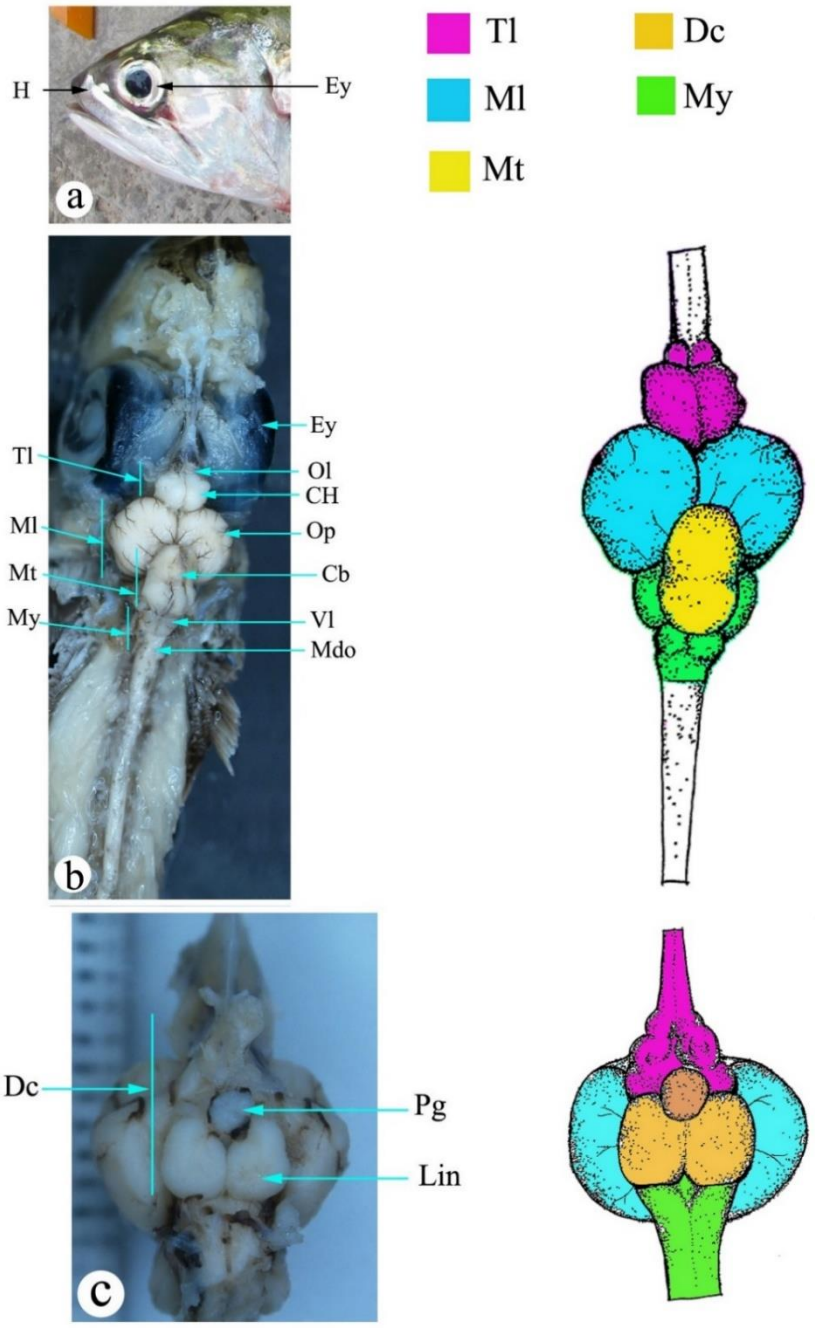

Figure 5.2 Neuroanatomy and schematic diagram of the brain in *Rastrelliger brachysoma* including telencephalon (Tl), mesencephalon (Ml), diencephalon (Dc), metencephalon (Mt) and myelencephalon (My) (a-c); *CH = cerebral hemisphere, Ey = eye, H = head, Lin = inferior lobe of hypothalamus, Mdo = medullar oblongata, Ol = olfactory tract, Op = optic lobe, Pg = piyuitary gland, Vl = vagal lobe. (b = dorsal region and c = ventral region.*

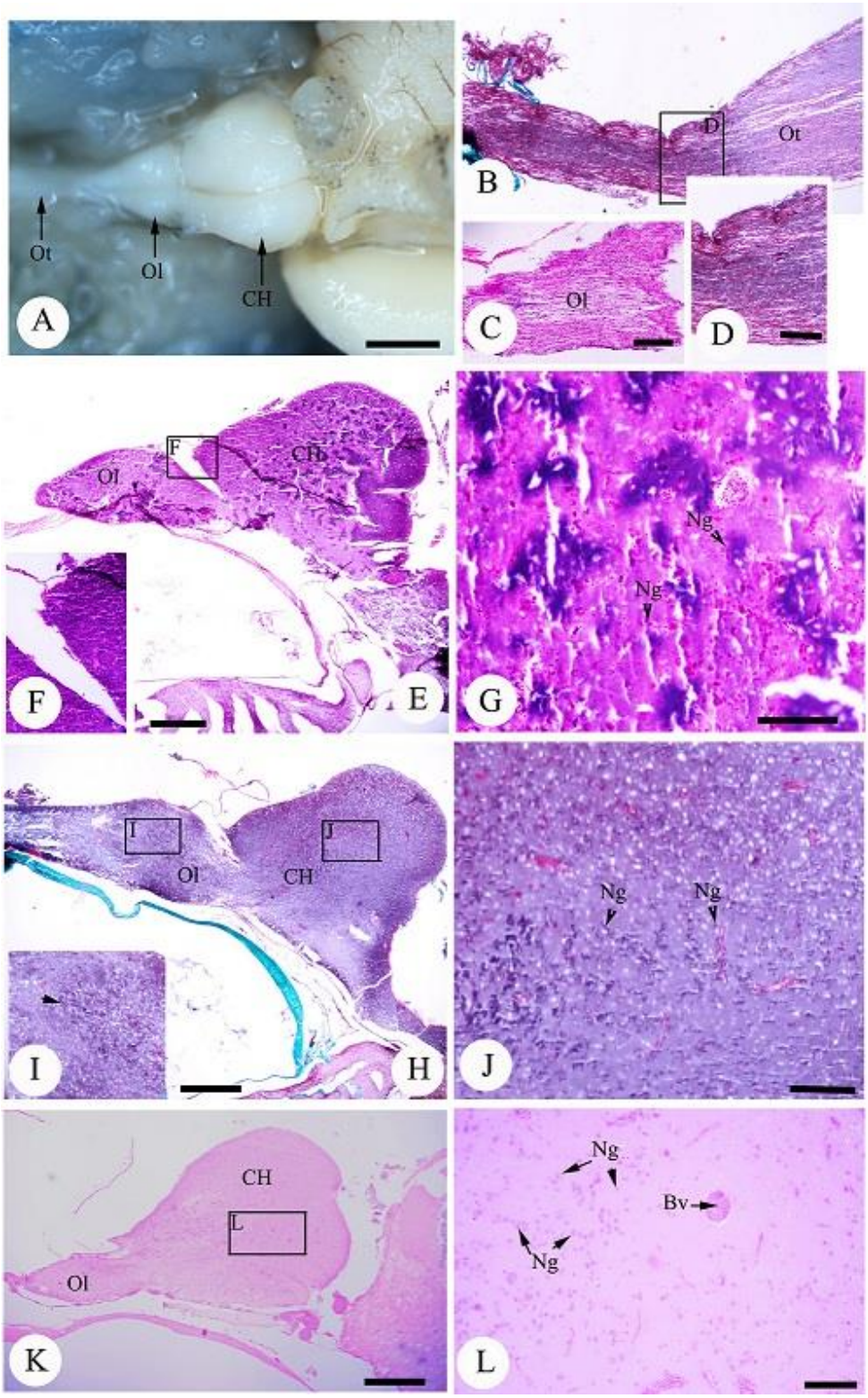

Figure 5.3 Neuroanatomy of the brain (A) and light micrograph (B-L) of telencephalon in *Rastrelliger brachysoma;* Scale bar: 200 μm (A, E, H, K), Scale bar: 20 μm (B, G, J, L)*; Bv = blood vessel, CH = cerebral hemisphere, Ng = neuroglia, Ol = olfactory lobe, Ot = olfactory tract.*

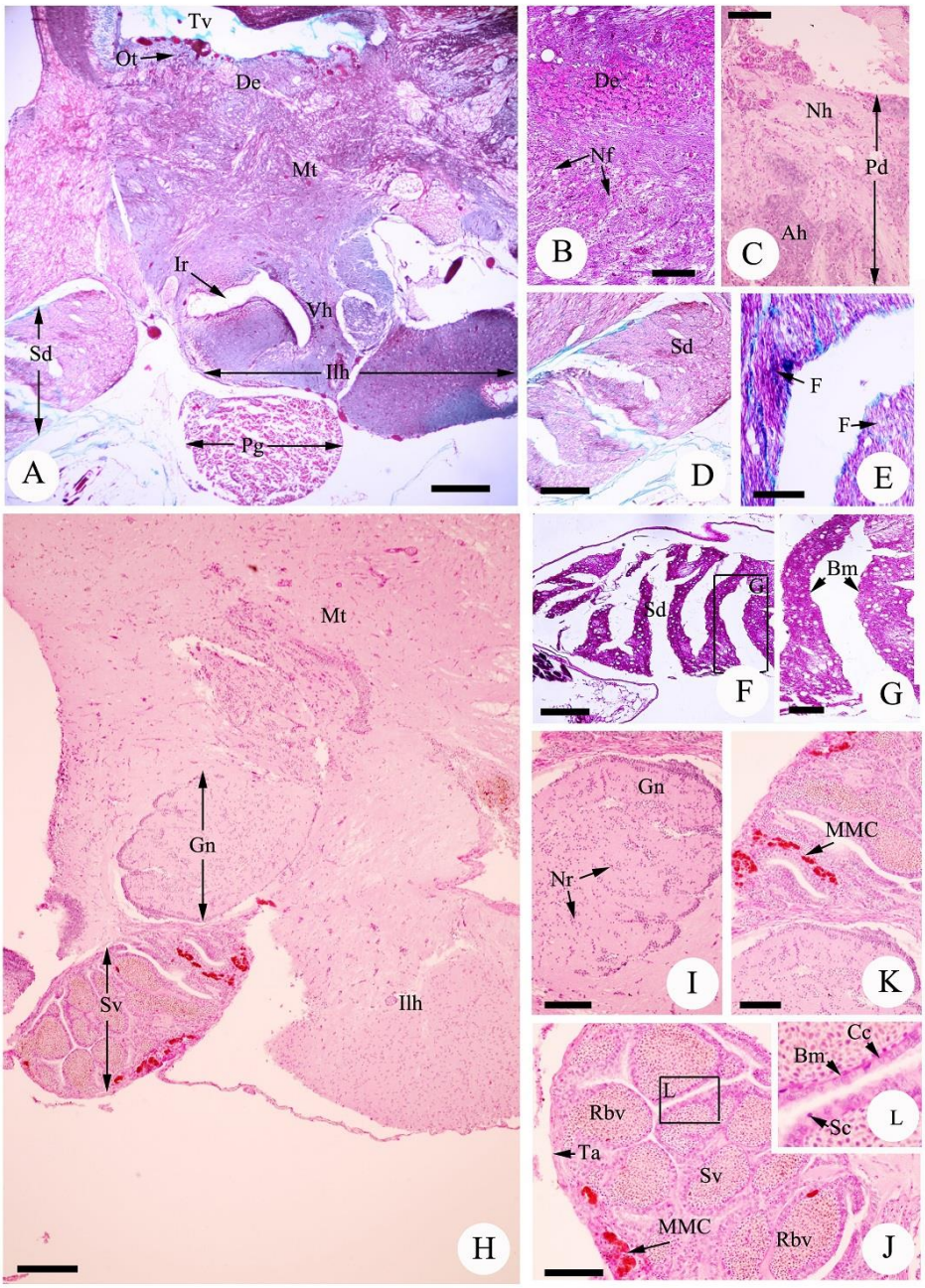

Figure 5.4 Light micrograph of diencephalon in *Rastrelliger brachysoma*; Scale bar: 200 µm (A,H), Scale bar: 20 µm (B-D, F, I-J), Scale bar: 10 µm (E, G, K). *Ah = adrenohypophysis, Bm = basement membrane, Cc = coronet cell, De = dorsal epithalamus, F = fiber, Gn = glomerular nucleus, Ir = infundibular recess, IIh = inferior lobe of hypothalamus, MMC = melanomacrophage center, Mt = middle thalamus, Nf = neuronal fiber, Nh = neurohypophysis, Nr = neuroglia, Ot = optic tectum, Pd = pituitary dorsal region, Pg = pituitary gland, Rbv = red blood vessel, Sc = supporting cell, Sd = saccus dorsali, Sv = saccus vasculosus,, Ta = tunica albuginea, Tv = third ventricle, Vh = ventral hypothalamus.*

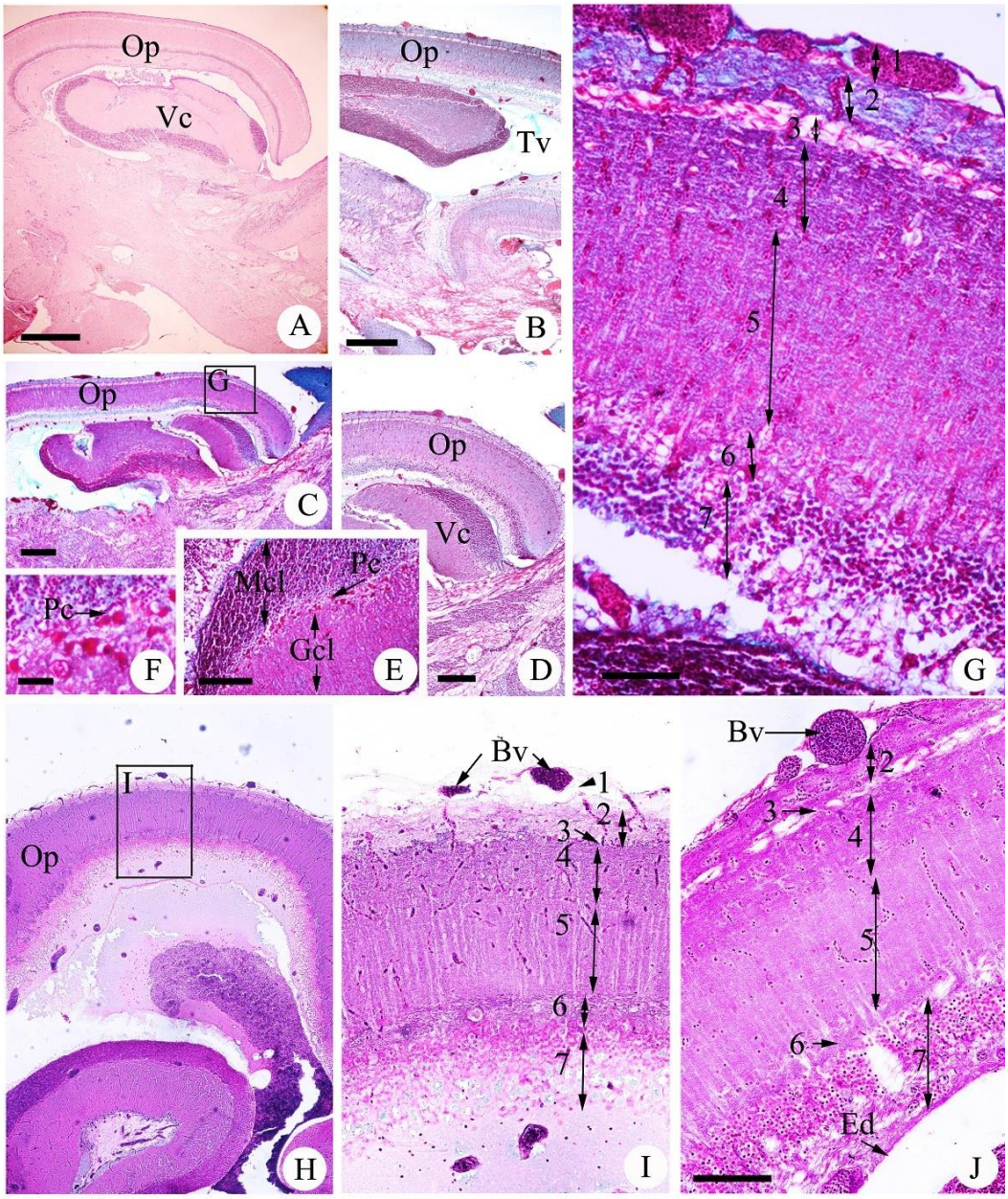

Figure 5.5 Light micrograph of mesencephalon and metencephalon in *Rastrelliger brachysoma*; Scale bar: 200 µm (A), Scale bar: 100 µm (B, H), Scale bar: 50 µm (C, D), Scale bar: 20 µm (E,G,J), Scale bar: 10 µm (F). *1 = Menix, 2 = stratum marginale,3 = stratum opticum,4 = stratum fibroetgricialem, 5 = stratum album central,6 = stratum griseum central,7 = stratum periventriculae, Bv = blood vessel, Ed = ependymal cell, Gcl = granulosa cell layer, Mcl = molecular cell layer, Op = optic lobe, Pc = PURKINJE cell layer, Tv = third ventricle, Vc = valvula cerebelli.*

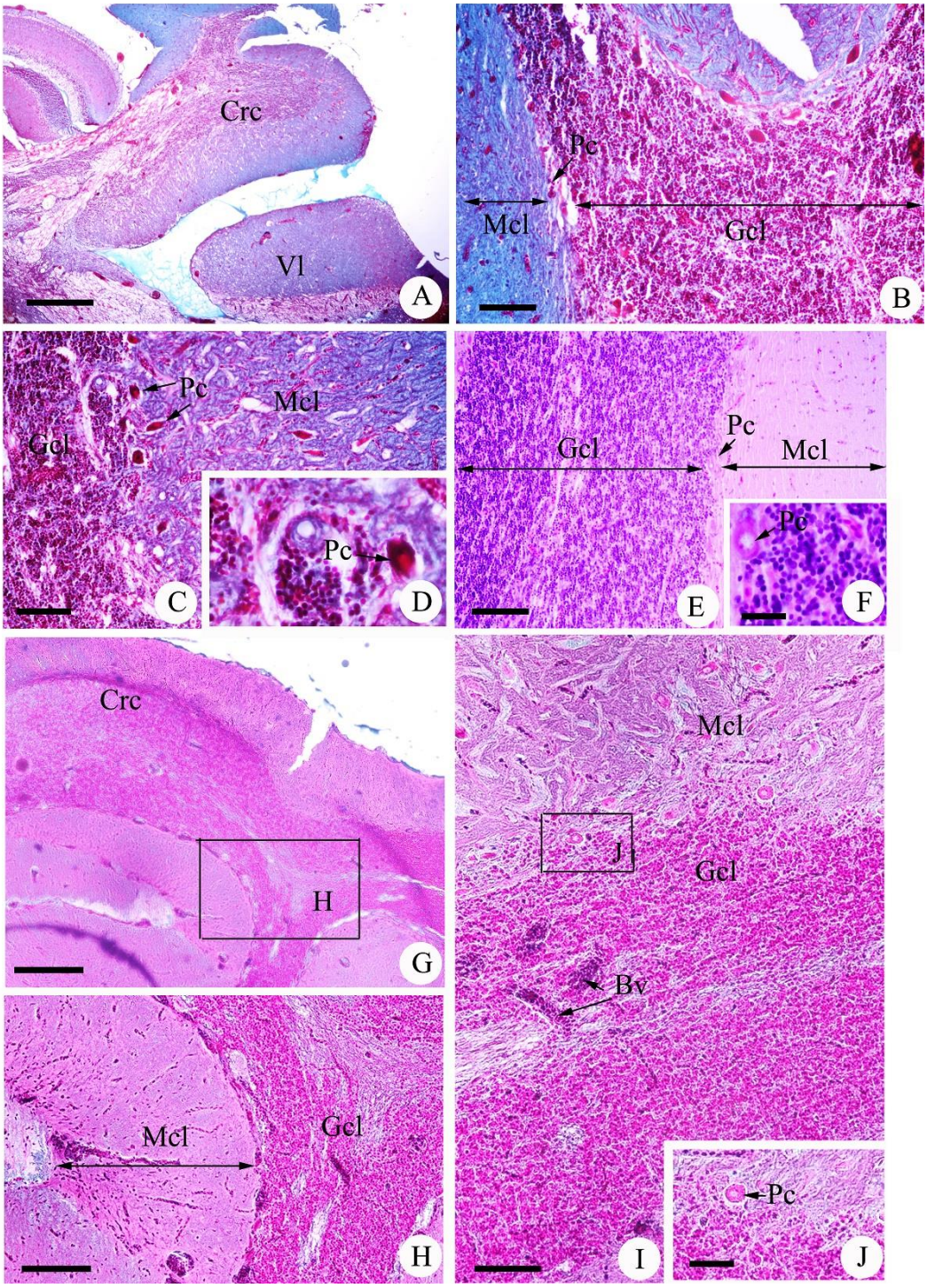

Figure 5.6 Light micrograph of metencephalon in *Rastrelliger brachysoma*; Scale bar: 200 µm (A), Scale bar: 100 µm (G), Scale bar: 20 µm (B, C, E, H, I), Scale bar: 10 µm (F, J). *Bv = blood vessel, Crc = corpus cerebelli, Gcl = granulosa cell layer, Mcl = molecular cell layer, Pc = Purkinje cell layer, Vl = vagal lobe.*

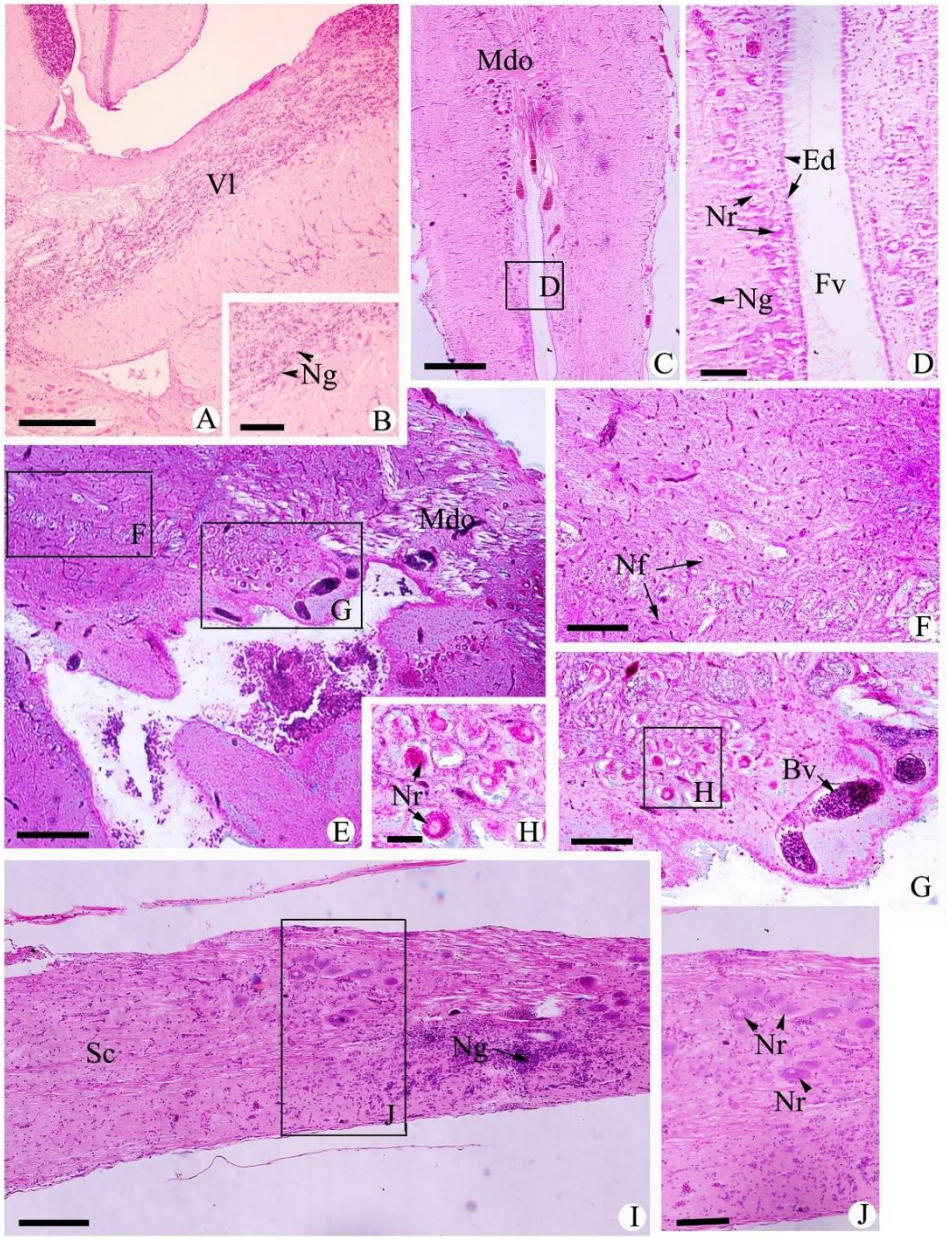

Figure 5.7 Light micrograph of myelencephalon and spinal cord in *Rastrelliger brachysoma*; Scale bar: 100 µm (A, E, I), Scale bar: 50 µm (C), Scale bar: 20 µm (D, F, G, J), Scale bar: 10 µm (B,H). *Bv = blood vessel, Ed = ependymal cell, Fv = fourth ventricle, Mdo = medullar oblongata, Nf = neuronal fiber, Ng = neuroglia, Nr = neurons, Sc = spinal cord, Vl = vagal lobe*

Chapter VI

DISTRIBUTION AND ALTERATION OF sbGnRH - GtH SYSTEM IN *Rastrelliger brachysoma* (Bleeker, 1851) FEMALE DURING BREEDING SEASON AND ITS COMPARED TO CAPTIVE BROODSTOCKS

Introduction

The gonadotropin releasing hormone (GnRH), a neuropeptide, is a conserved 10 amino-acids with N-terminal pyroglutamyl and C-terminal amidated glycine residue. It is the key neurotransmitter that acts as the master hormone which centrally plays an important role in the stimulate growth and reproduction of fish. GnRH isoforms in fish species were classified into three GnRH types (GnRH 1, 2 and 3) based on primary structure or complementary DNAs (cDNAs), neuroanatomical distributions, immunocytochemistry and *in situ* hybridization (Fernald & White, 1999). The GnRH-2 and GnRH-3 expressed mainly in olfactory bulbs, midbrain tegmentum, ventral telencephalon and preoptic area (Kauffman & Rissman, 2004). They play a critical role in reproductive behavior (Kauffman & Rissman, 2004, Temple et al., 2003). GnRH – 1 is a hydrophysiotropic form. It mainly expressed in neuronal population at the ventral surface of the forebrain, associated with the ventral telencephalon, preoptic area and hypothalamus. Therefore, it can be concluded that GnRH 1, particularly *sea bream* GnRH (sbGnRH) plays a key role in the reproduction of fishes, especially Scrombrids i.e. *Scomber japonicas* (Selvaraj et al., 2009). These neurons play a pivotal role in reproduction of all vertebrates by stimulating the gonadotropins secretion (GtH) (González-Martínez et al., 2001, González-Martínez et al., 2002, Gothilf et al., 1997,

Guilgur et al., 2006, Kah et al., 2007, Palevitch et al., 2009). GtHs: GtH I (FSH β -like) and GtH II (LH-like)) were produced by gonadotrops of the pituitary gland (Quérat et al., 2001, Sherwood & Adams, 2005). Previous investigations have shown that GtH I and GtH II possessed different functions in fishes. GtH I contributed to early spermatogenesis and follicular growth, while GtH II encouraged the maturation of gametes and was functionally induced in spermiation and ovulation (Planas et al., 1993, Tyler et al., 1991).

The short mackerel, *Rastrelliger brachysoma* (Bleeker, 1851) belonging to the family Scombridae is a vital important fish in Thai fishery industry. Moreover, this fish has been aimed to use as a potential candidate for marine fish aquaculture program. A preliminary culture project of *R. brachysoma* is set up in the Samut Sakhon Fisheries, Sumut Sakhon province, Thailand. The project was quite successful in terms of survival rate of the larvae. However, sexually matured fish used in this project were obtained from the natural population. In captive breeding condition, broodstock caught from the wild population usually showed the endocrinological dysfunction preventing completion of the reproductive system such as reduction of gonadosomatic index (GSI), decrease of germ cells in both quality and quantity. These changes may be influenced by lacking of gonadotrophin releasing hormone (GnRH) that is synthesized and released from the brain into the pituitary gland for stimulating and releasing of luteinizing hormone (LH) (Shiraishi et al., 2005, Zohar et al., 2010). The lack of this hormone was mainly caused by the differences in the culturing condition and their natural environment. These differences lead to acute and chronic stresses on reproductive physiology of fish (Selvaraj et al., 2009, Shiraishi et al., 2005, Zohar et al., 2010). To overcome this problem, the success in various aquaculture techniques

that increase the reproductive performance has been introduced, for examples, endocrine manipulative strategies, hormone priming, artificial fertilization, and production of recombinant fish gonadotropins. However, in order to optimize these manipulative procedures, a well understanding of basic knowledge of structure and regulation system of the reproductive neuroendocrine mechanisms of the fish is necessary.

In this research, the brain structure, the distribution and the changes of the gonadotropin-releasing hormone – gonadotropin system (sbGnRH-GtH system) in the brain in juvenile and sexually matured, *R. brachysoma* female in the Upper Gulf of Thailand were determined. The pattern of the distribution of sbGnRH-GtH system in the ovarian tissue was also investigated. Moreover, the differences of immunoreactivity and mRNA sbGnRH and GtH levels in brain between wild caught female fish and hatchery broodstocks fish at sexual maturation were investigated. The basic comprehensive knowledge of the reproductive neuroendocrine mechanisms underlying juvenile and sexual maturity of the species gained by this study could potentially be applied to the maturation regulation and the spawning induction, which will improve the breeding aquaculture system. Additionally, understandings of reproductive biology of *R. brachysoma* serve as the scaffold for equipping scientific advice to fisheries management in the future.

Materials and methods

Fish collections

The wild caught fish, juvenile (approx. < 13.4 cm in total length) and sexual maturation (approx. >16.5 cm in total length), *Rastrelliger brachysoma* female were

caught by bamboo strake trap from Samut Songkhram province, the Upper Gulf of Thailand (13°16’18.4” N, 100°02’13.4” E) during non-breeding season (October to December 2013) and breeding season (January to February 2014). Seventy-six individuals per sampling season (20 individuals in juvenile and 132 individuals in sexual maturation) were kept. Also, salinity and temperature (T) of sea water were measured on site during the samplings. All fish samples were kept in dry-ice and transported to the laboratory at Department of Marine Science, Faculty of Science, Chulalongkorn University.

The captive broodstocks of sexually matured *R. brachysoma* were reared at the Samut Songkhram Coastal Fisheries Research and Development Center, Samut Songkhram, Thailand to the total length at approx. 18 cm (2 year-old, 3 individuals in sexual maturation) during October to December 2013. The fish were kept and acclimatized in shaded concrete tanks filled with sea water at a temperature of 26-29 ˚C, salinity of 30-32 ppt and continuous aeration under a photoperiod of 12:12 h light-dark. They were fed with fresh squids and polychaetes twice daily. All fish were euthanized by rapidly cooling shock (Wilson et al., 2009). The experimental protocol was approved by the Animal Care and Use Committee of Faculty of Science in accordance with the guide for the care and use of laboratory animals prepared by Chulalongkorn University (Protocol Review No. 1423003).

Tissue collection and processing

The craniums of all fish were opened ventrally at the level of the whole brain situated while the posterior abdominal wall of the fish were also cut and collected the ovarian tissue. The ovarian tissues were immediately removed and measured the total

weight. All tissue (brain and ovarian tissue) and placed in fixative solution for further histological analyses. For gravimetric analysis, gonadosomatic indices (GSI) of *R. brachysoma* were calculated using the following formula (GSI = [gonadal weight/total weight x 100]). The remaining of fish samples were stored at -80 ºC for further GnRH and GtHs mRNA analysis using specific quantitative real-time PCR (qRT-PCR). .

Histological and histochemical observations

All tissues were rapidly fixed in Davidson's fixative for about 24 hrs at room temperature. After fixation, the tissues were dehydrated through a graded series of ethyl alcohol concentrations and embedded in paraffin. Serial of 4-5 µm sections were cut by rotary microtome. Finally, the serial of longitudinal, horizontal and cross sections were stained with Harris's hematoxylin and eosin (H&E) and specific stained with Masson's trichrome (MT) and Periodic Acid-Schiff (PAS) (Bancroft & Gamble, 2008, Humason, 1979) for identification of the brain structure and ovarian development. For determination of the ovarian development, section of ovarian tissue was examined in detail under light microscope in order to determine the stage of ovarian development according to Dietrich & Krieger (2009) for reproductive cycle analysis. Additionally, the counting the number of atretic follicles were quantified (50-100 oocytes/section/fish), as described by Blazer (2002).

Immunocytochemistry and immunofluorescence

Processing of tissues for Immunocytochemistry and immunofluorescence

Only sbGnRH antibody as type GnRH – 1 that previously tested for specificity

by scombrid, e.g., *S. japonicas* (Selvaraj et al., 2009) and marine perciforms (Kah et al., 1993, Mousa & Mousa, 1999, Powell et al., 1994, Selvaraj et al., 2012a, Selvaraj et al., 2009), were used in this study. Consecutive sections were tested for gonatrophic activity of FSHβ and LHβ followed the approach by Shimizu et al. (2003) and Selvaraj et al. (2009). Under observation in all antibodies, brains and pituitary glands were obtained from five fish per season. The ovarian tissues in wild fish were also collected at breeding season from three fish.

Immunoperoxidase detection

A Vectastain ABC Kit (Vector Laboratories, Burlingame, CA, USA) was used to detect the sbGnRH and GtH immunereactivity in the brain and various stages of the gonadal tissue. For immunoperoxidase detection, this research was followed the method from Selvaraj et al. (2009). In brief, sections from histological observation, they were cut throughout the midline of the brain. These sections were used for immunocytochemistry. They were deparaffinized, rehydrated and washed in phosphate-buffered saline (PBS) pH 7.4 at 4 °C (10 min). To reduce background noise and to enhance immureactivity signal, sections were subsequently blocked by immersing the sections in 0.3% Triton X-100 in PBST. Then the endogenous peroxidase activity was removed by immersing the section in 3% hydrogen peroxide in 0.1 M phosphate buffer (pH 7.4) for 30 min at room temperature. Then, they were incubated in a blocking solution, 10% normal goat serum (NGS, Vector Laboratories, Burlingame, USA) + 4% Bovine serum albumin (BSA) and finally, the sections were incubated at 4 ˚C overnight in the primary antibody, sbGnRH at dilution 1: 1000 and 1: 2,000 in a 0.1 M PBS, anti-Fh FSHβ 50-60 or anti-Fh LHβ at dilution 1: 1000 and 1: 2000 in PBS. (All antibodies

were donated from Prof. M. Amano and A. Shimizu) After three rinse, the sections were incubated for 1 h in the biotinylated goat anti-rabbit IgG solution (1: 500), washed in PBS three times and stained with 30, 30-diaminobenzidine tetrahydro- chloride (DAB) (Sigma, Germany) for 30 s to develop a brown color. Later the ultrapure water was used to stop the reaction. The sections counterstained with Mayer's hematoxylin. The overall localization and distribution of sbGnRH neuronal system in the brain were recorded, mapped, and photographed with a Canon EOS 1100D digital camera. The sections incubated with preimmune sera in place of pre-immune rabbit serum were the negative control.

Immunofluorescence detection

The consecutive sections from each set of sbGnRH and GtH immunoreactivity were confirmed by immunofluorescence. They were deparaffinized, rehydrated and the epitope-unmasking solution were incubated with 10 M citrate buffer (for antigen retrieval and reduce background staining). After then, non-specific binding of protein and other enzymes were blocked by incubating the section in a blocking solution (10% normal goat serum + 4% BSA in PBS 1 mM at room temperature). The sections were incubated in primary antiserum, sbGnRH (1: 1000 and 1: 2,000 in a 0.1 M PBS), anti-Fh FSHβ 50-60 or anti-Fh LHβ (1: 1000 and 1: 2000 in PBS) in overnight at room temperature. After three rinses, the sections were incubated with Alexa 488-conjugated goat anti-rabbit IgG (Molecular Probes, Eugene), at the dilution of 1: 500 in blocking solution. After the sections were washed, they were mounted in VECTA shield fluorescence mounting medium. The localization and distribution of sbGnRH and GtH immuoreactive cells were observed and photographed under with a Canon EOS 1100D

digital camera. Negative controls were examined by replacing the primary antibody with pre-immune rabbit serum.

Cell counting and staining intensities of sbGnRH-GtH immunoreactivities

Three representative sections of each brain and pituitary gland were observed for sbGnRH, FSH β and LH β immunonegative cells which were counted with a hand counter. The counting of these immunoreactive cells were classified and quantified for each antibody, stages and seasonality (thirty cells from three zones including the nucleus periventricularis, nucleus preopticus and nucleus lateralis tuberis per brain section were counted and 200 cells from four localities in proximal par distalis/per pituitary section under light microscope (10x and 40x). Furthermore, the intensities of these antibodies in the neurons, GtH cells and gonadal tissue were assessed by visual observation following score: − no immunoreactivity, + weak immunoreativity, ++ moderate immunoreactivity and +++ strong immunopositive, respectively.

sbGnRH and GtH mRNA expression using qRT - PCR

Sample preparations of sbGnRH profile were prepared from the brain (diencephalon) and pituitary following the modification method (Amano et al., 2004, Selvaraj et al., 2012a) using quantitative real-time PCR (qRT-PCR). In summation, the brains were fixed in RNA later (QIAGEN) after that their RNA extractions were performed by manufacturer's instructions (biotechrabbit, Hennigsdorf *Germany*). The yields of total RNA were measured by spectrophotometer with the absorption at 260/280 nm and then one step real time RT-PCR assay was used. Each reaction tube (20 µm) were added the reverse-transcribed into single stand cDNA which was

performed by using gene specific primers (Table 6.1). The thermocycling conditions were of 95 °C for 5 min and 35 cycles of 95 °C for 10 s and 60 °C for 30 s. The PCR products were checked by 0.5% agarose gel electrophoresis. Amplification of β-actin (house keeping gene) was used as positive control. Determination of RNA amount was used a relative quantification.

Table 6. 1 Gene-specific primers and amplicon size (bp) for each transcript in the quantitative real time PCR assays

Transcripts	Primers	Size (bp)
β-actin*	ACCGGTATTGTCATGGACTC TCATGAGGTAGTCTGTGAGGTC	127
sbGnRH	CTGGACAGCCTTTCAGAC TCCCTGTTGGTCACACTG	149
FSHβ	GTCATGGTAGCAGTGCTG CCTTCACACATGGTGGTG	131
LHβ*	GAAACAACCATCTGCAGCG AAAAGTCCCGATACGTGCAC	100

* Note: Nyuji et al. (2012b), Selvaraj et al. (2012a)

Statistical analysis

Two samples t-test was used to compare the average number of immunostained and mRNA in sbGnRH and GtH cells between non-breeding and breeding seasons in wild fish, and between wild and captive fish. These statistics were calculated using

Statistical Package for the Social Sciences (SPSS) software (version 15.0).

Results

Ambient environmental factors at the study site

The average ambient salinity was 26.32 ppt in non-breeding season (October to December 2013) and the average salinity during breeding season (January to February 2014) was 31.75 ppt. The average relative temperature during the non breeding season was 28.93˚C and the average temperature during breeding season was 29.05 ˚C.

Gonadosomatic index (GSI) and ovarian development

The female from the non-breeding season had 0.48±0.50 (SE) GSI. The GSI was significantly higher during the breeding season (2.82±1.93 (SE)) (Figure 6.1). The ovarian development stages in the wild *R. brachysoma* were identified based on the ovarian morphology and the proportion of oogenic cells. Undeveloped stage (stage 0, 94.73%) and early development stages (stage I, 5.26%) were the two major stage in non-breeding season. The undeveloped stage contained mainly oogonia, chromatin nucleolar stage oocyte and perinucleolar stage oocyte. The early development stage contained the perinucleolar stage, lipid and the cortical alveolar oocyte. In breeding season, the four major ovarian developments including undeveloped stage (stage 0, 40.67%), early development stage (stage I, 16.94), mid development stage (stage II, 5.08%). The mid development stage was mostly composed of the early vitellogenic and slight late vitellogenic oocytes. Late development stage (stage III, 37.29%) was comprised of the prominent late vitellogenic and post vitellogenic stages.

The highest prevalence of the ovarian histopathology were the degeneration and

disorganization in different stages of oocyte. This degeneration and disorganization is called atretic follicles. The atresia in oogonia and the prominent previtellogenic stage was shown in non-breeding season at 100% prevalence. In breeding season, the atresia was observed in many stages including oogonia (at 83.3% prevalence), previtellogenic stage (at 93.3% prevalence) and vitellogenic stage (100% prevalence). The vitellogenic stages which found high prevalance of atresia included early and late vitellogenic stages and mature stage. The number of atretic vitellogenic stage was observed only in breeding season at approximately 80.2 % prevalence (Figure 6.2 and Table 6.2).

In captive *R. brachysoma*, all samples from the Samut Songkhram Coastal Fisheries Research and Development Center, Samut Songkhram, Thailand exhibited mid development stage (100%, n = 3) in female fish. The prevalence of atresia in oogonia, previtellogenic and vitellogenic stages were shown at 21.3%, 56.66% and 100% prevalence, respectively (Figure 6.2 and Table 6.2).

Histological organization of the *R. brachysoma* brain and pituitary gland

Five major regions of the brain (telencephalon, diencephalon, mesencephalon, metencephalon and myelencephalon) in *R. brachysoma* were previously described (Senarat et al., 2015). As a whole, under transverse serial sections, the localization of the diencephalon was present the nucleus preopticus-periventricularis, which was classified into three zones: the nucleus periventricularis, nucleus preopticus and nucleus lateralis tuberis, which was considered to be homologous to the GnRH neuronal-producing cells (Palmieri et al., 2008, Selvaraj et al., 2009). Based on MT and PAS staining methods, the existence of the diencephalic neurons population in the nucleus preopticus-periventricularis could be distinctly classified into three types: small,

medium and large based on its distinct size. Their mean diameter size and the standard diviation (taken from ten cells) based on the three catagories were 7.84±0.26 μm, 30.6±2.11 μm and 50.9±1.36 μm, respectively (Figures 6.3C, 6.3E, 6.3F, 6.3G).

The nucleus periventricularis was observed in ventral part of the hypothalamus and composed of several nucleus layers (Figure 6.3C). However, only small cells were found and they were arranged in 12-15 layers. The nucleus preopticus exhibited at the ventro-lateral region of the mesencephalon where it was composed of neuronal populations. These neurons were medium and large sized cells. The nucleus lateralis tuberis exhibited at the inferior lobe of hypothalamus in the posterior end of both cross and longitudinal sections seen in the ventral part of the nucleus periventricularis. The muti-neurons with several sizes (small, middle and large sized-cells) was observed on the sagittal plane of this structure. The pituitary gland as another structure important in the diencephalon was found. The pituitary gland appeared to be attached to the ventral region of the hypothalamus.

The overall histological structure of the pituitary gland of *R. brachysoma* consisted of two components (the adenohypophysis and the neurohypophysis). In the adenohypophysis, it was consisted of a cluster of cell embeded and also divided into three distinguished areas; the rostral pars distalis (RPD), the proximal par distalis (PPD) and the pars intermedia (PI) (Figure 6.4 and schematic diagram 6.4A). Furthermore, the penetration of the neurohypophysial process to the the adrenohypophyseal area was present. The identification of cell types in the adrenohypophysis using H&E, MT and PAS staining methods were not easily identified to level of the hormonal producing cell. However, these methods could classify pituitary tissue in to four cell types: acidophil I, acidophil II, basophil and chromophil with distribution in different

adrenohypophyseal areas (Figures 6.4B-6.4J). Acidophils I and II were the major component in RPD. The acidophils I with cell staining red-orange was mainly arranged in cords bordering the neurohypophysis. They had the oval shape nucleus. The acidophil II was relatively small when compared with acidophil I. These cells occupied in the central – ventral parts of RPD. They had spherical nucleus stained with MT stain as red color. The common three cell types including acidophils I, II and basophils were observed in PPD. However, the basophils in this region were exclusively detected, which was considered to be homologous to the thyrotrope, somatotrope and gonadotrope (Hashimoto et al., 2003, Shimizu et al., 2003). A considerable increase of basophilic cells in PPD in the *R. brachysoma* pituitary female was observed in breeding season. In juvenile, the basophilic cells in pituitary gland was slightly shown in the PPD.

Immunocytochemistry and immunofluorescence

Distribution of sbGnRH-GtH immureactivity in the brain of the wild *R. brachysoma* female during juvenile stage

The distribution pattern of the sbGnRH immunoreactivity (-ir) was poorly detected in the brain. However, the immunostaining of the sbGnRH – ir occurred in some perikarya of the small sized-neurons of the nucleus preopticus. Medium and large-sized neurons were also detected in the nucleus lateralis tuberis (Figure 4.5). At this stage, immunostaining of FSH-ir was slightly found in ventral-central part in the PPD, the cytoplasm of these cells displayed a slight immunoreactivity. The occurrence of the LH-ir was located in the central-ventral parts of the PPD. Each cell showed a weak immunoreactivity.

Distribution of sbGnRH-GtH immunoreactivity in the brain of wild R. *brachysoma* female during sexual maturity

A strong sbGnRH-ir was found in the small –sized neurons of the nucleus periventricularis. The nucleus preopticus, sbGnRH-ir was detected in most of the medium and large-sized neurons. In the nucleus lateralis tuberis, strong immunoreactivities were present in several neuronal cells including the small, medium and large – sized neurons. Neuronal fibers from sbGnRH neurons were continuous with strong sbGnRH-ir and then it innervated in to the pituitary gland, as shown in the Immunofluorescence technique. The GtH-ir was also observed in this study, the intense of immunoreactive FSH cell were distributed and concentrated at the anterial – ventral regions of PPD, whereas the immunoreative LH cells were localized throughout the PPD, especially middle-ventral regions (Figures 6.6 and 6.7).

Distribution of sbGnRH-GtH immunoreactivity in the brain of captive *R. brachysoma* female during sexual maturity

The nucleus preopticus-periventricularis, sbGnRH – ir was detected in small-sized, medium-sized and large-sized neurons, as similarly seen in wild fish. However, note that all neurons were weakly detected. The intense of immunoreactive of the GtH-ir (FSH-ir and LH-ir) were similarly localized in the wild fish (Table 6.3).

Distribution and staining intensities of sbGnRH-GtH-immunoreactivity in the *R. brachysoma* ovarian tissue

The weak staining of sbGnRH-ir was observed in the follicular cells. In contrast to an intensed GtH-ir was observed in both the follicular cells and oogenic stages. Note

that a more intensed LH-ir was detected in same areas than FSH-ir. FSH – ir and LH – ir were found in the cytoplasm of the oogonia, previtellogenic, lipid and cortical stages and they appeared much weaker stained that what was detected in early and late vitellogenic stages (Table 6.4).

Changes in numbers and staining intensities of sbGnRH neurons GtH-immunoreactive cells in the brain

The numbers of sbGnRH immunoreactive neurons from three zones including the nucleus periventricularis, nucleus preopticus and nucleus lateralis tuberis were counted in both juvenile and sexually maturated female *R. brachysoma* from two seasons, are given in Figure 6.10. The numbers of sbGnRH immunoreactive neurons from all neuronal clusters in the sexual maturation was observed than the juvenile ($P<0.05$). The number of sbGnRH- immunoreactive neurons in female *R. brachysoma* from the three zones in the breeding season (28.66±0.47) were significantly higher in the non-breeding season (20.22±0.54) ($P<0.05$; Figure 6.9).

The number of GtH-immunoreactive neurons in PPD from sexually matured fish in the breeding season was higher than what was found in the juvenile. The number of FSH immunoreactive (ir) in the PPD from the non-breeding season (127.55±1.05 cells) was significantly higher than the breeding season (122±0.74 cells). The numbers of LH – ir from the breeding season was significantly higher ($P<0.05$) than the non-breeding season (Figure 6.10).

Comparison between wild and captive fish in the breeding season, the sbGnRH-GtH numbers in the brain showed that the wild fish were significantly higher ($P<0.05$) than the captive fish (Figure 6.10 and Table 6.3).

sbGnRH-GtH mRNA levels in the brain of *R. brachysoma* female during sexual maturity

As the non breeding season progress to the breeding season, the expression of the brain sbGnRH mRNA level increased and vice versa when the the breeding season progressed to the nonbreeding season. The sbGnRH mRNA level from the breeding season was significant higher ($P<0.05$) than the non breeding season (Figure 4.11). On the other hand, the expression of FSH and LH mRNA levels from the breeding season was significantly higher ($P<0.05$) than the non-breeding season. Based on a comparison between wild and captive fish, the sbGnRH-GtH mRNA levels in the brain of wild fish were higher than in the brain of captive fish with statistically significant difference ($P<0.05$, Figure 6.11).

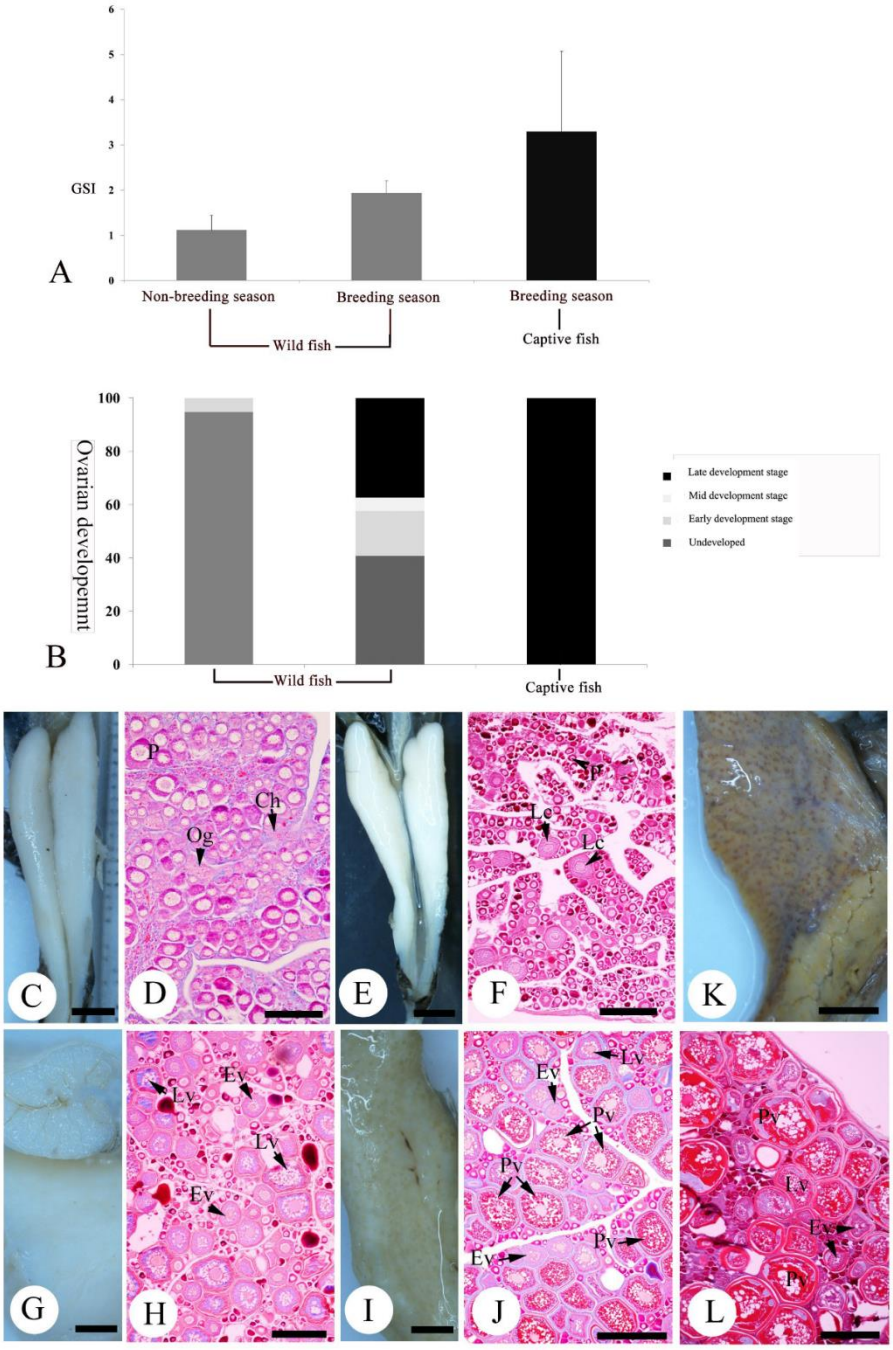

Figure 6.1 Histograms showing the gonadasomatic index (GSI) and percent of the ovarain development based on gross anatomy (A) and light photomicrograph of histopathological structure at four stages; stage 0, stage 1, stage 2 and stage 3 stained by Masson´s Trichrome in both wild and captive *Rastrelliger brachysoma*. Scale bar: 100 µm (D), 500 µm (F, H, J, L), 0.2 cm (C, E, G, I, K). *Ch = chromatin nucleolar stage, Ev = early vitellogenic stage, Lv = late vitellogenic stage, Og = oogonia, P = perinucleolar stage, Pv = post vitellogenic stage.*

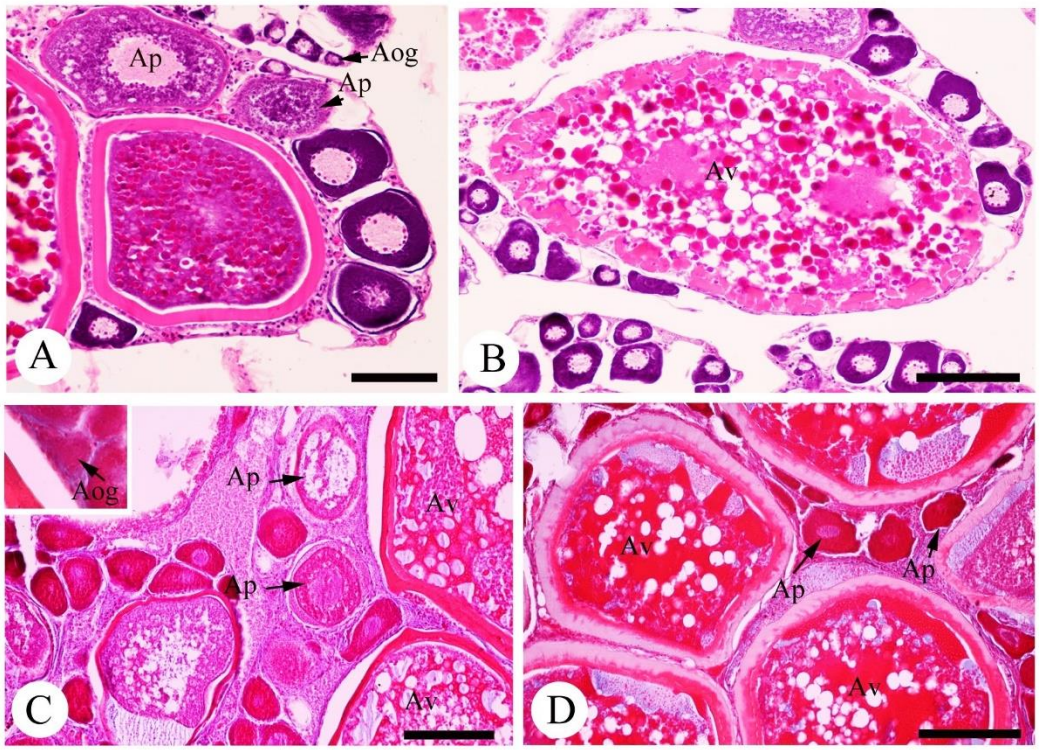

Figure 6.2 Light photomicrograph of histopathological alterations of the ovarian tissue, atresia of oogonia (Aog), atresia of previtellogenic stage (Ap), atresia in vitellogenic stage (Av). Scale bar: 100 µm (A-B), 200 µm (C-D)

Table 6.2 showing the number of atresia at different stages of oocytes.

Fish	Atresia	Seasons	
		Non-breeding	Breeding
Wild	Oogonia	23.90±3.03 (50 oocytes)	19.60±4.42 (50 oocytes)
	Pre-vitellogenic stage	63.50±3.83 (100 oocytes)	57.40±4.83 (100 oocytes)
	Vitellogenic stage	-	80.20 ± 3.45 (100 oocytes)
Captive	Oogonia	-	21.3 ±1.52 (50 oocytes)
	Pre-vitellogenic stage	-	56.66 ± 3.05 (100 oocytes)
	Vitellogenic stage	-	100 (100 oocytes)

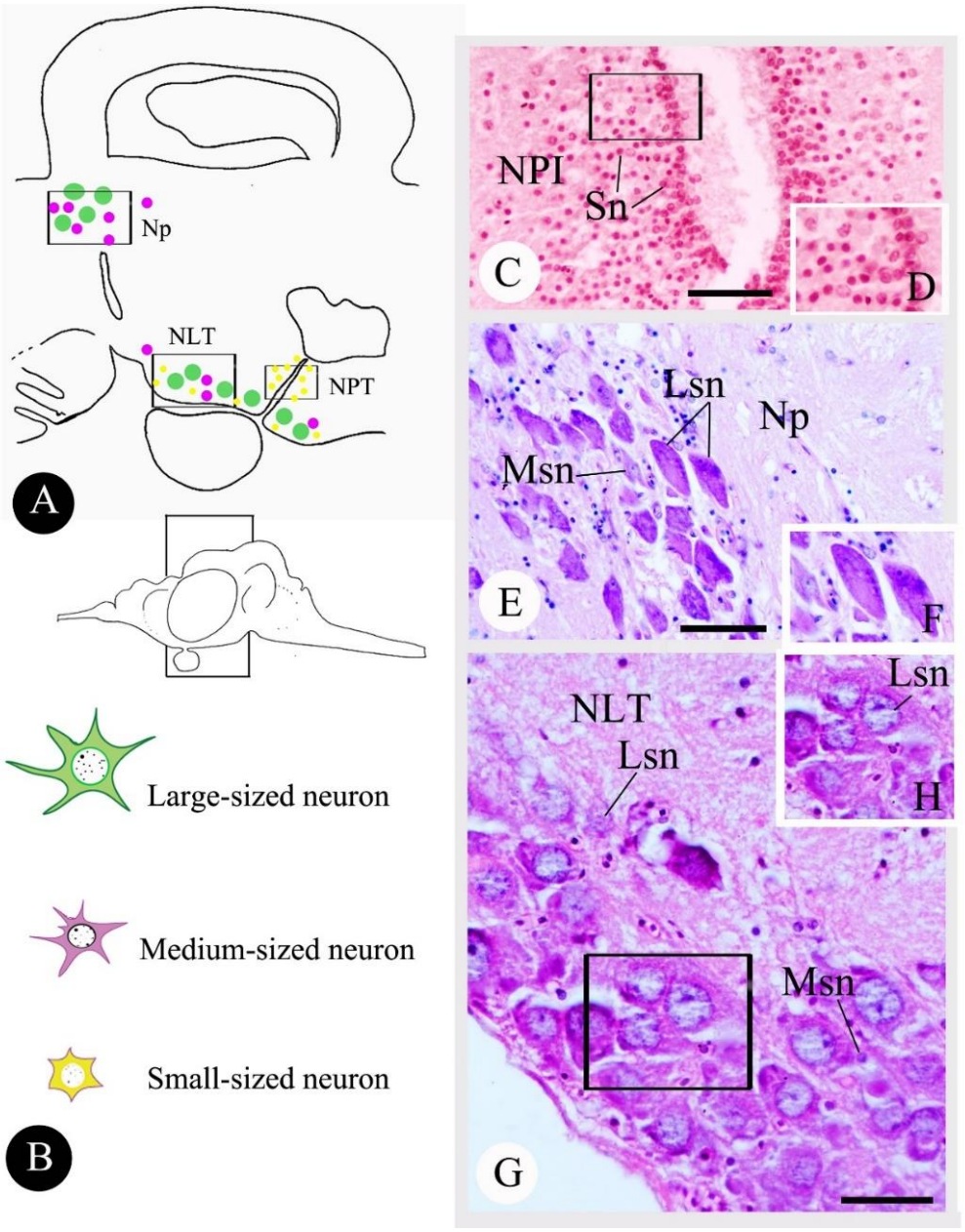

Figure 6.3 Schematic diagram (A-B) and light photomicrograph of histopathological structure of the diencephalon with special three areas including the nucleus periventricularis (NPI), the nucleus preopticus (Np) and nucleus lateralis tuberis (NLT) (C-H). Scale bar: 50 µm (C), 100 µm (E, G). *Sn = small sized-cell, Msn = middle sized-cell, Lsn = large sized-cell.*

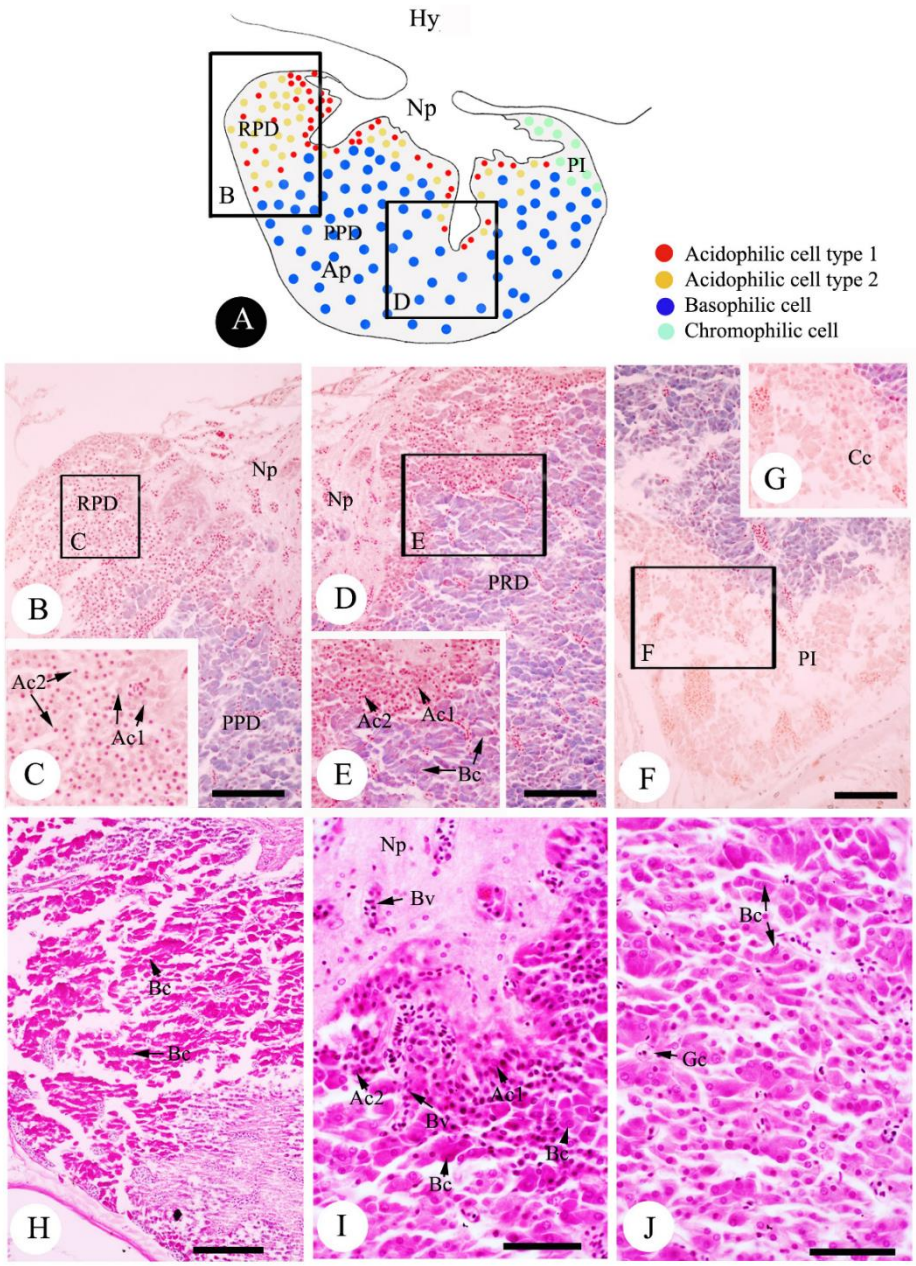

Figure 6.4 Schematic diagram (A) and light photomicrograph of pituitary histology (B-J) with composisting of two distinct areas including the adenohypophysis (Ap) and the neurohypophysis (Np)**.** Scale bar: 50 µm (B, D, F, H, I, J). *Ac1 = Acidophilic cell type, Ac2 = Acidophilic cell type, Bc = basophilic cell, Bv = blood vessel, Cc = chromophilic cell, Gc = granular cord, Hy = hypothalamus, PI = pars intermedia, PPD = proximal par distalis, RPD = rostral pars distalis.*

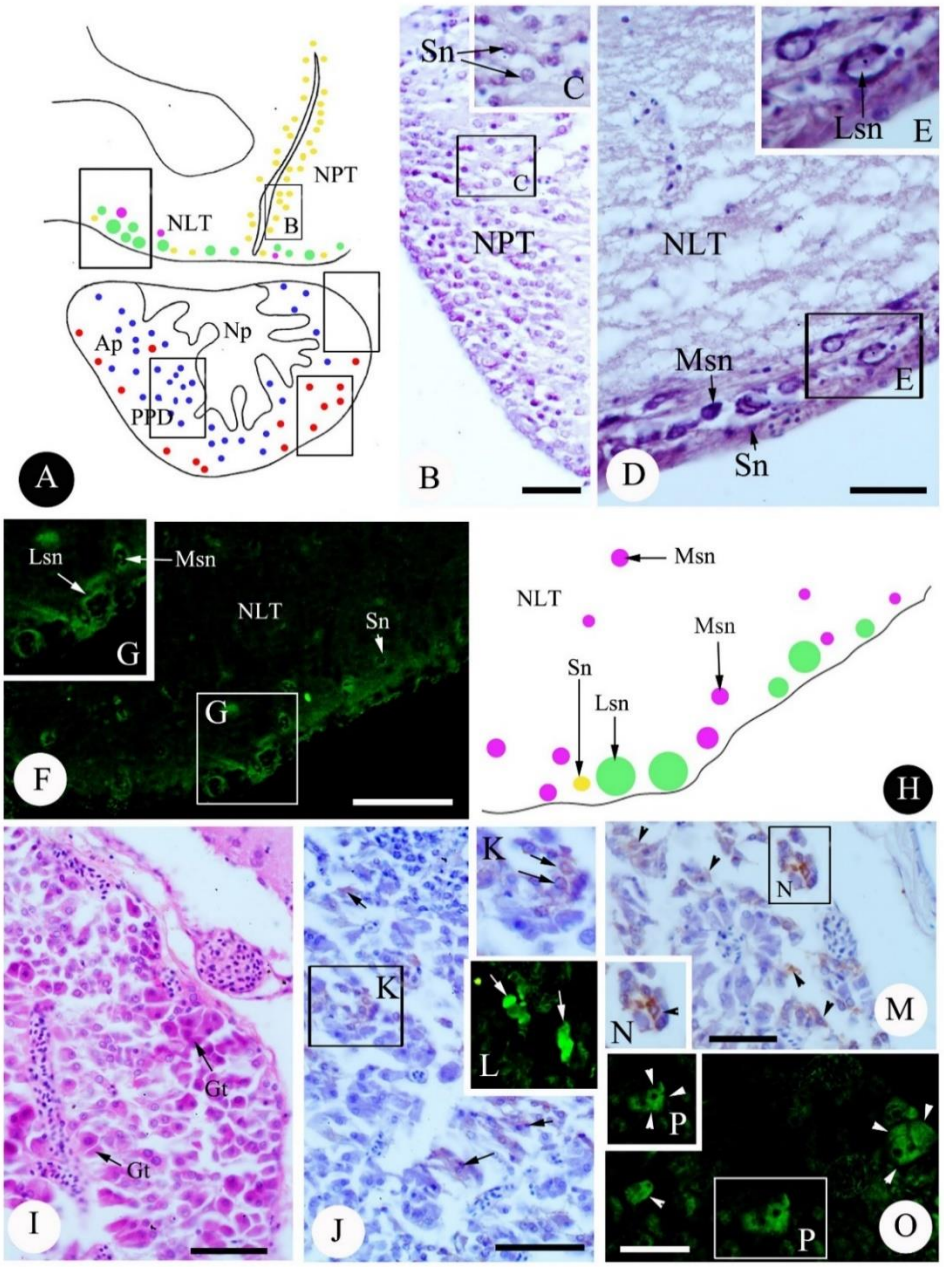

Figure 6.5 Schematic diagram (A, H) and light photomicrograph of immunolocalization of sbGnRH – ir (B-F) with three areas in the diencephalon including the nucleus periventricularis (NPT), the nucleus preopticus (Np) and nucleus lateralis tuberis (NLT) and GtH – ir (I-P) of Rastrelliger brachysoma during juvenile stage. Scale bar: 20 µm (M, O), 50 µm (B, D, F, I, J). *Ap = adrenohypophysis, Gt = gonadotropic cell, PPD = proximal par distalis, Sn = small sized-cell (yellow colour), Msn = middle sized-cell (puple colour), Lsn = large sized-cell (green colour), arrow = FSH – ir (blue colour), arrow head = LH- ir (red colour).*

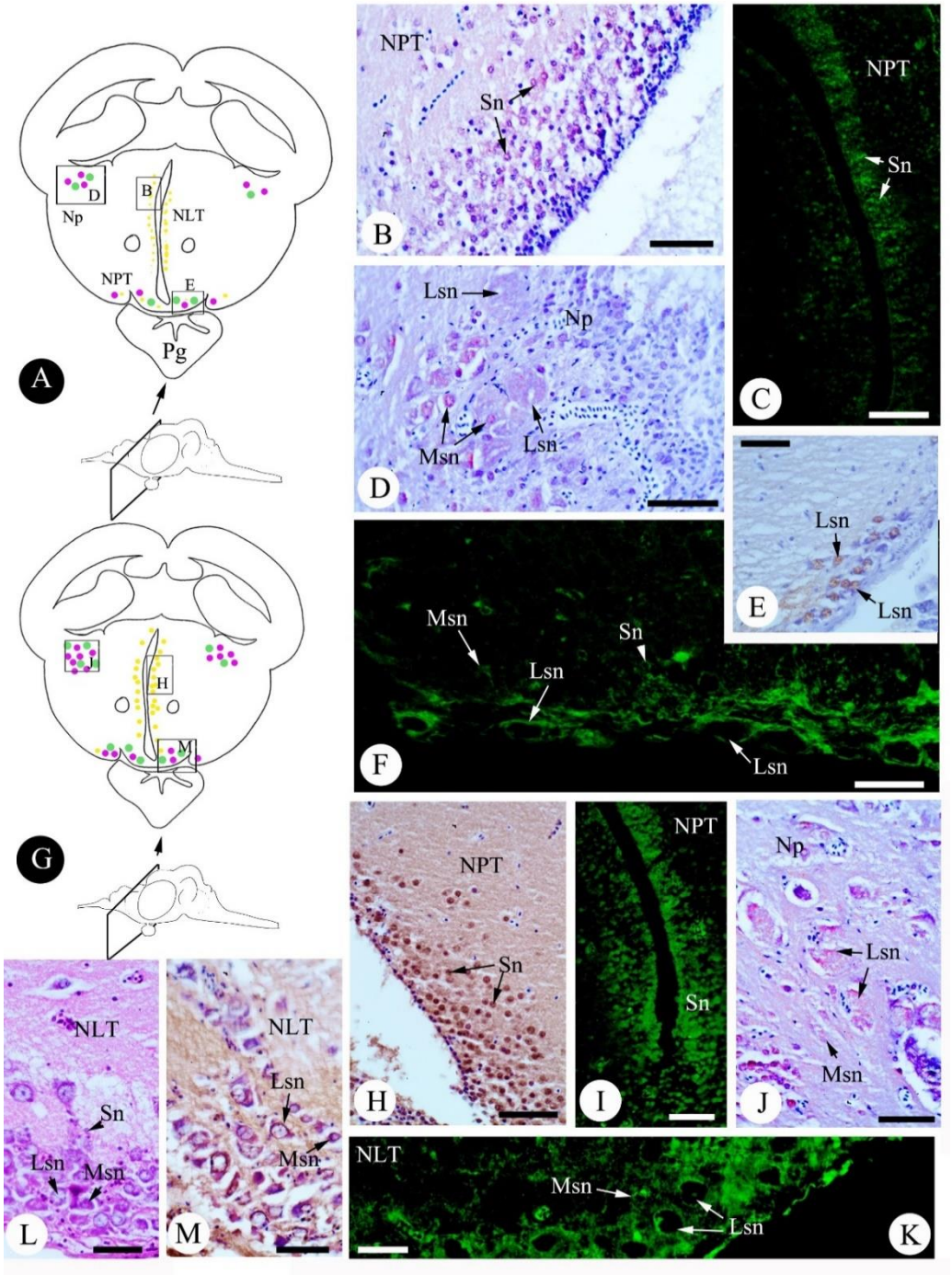

Figure 6.6 Schematic diagram (A, G) and light photomicrograph of immunolocalization of sbGnRH – ir (B-K) of the *Rastrelliger brachysoma* during non-breeding and breeding seasons. Scale bar: 50 µm (B-F, H-K), 100 µm (L, M). *NPT = nucleus periventricularis, Np = nucleus preopticus, NLT = nucleus lateralis tuberis, Pg = pituitary gland, Sn = small sized-cell (yellow colour), Msn = middle sized-cell (puple colour), Lsn = large sized-cell (green colour).*

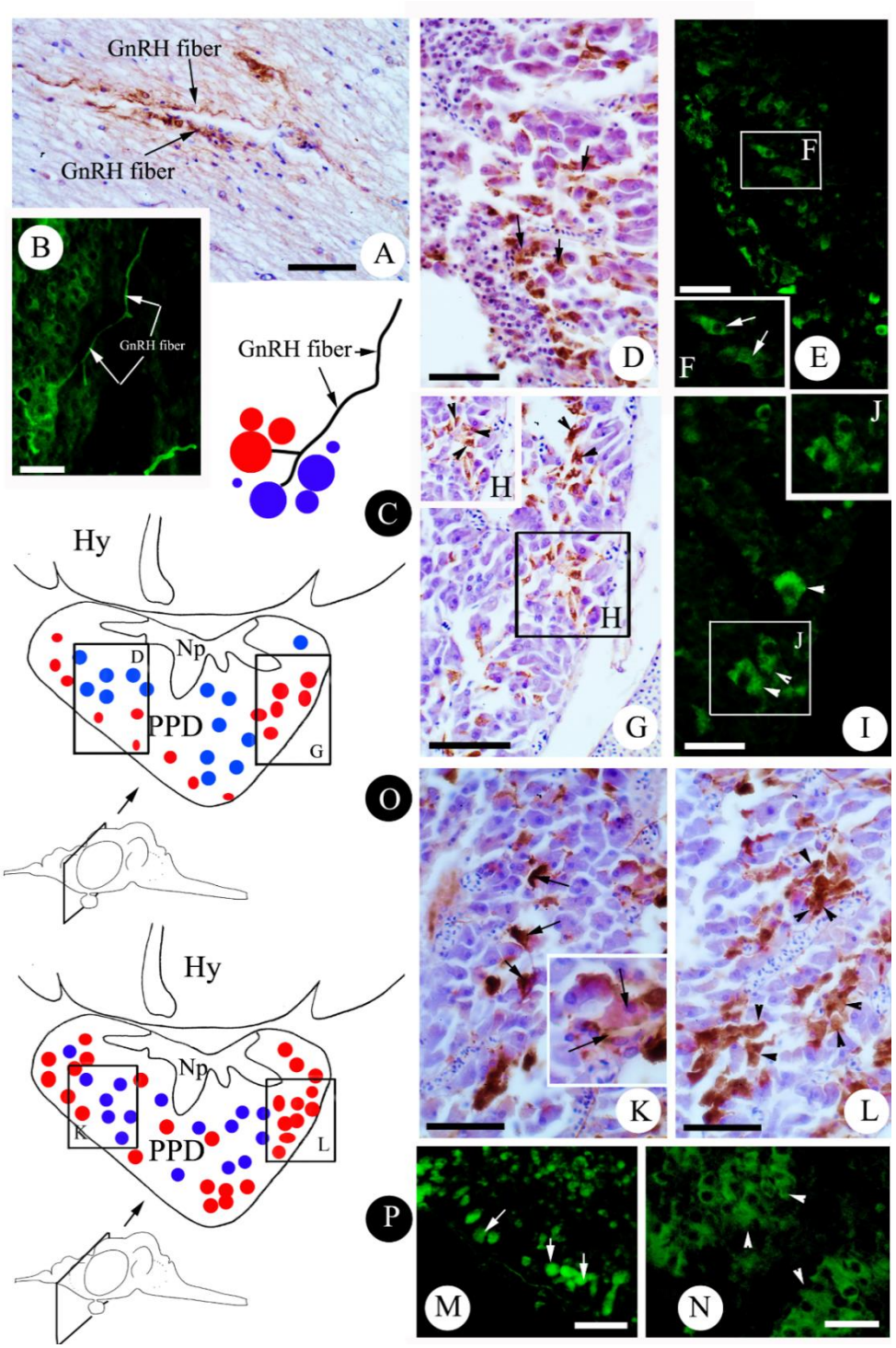

Figure 6.7 Light photomicrograph showing the sbGnRH fiber with protrude into the pituitary gland (A-C), light photomicrograph and schematic diagram of immunolocalization of FSH – ir (D, E, F, K, M, O) and LH – ir (G, I, L, N, P) of *Rastrelliger brachysoma* during non-breeding and breeding seasons. Scale bar: 20 µm (B), 50 µm (A, D, E, G, I, K, L, M, N). *PPD = proximal par distalis, arrow = FSH – ir (blue colour), arrow head = LH - ir (red colour).*

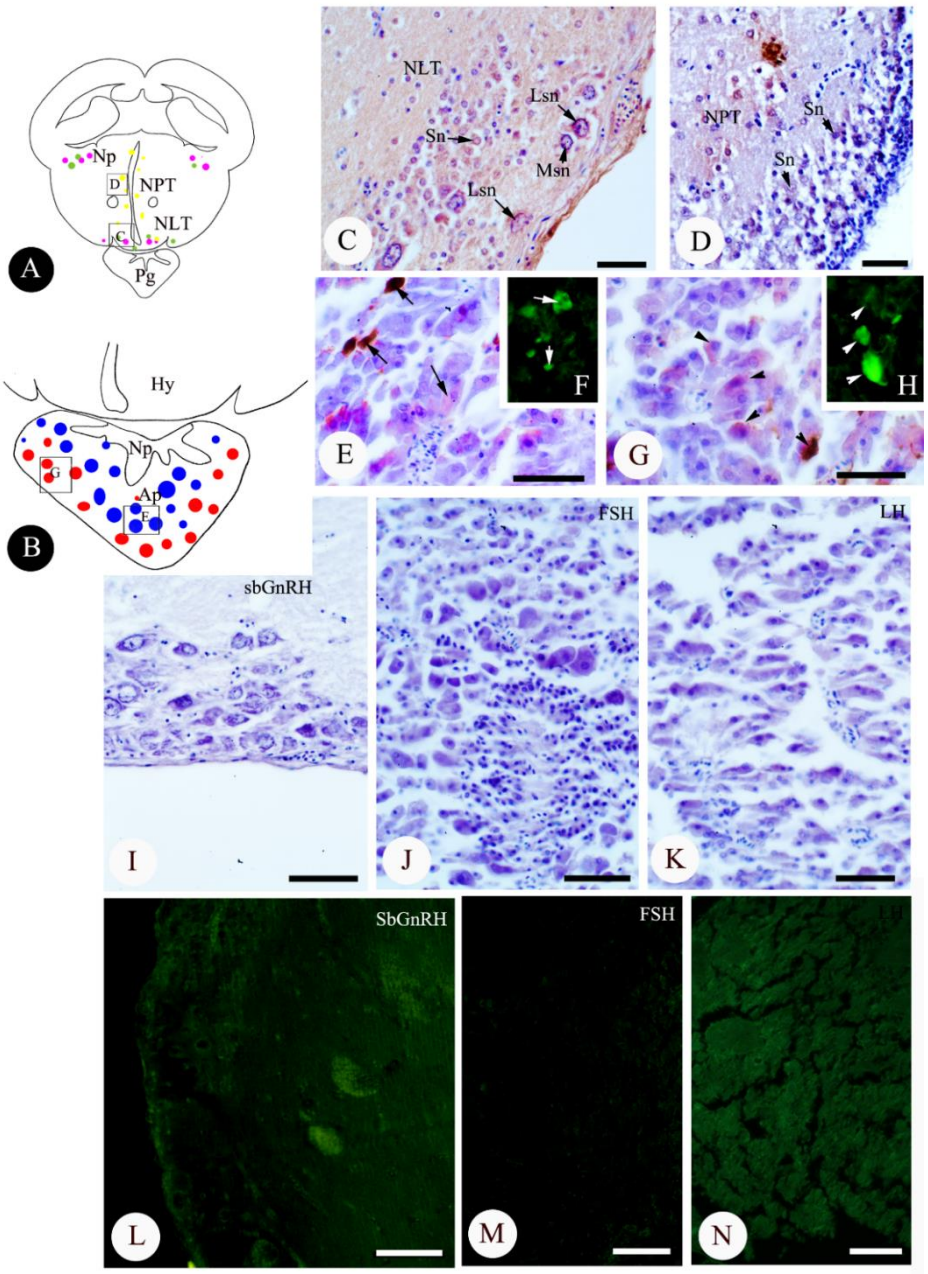

Figure 6.8 Schematic diagram (A, B) and light photomicrograph of immunolocalization of sbGnRH – ir (C-D) and GtH – ir (E-G) of captive *Rastrelliger brachysoma* during breeding season. Scale bar: 50 µm (C, D, E, G, J, K, M, N), 100 µm (I, L). *NPI = nucleus periventricularis, Np = nucleus preopticus, NLT = nucleus lateralis tuberis, Ap = adrenohypophysis, Hy = hypothalamus, Np =neurohypophysisSn = small sized-cell (yellow colour), Msn = middle sized-cell (puple colour), Lsn = large sized-cell (green colour), arrow = FSH – ir (blue colour), arrow head = LH - ir (red colour). Note that negative control sections showing no sbGnRH-ir and GtH-ir (I-N).*

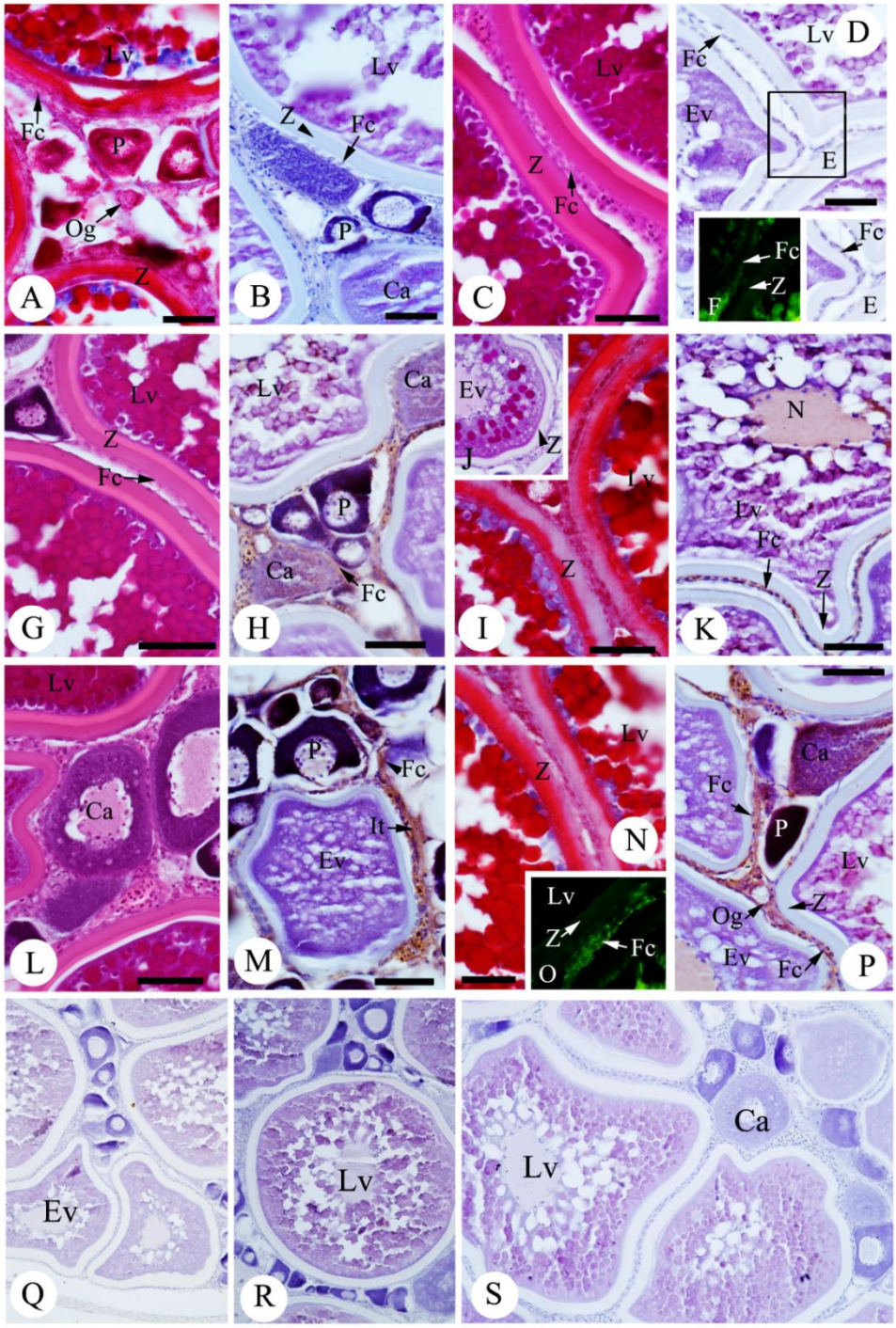

Figure 6.9 Light photomicrograph showing the sbGnRH, FSH and LH immunoreactivities in the ovarian tissue (A-P) and negative control (Q-S). Scale bar; 50 µm (A-P). *Ca = corltical alvelolar stage, Ev = early vitellogenic stage, Fc = follicular cell, Lv = late vitellogenic stage, N = nucleus, P = peirnucleolar stage, Og = oogonia, Z = zona pellucida.*

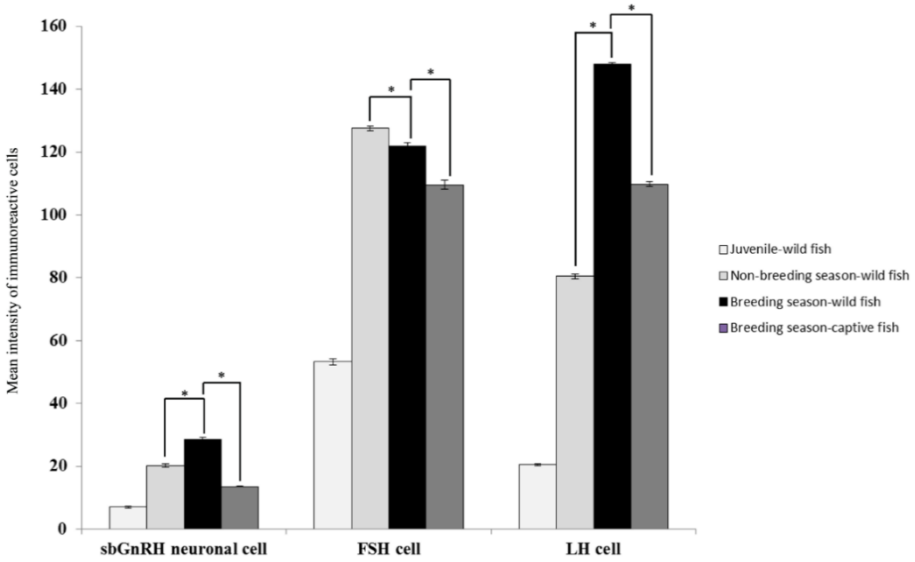

Figure 6.10 Histograms showing the mean numbers of sbGnRH immunoreactive neurons and GtH – ir (FSH – ir and LH - ir) in the brain of wild and captive *Rastrelliger brachysoma*. Values represent X ± SE; significantly different at *P<0.05

Table 6.3 Summary of the presence of sbGnRH neuronal immunoreactvity (-ir), FSH and LH – ir in female *Rastrelliger brachysoma*

Stages/Seasons	sbGnRH neuronal clusters/ir			FSH cells	LH cells
	NPT	Np	NLT		
Juvenile	+ (Sn) (R = 200, G = 168, B = 253) - (Msn) - (Lsn)	-	+ (Sn) (R = 140, G = 118, B = 180) + (Msn) (R = 118, G = 56, B = 179) + (Lsn) (R = 143, G = 107, B = 181)	+ (R = 149, G = 134, B = 215)	+ (R = 129, G = 78, B = 75)
Non-breeding (wild fish)	++ (Sn) (R = 200, G = 154, B = 242) - (Msn) - (Lsn)	+ (Sn) (R = 192, G = 94, B = 229) ++ (Msn) (R = 185, G = 113, B = 251) ++ (Lsn) (R = 182, G = 163, B = 227)	+ (Sn) (R = 136, G = 163, B = 216) ++ (Msn) (R = 118, G = 137, B = 151) ++ (Lsn) (R = 162, G = 156, B = 156)	++ (R = 173, G = 79, B = 98)	++ (R = 143, G = 44, B = 34)
Breeding (wild fish)	+++ (Sn) (R = 155, G = 89, B = 91) - (Msn) - (Lsn)	++ (Sn) (R = 168, G = 2, B = 174) +++ (Msn) (R = 215, G = 150, B = 254) +++ (Lsn) (R = 204, G = 60, B = 218)	++ (Sn) (R = 175, G = 109, B = 119) +++ (Msn) (R = 143, G = 52, B = 87) +++ (Lsn) (R = 101, G = 25, B = 53)	+++ (R = 52, G = 11, B = 14)	+++ (R = 98, G = 20, B = 15)
Breeding (Captive fish)	+ (Sn) (R = 199, G = 162, B = 196) - (Msn) - (Lsn)	+ (Sn) (R = 211, G = 130, B = 166) + (Msn) (R = 191, G = 87, B = 158) + (Lsn) (R = 182, G = 93, B = 144)	+ (Sn) (R = 205, G = 163, B = 219) ++ (Msn) (R = 187, G = 133, B = 172) +++ (Lsn) (R = 189, G = 150, B = 147)	++ (R = 207, G = 165, B = 252)	++ (R = 195, G = 103, B = 253)

(Note - Immunoreactivity: - no immunoreactivity; + weak immunoreactivity; ++ medium immunoreactivity and +++ strong immunoreactivity)

Table 6.4 Summary of the presence of sbGnRH – ir and GtH – ir in oogenic steps and their follicular cells of *Rastrelliger brachysoma*

Immunoreactivity	Steps of oogenic stages and follicular cells								
	Og	P	Fc	Ca	Fc	Ev	Fc	Lv	Fc
sbGnRH-ir	-	-	+	-	+	-	+	-	+
FSH – ir	-	+	++	++	++	+	+++	+	+++
LH – ir	-	+	++	+	++	+	+++	+	+++

Note- + weak immunoreactivity, ++ moderate immunoreactivity, +++ strong immunoreactivity, - no immunoreactivity
(Fc = follicular cells, Og = oogonia, P = previtellogenic, Ca = lipid and cortical stages Ev = early vitellogenic stage, Lv = late vitellogenic stage)

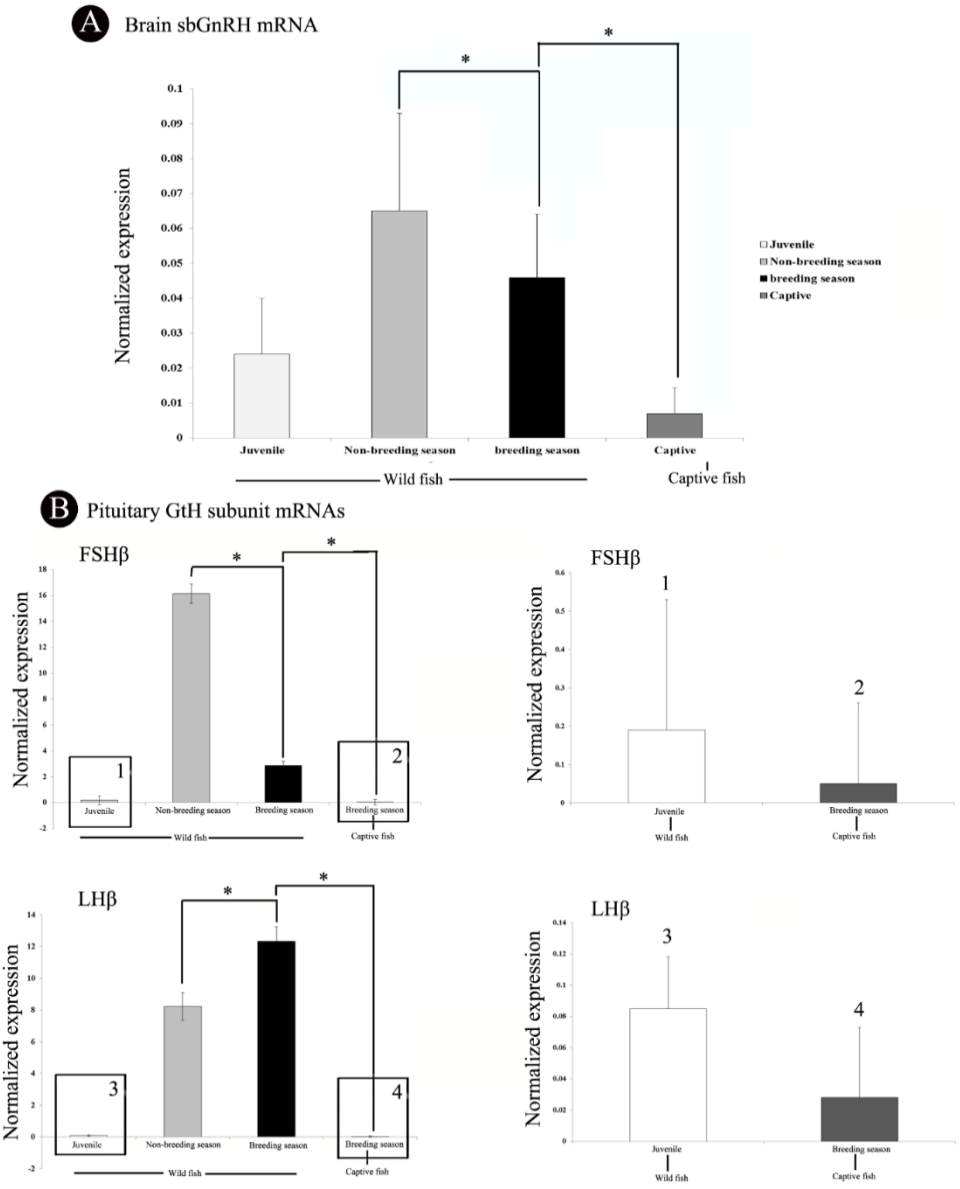

Figure 6.11 The gene expression levels of sbGnRH (A) and GtH (B) in the brain of wild and captive *Rastrelliger brachysoma.* Values represent X ± SE; significantly different at *P<0.05

Discussion

Specific localization, the presence of sbGnRH-positive neuronal cells with three neuronal cells including large, medium and small-sized neurons corresponded to three zones including the nucleus periventricularis, the nucleus preopticus and nucleus lateralis tuberis for the first time, whereas the antiserum against FSHβ and LHβ like-peptides also detected an intense immunoreactivity in the proximal par distalis (PPD) of the pituitary gland. This observation is supported by the sequence comparison as well as evolutionary trend because they did nearly cross react with *S. japonica* (Selvaraj et al., 2009). This was consistent with other fishes i.e. *Salmo salar* (Peter et al., 1991) and *T. thynnus* (Palmieri et al., 2008). It is of particular interest that the sbGnRH-ir immunoreactive fibers which project into the gonadotropic cells were also detected. It indicated the involvement with the pituitary gonadotrophs. I proposed that it may involve the sbGnR-GtHs like peptide in regard to oogenesis and ovarian maturation in *R. brachysoma*. This situation is often supported in other teleost, for example, in mature *S. japonicas* (Selvaraj et al., 2009), *Verasper moseri* (Amano et al., 2002) and *Japanese flounder* (Pham et al., 2008), *Carassius auratus* (Anglade et al., 1993) and *Pagrus major* (Okuzawa et al., 1997). All cases showed only sbGnRH which are related to the primary regulator of gonadotropin activity and gonadal development, were found in perciform fishes. Under immunocytochemical identification, the observation strongly showed that the distribution of the pituitary FSH and LH cells in *R. brachysoma* female was mainly located in the PPD. It was hypothesized that it was produced from different cells in the pituitary gland, as reported to those of *T. thynnus* (Kagawa et al., 1998), *Odontesthes bonariensis* (Miranda et al., 2001), *P. major* and *Micropterus dolomieu* (Shimizu et al., 2003). In contrast to presence in previous studies, the colocalization of

FSH and LH cells was shown in some cells including *Seriola dumerilii* (Hernández et al., 2002) and *Arasaki strain* (Shimizu et al., 2003). Unfortunately, it is unclear why the overlapping of FSH and LH immunoreactivities were in the same cell. The identification of FSH and LH receptors in *R. brachysoma* needs to be verified in further study. However, it indicated that the evidence of the physiological role for sbGnRH in *R. brachysoma* is related to central role in the regulation of gonadotropin secretion and the control of reproduction, the interacting of the sbGnRH and GtHs, as so called sbGnRH-GtH system. Similar pattern was examined in *S. japonicas* (Selvaraj et al., 2009), *Dicentrarchus labrax* (González-Martínez et al., 2002) and *V. moseri* (Amano et al., 2002).

Recent observations in the ovarian tissue suggested the existence of GnRH-like peptides in other invertebrates such as *Lymnea stagnalis* and *Helisoma trivolvis* (Young et al., 1999) and *H. asinina* (Nuurai et al., 2010). However, it is rare in fish. An earlier investigation in *Channa striatus* found, sbGnRH-ir in the pre-vitellogenic and post-vitellogenic stages with unclear figures (Swapna et al., 2005). This study showed that the existence of sbGnRH-ir in *R. brachysoma* was observed not only in the oocytes but also in the follicular cell together with interstitial tissue as the first clear-cut evidence. However, the mechanism and pathway involved with the function of sbGnRH on the oogenic activity is poorly known. Some studies suggested that sbGnRH is considered to play a role in regulating processes in ovarian cycle, either in autocrine or paracrine actions (Sherwood, 1997, Swapna et al., 2005). The expression of FSH and LH stimulate the sex steriods to regulate the oogenic growth and follicular development (Figure 4.12), which was very similar to what was found in some scombid and salmonids i.e. *S. japonicus* (Nyuji et al., 2013a) and *Salmo salar* (Andersson et al.,

2009). Another important observation is that strong immunoreacvity of FSH-ir was detected in the follicular cell in vitellogenic stages rather than the early oocyte differentiation (oogonia to cortical alveloli stage), implying that the potential role of its peptide may be involved with the steroidogenic acting function during vitellogenin synthesis (Figure 6.12). Nagahama (1994) explained that a pituitary FSH surge induces in follicular cells (theca and granulosa cells). It may be involved with the testosterone synthesis (T) in theca cells and its conversion by aromatase to Estrogen (E_2) in granulosa cells. Lastly, its E_2 was transported and stimulated the hepatocyte to produce the vitellogenin which is called the yolk granule before entering the oocyte. The results found strong intensity of LH-ir in follicular cell during early and late vitellogenic stages. This observation implied that a pituitary LH surge was triggered with respect to a switch in steroidogenic activity within the follicular cell, referring to granulosa cell, which these cells responsed to the maturation inducing hormone (MIS, a C21-steroids such as 17,20β-dihydroxy-4-pregnen-3-one (17,20β-P)). This switching from E_2 to MIS production involved with the regulation in the completion of oocyte maturation (germinal vesicle breakdown, GVB) and hydration (Figure 4.12) as well as the release of a fertilizable egg (Nagahama, 1994). I assumed that the existence of sbGnRH, FSH and LH like-peptides in *R. brachysoma* ovary was relating to oocyte differentiation and its activity. However, this hypothesis needs to be tested in the future by observing the activity of steroidogenic enzymes, level and gene expression/encoding of sex hormones.

Presently, the oogonia, chromatin nucleolar and prominent perinucleolar stages of the *R. brachysoma* female were seen in the non-breeding season. All of these stage were the so-called undeveloped stage. The GSI was still relatively low during this

stages. This was in contrast to the breeding season, the early and late vitellogenic stages were dominantly observed. These stages were the late development stage together with high GSI. At the same time, the results indicated that the number of sbGnRH, GtHs in both number and mRNA level were very much increased in parallel with the breeding season and decresed to the non-breeding season. In contrast, only sbGnRH mRNA level appered to be higher in the non-breeding season. It possible that the sbGnRH mRNA level in the brain may be rapidly transcripted during the breeding season. This hypothesis needs to be further examined. The number of FSH-immunoreactive cells reflected the peptide level together with FSH mRNA level in the non-breeding season was significantly higher than what was found in the breeding season throughout the juvenile stage. It was possible that FSH may controlled the early developed oocyte in both juvenile and adult stagea, as previously agreed by Nozaki et al. (1990b) and Naito et al. (1991). Interestingly, the peptide and level of FSH varied in the breeding season. It was suggested that this peptide hormone play an important role in regulating oocyte growth and vitellogenin synthesis during early and late vitellogenic stages in *R. brachysoma*. This characterization was similar to other fishes including *S. japonicas* (Nyuji et al., 2011, Selvaraj et al., 2012a) and *Paralichtys olivaceus* (Pham et al., 2008). However, FSH might not play such role in all fishes. For example in *P. major*, only LH was detected and involved in the vitellogenesis and final oocyte maturation (FOM) (Pham et al., 2008). Another important observation, the expression and the peptide of LH-immunoreactive cells in *R. brachysoma* during breeding season were significantly higher than GnRH and FSH producing cells. It was plausible that the increase of LH may concern and associate to final oocyte growth and the beginning of the ovulation in *R. brachysoma*. This study was supported by former studies including *S. japonicus*

(Nyuji et al., 2011) and other fish (Rosenfeld et al., 2007). This finding was also consistent with the most fish for example *Pagrus major* (Kagawa et al., 1998), *Dicentrachus labrax* (Forniés et al., 2003) and *Sparus aurata* (Gothilf et al., 1997). This study supported in the predominant role in both FSH and LH which possessed different functions in *R. brachysoma*. Both of which were responsible from sbGnRH activity; FSH predominant contributed to early oogenic growth, while LH encouraged the final maturation of oocytes and ovulation (Nyuji et al., 2011, Planas et al., 1993, Tyler et al., 1991).

The captive female *R. brachysoma* from breeding season had the highest GSI value but the level and peptides of sbGnRH, FSH and LH immunoreactive cells were clearly less than those of wild *R. brachysoma* in the breeding season. Concurrently, the detection of the histological observation indicated that the number of the atretic follicle, especially vitellogenic stages in captive fish was significantly higher than what was found in the wild fish. It was proposed that these lesions may be negatively reflected the impact of capture-induced stress, as similarly reported in *Trachurus japonicas* (Imanaga et al., 2014) and *Takifugu obscurus* (Yang & Chen, 2004). The stress induced atretic follicle probably caused by the decreasing of GnRH-1 expression. This could lead to the dysfunction of estrogen and the gonadotropins (GtHs) from pituitary gland (Imanaga et al., 2014). Guzmán et al. (2009) reported that the level of GnRH-1 expression in captive *Solea senegalesis* was much lower than those in wild fish. This study may also be explained the captive-rearing stress, inhibiting the transcription of GnRH-1. A low transcription of GnRH-1 may also be negatively affected in the reduction of FSH and LH expression, as similarly seen from *R. brachysoma* in captivity. Similar scenarios were also found in other studies. The dysfunction in endocrine system

result in blocking spontaneous ovulation and ultimately the reproductive system of *Salminus hilarii* females in captivity (Amaral et al., 2007, Honji et al., 2009, Honji et al., 2011). Although little evidence is known in the effects of GnRH-1 on GtH synthesis of captive broodstocks, the atretic follicles seemed to be the cause of the reduced oocyte quality and quantity. The atretic follicles causes impairment in the oogenic process as well as reproductive failure/problems, as suggested by several investigators (Guzmán et al., 2009, Levavi-Sivan et al., 2010). To resolve this problem, previous studies suggested the up-regulated of the GnRH-1 expression, the increasing production and efficiency of final oocyte maturation and ovulation is induced by HCG and an LH-like stimulus (hormonal therapies) (Levavi-Sivan et al., 2010, Nyuji et al., 2012a). All of these solutions could potentially be applied with the situation found in captive *R. brachysoma*.

Conclusion

The present study demonstrated the distribution and changes in the sbGnRH and GtHs (FSH and LH) in the brain in both juvenile and sexually matured individual. The highest levels of sbGnRH and GtH were detected in the breeding season implying that increased levels of these two hormones might be related to direct roles on ovarian maturation. Overall in this research, it could be confirm that the activities in the sbGnRH, FSH and LH correlating to oocyte differentiation in *R. brachysoma* female, were the function of hypothalamo-pituitary-ovarian axis. Additionally, the expression of sbGnRH, FSH and LH in wild fish has higher active reproductive succession when compared to captive fish. This suggested the capture-induced stress (Figure 6.12). All of the hormonal level changes found in this study could be applied in *R. brachysoma*

aquaculture. Note that the relationship between the sexual differentiation and expression of sbGnRH-GtH system during larval stage to puberty should be deeply investigated for further research.

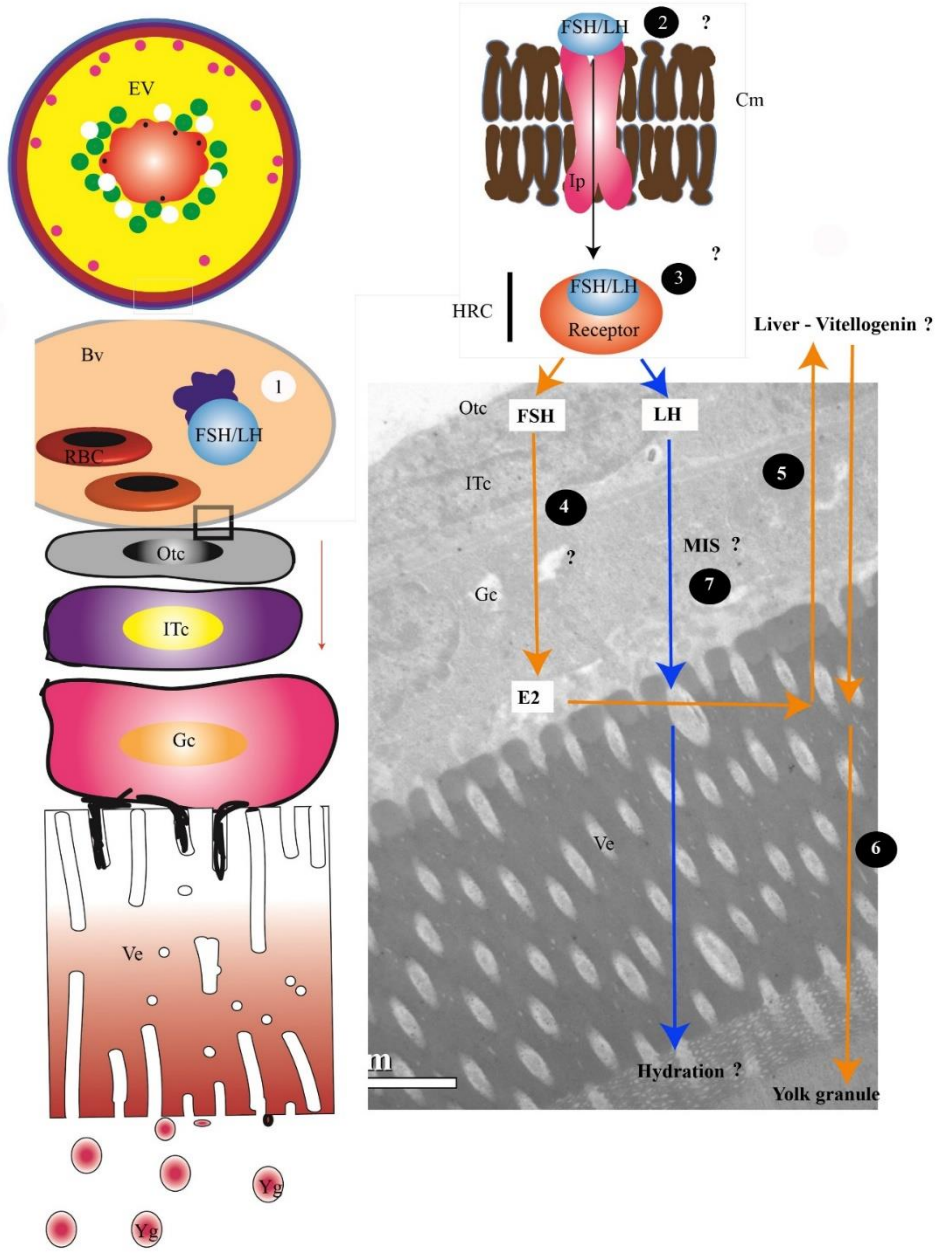

Figure 6.12 Schematic summary of the pathway of FSH and LH immunoreactiivty with expecting to role of these hormones on steriodogenic mechanism in follicular complex (outer theca cell (Otc), inner theca cell (ITc), granulosa cell (Gc) and vitelline envelope (Ve)). *Bv = blood vessel, Cm = cell membrane, E2 = estrogen, Ev = early vitellogenic stage, HRC = hormonal receptor complex, Ip = integral protein, MIS = maturation inducing hormone, RBC = red blood cellm Yg = yolk granules.*

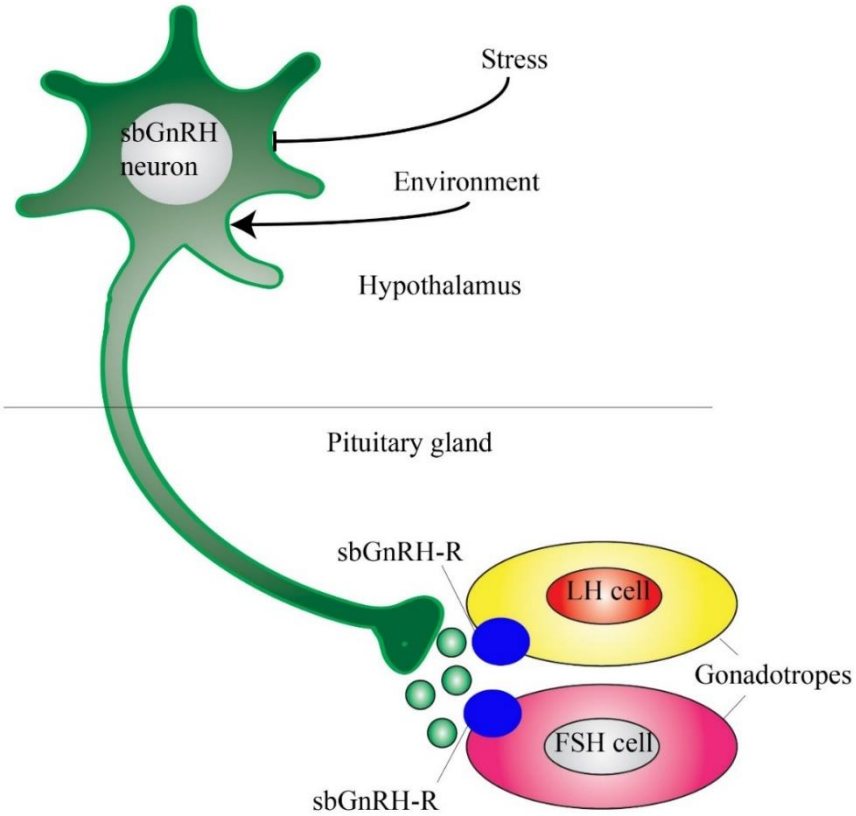

Figure 6.13 Schematic summary of the sbGnRH neuronal cell with entering to gonadotropes (LH and FSH cells) in the pituitary gland. *sbGnRH-R = sbGnRH receptor.*

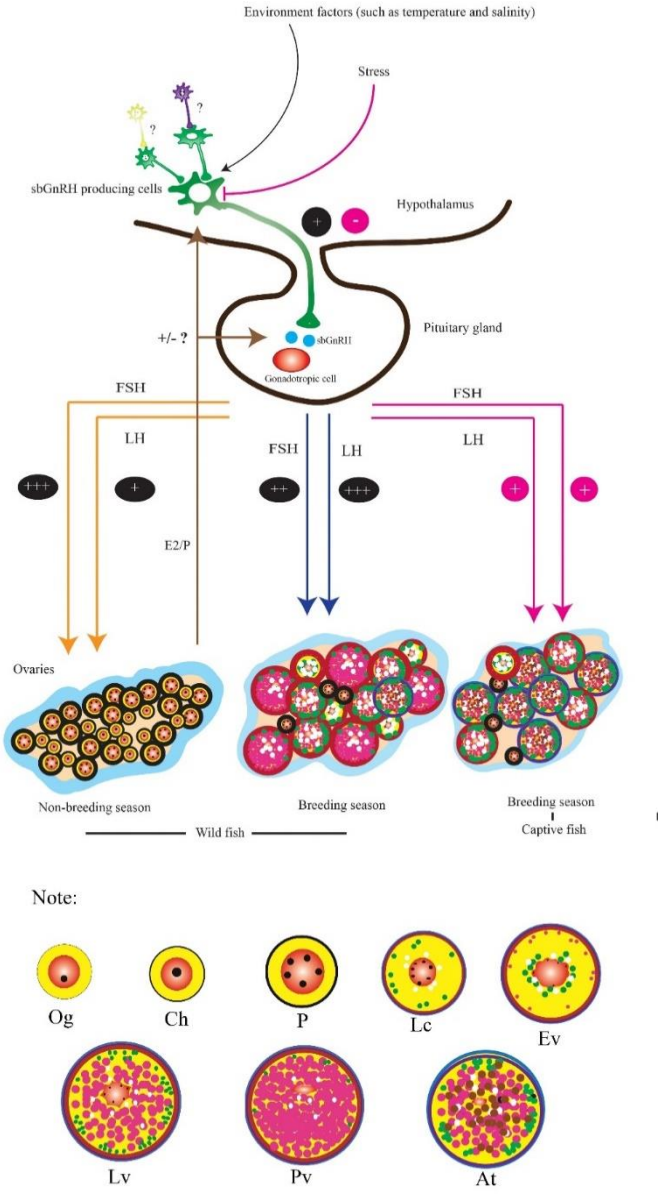

Figure 6.14 Schematic summary of the pathway of brain-pituitary ovarian axis in wild and captive *Rastrelliger brachysoma. At = atretic oocyte, Ca = cortical alveoli, Ch = chromatin nucleolar stage, Ev = early vitellogenic stage, Lc = lipid and cortical alveoli stage, Lv = late vitellogenic stage, Og = oognia, P = perinucleolar stage, Pv = post vitellogenic stage, Dark blue color = theca cell, light blue = tunica albuginea, red color = zona pellucida. Black color = follicular complex, Purple color = granulosa cells, Pink color = yolk granules, White color = lipid droplets, Light red = nucleus, Green color = cortical alveoli*

Chapter VII
DISTRIBUTION AND CHANGES IN sbGnRH and GtHs BETWEEN WILD AND CAPTIVE *Rastrelliger brachysoma* (Bleeker, 1851) MALE DURING BREEDING SEASON

Introduction

The gonadal maturation and its activity in many teleost fishes is regulated by various hormones in the hypothalomo–pituitary–gonadal axis (HPG axis) (Nagahama, 2000). It is integrated in the several neuroendocrines in hypothalamus. Their neuroendocrines are transported to the pituitary gland through the secretion of the neurohormones especially gonadotropin releasing hormone (GnRH) (King & Millar, 1992, Sherwood, 1997, Tucker & Hargreaves, 2004). GnRH was synthesized in hypothalamus and it release of two pituitary gonadotropic hormones (gonadotropins, GtHs): follicle stimulating hormone (FSH) and Luteinizing hormone (LH) (Quérat et al., 2001, Sherwood & Adams, 2005). Many previous investigations had shown that FSH involved with oogenic and follicular growths, whereas LH encouraged the maturation of oocytes and ovulation (Planas et al., 1993, Tyler et al., 1991).

The short mackerel (*Rastrelliger brachysoma*), a multiple-spawning fish is one of the most important fishery resources in Thailand. Up to date, this fish has been considered as one of the potential marine fish species for aquaculture. Under hatchery condition, broodstocks were caught from the wild population, which usually showed the endocrinological dysfunction preventing completion of the reproductive system. A good understanding of basic knowledge of structure and regulation of neuroendocrine mechanism, especially the gonadotropin releasing hormone (GnRH) as the master

signaling neuroendocrine decapeptide and central regulator for controlling reproductive growth of the fish, is needed to understand their physiological roles. Data on the distribution and alteration of sbGnRH-GtHs with which involved the ovarian maturation was previously recommended in *R. brachysoma*. Unfortunately, its precise information has not been investigated to clarify the male fish.

In this study, the structural classification of the brain in *R. brachysoma* was investigated together with the pattern of distribution and the changes of sbGnRH-GtHs system in male *R. brachysoma* during the breeding season. The the pattern of distribution and the changes of sbGnRH-GtHs system were also compared between the wild fish and the captive fish.

Materials and methods

Fish sampling

Juvenile (approx. <14.0 cm in total length) and sexually matured, *Rastrelliger brachysoma* (approx. >16.5 cm in total length, n = 56) were obtained from bamboo strake trap, the Upper Gulf of Thailand (13°16’18.4” N, 100°02’13.4” E). They were sampled during two seasons; non-breeding season (October to December 2013) and breeding season (January to February 2014). Salinity and temperature were also measured at collection site. The captive *R. brachysoma* were produced from the Samut Sakharm Fisheries, Sumut Sakhram Province, Thailand. The experimental protocol in this study was approved by the Animal Care and Use Committee of Faculty of Science in accordance with the guide for the care and use of laboratory animals prepared by Chulalongkorn University (Protocol Review No. 1423003).

Tissue collection and histological analysis

The brain and pituitary gland were dissected before separating into two groups. First group, they were fixed in Davidson's fixative for 24 hrs. Following dehydration and embedding in paraffin, serial of 5 µm sections were cut under standard histological technique. The longitudinal and cross section were histologically stained with Harris's hematoxylin and eosin (Bancroft & Gamble, 2008), Masson's Trichrome (MT) and Periodic acid schiff (PAS) (Bancroft & Gamble, 2008, Dietrich & Krieger, 2009) for identification in structure and cell types under light microscopethe. Last group were frozen and then stored in RNA later at -80 Cº to measure the GnRH and GtHs mRNA levels. The testicular tissue in fish was dissected and weighed for calculating the gonadosomatic indices (GSI). Subsequently, they were examined by standard histological technique (Bancroft & Gamble, 2008, Dietrich & Krieger, 2009). The testicular development was determined based on criteria by Dietrich & Krieger (2009).

Immunohistochemistry and immunofluorescence

This research examined the distribution and activity of sbGnRH, FSHβ and LHβ like-peptides using Immunohistochemistry and immunofluorescence by followed the approach of Senarat et al. (In progress) which was done for female *R. brachysoma*. The staining intensities and number of sbGnRH, FSH and LH immunoreactive cells was counted and recorded.

GnRH mRNA and GtHs mRNA expression using qualitative real time PCR (qPT-PCR)

The GnRH and GtHs mRNA levels was investigated using qRT-PCR method wth fined tune procedure from Senarat et al. (*In progress*), which was previously done in female *R. brachysoma*.

Statistical analysis

Student t – test was used to assess any significant different ($P < 0.05$) of the number and level of sbGnRH - GtHs between non-breeding and breeding seasons development and the sbGnRH-GtHs level between captive and wild fish during sexual maturity. These statistics were calculated using Statistical Package for the Social Sciences (SPSS) software (version 15.0).

Results

Ambient environmental factors at the study site

The average ambient salinity was 26.32 ppt in non-breeding season and the highest salinity during breeding season was 31.75 ppt. During this time the average relative temperature was 28.93˚C and the highest in breeding season was 29.05 ˚C.

Gonadosomatic index (GSI) and testicular development

The GSI of the sexually matured male *R. brachysoma* was 1.12±0.34 during non-breeding season and 1.94±0.26 during breeding season (Figure 5.1A). Note that the juvenile stage was not observed throughout in this research. Under the migration hypothesis of this species, they may be a fast movement fish. They could migrate into

and out of Samut Songkram area in just few week. Therefore, the pattern of migration of this fish would be a great interest in further study. Stages of testicular development in the wild *R. brachysoma* were identified according to the gonadal morphology and proportion of germ cells. In wild fish, only stage designed late spermatogenic stage (stage 3) was observed in non-breeding season (100%). The breeding seasons consisted of the spermatids and spermatozoa stages (Figures 7.1B-7.1F).

Captive *R. brachysoma*, GSI was 1.88±0.17. Only late spermatogenic stage (100%, n = 3) was found in this group (Figures 7.1B, 7.1G-7.1H).

Histological organization of the *R. brachysoma* brain and pituitary gland

The longitudinal section of *R. brachysoma* brain with five major regions including telencephalon, diencephalon, mesencephalon, metencephalon and myelencephalon were previously identified (Senarat et al., 2015). The nucleus preopticus-periventricularis was observed (Figure 7.2A), similarly to that in female *R. brachysoma*. It could be classified into three zones: the nucleus periventricularis, nucleus preopticus and nucleus lateralis tuberis. Based on its distinct size, there are small, medium and large. These cells were 7.64±0.30 μm, 30.2±2.51 μm and 50.1±2.46 μm, respectively (mean±SD of 10 cells) (Figures 7.2B-7.2C).

The histology and histochemistry in the pituitary gland were viewed by light microscopy. The adenohypophysis and the neurohypophysis were seen in the pituitary structure (Figures 7.2D-7.2F).The cross section of the adenohypophysis showed that it could be divided into three distinguished regions; the rostral pars distalis (RPD), the proximal par distalis (PPD) and the pars intermedia (PI). The PI contained four cell types (acidophil I, acidophil II, basophil and chromophil) (Figure 7.2E). Basophils were

mostly found in the PPD, which was previously considered to be homologous to the thyrotrope, somatotrope and gonadotrope (Shimizu et al., 2003). However, the the number and location of basophilic cells in male *R. brachysoma* from the non-breeding season were not significantly different from the males from the breeding seasons.

Immunocytochemistry and immunofluorescence

Distribution of sbGnRH-GtHs immunoreactivity system in the brain of wild *R. brachysoma* male during sexual maturation

Light immunostaining showed that the distribution pattern of sbGnRH immunostaining exhibited. Strong sbGnRH-ir in small–sized neurons in some areas of the nucleus periventricularis. In the nucleus preopticus, sbGnRH-ir was detected in some of the medium and large-sized neurons. More sbGnRH-ir positive neuronal cells were observed by immunocytochemistry and immunofluorescence in many small, medium and large – sized neurons of the nucleus lateralis tuberis. Additionally, the distribution of GtH-ir was present. The FSH-ir was detected in the anterial – ventral regions of PPD, whereas the LH-ir was found to be localized in middle-ventral regions (Figures 7.3-7.4)

Distribution and staining intensities of sbGnRH-GtHs immunoreactivity system in the *R. brachysoma* testis

Intense sbGnRH-ir was showed prominently in the tunica albuginea and spermatogenesis at the various stages excepting the spermatozoa. Interstial tissue of Leyding and Sertoli cells was exclusively detected in all specific antibodies as shown in Figure 7.5. Intense staining of FSH-ir appeared highest in the tunica albuginea and interstial tissue of Leyding cell. Similarly, intense staining of this antibody was also

observed in the spermatogonia, primary spermatocyte and, more intense in Sertoli cell with seminiferous lobule. Immunoreactivity of sbGnRH and LH was weakly exhibited at the spematogonia, primary spermatocytes and secondary spermatocytes. Immunoreactivity of sbGnRH and LH also exhibited at the interstitial cell of Leyding and Sertoli cell. However, it was quite intense as it was shown at the spematogonia, primary spermatocytes and secondary spermatocytes (Figure 7.5)

Numbers and staining intensities of sbGnRH-GtHs-immunoreactive neurons in the brain

The number of sbGnRH- immunoreactive neurons from three zones, FSH and LH immunoreactive cells with counting at breeding seasons was significantly different from those of the non-breeding season ($P<0.05$; Figure 7.6). During the breeding season, the total number of sbGnRH-immunoreactive neurons from the captive fish were significantly less ($P<0.05$) from wild fish (Figure 7.6).

The brain sbGnRH-GtH mRNA levels of *R. brachysoma* male during sexual maturity

The expression of the brain sbGnRH mRNA level from the non-breeding season was significantly higher ($P<0.05$) than the expression in the breeding season (Figure 7.6). On the other hand, the FSH mRNA level during the breeding season was higher ($P<0.05$) than what was found during the non-breeding season.

The LH mRNA level during non-breeding season was significantly less ($P<0.05$) than the level found during the breeding season. The comparative study between wild and captive fish revealed that the sbGnRH-GtH mRNA levels in wild fish were significant higher than captive fish ($P<0.05$).

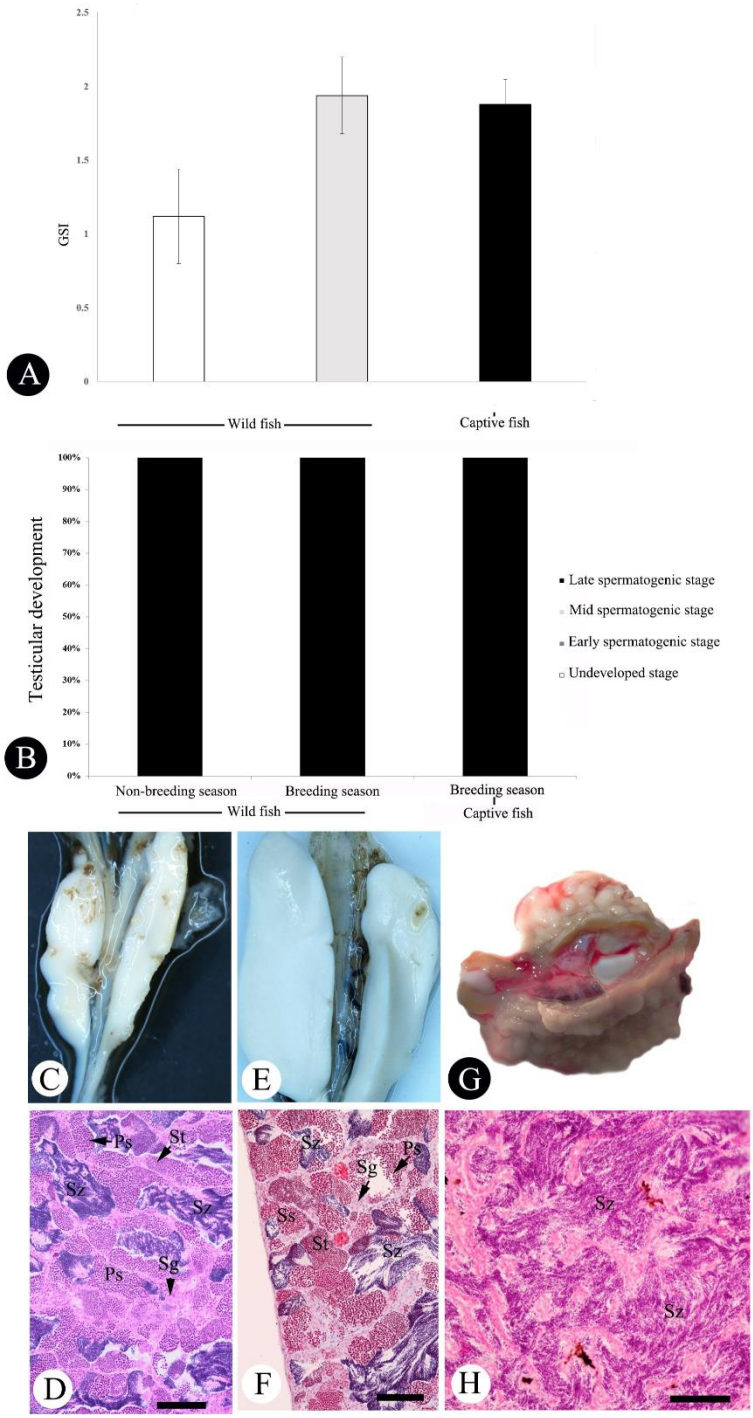

Figure 7. 1 Histograms showing the gonadasomatic index (GSI) (A) and percent of the testicular development (B) based on gross anatomy (C, E, G) and light photomicrograph of histopathological structure at four stages; stage 0, stage 1, stage 2 and stage 3 stained by Masson Trichrome in both wild and captive Rastrelliger brachysoma (D, F, H). Scale bar: 50 µm (H); 100 µm (D-F). *Ps = primary spermatocytes, St = spermatid, Sg = spermatogonia, Sz = spermatozoa.*

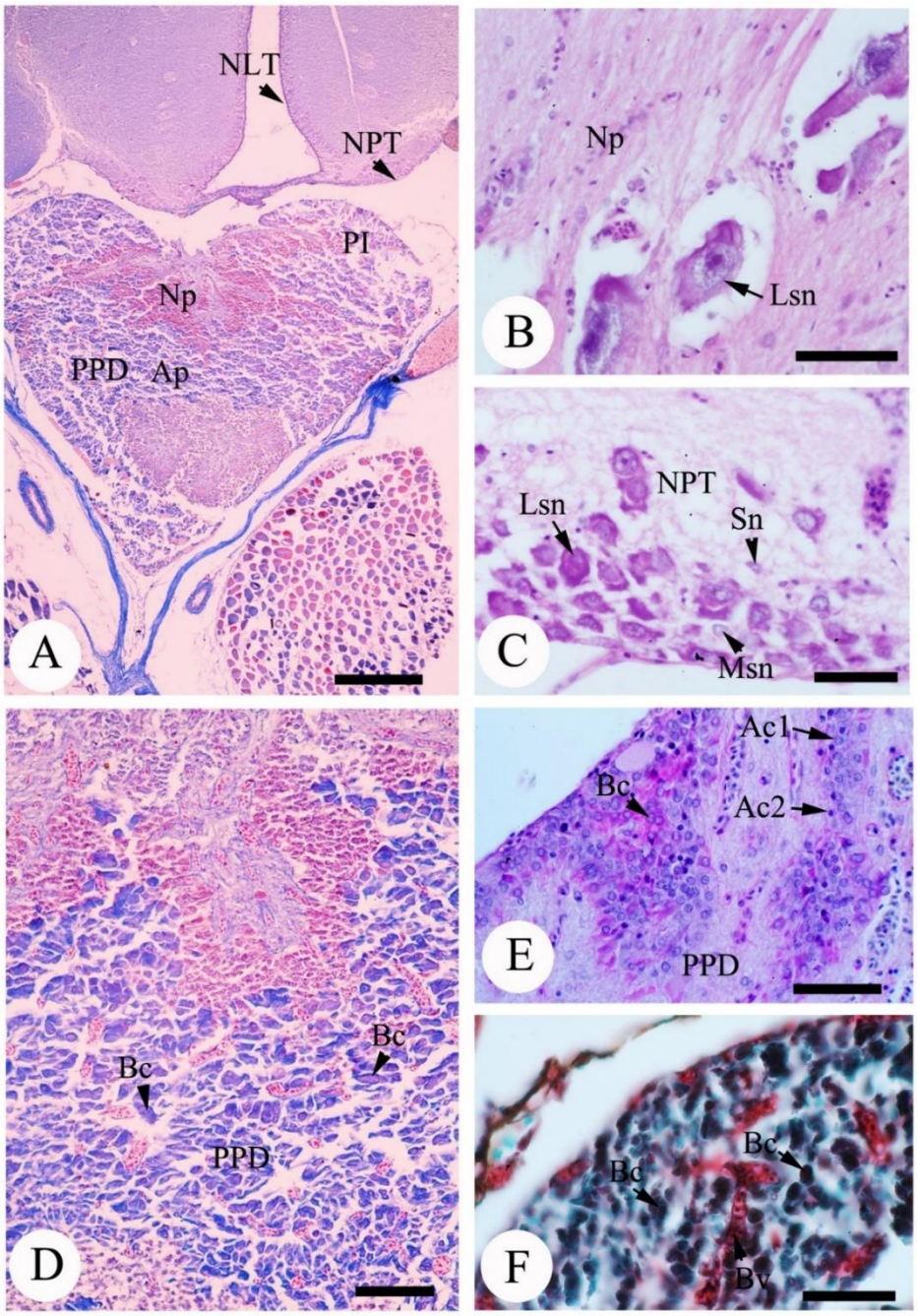

Figure 7.2 Light photomicrograph of histopathological structure of the diencephalon (A, B, C) with special three areas including and pituitary gland (A, D, E, F) Scale bar: 50 µm (C), 100 µm (E, G). *Ac1 = Acidophilic cell type, Ac2 = Acidophilic cell type, Ap = adrenohypophysis, Bc = basophilic cell, Lsn = large sized-cell.Msn = middle sized-cell NLT = nucleus lateralis tuberis, Np = neurohypophysis, PI = Par intermedia, NPT = the nucleus periventricularis, PPD = proximal par distalis, Sn = small sized-cell.*

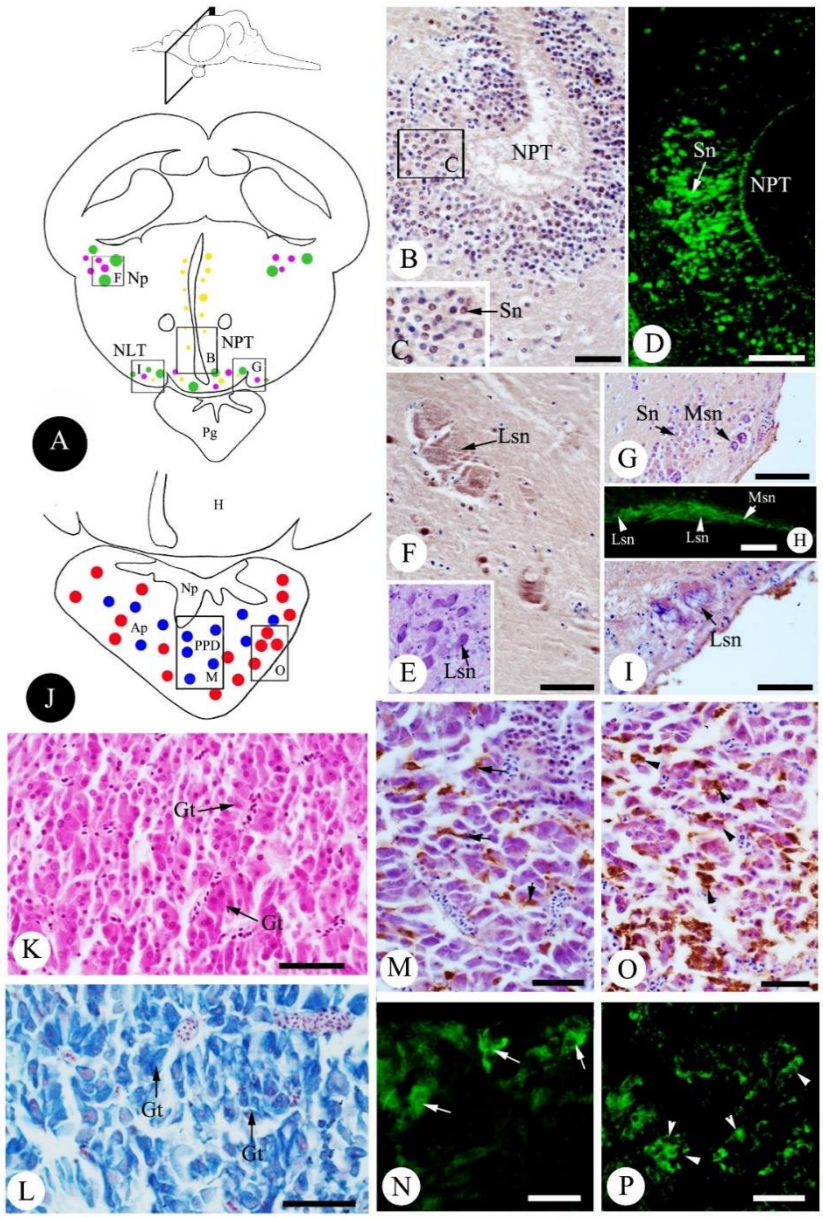

Figure 7.3 Schematic diagram (A, J) and light photomicrograph of immunolocalization of sbGnRH – ir with three areas in the diencephalon including the nucleus periventricularis (NPT) (B-C), the nucleus preopticus (Np) (E-F) and nucleus lateralis tuberis (NLT) (G-I) and GtH – ir (K-P) of *Rastrelliger brachysoma* during non-breeding season. Scale bar: 20 µm (M, O), 50 µm (B, D, F, I, J). *Ap = adrenohypophysis, Gt = gonadotropic cell, H = hypothalamus, Np = neurohypophysis, PPD = proximal par distalis, Sn = small sized-cell (yellow colour), Msn = middle sized-cell (puple colour), Lsn = large sized-cell (green colour), arrow = FSH – ir (blue colour), arrow head = LH- ir (red colour).*

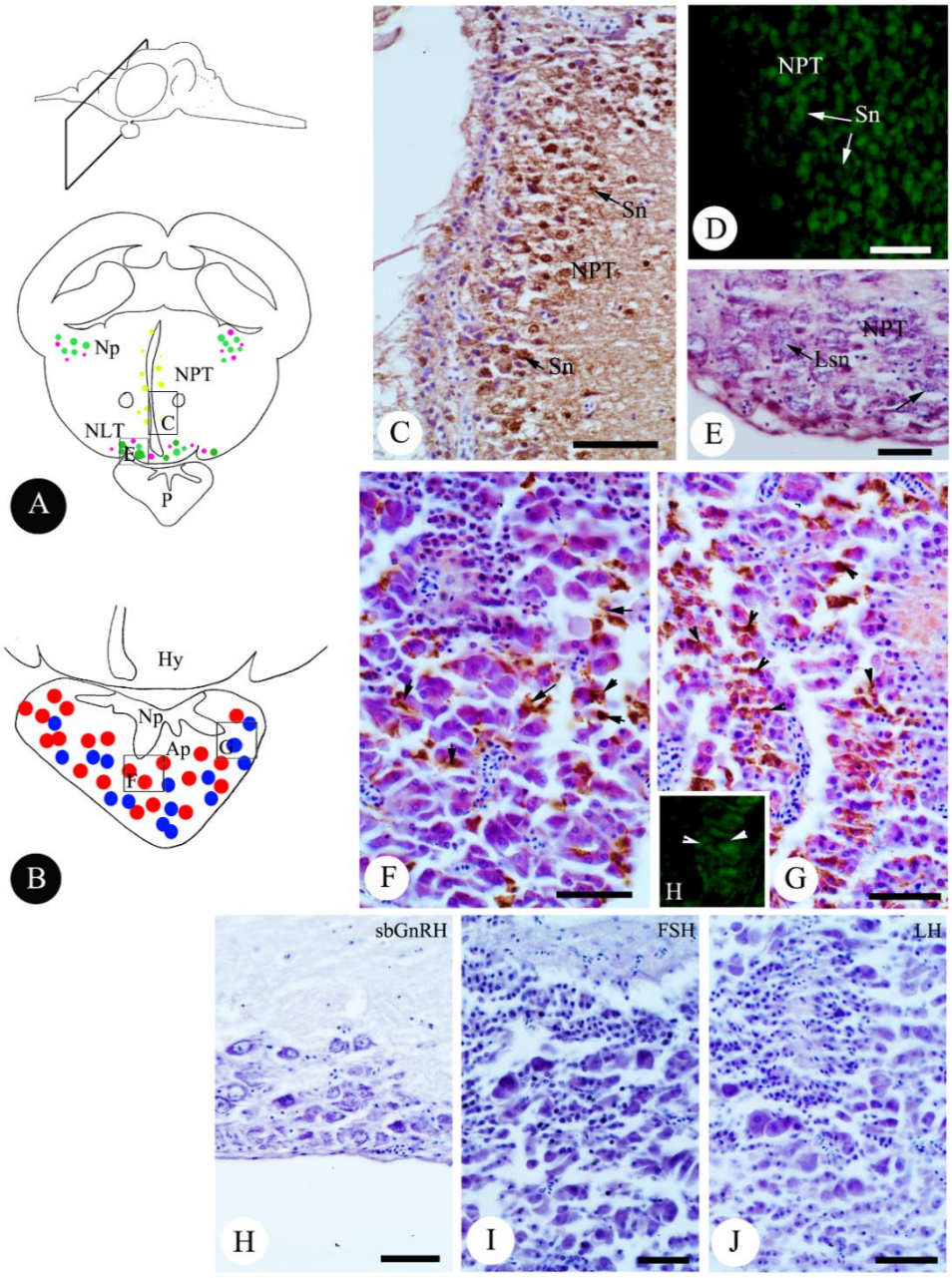

Figure 7.4 Schematic diagram (A-B) and light photomicrograph of immunolocalization of sbGnRH – ir (C-E) of the *Rastrelliger brachysoma* during breeding seasons. Scale bar: 50 µm (C-G). *Note that negative controls including sbGnRH (H), FSH (I) and LH (J) were present. Ap = adrenohypophysis, Hy = hypothalamus, Np = neurohypophysis, NPT = the nucleus periventricularis, Np = the nucleus preopticus, NLT = nucleus lateralis tuberis, Pg = pituitary gland, Sn = small sized-cell (yellow colour), Msn = middle sized-cell (puple colour), Lsn = large sized-cell (green colour).*

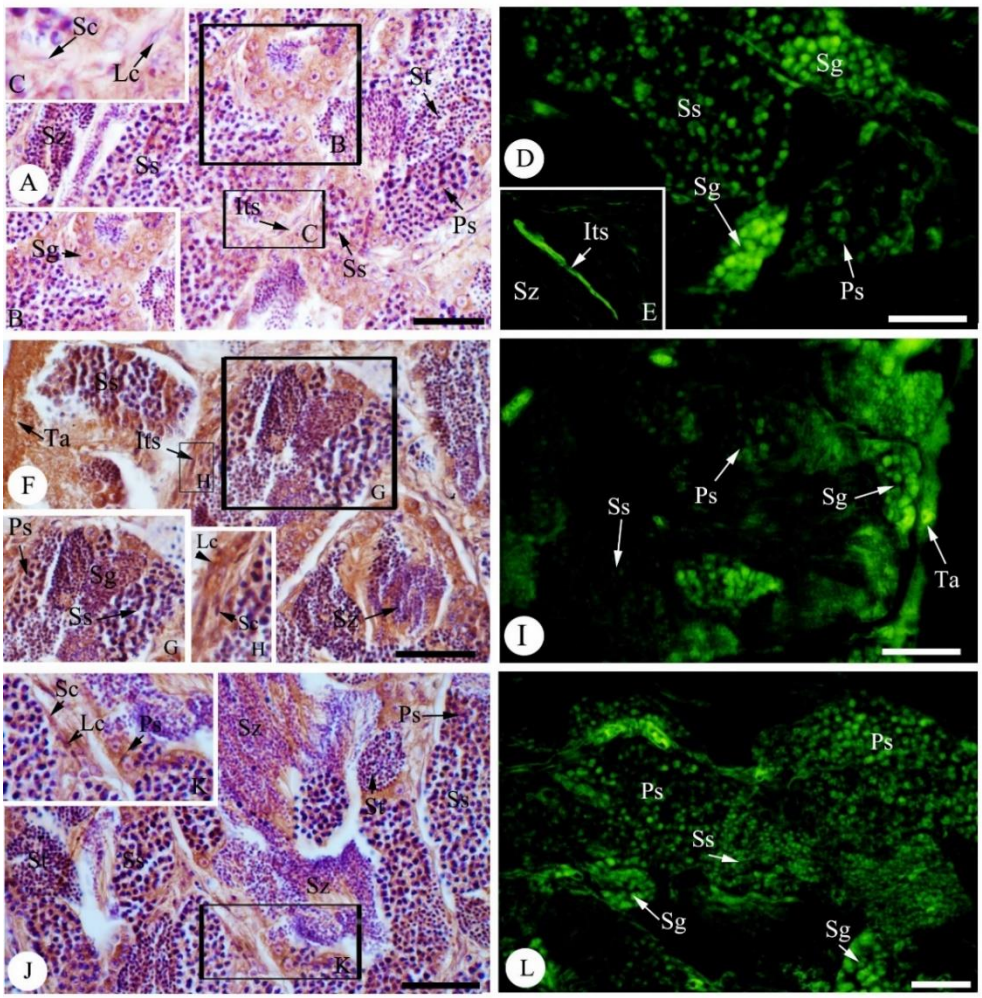

Figure 7.5 Light photomicrograph showing the sbGnRH (A-D), FSH (F-I) and LH (J-L) immunoreactivities in the testicular tissue. Scale bar; 50 µm (A-L). *Itc = interstitial cell and tissue, Lc = Leydig cell, Ps = primary spermatocytes, Sc = Sertoli cell, Ss = secondary spermatocytes, St = spermatid, Sg = spermatogonia, Sz = spermatozoa.*

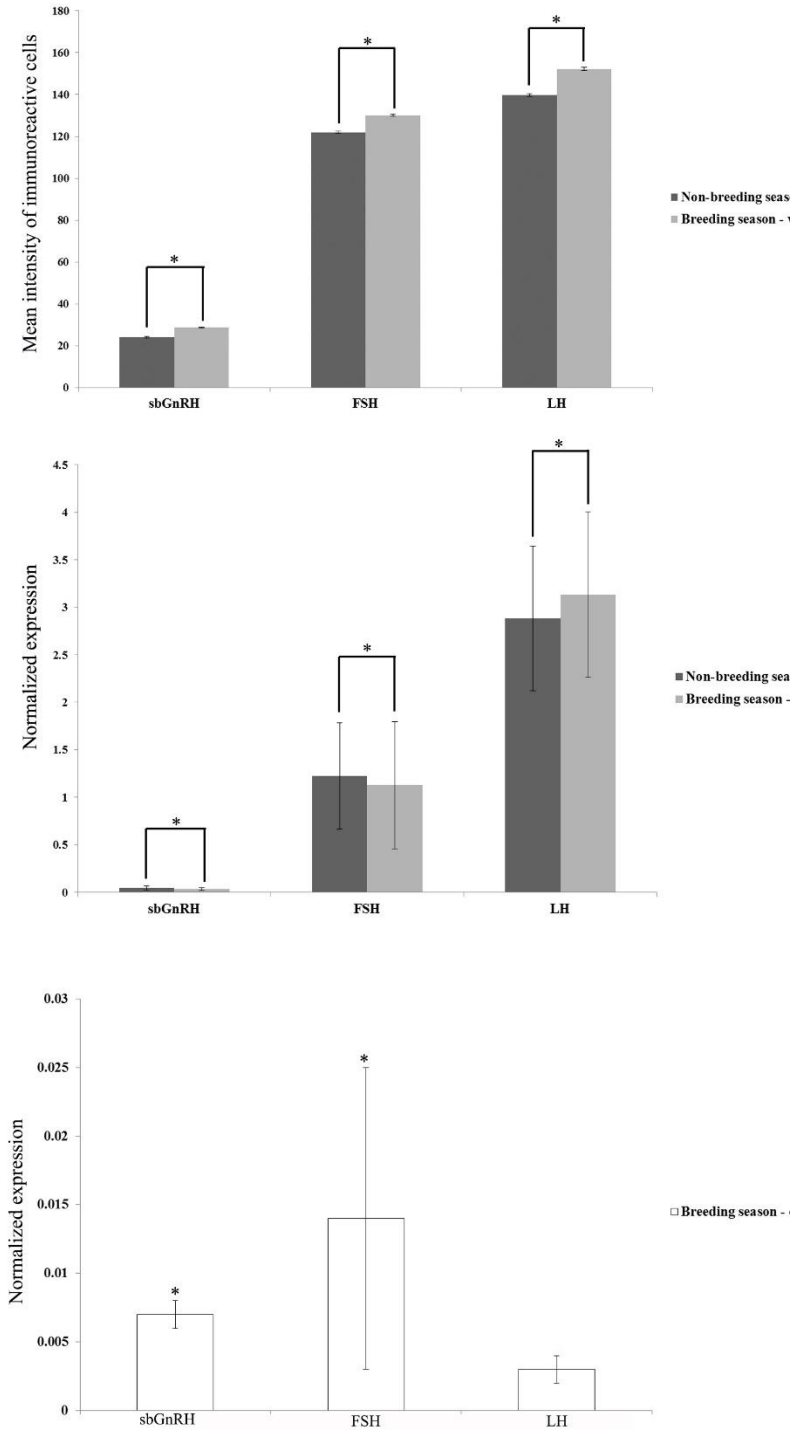

Figure 7.6 Histograms showing the mean numbers of sbGnRH immunoreactive neurons and GtHs – ir (FSH – ir and LH - ir) and their gene expression in the brain during non-breeding and breeding seasons of *Rastrelliger brachysoma*. Values represent X ± SE; significantly different at *P<0.05

Table 7.1 The distribution of sbGnRH neuronal cluters, FSH and LH immunoreactive cells in male *Rastrelliger brachysoma*

Stages/ Seasons	**sbGnRH neuronal clusters/ir**			**FSH cells**	**LH cells**
	NPT	**Np**	**NLT**		
Non-breeding	++ (Sn) - (Msn) - (Lsn)	+ (Sn) ++ (Msn) ++ (Lsn)	+ (Sn) +++ (Msn) ++ (Lsn)	+++	+++
Breeding	+++ (Sn) - (Msn) - (Lsn)	++ (Sn) +++ (Lsn) +++ (Lsn)	+ (Sn) +++ (Msn) +++ (Lsn)	+++	+++

(Note - Immunoreactivity: - no immunoreactivity; + weak immunoreactivity; ++ medium immunoreactivity and +++ strong immunoreactivity)

Table 7.2 *Summary of the presence of sbGnRH-ir, FSH - ir and LH-ir in spermatogenic stages of Rastrelliger brachysoma*

Immunoreactivity	Steps of spermatogenic stage						
	Sg	Ps	Ss	St	Sz	Sc	Lc
sbGnRH-ir	-	-	+	-	+	-	+
FSH – ir	-	+	++	++	++	+	++
LH – ir	-	+	++	+	++	+	+++

(Note immunoractivity; + weak immunoreactivity, ++ moderate immunoreactivity, +++ strong immunoreactivity, - no immunoreactivity. *Lc = Leydig cell, Ps = primary spermatocyte, Sc = Sertoli cell, Sg = spermatogonia, Ss = secondary spermatocyte, St = spermatid, Sz = spermatozoa*)

Discussion

This study investigated the existence of sbGnRH-producing cells from three zones including nucleus periventricularis, nucleus preopticus and nucleus lateralis tuberis for the first time. Three neuronal cell bodies including large, medium and small-sized neurons were positively detected by using immunocytochemistry and immunofluoresces. It suggested that these cells were related to producing the sbGnRH like peptide. The occurrence of these cells was highly similar to those identified in *S. japonicus* (Selvaraj et al., 2009), *T. thynnus* (Palmieri et al., 2008) and *Salmo salar* (Peter et al., 1991). Hence, it can be concluded that the diencephalon was the major neuroendocrine center which produced the sbGnRH peptide and provided a basis for future morpho-functional research in *R. brachysoma*. The sbGnRH-ir neuronal fibers protruded into the gonadotropic cells. Thus, it indicated that they strongly influenced on pituitary gonadotrophs and stimulated on testicular maturation and spermmiation. This supported by the former study in female *R. brachysoma* (Senarat et al., in progress), female *S. japonicas* (Selvaraj et al., 2009), *P. major* (Okuzawa et al., 1997) and *V. moseri* (Amano et al., 2002). This study suggested direct causal relationship with common pathway, as called sbGnRH-GtH system. It was in accordance with those of other fishes for example *S. japonicas* (Selvaraj et al., 2009), *Dicentrachus labrax* (González-Martínez et al., 2002) and *Verasper moseri* (Amano et al., 2002).

A wide distribution of the immunoreacvity confirmed the presence of sbGnRH - ir, FSH - ir and LH-ir in the testicular tissue of *R. brachysoma*, particularly Leydig cell, Sertoli cell and some stages of the spermogenesis. However, no corroborating investigation on this result was observed in the literature review. This is the first finding for such information for *R. brachysoma* as well as other Scombrids. According to the

hypothesis, the high sbGnRH - ir, FSH - ir and LH-ir intensity in both Leydig and Sertoli cells may be due to the location of sbGnRH and GtHs receptors (FSH and LH receptors). This was supported by what was found in other teleost fishes for example, *Danio rerio* (So et al., 2005) and *Oncorhynchus mykiss* (Sambroni et al., 2007). Similarly, Bouma & Nagler (2001) reported that the presence of the LH receptor on the surface of the Leydig cells of *Oncorhynchus mykiss*, acting in the process of producing the 11-ketotestosterone (11-KT). The FSH receptor was also detected on both Sertoli and Leydig cells. It involved with the germ cell development (Sambroni et al., 2007, So et al., 2005). Additionally, most of spermogonia, primary spermatocytes and secondary spermatocytes were still strongly immunoreacted with all peptides. It should be noted that these peptides concerned with gamete development and survival of spermatogenesis. It is possible that FSH peptide function also involved regulating the survival of spermatogonia and the meiosis via FSH receptor of the Sertoli cell, whereas LH peptide may be involved in controlling the differentiation of spermagenesis via LH receptor of the Leydig cell (Ruwanpura et al., 2010). I proposed that testicular tissue may be considered as a part of the principle source for sbGnRH and GtH productions or it may act as the paracrine mechanic to control the spermatogenic maturation. However, the effects of sbGnRH and GtH on spermatogenesis in *R. brachysoma* were still unclear and need to be further elucidated.

Although the investigation of the testicular morphology and GSI in the male *R. brachysoma* was different between the fish from the breeding season and the non breeding season. Testicular development were similarly observed during non-breeding and breeding seasons. Based on the testicular development, *R. brachysoma* in the gulf of Thailand is likely to produce sperm for the whole duration of this study.

Unfortunately the fish has not yet been collected in annual reproductive period. Further research about the fluctuation in reproductive cycle are needed.

The immunocytochemistry showed that the number of sbGnRH – ir and both number and mRNA levels for LH from the breeding season were significantly higher (all with $P<0.05$) than what were exhibited during the non-breeding season. Although, it is unclear, why sbGnRH and FSH mRNA was high expressed in the non-breeding season? It is interesting to note that these peptides related to controlling the size, morphology and maturation of the testicular tissue in *R. brachysoma* due to the correlation between sbGnRH and GtHs system (Figure 5.7). Hence, it was probably due to the increasing of sbGnRH number in diencephalon during the breeding season. Once the sbGnRH number increased, it probably controled the secretion of two gonadotropic peptide hormones (FSH and LH-like peptides) from the gonadotrops in the pituitary gland. This situation was consistent with previous observations in other fishes (Nyuji et al., 2011, Quérat et al., 2001, Sherwood & Adams, 2005). Immunocytochemistry showed that both the increasing of FSH and LH numbers during breeding season, which may indicated the differentiation and maturation of sperm cell as well as spermiation of both peptides (Figure 5.7) (Nyuji et al., 2011, Planas et al., 1993, Tyler et al., 1991).

In this study, the captive male *R. brachysoma* showed highest GSI value in the breeding season. On the contrary, when captive fish were compared with wild fish during the breeding season, wild fish had significantly higher levels of sbGnRH, FSH and LH mRNA than captive fish. This differences were problably caused by capture-induced stress (Figure 5.7). This result was consistence with previous investigations (Nyuji et al., 2012a) and (Nyuji et al., 2013b). Both studies suggested that the decreasing of GnRH-1 expression and dysfunction in the release the gonadotropins

(GtHs) from pituitary gland and estrogen could be caused by stress. Similar pattern were also observed in *Solea senegalesis* where the level of GnRH-1 expression in captive fish was much lower than those in wild fish (Guzmán et al., 2009). Although little is known in this about the relationship between GnRH-1 and GtH synthesis in captive broodstocks in *R. brachysoma*, this finding assured that the captive *R. brachysoma* is living under environmental stress. More studies including the up-regulated of the GnRH-1 expression and inducing in hormonal synthesis should be explored by further study.

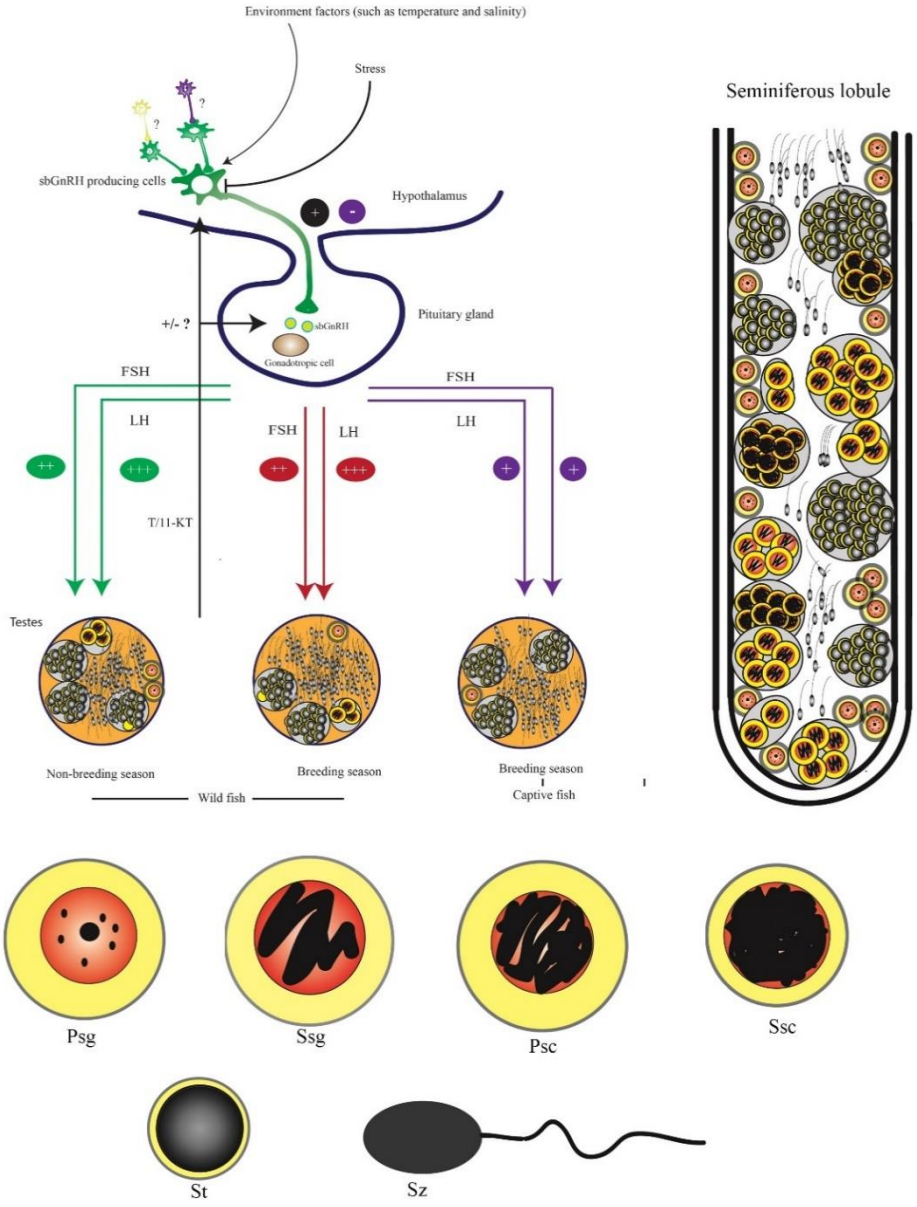

Figure 7.7 Schematic summary of the pathway of brain-pituitary testis axis in wild and captive *Rastrelliger brachysoma.* Psc = primary spermatocyte, Psg = primary spermatogonia, Ssc = secondary spermatocytes, Ssg = secondary spermatogonia, St = spermatid, Sz = spermatozoa.

Chapter VIII
GENERAL DISCUSSION AND CONCLUSION

The Short mackerel *Rastrelliger brachysoma* is one of the most economically important and a candidate for mariculture in Thailand, however, the aquaculture program of this species is hindered by reproductive problems in captivity. Therefore, an understanding in the neuroendocrine system which involves with the reproductive activity of the wild and captive fish are needed for this species.

The ovary of *R. brachysoma* was enclosed by the tunica albuginea. It was considered as an asynchronous developmental type, which could be classified into seven stages based on its histological characteristics. These seven stages were oogonium, chromatin nucleolar, perinucleolar, oil droplet and cortical alveolar, early, late and post vitellogenic stages throughout the atretic follicle. During the oogenic processes, the change and characterization of inclusions including lipids, cortical alveoli and yolk granules were detected by histolochemical techniques. The ultrastructure of female oogenesis was principally divided into five stages based on the nuclear characterization and cytoplasmic organelles; oogonium, previtellogenic, lipid and cortical alveolar, early and late vitellogenic stages, respectively. Initially, oogonium was present within cell nest in the epithelial compartment. Its cell was supported by prefollicular cells. The multiple nucleoli in previtellogenic stage, referring to primary growth stage were the first to appear and they were scattered around the peripheral of nuclear membrane with the increasing number of cytoplasmic organelles. Some microvilli of granulosa cell initially protruded into the vitelline envelope. A simple layer of flattened granulosa and theca cells was also observed. The lipid and

cortical alveolar stage under secondary growth oocyte accumulated two inclusions; the lipid droplets and cortical alveoli in the ooplasm. Another characterization, the increasing of numerous microvilli was also detected in the vitelline envelope. Finally, in the vitellogenic stage, a massive uptake and processing of proteins into yolk platelets due to embedding of the numerous microvilli in the largest vitelline envelope was observed.

The testicular parenchyma was a lobular organ, which jointed with testicular duct. It was classified as an unrestricted spermatogonial type. The classification of spermatogenetic stage could be classified into six stages based on the pattern of chromatin condensation and other characterizations at the light microscopic level. These six stages included the primary and secondary spermatogonium, primary and secondary spermatocyte, spermatid and spermatozoon. The spermatogenesis could be also classified another four stages based on the nuclear and cytoplasmic characterizations at the ultrastructural level. Spermatogonium was the early germ cell. It underwent a series of mitotic division to reach the primary spermatocyte. Secondary spermatocyte was shown with the heterochromatin surrounding the nuclear membrane which was rarely seen within seminiferous lobules. Stages during the spermatids differentiation comprised of early, intermediate and late stages. These stages under went the degree/change of chromatin condensation. Finally, the spermatozoon of *R. brachysoma* was an aquasperm primitive type. It composed of an oval head without an acrosome, a short mid-piece consisting of two basal bodies (proximal and distal centrioles) and a long flagella tail without lateral fins. The axonemes of classical form with 9+2 microtubules were present in the flagellum.

The anatomy and histological structure detailed of the brain and spinal cord which encompassed the central nervous system in the *R. brachysoma* revealed that the brain of *R. brachysoma* consisted of telencephalon, mesencephalon, diencephalon, metencephalon and myelencephalon, which followed posteriorly by the spinal cord. The telencephalon of *R. brachysoma* was less developed when compared to other parts. It mainly consisting of olfactory lobes and cerebral hemispheres. The largest part, the optic lobe located, in the mesencephalon region consisted of six histologically distinct layers; stratum marginale, stratum opticum, stratum fibroetgricialem, stratum album central, stratum griseum central and stratum periventriculae respectively. The diencephalon situated beneath mesencephalon. The epithalamus, thalamus and hypothalamus were distinctly seen in the diencephalon. The cerebellum in the metencephalon composed of the corpus and the valvula cerebelli. The most posterior portion of the brain was myelencephalon, which composed of the medulla oblongata and vagal lobes before joining the spinal cord. An understanding of the general and detailed anatomy of brain is an important part to apply the distribution and functions of neurotransmitters, involved with reproduction

The localization of the immunoreactivity of sbGnRH neurons revealed that it was distributed in neuronal cells of the nucleus preopticus-periventricularis witch were divided into three regions including nucleus periventricularis, nucleus preopticus and nucleus lateralis tuberis in the brain. The sbGnRH neuronal immunoreactive fibers were detected and protruded into the proximal par distalis where the gonadotrophs were present. These cells were also positive reacted, both FSHβ – ir and LHβ – ir. In the ovary, all peptides exhibited in the follicular cell and some oocytes. The alteration of GtHs levels using their number and mRNA level were detected at the highest level and

the breeding season fish was significant higher ($P<0.05$) than non-breeding season fish. The results in this part suggested significant involvement of sbGnRH and GtHs system with the ovarian development and maturation in this fish. In the comparative results, the number and mRNA levels of sbGnRH, FSHβ and LHβ in the wild broodstock were significantly higher than the level found in the cultured broodstock. This probably corresponded to the stressor in the culturing condition. It might be suggested the wild female fish showed more active oogenic process when compared to those captive fish. This result may be related to the endocrinological dysfunction.

The distribution the sbGnRH-immunoreactive neurons were detected in the nucleus preopticus-periventricularis in the brain of the *R. brachysoma* male which the similar pattern was observed in female. In the proximal par distalis, the gonadotrophs were positively detected, both FSHβ – ir and LHβ – ir. All peptides exhibited in the testicular tissue especially Leydig and Sertoli cells as well as some stages of spermatogenesis. The change of sbGnRH and GtHs levels according to their number and mRNA levels of *R. brachysoma* in the breeding season was significantly higher ($P<0.05$) than the non-breeding season. The presence of the sbGnRH and GtHs system in this part, indicated the involvement to the testicular maturation of this species. The numbers and the mRNA levels of sbGnRH, FSHβ and LHβ in wild fish were significantly higher than those of the cultured broodstocks. This novel finding provided valuable information regarding the endocrinological and reproductive dysfunctions.

In brief, the results from the current study could point out that the highest levels of sbGnRH and GtHs were detected in the breeding season. Therefore, this implied that the increased levels of these two hormones might be related to direct roles on gonadal maturation. I could confirm the activities in the sbGnRH, FSHβ and LHβ which

correlating to gonadal differentiation in *R. brachysoma*, as the function of hypothalamo-pituitary-ovarian axis. The expression of sbGnRH, FSHβ and LHβ reflects a more active reproductive development in wild fish when compared to captive fish. This suggested the capture-induced stress. The benefit from this study was not only to understand about physiological stress but also to support of the broodstock management program. The good examples of the knowledge gained for this study that could be benefit to such program were the up-regulated of the GnRH-1 expression, the increasing production and efficiency of final oocyte maturation and ovulation of *R. brachysoma* in captivity. The life cycle of *R. brachysoma* in the Gulf of Thailand was hypothesized that there were two spawning grounds and majority of the fish only spawned twice during the whole year. These two spawning grounds located in the area of Prachuap Khiri Khan, Chumporn and Surat Thani provinces. The spawning period covered from January to March ((Department of Fisheries, 1965, Menasveta, 1980). Based upon the histological study of gonadal structure and development of *R. brachysoma,* it can be presumed that the current hypothesis holds true for the multiple spawning fish and several long breeding periods per year. Based on the fact that the histological and hormonal studies reveal that these species spawn year round and ripe female were also observed on the year round basis as well. Several competing hypothesis could challenge the current one.

First, *R. brachysoma* population may spawn all year long which the spawning ground might not restricted to the two proposed areas. Second, *R. brachysoma* in the gulf of Thailand may have local population such as the one from Sumut Songkram Province. Last, the two spawning which were proposed earlier could still hold true for majority of the fish. However some fish may spawned year round along the proposed

migration route. This could highly influence the managing decision for this species. Consequently, the genetic diversity of this fish could be extremely high. I recommend extra protection for the spawning ground beyond the two previous proposed.

REFERENCES

Abascal F, Medina A (2005) Ultrastructure of oogenesis in the bluefin tuna, *Thunnus thynnus*. Journal of Morphology 264: 149-160

Abascal F, Medina A, Megina C, Calzada A (2002) Ultrastructure of *Thunnus thynnus* and *Euthynnus allettevatus* spermatozoa. Journal of Fish Biology 60: 147-153

Abascal FJ, Megina C, Medina A (2004) Testicular development in migrant and spawning bluefin tuna (*Thunnus thynnus* (L.)) from the eastern Atlantic and Mediterranean. Fishery Bulletin 102: 407-417

Abdalla FC, Cruz-Landim C (2003) Some histological and ultra-structural aspects of the oogenesis of *Piaractus mesopotamicus* Holmberg, 1887 (Teleostei). Brazilian Journal of Morphological Sciences 20: 3-10

Abdalla FC, Cruz-Landim C (2004) Occurrence and ultrastructural characterization of" nuage" during oogenesis and early spermatogenesis of *Piaractus mesopotamicus* Holmberg, 1887 (Teleostei). Brazilian Journal of Biology 64: 555-561

Abdel-Aziz SH, Al-Otaibi M, Osman AM, Ali TE-S, Bawazeer F (2012) Ultrastructural evidence of oogenesis of the Rusty Parrotfish, *Scarus ferrugineus* (Teleostei: Scaridae). Copeia 2012: 229-236

Abe H (1994) Regional variations in the ultrastructural features of secretory cells in the rat oviductal epithelium. The Anatomical Record 240: 77-85

Abe H, Oikawa T (1992) Examination by scanning electron microscopy of oviductal epithelium of the prolific Chinese Meishan pig at follicular and luteal phases. The Anatomical Record 233: 399-408

Abrahão VP, Shibatta OA (2015) Gross morphology of the brain of *Pseudopimelodus bufonius* (Valenciennes, 1840)(Siluriformes: Pseudopimelodidae). Neotropical Ichthyology 13: 255-264

Alberts B, Lewis J, Bray D (2000) Molecular biology of the cell. Garland Science

Amano M, Oka Y, Yamanome T, Okuzawa K, Yamamori K (2002) Three GnRH systems in the brain and pituitary of a pleuronectiform fish, the barfin flounder *Verasper moseri*. Cell and Tissue Research 309: 323-329

Amano M, Yamanome T, Yamada H, Okuzawa K, Yamamori K (2004) Effects of photoperiod on gonadotropin-releasing hormone levels in the brain and pituitary of underyearling male barfin flounder. Fisheries Science 70: 812-818

Amaral J, de Melo R, Honji R, Moreira R (2007) 10. Effects of migration impediment of *Salminus hilarii* (Teleost: Characidae) on the pituitary–gonad axis. Comparative Biochemistry and Physiology Part A: Molecular & Integrative Physiology 148: S44

Andersson E, Fjelldal PG, Klenke U, Vikingstad E, Taranger GL, Zohar Y, Stefansson SO (2001) Three forms of GnRH in the brain and pituitary of the turbot, *Scophthalmus maximus*: immunological characterization and seasonal variation. Comparative Biochemistry and Physiology Part B: Biochemistry and Molecular Biology 129: 551-558

Andersson E, Nijenhuis W, Male R, Swanson P, Bogerd J, Taranger GL, Schulz RW (2009) Pharmacological characterization, localization and quantification of expression of gonadotropin receptors in Atlantic salmon (*Salmo salar* L.) ovaries. General and Comparative Endocrinology 163: 329-339

Anglade I, Zandbergen T, Kah O (1993) Origin of the pituitary innervation in the goldfish. Cell and Tissue Research 273: 345-355

Baldacci A, Taddei A, Mazzini M, Fausto A, Buonocore F, Scapigliati G (2001) Ultrastructure and proteins of the egg chorion of the antarctic fish *Chionodraco hamatus* (Teleostei, Notothenioidei). Polar Biology 24: 417-421

Bancroft JD, Gamble M (2008) Theory and practice of histological techniques. Elsevier Health Sciences

Bartsch P, Britz R (1997) A single micropyle in the eggs of the most basal living actinopterygian fish, *Polypterus* (Actinopterygii, Polypteriformes). Journal of Zoology 241: 589-592

Bauchot R, Bauchot M, Platel R, Ridet J (1977) Brains of Hawaiian tropical fishes; brain size and evolution. Copeia 1: 42-46

Bauchot R, Diagne M, Ridet J-M, Bauchot M-L (1989) The brain of *Rhyacichthys aspro* (Rhyacichthyidae, Gobioidei). Japanese Journal of Ichthyology 36: 260-266

Bauchot R, Randall J, Ridet J, Bauchot M (1988) Encephalization in tropical teleost fishes and comparison with their mode of life. Journal fur Hirnforschung 30: 645-669

Bhatti MN, Al-Daham NK (1978) Annual cyclical changes in the testicular activity of a freshwater teleost, *Barbus luteus* (Heckel) from Shatt-Al-Arab, Iraq. Journal of Fish Biology 13: 321-326

Billard R (1970) Ultrastructure comparée de spermatozoïdes de quelques poissons téléostéens. Comparative Spermatology: 71-79

Billard R (1983) A quantitative analysis of spermatogenesis in the trout, *Salmo trutta* fario. Cell and Tissue Research 230: 495-502

Billard R (1984) Ultrastructural changes in the spermatogonia and spermatocytes of *Poecilia reticulata* during spermatogenesis. Cell and Tissue Research 237: 219-226

Billard R (1992) Reproduction in rainbow trout: sex differentiation, dynamics of gametogenesis, biology and preservation of gametes. Aquaculture 100: 263-298

Billard R, Richard M, Rombauts R (1982) Inhibition of spermatogenesis and vitellogenesis in rainbow trout by hormonal additives in the diet. The Progressive Fish-Culturist 44: 15-18

Blazer V (2002) Histopathological assessment of gonadal tissue in wild fishes. Fish Physiology and Biochemistry 26: 85-101

Bouma J, Nagler JJ (2001) Estrogen receptor-α protein localization in the testis of the rainbow trout (*Oncorhynchus mykiss*) during different stages of the reproductive cycle. Biology of Reproduction 65: 60-65

Brill RW, Holts D, Chang R, Sullivan S, Dewar H, Carey F (1993) Vertical and horizontal movements of striped marlin (*Tetrapturus audax*) near the Hawaiian Islands, determined by ultrasonic telemetry, with simultaneous measurement of oceanic currents. Marine Biology 117: 567-574

Brown-Peterson N, Thomas P, Arnold C (1988) Reproductive biology of the spotted seatrout, *Cynoscion nebulosus*, in south Texas. Fishery Bulletin 88: 373-388

Brown-Peterson NJ, Wyanski DM, Saborido-Rey F, Macewicz BJ, Lowerre-Barbieri SK (2011) A standardized terminology for describing reproductive development in fishes. Marine and Coastal Fisheries 3: 52-70

Brown-Peterson N, Grier H, Overstreet R (2002) Annual changes in germinal epithelium determine male reproductive classes of the cobia. Journal of Fish Biology 60: 178-202

Bruslé S (1981) Ultrastructure of spermiogenesis in *Liza aurata* risso, 1810 (Teleostei, Mugilidae). Cell and Tissue Research 217: 415-424

Bshary R, Wickler W, Fricke H (2002) Fish cognition: a primate's eye view. Animal cognition 5: 1-13

Buhi WC (2002) Characterization and biological roles of oviduct-specific, oestrogen-dependent glycoprotein. Reproduction 123: 355-362

Burke M, Leatherland J (1984) Seasonal changes in testicular histology of brown bullheads, *Ictalurus nebulosus* Lesueur. Canadian Journal of Zoology 62: 1185-1194

Butler A (2011) Functional morphology of the brains of ray-finned fishes. Encyclopedia of Fish Physiology: From Genome to Environment, Elsevier, New York: 37-45

Cayré P (1991) Behaviour of yellowfin tuna (*Thunnus albacares*) and skipjack tuna (*Katsuwonus pelamis*) around fish aggregating devices(FADs) in the Comoros Islands as determined by ultrasonic tagging. Aquatic Living Resources 4: 1-12

Chatchavalvanich K, Visattipat R (1997) Gross and microscopic structure of the female reproduction system in the White-tail Stingray (*Dasyatis bleekeri*). Thammasat International Journal of Science and Technology 2: 47-55

Chellappa S, Lima J, Araújo A, Chellappa N (2010) Ovarian development and spawning of Serra Spanish mackerel in coastal waters of Northeastern Brazil. Brazilian Journal of Biology 70: 451-456

Chung E-Y (2008) Ultrastructure of germ cells, the Leydig cells, and Sertoli cells during spermatogenesis in *Boleophthalmus pectinirostris* (Teleostei, Perciformes, Gobiidae). Tissue and Cell 40: 195-205

Cinquetti R (1994) Localization of steroidogenesis in the testis of *Padogobius martensi* (Pisces, Gobiidae): Histological, histochemical and ultrastructural investigation. Italian Journal of Zoology 61: 309-315

Cinquetti R, Dramis L (2003) Histological, histochemical, enzyme histochemical and ultrastructural investigations of the testis of *Padogobius martensi* between annual breeding seasons. Journal of Fish Biology 63: 1402-1428

Cruz-Landim Cd, Cruz-Hofling MAd (2001) Ultrastructure of ovarian follicular epithelium of the amazonian fish *Pseudotylosurus microps* (Gunther)(Teleostei, Belonidae): I. the follicular cells cycle of development. Revista Brasileira de Zoologia 18: 99-109

Culling CFA (2013) Handbook of histopathological and histochemical techniques: including museum techniques. Butterworth-Heinemann

Davison W, Axelsson M, Nilsson S, Forster ME (1997) Cardiovascular control in Antarctic notothenioid fishes. Comparative Biochemistry and Physiology Part A: Physiology 118: 1001-1008

de Vlaming V (1983) Oocytes developmental patterns and hormonal involvements, among teleost in control process. Control Processes in Fish Physiology, Room Helm, London

Dellovade TL, Hunter E, Rissman EF (1995) Interactions with males promote rapid changes in gonadotropin-releasing hormone immunoreactive cells. Neuroendocrinology 62: 385-395

Dellovade TL, Ottinger M, Rissman EF (1995) Mating alters gonadotropin-releasing hormone cell number and content. Endocrinology 136: 1648-1657

Department of Fisheries (1965) Reports on mackerel investigations 1963-1965. In Marine Fisheries Laboratory, Division of Research and Investigation, Department of Fisheries, Bangkok, Thailand,

Department of Fisheries (2009) Fisheries statistics of Thailand. [access 2 December 2014]. Available from http://www.fisheries.go.th/itstat/yearbook/data_2552/Yearbook/Yearbook2009.pdf.

Dietrich D, Krieger HO (2009) Histological analysis of endocrine disruptive effects in small laboratory fish. John Wiley & Sons

Dodd J (1983) Reproduction in Cartilaginous Fishes (Chondrichthyes). Fish Physiology, Elsevier 9: 31-95

Elofsson U, Winberg S, Francis RC (1997) Number of preoptic GnRH-immunoreactive cells correlates with sexual phase in a protandrously hermaphroditic fish, the dusky anemonefish (*Amphiprion melanopus*). Journal of Comparative Physiology A 181: 484-492

Esteban M, Muñoz J, Meseguer J (2000) Blood cells of sea bass (*Dicentrarchus labrax* L.). Flow cytometric and microscopic studies. The Anatomical Record 258: 80-89

FAO (1999) Report of the First Workshop on the Assessment of Fishery Stock Status in South and Southeast Asia. In pp Bangkok, 16-19 June 2009. FAO Fisheries and Agricultural Report No. 913, Rome, FAO, 30p

FAO (2010) Report of the First Workshop on the Assessment of Fishery Stock Status in South and Southeast Asia. In pp Bangkok, 16-19 June 2009. FAO Fisheries and Agricultural Report No. 913, Rome, FAO, 30p

Fawcett DW (1975) Ultrastructure and function of the Sertoli cell. In: Hamilton, DW, Greep, RD (Eds.), Handbook of physiology. Washington, American Physiological Society, pp 21-55.

Fernald RD, White RB (1999) Gonadotropin-releasing hormone genes: phylogeny, structure, and functions. Frontiers in Neuroendocrinology 20: 224-240

Fishelson L, Gibson R, Delarea Y (1990) Unusual cell organelles during spermiogenesis in two species of gobies (Gobiidae, Teleostei). Cell and Tissue Research 262: 397-400

Forniés M, Carrillo M, Mañanós E, Sorbera LA, Zohar Y, Zanuy S (2003) Relative potency of the forms of GnRH and their analogs on LH release in sea bass. Journal of Fish Biology 63: 73-89

Ganias K, Somarakis S, Koutsikopoulos C, Machias A, Theodorou A (2003) Ovarian atresia in the Mediterranean sardine, *Sardina pilchardus* sardina. Journal of the Marine Biological Association of the UK 83: 1327-1332

García-López A, Martínez Rodríguez G, Sarasquete C (2005) Male reproductive system in Senegalese sole *Solea senegalensis* (Kaup): anatomy, histology and histochemistry. Histology and Histopathology 20: 1179-1189.

Genten F, Terwinghe E, Danguy A (2008) Atlas of fish histology. Science Publishers, Enfield, NH: USA

González-Martínez D, Madigou T, Zmora N, Anglade I, Zanuy S, Zohar Y, Elizur A, Muñoz-Cueto JA, Kah O (2001) Differential expression of three different

prepro-GnRH (gonadotrophin-releasing hormone) messengers in the brain of the european sea bass (*Dicentrarchus labrax*). Journal of Comparative Neurology 429: 144-155

González-Martínez D, Zmora N, Mañanos E, Saligaut D, Zanuy S, Zohar Y, Elizur A, Kah O, Muñoz-Cueto JA (2002) Immunohistochemical localization of three different prepro-GnRHs in the brain and pituitary of the European sea bass (*Dicentrarchus labrax*) using antibodies to the corresponding GnRH-associated peptides. Journal of Comparative Neurology 446: 95-113

Gothilf Y, Meiri I, Elizur A, Zohar Y (1997) Preovulatory changes in the levels of three gonadotropin-releasing hormone-encoding messenger ribonucleic acids (mRNAs), gonadotropin beta-subunit mRNAs, plasma gonadotropin, and steroids in the female gilthead seabream, *Sparus aurata*. Biology of Reproduction 57: 1145-1154

Gresik EW, Quirk JG, Hamilton JB (1973) A fine structural and histochemical study of the Leydig cell in the testis of the teleost, *Oryzias latipes* (Cyprinidontiformes). General and Comparative Endocrinology 20: 86-98

Grier H (1975) Aspects of germinal cyst and sperm development in *Poecilia latipinna* (Teleostei: Poeciliidae). Journal of Morphology 146: 229-249

Grier H (1976) Sperm development in the teleost *Oryzias latipes*. Cell and Tissue Research 168: 419-431

GRIER H J (1993) Comparative organization of Sertoli cells including the Sertoli cell barrier. In: Russell LD, Griswold M D (Eds.), The Sertoli Cell. Cache River Press, pp. 704-739.

Grier H (2000) Ovarian germinal epithelium and folliculogenesis in the common snook, *Centropomus undecimalis* (Teleostei: Centropomidae). Journal of Morphology 243: 265-281

Grier H, Linton J, Leatherland J, De Vlaming V (1980) Structural evidence for two different testicular types in teleost fishes. American Journal of Anatomy 159: 331-345

Grier H, Taylor R (1998) Testicular maturation and regression in the common snook. Journal of Fish Biology 53: 521-542

Grier H, Van den Hurk R, Billard R (1989) Cytological identification of cell types in the testis of *Esox lucius* and *E. niger*. Cell and Tissue Research 257: 491-496

Grizzle JM, Rogers WA (1976) Anatomy and histology of the channel catfish. Auburn University, Agricultural Experiment Station

Grober MS, Fox SH, Laughlin C, Bass AH (1994) GnRH cell size and number in a teleost fish with two male reproductive morphs: sexual maturation, final sexual status and body size allometry. Brain, Behavior and Evolution 43: 61-78

Groman DB (1982) Histology of the striped bass. American Fisheries Society. Place published, Bethesda, Maryland

Guilgur LG, Moncaut NP, Canário AV, Somoza GM (2006) Evolution of GnRH ligands and receptors in gnathostomata. Comparative Biochemistry and Physiology Part A: Molecular & Integrative Physiology 144: 272-283

Guillette LJ, Fox SL, Palmer BD (1989) Oviductal morphology and egg shelling in the oviparous lizards *Crotaphytus collaris* and *Eumeces obsoletus*. Journal of Morphology 201: 145-159

Guzmán JM, Rubio M, Ortiz-Delgado JB, Klenke U, Kight K, Cross I, Sánchez-Ramos I, Riaza A, Rebordinos L, Sarasquete C (2009) Comparative gene expression of gonadotropins (FSH and LH) and peptide levels of gonadotropin-releasing hormones (GnRHs) in the pituitary of wild and cultured Senegalese sole (*Solea senegalensis*) broodstocks. Comparative Biochemistry and Physiology Part A: Molecular & Integrative Physiology 153: 266-277

Gwo JC, Gwo HH, Chang SL (1993) Ultrastructure of the spermatozoon of the teleost fish *Acanthopagrus schlegeli* (Perciformes: Sparidae). Journal of Morphology 216: 29-33

Halpern-Sebold LR, Schreibman MP, Margolis-Nunno H (1986) Differences between early-and late-maturing genotypes of the platyfish (*Xiphophorus maculatus*) in the morphometry of their immunoreactive luteinizing hormone releasing hormone-containing cells: A developmental study. Journal of Experimental Zoology 240: 245-257

Hamaguchi S (1993) Alterations in the morphology of nuages in spermatogonia of the fish, *Oryzias latipes*, treated with puromycin or actinomycin D. Reproduction Nutrition Development 33: 137-141

Hamlett WC, Hysell MK, Galvin J, Spieler RE (1998) Reproductive accomodations for gestation in the Atlantic guitarfish, *Rhinobatos lentiginosus*, Rhinobatidae. Journal of the Elisha Mitchell Scientific Society 114: 199

Hara M, Okiyama M (1998) An ultrastructural review of the spermatozoa of Japanese fishes. Bulletin of the Ocean Research Institute, University of Tokyo 33: 1-138

Harder W (1975) Anatomy of fishes, part I: text. E Schweizerbartsche Verlagsbuchhandlung, Stuttgart

Hashimoto S, Kurihara R, Strüssmann CA, Yamasaki T, Soyano K, Hara A, Shiraishi H, Morita M (2003) Gonadal histology and serum vitellogenin levels of bigeye tuna *Thunnus obesus* from the Northern Pacific Ocean—absence of endocrine disruption bio-indicators. Marine Pollution Bulletin 46: 459-465

Hernández MPGa, Ayala AGa, Zandbergen MA, Agulleiro B (2002) Investigation into the duality of gonadotropic cells of Mediterranean yellowtail (*Seriola dumerilii*, Risso 1810): immunocytochemical and ultrastructural studies. General and Comparative Endocrinology 128: 25-35

Honji R, Narcizo A, Borella M, Romagosa E, Moreira R (2009) Patterns of oocyte development in natural habitat and captive *Salminus hilarii* Valenciennes, 1850 (Teleostei: Characidae). Fish Physiology and Biochemistry 35: 109-123

Honji RM, Mello PH, Araújo BC, Rodrigues-Filho JA, Hilsdorf AW, Moreira RG (2011) Influence of spawning procedure on gametes fertilization success in *Salminus hilarii* Valenciennes, 1850 (Teleostei: Characidae): implications for the conservation of this species. Neotropical Ichthyology 9: 363-370

Huber R, Staaden M, Kaufman L, Liem K (1997) microhibitat use, trophic patterns, and the evolution of brain structure in African cichids. Brain, Behavior and Evolution 50: 167-182

Humason GL (1979) Animal Tissue Techniques. 4th. San Francisco: Freeman

Imanaga Y, Nyuji M, Amano M, Takahashi A, Kitano H, Yamaguchi A, Matsuyama M (2014) Characterization of gonadotropin-releasing hormone and gonadotropin in jack mackerel (*Trachurus japonicus*): Comparative gene expression analysis with respect to reproductive dysfunction in captive and wild fish. Aquaculture 428: 226-235

Jalali MA, Ahmadifar E, Sudagar M, Takami GA (2009) Growth efficiency, body composition, survival and haematological changes in great sturgeon (*Huso huso* Linnaeus, 1758) juveniles fed diets supplemented with different levels of Ergosan. Aquaculture Research 40: 804-809

Jamieson B, Grier H (1993) Influences of phylogenetic position and fertilization biology on spermatozoal ultrastructure exemplified by exocoetoid and poeciliid fish. Hydrobiologia 271: 11-25

Jamieson BG, Leung L-P (1991) Fish evolution and systematics: evidence from spermatozoa: with a survey of lophophorate, echinoderm and protochordate sperm and an account of gamete cryopreservation. Cambridge University Press

Kagawa H, Tanaka H, Okuzawa K, Kobayashi M (1998) GTH II but not GTH I induces final maturation and the development of maturational competence of oocytes of red seabreamin vitro. General and Comparative Endocrinology 112: 80-88

Kah O, Anglade I, Leprêtre E, Dubourg P, de Monbrison D (1993) The reproductive brain in fish. Fish Physiology and Biochemistry 11: 85-98

Kah O, Lethimonier C, Somoza G, Guilgur L, Vaillant C, Lareyre J-J (2007) GnRH and GnRH receptors in metazoa: a historical, comparative, and evolutive perspective. General and Comparative Endocrinology 153: 346-364

Kauffman AS, Rissman EF (2004) A critical role for the evolutionarily conserved gonadotropin-releasing hormone II: mediation of energy status and female sexual behavior. Endocrinology 145: 3639-3646

Khanna S, Singh H (1967) Histology and histochemistry of the saccus vasculosus in some teleosts (Pisces). Cells Tissues Organs 67: 304-311

King JA, Millar RP (1992) Evolution of gonadotropin-releasing hormones. Trends in Endocrinology and Metabolism 3: 339-346

Kotrschal K, Junger H (1987) Patterns of brain morphology in mid-European Cyprinidae (Pisces, Teleostei): a quantitative histological study. Journal fur Hirnforschung 29: 341-352

Kuchnow KP, Scott JR (1977) Ultrastructure of the chorion and its micropyle apparatus in the mature *Fundulus heteroclitus* (Walbaum) ovum. Journal of Fish Biology 10: 197-201

Lagler K, Bardach J, Miller R, Passino D (1977) Ichthyology. 506 pp. In John Wiley and Sons

Lahnsteiner F, Patzner R (1990) The spermatic duct of blenniid fish (Teleostei, Blenniidae): Fine structure, histochemistry and function. Zoomorphology 110: 63-73

Lahnsteiner F, Weismann T, Patzner R (1997) Structure and function of the ovarian cavity and oviduct and composition of the ovarian fluid in the bleak, *Alburnus alburnus* (Teleostei, Cyprinidae). Tissue and Cell 29: 305-314

Levavi-Sivan B, Bogerd J, Mañanós EL, Gómez A, Lareyre J-J (2010) Perspectives on fish gonadotropins and their receptors. General and Comparative Endocrinology 165: 412-437

Mandich A, Massari A, Bottero S, Marino G (2002) Histological and histochemical study of female germ cell development in the dusky grouper *Epinephelus marginatus* (Lowe, 1834). European Journal of Histochemistry 46: 87

Manni L, Rasotto M (1997) Ultrastructure and histochemistry of the testicular efferent duct system and spermiogenesis in *Opistognathus whitehurstii* (Teleostei, Trachinoidei). Zoomorphology 117: 93-102

Matsuyama M, Nagahama Y, Matsuura S (1991) Observations on ovarian follicle ultrastructure in the marine teleost, Pagrus major, during vitellogenesis and oocyte maturation. Aquaculture 92: 67-82

Mattei X (1988) The flagellar apparatus of spermatozoa in fish. Ultrastructure and evolution. Biology of the Cell 63: 151-158

Mattei X (1991) Spermatozoon ultrastructure and its systematic implications in fishes. Canadian Journal of Zoology 69: 3038-3055

Mayer I, Shackley S, Ryland J (1988) Aspects of the reproductive biology of the bass, *Dicentrarchus labrax* LI An histological and histochemical study of oocyte development. Journal of Fish Biology 33: 609-622

McMillan DB (2007) Fish histology: female reproductive systems. Springer Science & Business Media

Menasveta D (1980) Resources and fisheries of the Gulf of Thailand. Training Department, Southeast Asian Fisheries Development Center, Department of Fisheies, Thailand

Miranda LA, Strüssmann CA, Somoza GM (2001) Immunocytochemical identification of GtH1 and GtH2 cells during the temperature-sensitive period for sex determination in pejerrey, *Odontesthes bonariensis*. General and Comparative Endocrinology 124: 45-52

Mousa HA, Mousa MA (1999) Immunocytochemical and histological studies on the hypophyseal-gonadal system in the freshwater Nile Tilapia, *Oreochromis*

niloticus (L.), during sexual maturation and spawning in different habitats. Journal of Experimental Zoology 284: 343-354

Nagahama Y (1983) The functional morphology of teleost gonads. Fish Physiology 9: 223-275

Nagahama Y (1994) Endocrine regulation of gametogenesis in fish. International Journal of Developmental Biology 38: 217-217

Nagahama Y (2000) Gonadal steroid hormones: major regulators of gonadal sex differentiation and gametogenesis in fish. In International Symposium on the Reproductive Physiology of Fish, Bergen, Norway, July 4-9, 1999. pp. 211-222

Naito N, Hyodo S, Okumoto N, Urano A, Nakai Y (1991) Differential production and regulation of gonadotropins (GTH I and GTH II) in the pituitary gland of rainbow trout, *Oncorhynchus mykiss*, during ovarian development. Cell and Tissue Research 266: 457-467

Neidig CL, Skapura DP, Grier HJ, Dennis CW (2000) Techniques for spawning common snook: broodstock handling, oocyte staging, and egg quality. North American Journal of Aquaculture 62: 103-113

New JG (2001) Comparative neurobiology of the elasmobranch cerebellum: theme and variations on a sensorimotor interface. In The behavior and sensory biology of elasmobranch fishes: an anthology in memory of Donald Richard Nelson, pp 93-108. Springer

Northcutt RG (1981) Localization of neurons afferent to the telencephalon in a primitive bony fish, *Polypterus palmas*. Neuroscience Letters 22: 219-222

Nostro FL, Grier H, Meijide F, Guerrero G (2003) Ultrastructure of the testis in *Synbranchus marmoratus* (Teleostei, Synbranchidae): the germinal compartment. Tissue and Cell 35: 121-132

Nostro FLL, Antoneli FN, Quagio-Grassiotto I, Guerrero GA (2004) Testicular interstitial cells, and steroidogenic detection in the protogynous fish, *Synbranchus marmoratus* (Teleostei, Synbranchidae). Tissue and Cell 36: 221-231

Nozaki M, Naito N, Swanson P, Miyata K, Nakai Y, Oota Y, Suzuki K, Kawauchi H (1990b) Salmonid pituitary gonadotrophs I. Distinct cellular distributions of two gonadotropins, GTH I and GTH II. General and Comparative Endocrinology 77: 348-357

Nuurai P, Poljaroen J, Tinikul Y, Cummins S, Sretarugsa P, Hanna P, Wanichanon C, Sobhon P (2010) The existence of gonadotropin-releasing hormone-like peptides in the neural ganglia and ovary of the abalone, *Haliotis asinina* L. Acta Histochemica 112: 557-566

Nyuji M, Fujisawa K, Imanaga Y, Kitano H, Yamaguchi A, Matsuyama M (2013b) GnRHa-induced spawning of wild-caught jack mackerel *Trachurus japonicus*. Fisheries Science 79: 251-258

Nyuji M, Kitano H, Shimizu A, Lee JM, Kusakabe T, Yamaguchi A, Matsuyama M (2013a) Characterization, localization, and stage-dependent gene expression of gonadotropin receptors in chub mackerel (*Scomber japonicus*) ovarian follicles. Biology of Reproduction 88: 148

Nyuji M, Selvaraj S, Kitano H, Shiraishi T, Yamaguchi A, Shimizu A, Matsuyama M (2012b) Immunoreactivity of gonadotrophs (FSH and LH Cells) and

gonadotropin subunit gene expression in the male chub mackerel *Scomber japonicus* pituitary during the reproductive cycle. Zoological Science 29: 623-629

Nyuji M, Shiraishi T, Kitano H, Irie S, Yamaguchi A, Matsuyama M (2012a) Induction of final oocyte maturation and ovulation in jack mackerel, *Trachurus japonicus*, temporarily reared in captivity. Journal of the Faculty of Agriculture, Kyushu University 57: 427-430

Nyuji M, Shiraishi T, Selvaraj S, Van In V, Kitano H, Yamaguchi A, Okamoto K, Onoue S, Shimizu A, Matsuyama M (2011) Immunoreactive changes in pituitary FSH and LH cells during seasonal reproductive and spawning cycles of female chub mackerel *Scomber japonicus*. Fisheries Science 77: 731-739

Okochi Y, Abe O, Tanaka S, Ishihara Y, Shimizu A (2016) Reproductive biology of female Pacific bluefin tuna, *Thunnus orientalis*, in the Sea of Japan. Fisheries Research 174: 30-39

Okubo K, Nagahama Y (2008) Structural and functional evolution of gonadotropin-releasing hormone in vertebrates. Acta Physiologica 193: 3-15

Okuzawa K, Gen K, Bruysters M, Bogerd J, Gothilf Y, Zohar Y, Kagawa H (2003) Seasonal variation of the three native gonadotropin-releasing hormone messenger ribonucleic acids levels in the brain of female red seabream. General and Comparative Endocrinology 130: 324-332

Okuzawa K, Granneman J, Bogerd J, Goos HT, Zohar Y, Kagawa H (1997) Distinct expression of GnRH genes in the red seabream brain. Fish Physiology and Biochemistry 17: 71-79

Olson KR (2000) Circulation System. In The Laboratory Fish, GK O (ed) pp 369- 378. United Kingdom: Academic Press

Palevitch O, Abraham E, Borodovsky N, Levkowitz G, Zohar Y, Gothilf Y (2009) Nasal embryonic LHRH factor plays a role in the developmental migration and projection of gonadotropin-releasing hormone 3 neurons in zebrafish. Developmental Dynamics 238: 66-75

Palmieri G, Acone F, Desantis S, Corriero A, Ventriglia G, Addis P, Genovese S, Aprea A, Spedicato D, Losurdo M (2008) Brain morphology and immunohistochemical localization of the gonadotropin-releasing hormone in the bluefin tuna, *Thunnus thynnus*. European Journal of Histochemistry: 52: 19-28

Parenti LR, Grier HJ (2004) Evolution and phylogeny of gonad morphology in bony fishes. Integrative and Comparative Biology 44: 333-348

Peter R, Crim L, Billard R (1991) A stereotaxic atlas and implantation technique for nuclei of the diencephalon of Atlantic salmon (*Salmo salar*) parr. Reproduction Nutrition Development 31: 167-186

Pham KX, Amano M, Kurita Y, Shimizu A, Fujinami Y, Amiya N, Yamamori K (2008) Changes in the immunostaining intensities of follicle-stimulating hormone and luteinizing hormone during ovarian maturation in the female Japanese flounder. Fish Physiology and Biochemistry 34: 357-365

Planas JV, Swanson P, Dickhoff WW (1993) Regulation of testicular steroid production in vitro by gonadotropins (GTH I and GTH II) and cyclic AMP in coho salmon (*Oncorhynchus kisutch*). General and Comparative Endocrinology 91: 8-24

Poirier GR, Nicholson N (1982) Fine structure of the testicular spermatozoa from the channel catfish, *Ictalurus punctatus*. Journal of Ultrastructure Research 80: 104-110

Potter H, Kramer CR (2000) Ultrastructural observations on sperm storage in the ovary of the platyfish, *Xiphophorus maculatus* (Teleostei: Poeciliidae): the role of the duct epithelium. Journal of Morphology 245: 110-129

Powell J, Zohar Y, Elizur A, Park M, Fischer W, Craig A, Rivier J, Lovejoy D, Sherwood N (1994) Three forms of gonadotropin-releasing hormone characterized from brains of one species. Proceedings of the National Academy of Sciences 91: 12081-12085

Puchtler H, Waldrop FS (1978) Silver impregnation methods for reticulum fibers and reticulin: A re-investigation of their origins and specifity. Histochemistry 57: 177-187

Quagio-Grassiotto I, Oliveira C (2008) Sperm ultrastructure and a new type of spermiogenesis in two species of Pimelodidae, with a comparative review of sperm ultrastructure in Siluriformes (Teleostei: Ostariophysi). Zoologischer Anzeiger-A Journal of Comparative Zoology 247: 55-66

Quagio-Grassiotto I, Guimarães A (2003) Follicular epithelium, theca and egg envelope formation in *Serrasalmus spilopleura* (Teleostei, Characiformes, Characidae). Acta Zoologica 84: 121-129

Quérat B, Tonnerre-Doncarli C, Géniès F, Salmon C (2001) Duality of gonadotropins in gnathostomes. General and Comparative Endocrinology 124: 308-314

Roberts RJ (2012) Fish pathology. John Wiley & Sons, Wiley-Blackwel

Romagosa E (1991) Mudanças morfológicas (microscopia de luz e eletrônica) das

gônadas de Pacu, *Piaractus mesopotamicus* (Homberg, 1887) durante o ciclo reprodutivo, em condições de confinamento. In Instituto de Biociências de Rio Claro da Universidade Estadual Paulista.

Romagosa E, Narahara M, Borella M, Parreira S, Fenerich-Verani N (1999) Ultrastructure of the germ cells in the testis of matrinxã, Brycon cephalus (Teleostei, Characidae). Tissue and Cell 31: 540-544

Rosenfeld H, Meiri I, Elizur A (2007) Gonadotropic regulation of oocyte development. In The Fish Oocyte, pp 175-202. Springer

Ruwanpura SM, McLachlan RI, Meachem SJ (2010) Hormonal regulation of male germ cell development. Journal of Endocrinology 205: 117-131

Saidapur SK (1978) Follicular atresia in the ovaries of nonmammalian vertebrates. International Review Cytology 54: 225-244

Sambroni E, Le Gac F, Breton B, Lareyre J-J (2007) Functional specificity of the rainbow trout (*Oncorhynchus mykiss*) gonadotropin receptors as assayed in a mammalian cell line. Journal of Endocrinology 195: 213-228

Santos J, Veloso-Júnior V, Andrade Oliveira D, Hojo R (2010) Morphological characteristics of the testis of the catfish *Pimelodella vittata* (Lütken, 1874). Journal of Applied Ichthyology 26: 942-945

Sarasquete C, Cardenas S, González de Canales ML, Pascual E (2002) Oogenesis in the bluefin tuna, *Thunnus thynnus* L. A histological and histochemical study. Histology and Histopathology 17: 775-788.

Satchell GH (1991) Physiology and form of fish circulation. Cambridge University Press

Sattari M (2002) Ichthyology: Anatomy and Physiology. Naghsh Mehr Publication, 659p

Savari S, Safahieh A, Archangi B, Savari A, Abdi R (2013) Brain Anatomy and Histology of Orange Spotted Grouper (*Epinephelus coioides*). Journal of the Persian Gulf 4: 1-13

Selman K, Wallace RA (1982) Oocyte growth in the sheepshead minnow: Uptake of exogenous proteins by vitellogenic oocytes. Tissue and Cell 14: 555-571

Selman K, Wallace RA (1983) Oogenesis in *Fundulus heteroclitus*. III. vitellogenesis. Journal of Experimental Zoology 226: 441-457

Selman K, Wallace RA (1986) Gametogenesis in *Fundulus heteroclitus*. American Zoologist 26: 173-192

Selman K, Wallace RA (1989) Cellular aspects of oocyte growth in teleosts. Zoological Science 6: 211-231

Selman K, Wallace RA, Barr V (1986) Oogenesis in *Fundulus heteroclitus* IV. Yolk-vesicle formation. Journal of Experimental Zoology 239: 277-288

Selman K, Wallace RA, Barr V (1988) Oogenesis in *Fundulus heteroclitus*. V. The relationship of yolk vesicles and cortical alveoli. Journal of Experimental Zoology 246: 42-56

Selman K, Wallace RA, Sarka A, Qi X (1993) Stages of oocyte development in the zebrafish, *Brachydanio rerio*. Journal of Morphology 218: 203-224

Selvaraj S, Kitano H, Amano M, Nyuji M, Kaneko K, Yamaguchi A, Matsuyama M (2012a) Molecular characterization and expression profiles of three GnRH forms in the brain and pituitary of adult chub mackerel (*Scomber japonicus*) maintained in captivity. Aquaculture 356: 200-210

Selvaraj S, Kitano H, Amano M, Ohga H, Yoneda M, Yamaguchi A, Shimizu A, Matsuyama M (2012b) Increased expression of kisspeptin and GnRH forms in the brain of scombroid fish during final ovarian maturation and ovulation. Reproductive Biology and Endocrinology 10: 64

Selvaraj S, Kitano H, Fujinaga Y, Amano M, Takahashi A, Shimizu A, Yoneda M, Yamaguchi A, Matsuyama M (2009) Immunological characterization and distribution of three GnRH forms in the brain and pituitary gland of chub mackerel (*Scomber japonicus*). Zoological Science 26: 828-839

Senarat S, Jiraungkoorskul W, Kettratad J (2015) Neuroanatomy and histology of the central nervous system in short mackerel, *Rastrelliger brachysoma* (Bleeker, 1865). Walailak Journal of Science and Technology 13: 531-541

Sherwood N (1997) Origin and evolution of GnRH in vertebrates and invertebrates. GnRh neurons Gene to behavior: 3-25

Sherwood NM, Adams BA (2005) Gonadotropin-releasing hormone in fish: evolution, expression and regulation of the GnRH gene. In Melamed, P. and Sherwood, N. (Eds). Hormones and Their Receptors in Fish Reproduction. World Scientific Publishing pp. 1-39

Shimizu A, Tanaka H, Kagawa H (2003) Immunocytochemical applications of specific antisera raised against synthetic fragment peptides of mummichog GtH subunits: examining seasonal variations of gonadotrophs (FSH cells and LH cells) in the mummichog and applications to other acanthopterygian fishes. General and Comparative Endocrinology 132: 35-45

Shiraishi T, Ohta K, Yamaguchi A, Yoda M, Chuda H, Matsuyama M (2005) Reproductive parameters of the chub mackerel *Scomber japonicus* estimated

from human chorionic gonadotropin-induced final oocyte maturation and ovulation in captivity. Fisheries Science 71: 531-542

Skinner MK (1991) Cell-Cell Interactions in the Testis. Endocrine Reviews 12: 45-77

So W-K, Kwok H-F, Ge W (2005) Zebrafish gonadotropins and their receptors: II. Cloning and characterization of zebrafish follicle-stimulating hormone and luteinizing hormone subunits—their spatial-temporal expression patterns and receptor specificity. Biology of Reproduction 72: 1382-1396

Sprando R, Russell L (1988) Spermiogenesis in the bluegill (*Lepomis macrochirus*): a study of cytoplasmic events including cell volume changes and cytoplasmic elimination. Journal of Morphology 198: 165-177

Sritakon. T. SN, Chotithammo, S. and Vechprasit, S (2006) Reproductive biology of short mackerel *Rastrelliger brachysoma* (Bleeker, 1851) and Indian mackerel *R. kanagurta* (Cuvier, 1817) in the Southern Gulf of Thailand. In Department of Fisheries

Sutthakorn P (1998) Biological aspects of short mackerel, *Rastrelliger brachysoma* (Bleeker, 1851) of the Andaman Sea Coast of Thailand. Department of Fisheires

Swapna I, Sreenivasulu G, Rasheeda M, Thangaraj K, Kirubagaran R, Okuzawa K, Kagawa H, Senthilkumaran B (2005) Seabream GnRH: partial cDNA cloning, localization and stage-dependent expression in the ovary of snake head murrel, *Channa striatus*. Fish Physiology and Biochemistry 31: 157-161

Temple JL, Millar RP, Rissman EF (2003) An evolutionarily conserved form of gonadotropin-releasing hormone coordinates energy and reproductive behavior. Endocrinology 144: 13-19

Todd P (1976) Ultrastructure of the spermatozoa and spermiogenesis in New Zealand freshwater eels (Anguillidae). Cell and Tissue Research 171: 221-232

Tomkiewicz J, Tybjerg L, Jespersen Å (2003) Micro-and macroscopic characteristics to stage gonadal maturation of female Baltic cod. Journal of Fish Biology 62: 253-275

Tucker CS, Hargreaves JA (2004) Biology and culture of channel catfish. Elsevier Science

Turkmen S, Mumford S, Heidel J, Smith C, Morrison J, MacConnell B (2007) Fish Histology and Histopathology. USFWS-NCTC Shepherdstown, West Virginia, USA: 32-2

Tyler C, Sumpter J, Kawauchi H, Swanson P (1991) Involvement of gonadotropin in the uptake of vitellogenin into vitellogenic oocytes of the rainbow trout, *Oncorhynchus mykiss*. General and Comparative Endocrinology 84: 291-299

Ueda IK, Egami MI, Sasso WdS, Matushima ER (2001) Cytochemical aspects of the peripheral blood cells of *Oreochromis* (Tilapia) *niloticus* (Linnaeus, 1758)(Cichlidae, Teleostei): part II. Brazilian Journal of Veterinary Research and Animal Science 38: 273-277

van der Straten KM, Collette BB, Leung LK-P, Johnston SD (2006) Sperm morphology of the black marlin (*Makaira indica*) differs from scombroid sperm. Bulletin of Marine Science 79: 839-845

Vázquez GR, Guerrero G (2007) Characterization of blood cells and hematological parameters in *Cichlasoma dimerus* (Teleostei, Perciformes). Tissue and Cell 39: 151-160

Vidal B (1988) Histochemical and anisotropical properties characteristics of silver impregnation: the differentiation of reticulin fibers from the other interstitial collagens. Zoologische Jahrbuecher Abteilung fuer Anatomie 117: 485-494

Volkoff H, Peter R (1999) Actions of two forms of gonadotropin releasing hormone and a GnRH antagonist on spawning behavior of the goldfish *Carassius auratus*. General and Comparative Endocrinology 116: 347-355

Wallace RA, Selman K (1981) Cellular and dynamic aspects of oocyte growth in teleosts. American Zoologist 21: 325-343

Wallace RA, Selman K (1990) Ultrastructural aspects of oogenesis and oocyte growth in fish and amphibians. Journal of Electron Microscopy Technique 16: 175-201

West G (1990) Methods of assessing ovarian development in fishes: a review. Marine and Freshwater Research 41: 199-222

Wiegand MD (1996) Composition, accumulation and utilization of yolk lipids in teleost fish. Reviews in Fish Biology and Fisheries 6: 259-286

Wilson JM, Bunte RM, Carty AJ (2009) Evaluation of rapid cooling and tricaine methanesulfonate (MS222) as methods of euthanasia in zebrafish (*Danio rerio*). Journal of the American Association for Laboratory Animal Science 48: 785-789

Yang Z, Chen Y-F (2004) Induced ovulation in obscure puffer Takifugu obscurus by injections of LHRH-a. Aquaculture International 12: 215-223

Yön NDK, Akbulut C (2012) Electron and light microscopic investigations of follicular epithelium in vitellogenic oocyte of zebrafish (*Danio rerio*). Pakistan Journal of Zoology 44: 1581-1586

Young KG, Chang JP, Goldberg JI (1999) Gonadotropin-releasing hormone neuronal system of the freshwater snails *Helisoma trivolvis* and Lymnaea stagnalis: possible involvement in reproduction. Journal of Comparative Neurology 404: 427-437

Zohar Y, Muñoz-Cueto J, Elizur A, Kah O (2010) Neuroendocrinology of reproduction in teleost fish. General and Comparative Endocrinology 165: 438-455

Zohar Y, Mylonas CC (2001) Endocrine manipulations of spawning in cultured fish: from hormones to genes. Aquaculture 197: 99-136

APPENDIX

VITA

Mr. Sinlapachai Senarat was born on December 18, 1985 in Nakhon Si Thammarat Province, Thailand. He graduated with his Bachelor of Science in Biology from the Faculty of Science, Prince of Songkla University in 2008. Afterwards, he enrolled as a graduate student in the Zoology program, Department of Biology, Faculty of Science, Chulalongkorn University in 2009. He obtained his Master of Science in 2011 then continued his Ph.D. study in the Department of Marine Science, Faculty of Scince, Chulalongkorn University. He was awarded the scholarship from the 100th Anniversary, Chuulalongkorn University for his study.

PUBLICATIONS

Senarat, S., Kettretad, J. and Jiraungkoorskul, W. 2015. Classification stages of novel atretic structure in short mackerel Ratrelliger brachysoma (Bleeker, 1851) from the Upper Gulf of Thailand. Songklanakarin Journal of Science and Technology 37: 569-573.

Senarat, S., Kettretad, J. and Jiraungkoorskul, W. 2015. Morpho-histology of the reproductive duct in short mackerel Rastrelliger brachysoma (Bleeker, 1851). Advances in Environmental Biology 9: 210-215.

Senarat, S., Kettretad, J. and Jiraungkoorskul, W. 2016. Neuroanatomy and histology of the central nervous system in short mackerel, Rastrelliger brachysoma (Bleeker, 1851) Walailak Journal of Science and Technology 13: 531-541.

Senarat, S., Kettretad, J. and Jiraungkoorskul, W. 2016. Histological evidence of the heart and ovarian vessels in the short mackerel, Rastrelliger brachysoma. EurAsian Journal of BioSciences 10: 13-21.

Senarat, S., Kettretad, J. and Jiraungkoorskul, W. 2016. Testicular structure and spermatogenesis of short mackerel, Rastrelliger brachysoma (Bleeker, 1851) in The Upper Gulf of Thailand. Asia Pacific Journal of Molecular Biology and Biotechnology. 24: xx-xx (Article in press).

Senarat, S., Kettretad, J. and Jiraungkoorskul, W. 2016. Ovarian histology and reproductive health of short mackerel, Rastrelliger brachysoma (Bleeker, 1851), as threatened marine fish in Thailand. Songklanakarin Journal of Science and Technology (Article in press).